SCUOLA DI DOTTORATO
UNIVERSITÀ DEGLI STUDI DI MILANO-BICOCCA

Department of Biotechnologies and Biosciences

Ph.D. Program in Translational and Molecular Medicine (DIMET)
Cycle XXXII

Role of the Sox2 and COUP-TF1 transcription factors in the development of the visual system by conditional knock-out in mouse

Dr. Linda Serra

Registration number: 823235

Tutor: Prof. Silvia K. Nicolis

Co-tutor: Dr. Michèle Studer

Coordinator: Prof. Andrea Biondi

ACADEMIC YEAR 2018/2019

TABLE OF CONTENTS

CHAPTER 1:

GENERAL INTRODUCTION p. 7

1. The visual system: organizations and development in the mouse p. 7

1.1 The development of the cerebral cortex in mice p. 9

1.2 The development of the thalamus in mice p. 13

1.3 Factors that regulate visual system development in mice p. 15

1.3.1 Key molecules necessary for the development of retino-thalamic connections p. 16

1.3.2 Key molecules necessary for the development of thalamo-cortical connections p. 18

1.3.3 Role of serotonin in the development of thalamic neurons and their connections p. 20

2. The Sox2 transcription factor p. 23

2.1 Sox2 expression and functions during nervous system embryonic development p. 24

2.2 Sox2 function in eye development p. 26

2.3 SOX2 and human disease p. 28

3. The COUP-TF1 transcription factor p. 29

3.1 COUP-TF1 functions in nervous system development p. 30

3.2 COUP-TF1 and human disease p. 32

4. Mouse genetic models used in my thesis project p. 32

AIM OF THE THESIS p. 34

References p. 36

CHAPTER 2:
Sox2 acts in thalamic neurons to control the development of retina-thalamus-cortex connectivity p. 45

CHAPTER 3:
Characterization of Sox2 and COUP-TF1 targets in the dLGN p. 106

CHAPTER 4:
Mouse *Nr2f1* haploinsufficiency unveils new pathological mechanisms of a human optic atrophy syndrome p. 123

CHAPTER 5:
SUMMARY p. 192
CONCLUSIONS AND FUTURE PERSPECTIVES p. 194
1. Sox2 is required not only in neural stem cells but also in differentiated neurons of the thalamus p. 194
2. *SOX2* defective function in the thalamus could be linked in humans to cerebral visual impairment p. 197
3. Sox2 and COUP-TF1: why are they co-expressed in thalamic neurons? p. 199
References p. 201

CHAPTER 6:
Review
"More than just Stem Cells: Functional Roles of the Transcription Factor Sox2 in Differentiated Glia and Neurons" p. 205

CHAPTER 1
GENERAL INTRODUCTION

1. The visual system: organization and development in the mouse

The visual system in mice is composed of three components closely interconnected: the eye, the dorsolateral geniculate nucleus (dLGN) in the thalamus and the visual cortex (Figure 1).

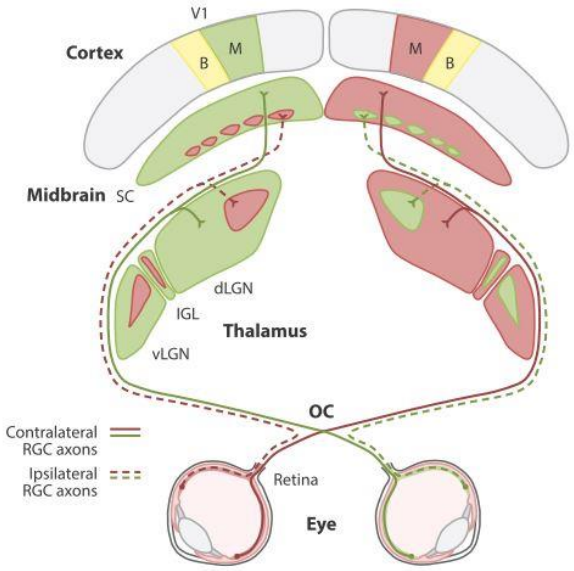

Figure 1. Schematic representation of the complexity of the mouse visual system. Neuronal projections from each eye reach the dLGN in the thalamus. A portion of contralateral and ipsilateral projections from the eye reach the superior colliculus (SC). Axon terminals of thalamic neurons project to the visual cortex. The monocular and binocular zones of the visual cortex elaborate information from the contralateral eye and both eyes respectively.

In turn, neurons of the visual cortical area send their efferents to the dLGN, generating a cortex-thalamus loop (image from Seabrook et al., 2017).

The dLGN receives visual information from the retina; here, axons of the retinal ganglion cells (RGCs) from both eyes exit the eyeball and meet at the optic chiasm, where they give rise to two different neuronal projections: 97-98% of RGCs produce contra-lateral projections, that cross and reach the opposite hemisphere, whereas only 2-3% give rise to ipsi-lateral projections, which reach the corresponding hemisphere (Diao et al., 2018). While ipsi-lateral projections originate from RGCs localized in the ventrolateral retina, contra-lateral ones originate from RGCs distributed along the whole retina. Their uncrossing or crossing is regulated by the interaction of guidance cues expressed by RGCs and along the path of retinal fibers (Diao et al., 2018).

Contra-lateral projections reach the dLGN between embryonic day 16 (E16) and postnatal day 0 (P0) and occupy about 90% of the dLGN area. The ipsi-lateral projections arrive to the dLGN between postnatal day 0 (P0) and postnatal day 2 (P2) and occupy 10% of the total area corresponding to the dorso-medial region of the dLGN (Guido, 2018).

At this stage, contra-lateral and ipsi-lateral projections show some overlap, but later in development (at the end of the first postnatal week) they are clearly segregated and at postnatal day 12, when eyes open, they show and adult-like segregation pattern (Guido, 2018).

In mice and, more in general, in rodents, 10% of dLGN cellular composition is represented by interneurons, and the remaining part is composed of thalamocortical relay neurons; both neuron types receives visual inputs from the retina, but only relay neurons project their

terminal axons to the visual areas of the cortex (Kerschensteiner and Guido, 2017).

In mice, the cortical primary visual area is subdivided in two zones: the monocular zone and the binocular zone (see Figure 1), that receive and elaborate the visual information coming from the contralateral eye and from both eyes respectively (Seabrook et al., 2017). Cortical neurons of the visual area, in turn, project to the dLGN giving rise to a complex neuronal circuit.

In the following sections I will discuss the development of the two components of the visual system in the mouse that I mainly studied during my thesis project, the cerebral cortex and the thalamus, and some of the molecular mechanisms underlying their formation and interconnection.

1.1 The development of the cerebral cortex in mice

In mammals, the most expanded region of the cerebral cortex is the neocortex, which is subdivided into six radially organized layers. The majority of neocortical neurons is glutamatergic and originate from the ventricular zone (VZ) starting at embryonic day (E) 10.5; initially, the first post-mitotic neurons accumulates on the top of the VZ originating a primitive structure called the preplate (PP). Subsequent waves of neurons born in the VZ migrate along the radial glia giving rise to the cortical plate (CP), which subdivides the preplate into a deeper layer, the subplate (SP), and a more superficial layer, the marginal zone (MZ). The MZ will give rise to layer 1 of the neocortex populated by Cajal-Retzius cells, expressing Reelin (Figure 2) (O'Leary and Nakagawa, 2002, Alfano and Studer 2013).

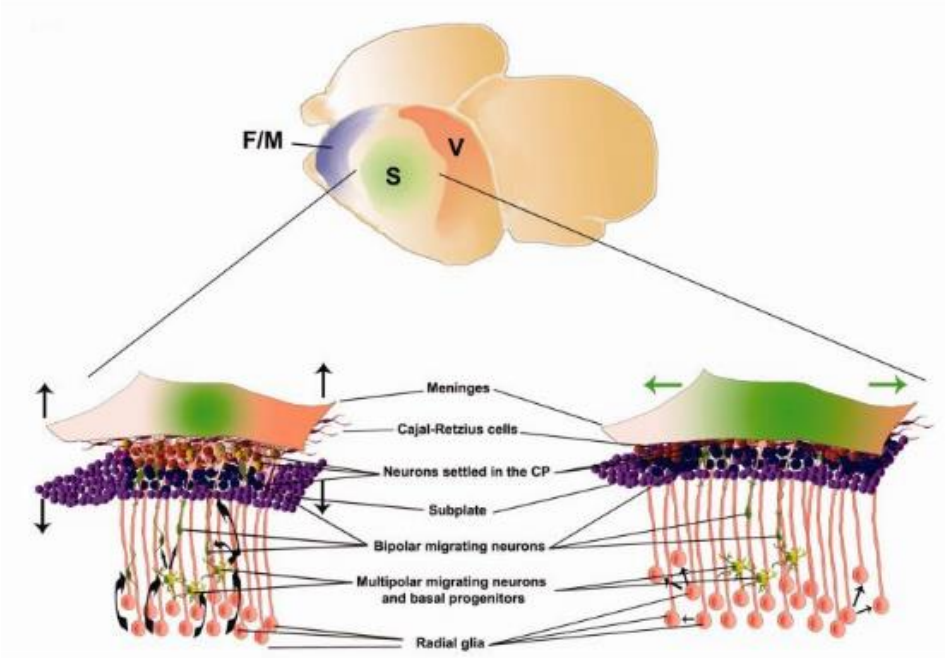

Figure 2. **Schematic representation of the development of the mouse cerebral cortex** (from Alfano and Studer 2013).

Subsequent waves of new-born neurons leave the proliferative zone and rise towards the cortical plate, expanding it through an inside-out process. Precisely, neurons generated early occupy the deeper layers, while neurons generated later in successive waves migrate overtaking the existing neurons, and they occupy the most superficial layers. Thus, layers VI, V, IV, III and II are progressively generated. Reelin, expressed by Cajal-Retzius cells in layer 1, is a secret protein important in guiding radial migration of neocortical neurons and, therefore, has a key role in the layering of the neocortex (O'Leary and Nakagawa, 2002).

The neocortex is tangentially organized into specialized areas, morphologically and functionally distinct, that are specified during the arealization process. Precisely four cortical primary areas, interconnected to higher order areas, can be identified: the primary visual area (V1), that processes visual information coming from the retina, the primary somatosensory area (S1), that receives information from the body's periphery, the primary auditory area (A1), that receives information from the inner ear, and the primary motor area (M1), that controls voluntary movements (O'Leary and Sahara, 2008).

The arealization process is regulated both by intrinsic and extrinsic factors (Figure 3). Regarding intrinsic factors, there are four patterning centers localized in the perimeter of the telencephalon: the commissural plate (CoP), the cortical hem, the antihem and some domains of the ventral telencephalon, that produce and secrete specific morphogens such as Fgfs, Bmps, Tgfα and Shh respectively (Figure 3).

These secreted molecules act on cortical progenitors establishing gradients of expression of specific transcription factors crucial for area identity that include: Emx2, Pax6, Sp8 and COUP-TF1.

However, the specification of cortical areas is fully achieved thanks to the combination of intrinsic mechanisms of gene regulation and extrinsic cues to the cortex. In fact, each primary cortical area receives inputs from thalamo-cortical afferents, which convey sensory information from specific dorsal thalamic nuclei (O'Leary and Sahara, 2008) (Figure 3).

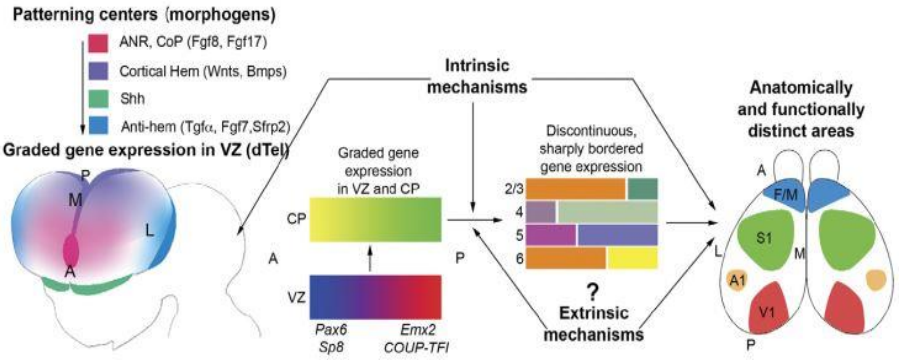

Figure 3. **The arealization process.** The combination of intrinsic genetic mechanisms and signals extrinsic to the cortex lead to the definition of different cortical areas, with specific morphological and functional peculiarities (from O'Leary and Sahara 2008).

Precisely, the V1 receives projections from the dorsolateral geniculate nucleus (dLGN), the S1 from the ventroposterior nucleus (VPN), the A1 from the medial geniculate nucleus (MGN) and the M1 from the ventrolateral nucleus (VLN). Neurons of each thalamic nucleus send their terminals to layer IV of the corresponding cortical area and, in turn, layer V and VI neurons send back cortico-thalamic afferents to the respective nucleus (Alfano and Studer, 2013). The cortico-thalamic projections seem to shape the activity of the thalamic nuclei (Alfano and Studer, 2013), while thalamo-cortical afferents are important for the correct shaping of cortical areas, distinguishing them from surrounding higher order areas. In fact, lack of thalamo-cortical projections to the prospective visual area results in failure to specify primary visual area and higher-order visual areas (Chou et al., 2013).

1.2 The development of the thalamus in mice

The thalamus is a bilaterally symmetrical structure positioned in the central part of the forebrain in mammals, important for the transmission of sensory and motor information coming from the periphery to the cerebral cortex, but also for the transmission of inputs between cortical areas. Indeed, some thalamic nuclei relay information from layer V of a distinct cortical area to another cortical area. The relay can occur from a cortical primary area to a high order area or between two higher order cortical areas (Sherman 2007).

During early development, the thalamus originates from prosomere 2 of the diencephalon during a specific temporal window, with thalamic progenitor cells proliferating between E10 and E15 according to lateromedial and caudorostral gradients, before they differentiate into neurons (Gezelius and Lopez-Bendito, 2017). The thalamus can be distinguished from the hypothalamus after E12 and it is possible to discriminate between dorsal and ventral thalamus at E13. Later in development (E16-E17) thalamic neurons start to aggregate in specific nuclei, first in the epithalamus and ventral thalamus and, then, in the dorsal thalamus (Lopez-Bendito and Molnar, 2003).

Thalamic neurons are organized in approximately 30 specific nuclei, distinguishable according to their morphology and cellular density, that establish connectivity patterns with specific brain structures such as cortical areas, hippocampus, amygdala, spinal cord and many others. The dorsal thalamus and the cortex are strongly interconnected and in the mouse they start to interact through reciprocal connections between E13 and E18.

At E13.5 thalamic axons leave the dorsal thalamus, descend ventrally and then they turn dorsalaterally crossing the diencephalic-telencephalic boundary. Subsequently, they cross the medial and lateral ganglionic eminences and they stop before reaching the subpallium-pallium boundary at E15.

At the same time, cortical axons leave the cortex and stop at the same boundary. Here they start to strictly associate ("handshake") and at E18.5 thalamic and corticofugal projections reach their specific targets (Figure 4) (Lopez-Bendito and Molnar, 2003).

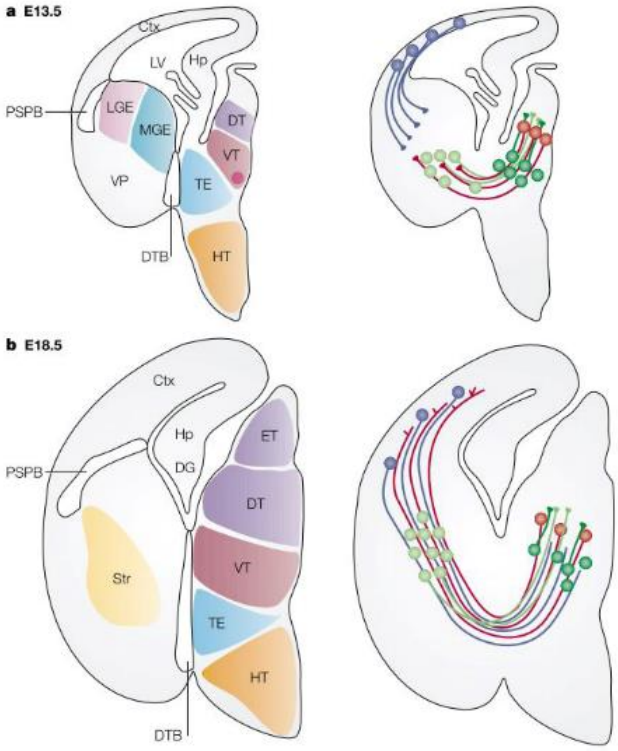

Figure 4. The development of thalamo-cortical and cortico-thalamic neural projections (image from Lopez-Bendito and Molnar, 2003). a) At E13.5 thalamic axons from the dorsal thalamus (DT), represented as red lines,

descend among the cell of the ventral thalamus (VT) and cross the diencephalon-telencephalon boundary (DTB). At the same time, cortical axons, represented as blue lines, leave the cortex and transiently stop at the pallial-subpallial boundary (PSPB). b) At E18.5 thalamo-cortical (red) and corticofugal projections (blue) are reaching their respective targets.

Thalamic sensory nuclei located in the dorsal thalamus, such as dLGN, VPN and MGN, project to specific and specialized primary cortical areas, V1, S1 and A1 respectively, while other nuclei that integrate signals from several sources project more diffusely to larger areas of the cortex (Bibollet-Bahena et al., 2017).

1.3 Factors that regulate visual system development in mice

The patterning of the visual system in mouse depends on the combination of different factors: molecular guidance cues, retinal waves and sensory visual experience that together orchestrate visual axis development and interconnection. During development, the segregation of retinal fibers that reach the dLGN undergoes a refinement process. The retinogeniculate pathway refinement in mouse is due to the combination of molecular guidance cues, that first establish the initial positioning of retinal axons and contribute to the localization of eye-specific domains, and of neural activity. In fact, before the natural eye-opening, adjacent RGCs show a spontaneous activity that spreads through the retina in form of retinal waves. Retinal waves are essential for the visual pathway patterning, particularly in the first two postnatal weeks, and when they are perturbed, retinal axon arbors do not properly segregate in the dLGN. Moreover, there is also a remodelling of synaptic connections, which is achieved by means of

synaptic pruning; precisely, at the beginning, a single neuron of the dLGN receives inputs from many RGCs, but during the first three postnatal weeks the event of synaptic pruning leaves only few functional inputs. Therefore, weak synaptic inputs are removed while the remaining inputs are strengthened. After eye-opening, that in mouse occurs at about postnatal day 12, spontaneous retinal waves are replaced by visually evoked activity, which is important for the continued strengthening and stabilization of the connectivity pattern typical of the adults. Infact, the elimination of visual stimuli during this phase strongly affects the connectivity between the eye and the dLGN; neurons of the dLGN receive many weak inputs from the RGCs and they appear immature (Guido 2018). Thus, the alteration of all these factors is causative of an aberrant development of the visual system.
In the following paragraphs I will focus on some molecular guidance cues involved in the development of connections between the eye, the thalamus and the cortex.

1.3.1 Key molecules necessary for the development of retino-thalamic connections

The Eph-Ephrin receptor-ligand signalling pathway exerts a crucial role in guiding retinal axons growth towards the dLGN. The Eph family is composed of tyrosine kinase receptors subdivided into two subclasses - A and B - according to their affinity to ephrinA or ephrinB ligands (Williams et al., 2003). EphA receptors and EphrinAs ligands are expressed in the RGC layer of the retina or in the dLGN with opposite gradients.

Components of the EphrinA/EphA family important for the visual system are EphrinA2, A3 and A5. In the dLGN, the expression of *EphrinA2, EphrinA3* and *EphrinA5* have been described; *EphrinA2* and *A5* show a high ventrolateral-anterior to low dorsomedial-posterior graded expression pattern, while *EphrinA3* is expressed at low levels. Triple knock-out of *EphrinA2, EphrinA3* and *EphrinA5* in mice reveals that EphrinA ligands are important for the correct targeting of ipsilateral projections to the dLGN, which in fact occupy irregular and patchy areas in the mutant dLGN (Pfeiffenberger et al., 2005).

Compontents of the EfnaB/EphB family important for the visual system are, for example, EphrinB2 and its receptor EphB1.

The ligand EphrinB2, which is expressed by radial glia in the optic chiasm midline, interacts with the receptor EphB1, expressed in RGCs of the ventrotemporal retina. EphrinB2 is required for ipsilateral projections to form by repulsing EphB1 positive axons coming from the retina and guiding them to the ipsilateral hemisphere and when EphB1 is knocked-out a dramatic reduction of ipsilateral projections can be observed (Williams et al., 2003; reviewed in Diao et al., 2018).

Another molecule important for the regulation of eye-specific patterning is *Ten-m3*, a highly conserved type II transmembrane protein expressed both in the retina and in the dLGN. Within the RGC layer, Ten-m3 shows a linear high-ventral to low-dorsal gradient, and within the dLGN it shows an expression pattern higher dorsally and lower ventrally. *Ten-m3 KO* mice present a dramatic change in the targeting of ipsilateral projections. Caudally, ipsilateral projections are more expanded in the dorso-medial part of the dLGN, while, centrally, they

are dramatically elongated along the the ventrolateral and dorsomedial axis of the dLGN (Leamey et al., 2007, reviewd in Diao et al., 2018).
Two other crucial factors in the correct patterning of the dLGN belong to the Zinc finger transcription factor family and are *Zic4* and *Zic2*.
Zic4 is expressed in a gradient both in the RGC layer in the retina and in the dLGN; *Zic4 null* mice show disorganized ipsilateral projections that target the dLGN, with an increase of ipsilateral projections clusters and of the percentage of dLGN surface occupied by them (Horng et al., 2009). This phenotype resembles that observed in *EphrinA2/A3/A5 triple KO-mice*.
Zic2 is expressed in retinal ganglion cells that give rise to ipsilateral projections, when these cells grow their axons towards the optic chiasm. Zic2 is important in the establishment of retinal ganglion cells identity, in fact reduced levels of Zic2 in mice lead to a reduction of retinal axons that project ipsilaterally at the optic chiasm (Herrera et al., 2003).

1.3.2 Key molecules necessary for the development of thalamo-cortical connections

The production of attractive and repulsive factors from the cortex is thought to have an essential role in guiding the outgrowth of projections coming from the thalamus to all cortical regions (O'Leary and Nakagawa 2002, Lopez-Bendito and Molnar 2003).
Some examples of molecules involved in the set-up of these projections are semaphorins, a family of transmembrane and secreted proteins that can act as attractive or repulsive guidance cues. A member of this family, *Semaphorin6A*, is highly expressed in the developing thalamus, amygdala and ventral telencephalon when thalamic axons start to grow

towards their cortical targets. In *Semaphorin-6A* deficient mice, axons from the dLGN are misrouted to the ventral telencephalon and fail to reach the visual cortex, which gets innervated by somatosensory axons (Little et al., 2009).

Other important guidance molecules belong to the Ephrins-Ephs family, that, as already mentioned, are also necessary for the correct patterning of retinal projections to the dLGN. The interaction between these ligands and their receptors mediate the branching of thalamic axons in their cortical targets and, consequently, the establishment of layer-specific connections (Mann et al., 2002). For example, it has been demonstrated that EphrinA5 in the cortex acts in a repulsive fashion for thalamo-cortical axons that express certain levels of EphA receptors, leading to a precise topographic organization of the somatosensory cortex (Dufour et al., 2003).

Defects in thalamo-cortical development are also identified in mice lacking the homeodomain transcription factor *Gbx2*.

Gbx2 is specifically expressed in the developing thalamus, where it is essential in the specification and differentiation of the distinct thalamic nuclei (Li et al., 2012). In *Gbx2* mutant mice in fact, thalamic axons fail to reach the cortex, leading to a complete loss of thalamic innervation, that could be explained by a defective production of guidance cues (reviewed in Lopez-Bendito and Molnar, 2003; Diao et al., 2018).

Another example is represented by the ligand Netrin-1 and the receptor DCC. Netrin-1 is a membrane-associated protein expressed in the ventral telencephalon and in the internal capsule region (the major axon tract that reciprocally connects the cortex with subcortical regions) and interacts with the receptor DCC, which is instead expressed by neurons

of the dorsal thalamus that project to the cortex. In *Netrin-1* knock-out mice, thalamo-cortical afferents are able to leave the dorsal thalamus and reach the dorsal cortex; however, they show a disorganized and abnormally restricted pathway through the internal capsule region and the number of axons that reach the cortex is reduced, demonstrating that Netrin-1 is required to attract migrating axons toward the cortex through the interaction with its receptor DCC (Braisted et al., 2000).

1.3.3 Role of serotonin in the development of thalamic neurons and their connections

The serotonin neurotransmitter (5-HT) is involved in different developmental processes of the central nervous system, including differentiation, migration, growth and synaptogenesis. In the mouse, 5-HT is synthesized by neurons of the raphe nuclei, which are localized in the hindbrain (only a minor rostral part of the dorsal raphe is attributed to the midbrain) and they send their terminal axons to different brain targets, as shown in Figure 5 (Muzerelle et al., 2016).

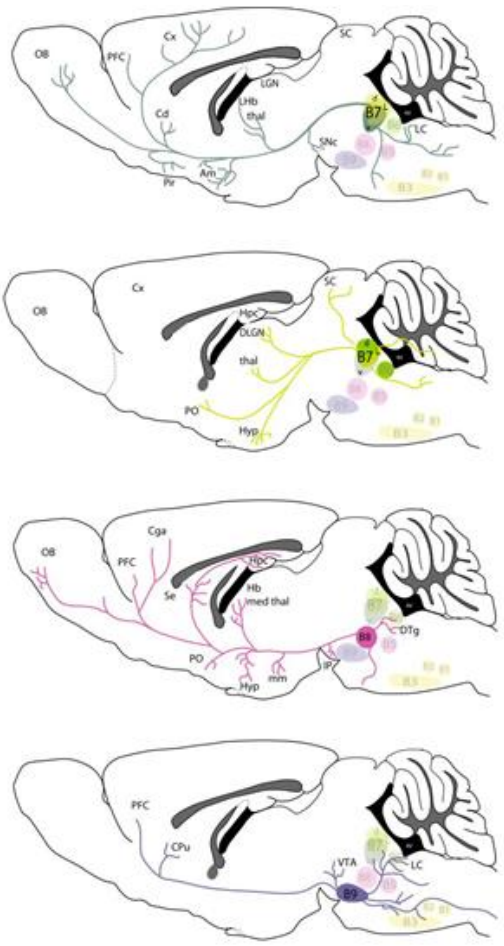

Figure 5. Different 5-HT raphe nuclei subgroups, such as B7, B8 and B9, target several areas of the mouse brain (from Muzerelle et al., 2016).

5-HT is transiently detectable in layer IV of V1, S1 and A1 cortices and in the dLG, VP and MG thalamic sensory nuclei in a very limited developmental time window, between birth (P0) and postnatal day 10 (P10).

However, thalamic neurons are not able to synthesize serotonin, but they can uptake it from the extracellular environment and concentrate it into their cellular bodies possibly to regulate extracellular 5-HT levels

or to further use it for serotonergic neurotransmission. This is due to the expression on cortical terminal axons of sensory thalamic neurons of the serotonin transporter, SERT, and of the vesicular monoamine transporter 2, V-MAT2. *SERT* and *VMAT2* are transiently expressed between P0 and P14 in dLG, VP and MG thalamic nuclei and are not detectable in the same nuclei in adults (Lebrand et al., 1996).

Thus, SERT takes-up serotonin into thalamic neurons, and V-MAT2 stores serotonin into synaptic vesicles protecting it from degradation mediated by the monoamine oxidase A enzyme (MAOA).

Raphe fibers project and release serotonin in different brain regions and the dLGN is one of them. Retinal ganglion terminal axons that reach the dLGN transiently express *SERT* and *V-MAT2*, therefore, they can internalize serotonin into their cellular bodies, precisely between E15 and P15. (Upton et al., 1999).

The transient presence of 5-HT and the expression of its molecular transporters in thalamic neurons and retinal ganglion cells is consistent with the idea that 5-HT acts as a modulator of the formation of retino-thalamic and thalamo-cortical connections. This is supported by several studies related to pharmacological or genetic manipulation of 5-HT levels in the brain, mainly focused on the somatosensory cortex. In mice, the primary somatosensory cortex has a characteristic organization; thalamocortical axons, arriving from the VP thalamic nucleus, reach the cortex and form clusters in cortical layer IV. Each cluster is surrounded by a distinct ring of cortical layer IV neurons, giving origin to what are called “barrels”, also known as barrel fields.

Pharmacological depletion of 5-HT in the developing postnatal mouse brain leads to a delay in barrel fields maturation in the somatosensory

cortical layer IV. Similar defects are observed in *V-MAT2-KO* mice, where the decrease of 5HT levels leads to a defective formation of barrel fields in layer IV of S1. On the other hand, also the increase of extracellular 5-HT levels in early postnatal brain in *MAOA-KO* and *SERT-KO* mice disrupts cortical development of barrel fields (van Kleef et al., 2012).

In addition, the increase of 5-HT levels in the brain of *MAOA-KO* mice during the first two postnatal weeks affects the segregation of ipsilateral and contralateral retinal projections that reach the dLGN. In these mice, retinal projections fail to perfectly segregate; the controlateral projections innervate the entire dLGN surface, including the territory normally occupied by ipsilateral projections, while ipsilateral projections cover a bigger volume in the dLGN (Upton et al., 1999).

Overall, these data show that serotonin is important for the correct development of the connections between the eye and the thalamus and between the thalamus and the cortex.

2. The Sox2 transcription factor

The SOX genes family [Sry-related High Mobility Group box] encodes for proteins expressed in different phases of embryonic development and cellular differentiation and involved in transcriptional regulation. Usually, a SOX protein presents three distinct functional domains: an activation or repression domain close to the C-terminal portion of the molecule, the HMG domain (High Mobility Group domain), essential for its binding to the DNA, and a region important for the interaction with other molecular partners. The peculiarity of the HMG domain is that, by interacting with the minor grove of DNA helix, it induces a

strong bending of the DNA molecule. The HMG domain, a 79-amino acid protein motif, recognises only 6-7 base pair DNA sequences (Kamachi et al., 2000). To date more than 20 SOX proteins have been identified and they are classified in Group A to G, according to the amino-acid sequence of the HMG domain; within the same group, SOX proteins show an HMG amino-acid sequence identity greater than 90%. SOX proteins act in a cell-specific way and this specificity is due to the interaction with different cell-specific partners (Kamachi et al., 2000).

2.1 Sox2 expression and functions during nervous system embryonic development

The *Sox2* gene, together with *Sox1* and *Sox3*, belongs to the Subgroup B1, that consists of transcriptional activators. *Sox2* has only one exon which encodes for a 2,4 kb transcript.

In the mouse, *Sox2* is expressed very early in development. It is detected in some morula cells at E2.5 and in the blastocyst inner cell mass (ICM) at E3.5, where it is important for the maintenance of embryonic stem cells pluripotency. *Sox2* is also expressed in the epiblast and extraembryonic ectoderm at E6.5, in the chorion and in the anterior region of the presumptive neuroectoderm at E7.5-E8. At E9.5 *Sox2* is expressed in the neural tube, sensory placodes, branchial arches and gut (Figure 6) (Avilion et al., 2003).

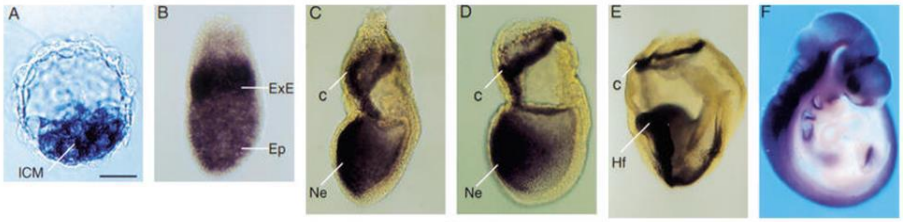

Figure 6. *Sox2* mRNA detection during embryonal development in mice (from Avilion et al., 2003). *Sox2* is expressed in the inner cell mass of the blastocyst (A), in the epiblast and in the extraembryonic ectoderm at E6.5 (B), in the chorion and in the anterior region of the presumptive neuroectoderm at E7.5-E8 (C,D), in the chorion, headfolds and neural tube (E), and is expressed throughout the nervous system by E9.5 (F).

In the differentiating neural tube *Sox2* is detected in the proliferating ventricular zone (VZ) and, in the adult brain, *Sox2* expression is found in some differentiated cells, including pyramidal cells in the cerebral cortex, striatal and thalamic neurons and ependymal cells (Ferri et al., 2004; Mercurio et al., 2019; Cheng et al., 2019).

Sox2 is such an important gene during development that its constitutive knock-out in mice is embryonic lethal. Mutant embryos fail to survive after implantation *in utero* because of embryonic stem cells loss (Avilion et al., 2003). Therefore, the Nicolis laboratory generated different *Sox2* conditional knock-out mouse models in order to study its role in the development of the central nervous system; in these mouse models, the *Sox2* gene is flanked by two loxP sites recognised by specific Cre-recombinases, whose expressions is controlled by tissue-specific promoters, mediating *Sox2* deletion in a tissue and time-specific fashion (Favaro et al., 2009).

Sox2 is required in neural stem cells maintenance during the development of the central nervous system. In fact, *Sox2* conditional ablation in all the neural tube at E12.5 leads to a slightly reduced hippocampus and to the enlargement of the lateral ventricle at birth; the hippocampal defect worsens at postnatal day 7, when the dentate gyrus of the hippocampus is almost absent (Favaro et al., 2009). Interestingly, brain developmental defects are more dramatic when *Sox2* is ablated earlier in development. Indeed, *Sox2* deletion in the developing telencephalon at E9.5 leads to a compromised ventral telencephalon, microcephaly, under-developed eyes and death before birth (Ferri et al., 2013).

Sox2 is also required in the development and neurogenesis of the olfactory ephitelium (Panaliappan et al., 2018).

2.2 Sox2 function in eye development

In vertebrates, the eye is composed of a neurogenic and a non neurogenic region, that are the retina and epithelial tissue, respectively. They originate from a common pool of progenitors in the optic vesicle; in mice, at E10.5 the optic vesicle starts to invaginate giving rise to the optic cup, where the optic cup inner layer gives origin to the neural retina and the outer layer to the retinal pigment epithelium (Figure 7). The interface of these two domains is the peripheral optic cup margin that generates the ciliary body epithelium and the inner iris epithelium (Matsushima et al., 2011).

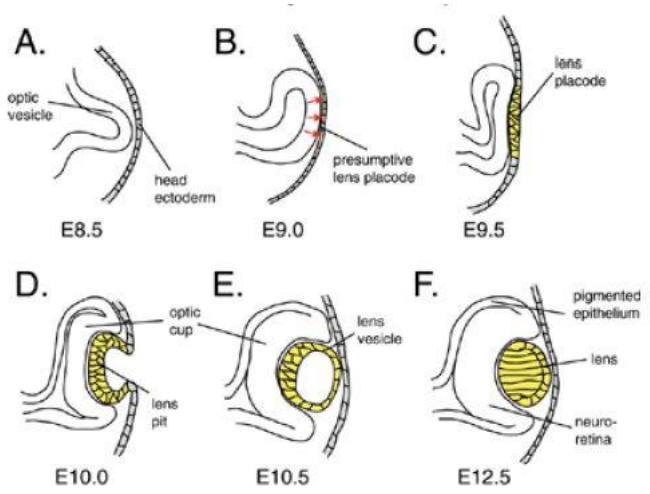

Figure 7. Representation of eye development in vertebrates. In mice, the optic vesicle forms at E8.5 and contacts the head ectoderm at E9. Lens placode formation occurs at E9.5 thanks to signals from the optic vesicle. At E10, the optic vesicle invaginates to create the optic cup. At E12.5, the optic cup inner layer forms the neuroretina and the outer layer comprising the retinal pigment epithelium (from Wawersik and Maas, 2000).

Sox2 is required for the proliferative and differentiation capacity of retinal progenitors, in fact its conditional ablation in the mouse retina leads to complete loss of the neural progenitor competence to properly divide and differentiate (Taranova et al., 2006).

Interestingly, the transcription factor Sox2 is co-expressed with Pax6 in the optic vesicle before optic cup formation. When the optic cup starts to form, Sox2 and Pax6 show opposite expression gradients, with high Sox2 expression in the central optic cup (that will give rise to the neural retina) and high Pax6 expression in the peripheral optic cup margin (that will give rise to the ciliary body epithelium). Conditional *Sox2* ablation in progenitors throughout the optic cup leads to the loss of neural

characteristics, in fact *Sox2* deleted cells lack the expression of neural retinal markers such as Hes5 and Notch1.

Moreover, a strong upregulation of Pax6 in central optic cup progenitors is observed, with a transition from neurogenic retina to non-neurogenic ciliary epithelium cell fate. Pax6 upregulation in *Sox2* mutant cells suggests that Sox2 antagonizes Pax6 in order to keep neural retina identity. The neuronal differentiation capacity is rescued when *Sox2* is ablated in mice carrying a spontaneous mutation in the Pax6 gene (the mutation gives rise to a truncated and functionally inactive Pax6 protein). Thus, the correct regionalization of the optic cup in the developing eye strongly depends on the balance of Sox2 and Pax6 dosage (Matsushima et al., 2011). Sox2 is also required in a differentiated cell type of the retina, the Müller glia, as discussed in the review in Chapter 6 "More than just stem cells: functional roles of the transcription factor Sox2 in differentiated glia and neurons" that I wrote with Dr. Sara Mercurio and Prof. Silvia Nicolis.

2.3 SOX2 and human disease

The requirement of the Sox2 transcription factor for the development of the eye and nervous system makes it a good candidate gene linked to eye and central nervous system defects in human. Indeed, heterozygous missense, non-sense and frameshift mutations have been identified in the *SOX2* human gene, and usually lead to *SOX2* loss-of-function (Fantes et al., 2003; Ragge et al., 2005; Schneider et al., 2009). Human patients carrying these mutations show severe eye developmental disorders represented by anophthalmia (absent eye), microphthalamia (small eye) and coloboma (failure of optic fissure closure), that often

affect both eyes. Different extra-ocular defects can be observed, such as brain malformations, seizure, motor defects, postnatal growth failure, cranio-facial dysmorphism, and male genital tract abnormalities (Ragge et al., 2005; Kelberman et al., 2006; Williamson and FitzPatrick, 2014). Some other defects include the hypothalamo-pituitary-gonadal system, such as pituitary hypoplasia, endocrine deficits and hypogonadism (Kelberman et al., 2006), and hippocampal malformations, that lead to learning disabilities, and epilepsy (Sisodya et al., 2006). Some defects of the *SOX2* human disease have been reproduced in mice by the Nicolis laboratory, therefore the mouse represents a good model for the study of the human disease.

3. The COUP-TF1 transcription factor

COUP-TF1 (Chicken Ovalbumin Upstream Promoter-Transcription Factor 1), also known as Nr2f1, and COUP-TF2 (Chicken Ovalbumin Upstream Promoter-Transcription Factor 2), also known as Nr2f2, belong to the superfamily of steroid/thyroid hormone receptors. They are also called orphan receptors, because their ligands are still unknown. COUP-TFs are characterized by two highly conserved motifs: a DNA-binding domain that contains two zinc fingers and a ligand-binding domain with two conserved regions. COUP-TFs form homodimers and bind AGGTCA motifs (Lin et al., 2011).

COUP-TFs are involved in several developmental processes, where they regulate cell fate determination, differentiation, cellular survival and migration.

3.1 COUP-TF1 functions in nervous system development

COUP-TF1 is a master regulator of cortical patterning and its graded expression in cortical progenitors is essential for the establishment of cortical area identity; it is highly expressed in cortical progenitors that give rise to cortical sensory areas (visual, auditory and somatosensory areas), while it is expressed at lower levels in cortical progenitors that will give rise to frontal-motor areas. The high expression of COUP-TF1 inhibits frontal/motor cortical area identity and promotes sensory areas identity. In fact, when *COUP-TF1* is conditionally ablated in cortical progenitors of the dorsal telencephalon, neocortical area patterning is dramatically compromised. Frontal areas, including motor areas, are strongly expanded and cover almost the entire emisphere, and consequently cortical sensory areas are shifted and mis-localized to the caudal part of the developing cortex. The cortical shift is also accompanied by a thalamo-cortical projections shift, highlighting COUP-TF1 role in the specification of positional information in the cortex (Armentano et al., 2007).

COUP-TF1 in cortical progenitors is also crucial for corticospinal motor neuron (CSMN) differentiation. Briefly, in the adult primary motor cortex, CSMNs project subcerebrally, including the spinal cord. In the developing cortex they are mainly localized in the motor cortex, where COUP-TF1 expression is low. When COUP-TF1 is ablated in cortical progenitors, CSMN undergo abnormal differentiation and the majority of them fails to project to the spinal cord. In addition, layer VI neurons of the S1 are partially re-specified to layer V pyramidal neurons, that are subcerebral projecting neurons, and form a "motorized" layer VI projecting to the spinal cord, and genuine layer V

pyramidal neurons are mis-specified. Indeed, the majority of their axons do not reach the spinal cord and accumulate in the brainstem region (Tomassy et al., 2010).

Interestingly, COUP-TF1 is not only expressed in progenitors, but also in differentiated cortical neurons, and its deletion in post-mitotic cortical neurons strongly affects the specification of cortical areas, similarly to what observed when *COUP-TF1* is deleted in cortical precursors. These defects are rescued when it is reintroduced in post-mitotic cortical neurons, showing that COUP-TF1 in post-mitotic neurons is necessary and sufficient to confer sensory cortical identity to new born cortical neurons (Alfano et al., 2014).

In addition to a role for COUP-TF1 in post-mitotic telencephalic neurons, it has been shown to play a crucial role also in post-mitotic neurons of the thalamus. Here, COUP-TF1 is expressed in specific nuclei of the dorsal thalamus, including the visual nucleus, dLGN. COUP-TF1 is essential for the correct development of these nucleus, in fact its conditional deletion specifically in the dLG, VP and MG thalamic nuclei, when thalamic neurons are already post-mitotic, strongly affects the dLGN, that is almost absent at (P7), but less the VPN and MGN (Chou et al., 2013).

Consequently, the projections that from the dLGN reach the visual cortex are absent and the visual cortical area is not correctly patterned at postnatal stages. These findings demonstrate that the identity of the visual area is not only defined by the graded expression of certain transcription factors in cortical progenitors, but also by the arrival of neuronal projections coming from the dLGN. These thalamo-cortical

afferents are essential to establish primary cortical area identity versus visual higher order area identity (Chou et al., 2013).

3.2 COUP-TF1 and human disease

In humans, *de novo* heterozygous missense mutations and deletions have been identified in the *COUP-TF1* gene (*NR2F1* in humans). These mutations are localized at the DNA-binding domain, or in ligand-binding domain. Some patients carrying mutations in the *NR2F1* gene show cerebral visual impairment (CVI), that is a defect in the projection and interpretation of visual inputs to the brain, and different grades of intellectual disabilities and optic nerve atrophy. These findings reveal a crucial role of COUP-TF1 in the correct neurodevelopment of the visual system (Bosch et al., 2014).

4. Mouse genetic models used in my thesis project

To study the role of the transcription factors Sox2 and COUP-TF1 in the development of the visual system, the objective of my thesis project, I used two lines of conditional knock-out mice: the $Sox2^{flox/flox}$; RORα-Cre (Mercurio et al., 2019) and the COUP-$TF1^{flox/flox}$; RORα-Cre (Chou et al., 2013), where *Sox2* and *COUP-TF1* genes are flanked by two loxP sites.

The expression of the Cre recombinase is placed under the control of the RORα gene promoter by knock-in to the 3' UTR of the *RORα* gene (Chou et al., 2013). The RORα-Cre knock-in is active in the dorsal thalamus (dTh) starting at E14.5 and can be detected at P0 and P7 in the principal sensory nuclei, including the dorsolateral geniculate nucleus

(dLGN), the ventroposterior nucleus (VPN) and the medial geniculate nucleus (MGN) (Chou et al., 2013).

Therefore, the RORα-Cre knock-in drives *Sox2* and *COUP-TF1* deletion in the RORα gene expression domain starting at E14.5 in the dorsal thalamus. Ablation occurs in post-mitotic neurons of the dorsal thalamus at E15.5 and later at E18.5-P0 and P8 is observed in neurons of the dLGN, VPN and MGN (Mercurio et al., 2019, Chou et al., 2013), while the expression of *Sox2* and *COUP-TF1* appears untouched in the cortex as shown in Figure 8.

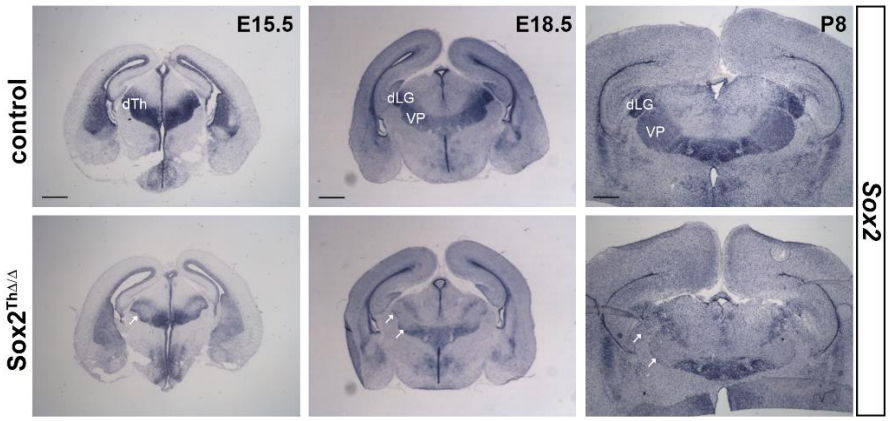

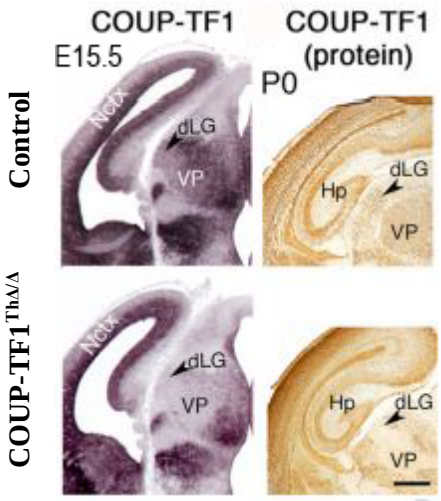

Figure 8. On top, Sox2 thalamic ablation mediated by the Rorα-Cre recombinase at E15.5, E18.5 and P8 (Mercurio et al., 2019). Below, COUP-TF1 thalamic ablation mediated by the Rorα-Cre recombinase at E15.5 and P0 (Chou et al., 2013).

AIM OF THE THESIS

The aim of my PhD thesis is to characterize the role of the Sox2 and COUP-TF1 transcription factors in the development of the visual system by dissecting the gene regulatory network controlled by the two factors, using the mouse as a model system. Heterozygous mutations in the *SOX2* and *COUP-TF1* genes in human patients are linked to a spectrum of nervous system defects, including visual defects, as reported in the General Introduction. Interestingly, Sox2 and COUP-TF1 are expressed in all the three components of the visual system in mice: the eye, the thalamic dLGN (visual thalamus) and the cortex.

Sox2 role in eye development is well characterized (Taranova et al., 2006; Matsushima et al., 2011), but nothing is known about its role in the visual thalamus. Regarding COUP-TF1, it has been recently shown that it is required for the correct development of the visual thalamus and, consequently, for proper visual cortical patterning; indeed, when *COUP-TF1* is conditionally ablated in neurons of the dLGN, the dLGN itself is highly reduced in size and the primary visual area is not defined from surrounding cortical areas (Chou et al., 2013).

Studying how Sox2 and COUP-TF1 orchestrate the development of the visual system in mice is a useful strategy to understand human diseases of vision.

Therefore, during my PhD, I first aimed to study Sox2 role in the visual thalamus and how its expression in the thalamus is important in regulating the development of the visual axis, by using *Sox2* thalamic conditional knock-out mice. We found that *Sox2* deletion in differentiated thalamic neurons, mediated by the same deleter used by Chou et al., 2013 to ablate *COUP-TF1* in differentiated thalamic neurons of the dLGN, affects the development of the visual axis, to an extent similar to what previously described for *COUP-TF1* thalamic mutant mice (Chou et al., 2013).

Consequently, my second aim was to identify genes whose deregulation in the dLGN could mediate Sox2 function in the visual thalamus, and that therefore could explain the defects we observed in mutant mice. We first adopted a candidate gene approach and subsequently a genome-wide approach (RNA-sequencing).

Interestingly, I observed that SOX2 and COUP-TF1 are largely co-localized in the same neurons of the dLGN. Therefore, considering their co-localization in the visual thalamus and the similarities of the visual developmental defects observed in *Sox2* and *COUP-TF1* single thalamic mutants, I started to investigate the relationship of Sox2 and COUP-TF1 in these thalamic neurons, in order to understand whether these two transcription factors are involved in the same genetic pathway.

We are currently performing an RNA sequencing also on *COUP-TF1* mutant dLGNs. In this way we will combine the deregulated genes in *Sox2* mutants and in *COUP-TF1* mutants to identify potential common de-regulated genes. To understand the relationship between the two transcription factors, we generated *Sox2* and *COUP-TF1* double mutant

mice that I am currently analyzing. During my PhD I also spent a research period in the laboratory of my thesis co-director Dr. Michèle Studer in Nice, where I characterized the thalamus in *COUP-TF1* constitutive knock-out, a mouse model in which COUP-TF1 is lacking from the beginning of the development.

Chapter 2 (published paper) includes the description of the unexpected and completely new function of Sox2 in post-mitotic thalamic neurons of the dLGN.
Chapter 3 (ongoing work) includes the description of the search for genes regulated by Sox2 and COUP-TF1 in the dLGN to understand their relationship in the visual thalamus.
Chapter 4 (published paper) includes the description of the function of COUP-TF1 in the eye. *COUP-TF1* constitutive knock-out recapitulates COUP-TF1 human patients defects, therefore it represents an important and unique mouse model for human disease.
Chapter 5 includes the general discussion of the results obtained in my research project and future perspectives.
Chapter 6 (published review) includes an additional discussion about the importance of Sox2 in differentiated neurons and glia.

References

Alfano, C., Magrinelli, E., Harb, K., Hevner, R.F., Studer, M., 2014. Postmitotic control of sensory area specification during neocortical development. Nat Commun 5, 5632.

Alfano, C., Studer, M., 2013. Neocortical arealization: evolution, mechanisms, and open questions. Dev Neurobiol 73(6), 411-447

Armentano, M., Chou, S.-J., Srubek Tomassy, G., Leingärtner, A., O'Leary, D.D.M., Studer, M., 2007. COUP-TFI regulates the balance of cortical patterning between frontal/motor and sensory areas. Nature Neuroscience 10, 1277

Avilion, A.A., Nicolis, S.K., Pevny, L.H., Perez, L., Vivian, N., Lovell-Badge, R., 2003. Multipotent cell lineages in early mouse development depend on SOX2 function. Genes Dev 17(1), 126-140.

Bibollet-Bahena, O., Okafuji, T., Hokamp, K., Tear, G., Mitchell, KJ., 2017. A dual-strategy expression screen for candidate connectivity labels in the developing thalamus. PLoS One 12(5):e0177977.

Bosch, DG., Boonstra, FN., Gonzaga-Jauregui, C., Xu, M., de Ligt, J., Jhangiani,S., Wiszniewski, W., Muzny, DM., Yntema, HG., Pfundt, R., Vissers, LE., Spruijt, L., Blokland, EA., Chen, CA., Baylor-Hopkins Center for Mendelian Genomics, Lewis, RA., Tsai, SY., Gibbs, RA., Tsai, MJ., Lupski, JR., Zoghbi, HY., Cremers, FP., de Vries, BB., Schaaf, CP., 2014. NR2F1 mutations cause optic atrophy with intellectual disability. Am J Hum Genet. 94(2):303-9.

Braisted, J.E., Catalano, S.M., Stimac, R., Kennedy, T.E., Tessier-Lavigne, M., Shatz, C.J., O'Leary, D.D., 2000. Netrin-1 promotes thalamic axon growth and is required for proper development of the thalamocortical projection. J Neurosci 20(15), 5792-5801.

Cheng, AH., Bouchard-Cannon, P., Hegazi, S., Lowden, C., Fung, SW., Chiang, CK., Ness, RW., Cheng, HM., 2019. SOX2-Dependent Transcription in Clock Neurons Promotes the Robustness of the Central Circadian Pacemaker. Cell Rep. 26(12):3191-3202.

Chou, S.J., Babot, Z., Leingartner, A., Studer, M., Nakagawa, Y., O'Leary, D.D., 2013. Geniculocortical input drives genetic distinctions between primary and higher-order visual areas. Science 340(6137), 1239-1242.

Diao, Y., Chen, Y., Zhang, P., Cui, L., Zhang, J., 2018. Molecular guidance cues in the development of visual pathway. Protein Cell 9(11), 909-929.

Dufour, A., Seibt, J., Passante, L., Depaepe, V., Ciossek, T., Frisén, J., Kullander, K., Flanagan, JG., Polleux, F., Vanderhaeghen, P., 2003. Area specificity and topography of thalamocortical projections are controlled by ephrin/Eph genes. Neuron 39(3), 453-65.

Fantes, J., Ragge, NK., Lynch, SA., McGill, NI., Collin, JR., Howard-Peebles, PN., Hayward, C., Vivian, AJ., Williamson, K., van Heyningen, V., FitzPatrick, DR., 2003. Mutations in SOX2 cause anophthalmia. Nat Genet. 33(4):461-3.

Favaro, R., Valotta, M., Ferri, A.L., Latorre, E., Mariani, J., Giachino, C., Lancini, C., Tosetti, V., Ottolenghi, S., Taylor, V., Nicolis, S.K., 2009. Hippocampal development and neural stem cell maintenance require Sox2-dependent regulation of Shh. Nat Neurosci 12(10), 1248-1256.

Ferri, A., Favaro, R., Beccari, L., Bertolini, J., Mercurio, S., Nieto-Lopez, F., Verzeroli, C., La Regina, F., De Pietri Tonelli, D., Ottolenghi, S., Bovolenta, P., Nicolis, S.K., 2013. Sox2 is required for embryonic development of the

ventral telencephalon through the activation of the ventral determinants Nkx2.1 and Shh. Development 140(6), 1250-1261.

Ferri AL, Cavallaro M, Braida D, Di Cristofano A, Canta A, Vezzani A, Ottolenghi S, Pandolfi PP, Sala M, De Biasi S, Nicolis SK. 2004. Sox2 deficiency causes neurodegeneration and impaired neurogenesis in the adult mouse brain. Development 131: 3805-19.

Gezelius, H., Lopez-Bendito, G., 2017. Thalamic neuronal specification and early circuit formation. Dev Neurobiol, 77, 830-843

Guido W., 2018. Development, form, and function of the mouse visual thalamus. J Neurophysiol. 120(1): 211-25.

Herrera, E., Brown, L., Aruga, J., Rachel, RA., Dolen, G., Mikoshiba, K., Brown, S., Mason, CA., 2003. Zic2 patterns binocular vision by specifying the uncrossed retinal projection. Cell 114(5): 545-57.

Horng, S., Kreiman, G., Ellsworth, C., Page, D., Blank, M., Millen, K., Sur, M., 2009. Differential gene expression in the developing lateral geniculate nucleus and medial geniculate nucleus reveals novel roles for Zic4 and Foxp2 in visual and auditory pathway development. J Neurosci 29(43), 13672-13683.

Kamachi, Y., Uchikawa, M., Kondoh, H., 2000. Pairing SOX off: with partners in the regulation of embryonic development. Trends Genet 16(4), 182-187.

Kelberman, D., Rizzoti, K., Avilion, A., Bitner-Glindzicz, M., Cianfarani, S., Collins, J., Chong, W.K., Kirk, J.M., Achermann, J.C., Ross, R., Carmignac,

D., Lovell-Badge, R., Robinson, I.C., Dattani, M.T., 2006. Mutations within Sox2/SOX2 are associated with abnormalities in the hypothalamo-pituitary-gonadal axis in mice and humans. J Clin Invest 116(9), 2442-2455.

Kerschensteiner, D., Guido, W., 2017. Organization of the dorsal lateral geniculate nucleus in the mouse. Vis Neurosci. 34:E008. doi: 10.1017/S0952523817000062.

Leamey, CA., Merlin, S., Lattouf, P., Sawatari, A., Zhou, X., Demel, N., Glendining, KA., Oohashi, T., Sur, M., Fässler, R., 2007. Ten_m3 regulates eye-specific patterning in the mammalian visual pathway and is required for binocular vision. PLoS Biol. 2007 Sep;5(9):e241.

Lebrand, C., Cases, O., Adelbrecht, C., Doye, A., Alvarez, C., El Mestikawy, S., Seif, I., Gaspar, P., 1996. Transient Uptake and Storage of Serotonin in Developing Thalamic Neurons. Neuron 17(5), 823-835.

Li, K., Zhang, J., Li, J.Y., 2012. Gbx2 plays an essential but transient role in the formation of thalamic nuclei. PLoS One 7(10), e47111.

Lin, FJ., Qin, J., Tang, K., Tsai, SY., Tsai, MJ., 2011. Coup d'Etat: an orphan takes control. Endocr Rev. 32(3): 404-21.

López-Bendito, G., Molnár, Z., 2003. Thalamocortical development: how are we going to get there? Nature Reviews Neuroscience 4(4), 276-89.

Mann, F., Peuckert, C., Dehner, F., Zhou, R., Bolz, J., 2002. Ephrins regulate the formation of terminal axonal arbors during the development of thalamocortical projections. Development 129(16), 3945-55.

Matsushima, D., Heavner, W., Pevny, L.H., 2011. Combinatorial regulation of optic cup progenitor cell fate by SOX2 and PAX6. Development 138(3), 443-454.

Mercurio, S., Serra, L., Motta, A., Gesuita, L., Sanchez-Arrones, L., Inverardi, F., Foglio, B., Barone, C., Kaimakis, P., Martynoga, B., Ottolenghi, S., Studer, M., Guillemot, F., Frassoni, C., Bovolenta, P., Nicolis, SK., 2019. Sox2 Acts in Thalamic Neurons to Control the Development of Retina-Thalamus-Cortex Connectivity. iScience 15:257-273.

Muzerelle, A., Scotto-Lomassese, S., Bernard, J.F., Soiza-Reilly, M., Gaspar, P., 2016. Conditional anterograde tracing reveals distinct targeting of individual serotonin cell groups (B5–B9) to the forebrain and brainstem. Brain Structure and Function 221(1), 535-561.

O'Leary, D.D., Nakagawa, Y., 2002. Patterning centers, regulatory genes and extrinsic mechanisms controlling arealization of the neocortex. Curr Opin Neurobiol 12(1), 14-25.

O'Leary, DD., Sahara, S., 2008. Genetic regulation of arealization of the neocortex. Curr Opin Neurobiol 18(1):90-100

Panaliappan, TK., Wittmann, W., Jidigam, VK., Mercurio, S., Bertolini, JA., Sghari, S., Bose, R., Patthey, C., Nicolis, SK., Gunhaga, L., 2018. Sox2 is required for olfactory pit formation and olfactory neurogenesis through BMP restriction and Hes5 upregulation. Development 145(2) doi: 10.1242/dev.153791.

Pfeiffenberger, C., Cutforth, T., Woods, G., Yamada, J., Rentería, R.C., Copenhagen, D.R., Flanagan, J.G., Feldheim, D.A., 2005. Ephrin-As and

neural activity are required for eye-specific patterning during retinogeniculate mapping. Nature Neuroscience 8(8), 1022-27.

Ragge, N.K., Lorenz, B., Schneider, A., Bushby, K., de Sanctis, L., de Sanctis, U., Salt, A., Collin, J.R., Vivian, A.J., Free, S.L., Thompson, P., Williamson, K.A., Sisodiya, S.M., van Heyningen, V., Fitzpatrick, D.R., 2005. SOX2 anophthalmia syndrome. Am J Med Genet A 135(1), 1-7; discussion 8.

Seabrook, T.A., Burbridge, T.J., Crair, M.C., Huberman, A.D., 2017. Architecture, Function, and Assembly of the Mouse Visual System. Annu Rev Neurosci 40(1), 499-538.

Schneider, A., Bardakjian, T., Reis, LM., Tyler, RC., Semina, EV., 2009. Novel SOX2 mutations and genotype-phenotype correlation in anophthalmia and microphthalmia. Am J Med Genet A. 149A(12):2706-15.

Sherman, SM., 2007. The thalamus is more than just a relay. Curr Opin Neurobiol. 2007 17(4):417-22.

Sisodiya, S.M., Ragge, N.K., Cavalleri, G.L., Hever, A., Lorenz, B., Schneider, A., Williamson, K.A., Stevens, J.M., Free, S.L., Thompson, P.J., van Heyningen, V., Fitzpatrick, D.R., 2006. Role of SOX2 mutations in human hippocampal malformations and epilepsy. Epilepsia 47(3), 534-542.

Taranova, O.V., Magness, S.T., Fagan, B.M., Wu, Y., Surzenko, N., Hutton, S.R., Pevny, L.H., 2006. SOX2 is a dose-dependent regulator of retinal neural progenitor competence. Genes Dev 20(9), 1187-1202.

Tomassy, G.S., De Leonibus, E., Jabaudon, D., Lodato, S., Alfano, C., Mele, A., Macklis, J.D., Studer, M., 2010. Area-specific temporal control of

corticospinal motor neuron differentiation by COUP-TFI. Proc Natl Acad Sci U S A 107(8), 3576-3581.

Upton, AL., Salichon, N., Lebrand, C., Ravary, A., Blakely, R., Seif, I., Gaspar, P., 1999. Excess of serotonin (5-HT) alters the segregation of ispilateral and contralateral retinal projections in monoamine oxidase A knock-out mice: possible role of 5-HT uptake in retinal ganglion cells during development. J Neurosci. 19(16): 7007-24.

van Kleef, E.S., Gaspar, P., Bonnin, A., 2012. Insights into the complex influence of 5-HT signaling on thalamocortical axonal system development. Eur J Neurosci 35(10), 1563-1572.

Wawersik S1, Maas RL., 2000. Vertebrate eye development as modelled in *Drosophila*. Hum Mol Genet. 9(6):917-25.

Williams, SE., Mann, F., Erskine, L., Sakurai, T., Wei, S., Rossi, DJ., Gale, NW., Holt, CE., Mason, CA., Henkemeyer, M., 2003. Ephrin-B2 and EphB1 mediate retinal axon divergence at the optic chiasm. Neuron 39(6), 919-35.

Williamson, KA., FitzPatrick, DR., 2014. The genetic architecture of microphthalmia, anophthalmia and coloboma. Eur J Med Genet. 57(8):369-80.

One of the interests of the laboratory of Prof. Silvia Nicolis is the study of the role of Sox2 in the development of the visual axis in mouse. Precisely, the focus is on the role played by Sox2 in an important cerebral structure of the visual system, the visual thalamus. To perform this study the laboratory uses a mouse model of *Sox2* conditional knock-out, in which the *Sox2* gene is specifically deleted in post-mitotic projection neurons of the visual thalamus during embryonic development.

Shortly before my arrival in the Nicolis laboratory, the phenotypic analysis of *Sox2* thalamic mutants had revealed defects in the size of the visual thalamus and the patterning of the visual cortex in these mutants, but the mechanisms underlying these developmental defects were mostly unknown. Therefore, during my PhD I characterized and analysed the neuronal projections between the eye, the visual thalamus and the visual cortex in control and *Sox2* thalamic mutant mice by using different *in vivo* and *ex vivo* techniques. I found that the whole visual axis is compromised after *Sox2* conditional ablation in the thalamus. Subsequently, to identify potential target genes that could mediate Sox2 function in the visual thalamus and in the development of its connections with the eye and the visual cortex, I analysed, by in situ hybridization on mouse brain sections, the expression of genes known to be important for the correct development of the visual axis. Interestingly, I found some genes whose expression in the visual thalamus is downregulated following *Sox2* conditional deletion and that could, at least in part, explain the observed developmental defects. The novel function of Sox2 in post-mitotic neurons of the dLGN and the

analyses of the defects associated to its deletion in the thalamus are presented in Chapter 2.

CHAPTER 2

Sox2 acts in thalamic neurons to control the development of retina-thalamus-cortex connectivity

Sara Mercurio[1], Linda Serra[1,5], Alessia Motta[1], Lorenzo Gesuita[1], Luisa Sanchez-Arrones[3], Francesca Inverardi[2], Benedetta Foglio[2], Cristiana Barone[1], Polynikis Kaimakis[3], Ben Martynoga[4], Sergio Ottolenghi[1], Michèle Studer[5], Francois Guillemot[4], Carolina Frassoni[2], Paola Bovolenta[3] and Silvia K. Nicolis[1*]

[1]Department of Biotechnology and Biosciences, University of Milano-Bicocca, piazza della Scienza 2, 20126 Milano, Italy

[2]Clinical and Experimental Epileptology Unit, Fondazione I.R.C.C.S. Istituto Neurologico "Carlo Besta", c/o AMADEOLAB, via Amadeo 42, 20133 Milano, Italy

[3]Centro de Biología Molecular Severo Ochoa, Consejo Superior de Investigaciones Científicas – Universidad Autónoma de Madrid and CIBER de Enfermedades Raras (CIBERER), ISCIII Madrid Spain

[4]The Francis Crick Institute, Midland Road, London NW 1AT, UK

[5]Université Côte d'Azur, CNRS, Inserm, iBV, Nice, France

Published on iScience, 2019 15:257-273.

Summary

Visual system development involves the formation of neuronal projections connecting the retina to the thalamic dorsolateral-geniculate nucleus (dLGN), and the thalamus to the visual cerebral cortex. Patients carrying mutations in the *SOX2* transcription factor gene present severe visual defects, thought to be linked to SOX2 functions in the retina. We show that Sox2 is strongly expressed in mouse postmitotic thalamic projection neurons. Cre-mediated deletion of Sox2 in these neurons causes reduction of the dLGN, abnormal distribution of retino-thalamic and thalamo-cortical projections and secondary defects in cortical patterning. Reduced expression, in mutants, of Sox2 target genes encoding ephrin-A5 and the serotonin-transport molecules SERT and vMAT2 (important for establishment of thalamic connectivity) likely provides a molecular contribution to these defects. These findings unveil thalamic SOX2 function as a novel regulator of visual system development and a plausible additional cause of brain-linked genetic blindness in humans.

Introduction

The development of specific neuron-to-neuron connections is central to the formation and function of the nervous system. In the mammalian visual system, the retina sends visual information to the thalamic dorso-lateral geniculate nucleus (dLGN); the dLGN neurons in turn connect to the visual cerebral cortex, that elaborates visual information. In development, retinal axons, forming the optic nerve, outgrow towards the dLGN, and then generate connections with a precise spatial distribution, linking retinal projections from each specific eye to

specific dLGN subregions, in response to region-specific signals produced by the dLGN. In turn, dLGN neurons develop precise connections to the visual cerebral cortex (Garel and Lopez-Bendito, 2014, Gezelius and Lopez-Bendito, 2017). The gene regulatory networks active in dLGN neurons, specifying their connectivity programs, are still poorly understood, and are being investigated (Gezelius and Lopez-Bendito, 2017, Horng et al., 2009).

In humans, mutations in the gene encoding the Sox2 transcription factor cause severe visual disease (Fantes et al., 2003, Williamson and FitzPatrick, 2014). Conditional eye-specific knockout (KO) in mice showed that, in the visual system, Sox2 plays important functions in retinal and lens progenitor cells development (Pevny and Nicolis, 2010, Taranova et al., 2006, Smith et al., 2009, Kamachi et al., 2001). However, roles for Sox2 in other components of the visual system, in particular the dLGN, are still unexplored. So far, Sox2 function has been prominently demonstrated in stem cells (embryonic, neural) (Arnold et al., 2011, Avilion et al., 2003, Favaro et al., 2009, Pevny and Nicolis, 2010, Bertolini et al., 2019); instead, neuronal differentiation implies Sox2 extinction, with rare exceptions (Graham et al., 2003, Lee et al., 2014).

Here, we report that SOX2 is highly expressed in postmitotic, fully differentiated projection neurons of the dLGN. We find that its thalamic-specific ablation in these neurons impairs the development of dLGN, in particular its connectivity with the retina and the visual cortex, and we identify specific SOX2 downstream target genes which likely contribute to these defects.

Results

Sox2 is expressed in thalamic projection neurons

We first investigated Sox2 expression in the thalamus by *in situ* hybridization (ISH) and immunofluorescence (IF) (Fig. 1). ISH detects high Sox2 expression in the dorsal thalamus at perinatal stages (E17.5), and in the sensory thalamic nuclei, including the dLGN, at postnatal stages (P8), (Fig. 1A). At these late stages, thalamic cells consist of differentiated neurons and glia (Gezelius and Lopez-Bendito, 2017). Indeed, IF on the postnatal dLGN shows that the vast majority of cells positive for NEUN (a general marker of differentiated neurons) are strongly positive for SOX2 (Fig. 1B,D). A proportion of glial cells (about 50%), marked by S100ß, are also weakly SOX2-positive (Fig. 1C,D). Overall, most (89%) SOX2-positive dLGN cells are represented by neurons (Fig. 1E). On the other hand, interneurons, marked by GAD-67, are SOX2-negative (Fig. S1A), indicating that, within neurons, SOX2 activity is mainly restricted to glutamatergic (projection) neurons. The majority of oligodendrocytes, marked by OLIG2, are SOX2-negative with some minor exceptions (Fig. S1B).

Sox2 deletion in the developing thalamus leads to reduced dLGN size and reduced retinal afferents to the dLGN

To delete Sox2 in the thalamus, we used a $Sox2^{flox}$ allele that we had previously generated (Favaro et al., 2009), in combination with a RORα-Cre transgene, active from embryonic day (E) 14.5, when thalamic neurons are already postmitotic (Chou et al., 2013). Sox2 efficient ablation was observed by ISH, already at E15.5 in the dorsal thalamus (Fig. 1F,F'), and, subsequently (E18.5, P8; Fig. 1G-H'), in the

dLGN, and in the adjacent somatosensory thalamic nucleus (ventro-posterior nucleus, VPN) (Chou et al, 2013). Sox2 thalamic mutants are termed $Sox2^{Th\Delta/\Delta}$ hereafter. IF shows that SOX2 is efficiently ablated from neurons, though it persists in at least some glia (Fig. S1C,D).

To determine if Sox2 thalamic ablation results in defects in normal development of thalamic nuclei, in particular of the visual thalamic nucleus (dLGN), we analysed by ISH the expression of the transcription factor Lef1, present in the dLGN but almost absent in the adjacent vLGN (Fig. 2A-D'). At the end of gestation (E18.5), the mutant dLGN did not overtly differ in size from that of controls (Fig. 2A,A'); however, in postnatal development, the mutant dLGN failed to increase in size, contrary to controls, as seen by Lef1 ISH (Fig. 2B-D') and Nissl staining (Fig. 2E,E').

In normal development of visual system connectivity, retinal axons outgrow towards the dLGN, and establish neuron-to-neuron connections with the cell bodies of dLGN neurons. The dLGN provides molecular signals that guide and precisely pattern the outgrowth of incoming retinal axon terminals to form appropriately localized connections to the dLGN during the perinatal and early postnatal period; retinal afferents are, in turn, the source of important trophic signals, that allow the dLGN to complete its development and growth in early postnatal life (El-Danaf et al, 2015; Guido, 2018). Immunofluorescence with antibodies against the vesicular glutamate transporter 2 (vGLUT2) detects glutamatergic neuronal afferents from the retina, ensheathing and defining the dLGN. vGLUT2 IF showed an overall reduced area of the dLGN signal in the mutant at postnatal stages, confirming a reduced size (Fig. 2F,F'), a result that is also

observed at P16 and in adults (Fig. S2A-B'). Interestingly, the area covered by the incoming vGLUT2-positive fibers reaching the vLGN appeared slightly expanded (Fig. 2F; Fig. S2A-B'). In addition, in both P16 and adult mutants, the signal was less uniformly distributed than in controls, and more concentrated on the dorsal side of the dLGN (Fig. S2A-B').

A postnatally reduced size of the mutant dLGN (but not vLGN) was further confirmed by area measurements on DAPI-stained sections, in which retinal afferents had been stained with cholera toxin (Fig. S2C-E; cholera toxin labelling will be described in Fig. 3).

In the mutant dLGN (P8), the frequency of neurons (NEUN-positive cells) was reduced (by 18%), whereas that of glia (S100β-positive) was not significantly altered (Fig. 2G-L).

Taken together, these results highlight that the mutant dLGN does not grow, postnatally, contrary to the control dLGN, and that, concomitantly, a reduction of retinal afferents reaching the mutant dLGN is observed.

Retino-thalamic projections are abnormally distributed in Sox2 thalamic mutants

In normal development, nasal-temporal retinal projections from each eye cross on the brain midline (optic chiasm) to reach a specific region of the contralateral dLGN, whereas a minority of the fibers from the ventro-temporal crescent of the retina do not cross, and project onto the ipsilateral dLGN. dLGN regions receiving the contra- or ipsilateral fibres have well-defined, complementary, mutually exclusive shapes, that can be visualized by separately marking the retinal fibers

originating from the right and left eye with cholera toxin subunit B (CTB) labelled with different fluorochromes (Fig. 3; see drawing in Fig. 3K). We labelled retinal afferents at three time points (P0, P7, P21), defining successive steps of afferents arrival to the dLGN, and segregation within it, and analysed the projections to the thalamus one to three days later (P1, P9 and P24, Fig. 3A-H''). In mutants, retinal afferents to the dLGN are reduced already at the earliest time point (P1, Fig. 3A,B), particularly in the medial dLGN region (arrows). Of note, the size of the dLGN is still comparable in mutants and control at this early stage. At later stages (P9, P24), in controls, contra (green)- and ipsilateral (red) afferents complete their segregation to different regions of the dLGN, as expected (Fig. 3C,E). In mutants, segregation occurs, but the pattern of ipsi- and contra-lateral afferent fibers appears abnormal: ipsilateral (red) fibers show a different distribution (compare the mutants in Fig. 3D, and particularly 3G,H, versus controls in Fig. 3C and 3E,F, respectively); contralateral (green) fibers also look abnormal, with a somewhat fragmented, "clumpy" fibers distribution, in particular the most anterior (left) sections (Fig. 3D compared to C, Fig. 3G compared to E; arrowheads in D and G point to "clumps", i.e. local dishomogeneities, in mutant). In addition, at both early (P1) and later (P9, P24) stages, in mutants, the fraction of retinal afferents reaching the vLGN (measured as the green area in the vLGN) is proportionally higher than that reaching the dLGN as compared to controls, suggesting afferents misrouting (Fig. 3D versus C, and G,H versus E,F; see I,J for quantifications). Finally, in mutants, an abnormally increased fraction of contralateral fibers was also apparent in the intermediate lateral geniculate nucleus (iLGN) (Fig. 3 G versus

E), and, within the vLGN, some overlap between contra- and ipsi-lateral projections was visible, possibly as a result of the excess fibers projecting to the vLGN in mutants (see above; Fig 3G compared to E). We also traced the retinal axons reaching the dLGN through DiI labelling in early postnatal life (at P0, and P5) (Fig. S2F-G'). In thalamic Sox2 mutants, an overall reduction of retinal afferents reaching the dLGN is seen already at P0, and, more markedly, at P5 (Fig. S2F-G'), matching the abnormality observed in the mutant by cholera toxin labelling.

Of note, the thalamic defects did not result in gross alterations of the adult retina or in changes of the number and distribution of the retinal ganglion cells (RGC; Fig. S2H-I), indicating that, in spite of abnormal targeting, RGC viability is preserved.

Overall, these data indicate a role for Sox2 within dLGN cells, in the generation of appropriate connections of retinal afferents to the thalamus, suggesting a possible role for Sox2 in regulating guidance cues in the thalamus.

Thalamo-cortical connections and normal postnatal patterning of the cerebral cortex are perturbed in Sox2 thalamic mutants

To directly investigate thalamo-cortical connections in mutants, we performed immunohistochemistry (on cortical flat-mounts, scheme in Fig. 4A, and telencephalon coronal sections) with antibodies against vGLUT2 (Fig. 4B,D), the serotonin transporter (SERT) (Fig. 4C,E), and serotonin (5-hydroxytryptamine, 5-HT) (Fig. 4F), all marking the developing thalamo-cortical axons (TCA) in the young postnatal brain (Chou et al., 2013, Lebrand et al., 1996). With all three antibodies, a

reduction of the staining was observed in the visual cortex (V1) in $Sox2^{Th\Delta/\Delta}$ mutants (Fig. 4B'-F', compared to B-F), indicating that TCA originating from mutant dLGN are strongly abnormal.

The correct development of TCA, projecting from the dLGN to the visual cortex, is essential for the development of the cortical visual areas, in particular for the diversification of the primary visual area (V1) and the adjacent higher-order visual areas (V^{HO}) (Chou et al, 2013). In the normal postnatal brain (P7), the *Lmo4* gene is expressed in V^{HO}, but not in the adjacent V1, with a clear boundary between positive and negative regions; in the mutant, however, this boundary is not well defined, and expression in V1 is more pronounced and more similar to that in V^{HO} (Fig. 4G,G'). We also obtained similar results with two different markers, *Bhlhb5*, normally expressed in the V1, but less so in the V_{H0} area (Fig. 4H,H') and *Rorβ* (not shown). The observed cortical defect is reminiscent of alterations previously found in Nr2f1 (COUP-TF1) thalamic mutants obtained by RORα-Cre -mediated deletion of the *Nr2f1* gene, encoding a transcription factor important for dLGN neurons development. In these mutants, the cortical defects are thought to be secondary to defective TCA connections of the dLGN to the visual cortex (Chou et al., 2013).

Overall, the detection of a cortical patterning defect in our thalamic mutant, together with the abnormalities of the incoming thalamic connections (as indicated by the reduced vGLUT2 staining), indicates a defect in the development of TCA, affecting their ability to correctly pattern the postnatal cortex.

The thalamus is also the target of cortico-thalamic axon afferents (CTA) (Garel and Lopez-Bendito, 2014). We injected DiI (red) and DiA

(green) in the visual and somatosensory cortex, respectively (scheme in Fig. 4I"); these compounds diffuse along the neuronal membranes, allowing visualization of neuronal projections. Labelling of visual cortex with DiI showed that development of CTA to the dLGN was compromised in $Sox2^{Th\Delta/\Delta}$ mutants, while the connections between the somatosensory cortex and the VP nucleus were comparatively less affected (Fig. 4I-I'').

Overall, our observations show that Sox2 ablation affects TCA development, and, secondarily, cortical patterning, and CTA development.

Specific genes important for dLGN development are downregulated in the mutant dLGN

To identify Sox2 target genes whose deregulation in Sox2 mutants might be responsible for the observed defects of connectivity, we studied the expression of candidate genes known to play key roles in dLGN development, by ISH and immunohistochemistry (Fig. 5; Fig. S3). In the dLGN, (and VP), Sox2 was co-expressed with Nr2f1 (data not shown); however, no important reduction was detected, in mutants, in the expression of *Nr2f1* by ISH (Fig. 5B,B') or immunohistochemistry (at E18.5 and P8, not shown). Also, no change was found in the expression of other genes normally active, and important, in/for the dLGN, tested at E18.5 and/or at E15.5: *Zic4* (Horng et al., 2009), *NtnG1*, *Sema6A* (Gezelius and Lopez-Bendito, 2017, Little et al., 2009), *Gbx2* (Miyashita-Lin et al., 1999, Sur and Rubenstein, 2005), *Sox11*, *Klf6*, *Zic1*, *Ntn1* (Braisted et al., 2000) (Fig.

5C-E'; Fig. S3B-D',F-H'). This indicates that a "general" dLGN gene expression program was retained in mutant dLGN.

However, in the mutant dLGN we observed a strong reduction in the expression of *ephrin-A5* (encoded by the *Efna5* gene) by ISH E18.5, i.e. prior to the visible patterning defect, and postnatally (P7) (Fig. 5F-H"). Of note, some reduction was consistently observed also in heterozygotes (Fig. 5G', H', compared to G,H).

Ephrin-A5 is a signaling molecule involved in axon guidance in the developing brain (Kania and Klein, 2016), and is expressed, in the normal dLGN, in a gradient. Germline knockout studies showed that, in the absence of Efna5, 2 and 3, the establishment of the correct pattern of contra- and ipsilateral retina-dLGN projections is severely disrupted (Huberman et al., 2005, Pfeiffenberger et al., 2005, Vanderhaeghen et al., 2000); these previous results suggest that Efna5 downregulation in Sox2 mutants may significantly contribute to the observed defective patterning of retinal afferents. Interestingly, SOX2 ChIPseq detects two SOX2-bound regions in the *Efna5* gene in neural stem/progenitor cells, located in the first intron (Fig. 5I). We cloned each of the two DNA regions encompassing the SOX2 peaks upstream of a minimal promoter and a luciferase reporter gene (Fig. 5J), and co-transfected the constructs with increasing amounts of a SOX2 expression vector (Ferri et al., 2013, Mariani et al., 2012, Panaliappan et al., 2018) into neural (Neuro-2a) cells (Fig. 5K). The most upstream peak (5' peak) did not show any response over the SOX2 amounts tested; the 3' peak, however, showed a strong dose-dependent transactivation of the luciferase reporter, to an extent similar to that previously observed with the promoter of the Nkx2.1 gene, a previously identified SOX2 target

(Ferri et al., 2013) (Fig. 5K). These observations indicate the presence of a SOX2-responsive regulatory region (putative enhancer) within the Efna5 gene.

Further to Efna5 downregulation, we had observed a reduction of serotonin (5-HT), and its transporter SERT in thalamo-cortical axons at P8 (see above, Fig. 4). As serotonin levels in the first two postnatal weeks have been shown to have a role in regulating thalamo-cortical projections (see below), we investigated in more detail the levels of serotonin, and of components of its pathway, during development, following Sox2 thalamic loss.

5-HT marks the TCA during the time window when they first establish their patterned connections with cortical neurons. 5-HT is not synthesized by thalamic neurons, but transiently uptaken by TCA via the serotonin transporter SERT (Lebrand et al., 1996); pharmacological manipulation of 5-HT uptake, or knock-out of the SERT-encoding gene, perturbs sensory TCA development, particularly to the somatosensory cortex, indicating a developmental function for this transient 5-HT uptake (Chen et al., 2015, Gaspar et al., 2003, Persico et al., 2001). This raised the possibility that an early reduction in 5-HT content within thalamic neurons might, as well, contribute to the observed dLGN TCA development defect in Sox2 mutants. Indeed, we observed a reduction of 5-HT levels in cell bodies and axons in the mutant dLGN (more pronounced in homozygous mutants, but also detected in heterozygotes) already at P1 (when the dLGN size is still not importantly reduced in homozygous mutants) (Fig. 6A-A''), and at P8 (Fig. 6B-B''). Further, IF for 5-HT indicated that intracellular 5-HT accumulation is not observed in the mutants at P8 (Fig. 6C-C''';

compare C,C', control, showing intracellular perinuclear red 5-HT staining, to C'',C''', mutant, showing strongly reduced intracellular 5-HT). We then investigated the expression of the SERT-encoding gene by ISH at early stages (E18.5), preceding the overtly defective phenotype (Fig. 6D-D''). SERT mRNA signal intensity was reduced in $Sox2^{Th\Delta/\Delta}$ and, to a lesser extent, in heterozygotes, at E18.5 (Fig. 6D-D'') (when the mutant dLGN size is similar to control), and P7 (Fig. S3I'-I''). We also observed, at E18.5, a reduction in the expression of the mRNA encoding the Vesicular Mono Amine Transporter 2 (vMAT2) (Fig. S3J-J''), the transporter that packages 5-HT into synaptic vesicles, protecting it from degradation (Gaspar et al., 2003). These findings indicate that 5-HT metabolism/transport is compromised in Sox2 thalamic mutants, which might plausibly contribute to the abnormal development of thalamo-cortical connectivity, in accordance with previous observations on the somatosensory TCA connections (Persico et al., 2001, Chen et al., 2015) (Gaspar et al., 2003). SOX2 ChIPseq in neural stem/progenitor cells detects low level SOX2 binding to the promoter region of the SERT-encoding gene Slc6a4 (Fig. S4A) while in the vMAT2-encoding gene (Slc18a2), three intragenic SOX2 binding peaks are detected (Fig. S4B). This suggests that SOX2 might directly participate in the regulation of the vMAT2- and, possibly, the SERT-encoding gene.

Overall, our findings indicate that Sox2 controls, possibly through direct binding, downstream target genes important for dLGN development.

Alterations of the thalamo-cortical connections and of the patterning of the cerebral cortex are also observed in the somatosensory axis in Sox2 thalamic mutants

In examining the components of the visual system, the focus of the present paper (dLGN, visual cortex), we noticed that the VP somatosensory thalamic nucleus and VP thalamo-cortical connectivity also showed abnormal features, suggestive of a more general role for Sox2 in the development of sensory organs-thalamo-cortical connectivity. Within the VP thalamic nucleus, that receives somatosensory input from the periphery and, in turn, projects to the somatosensory cortex, Sox2 is highly expressed in wild type mice, similarly to the dLGN, but is absent in the Sox2-mutant (Fig. 1). We found, by vGLUT2 immunohistochemistry, that the map organization of barreloids in the mutant VP nucleus appears perturbed (Fig. 7A-A''). We then visualized TCA from the VP to the somatosensory primary cortex (S1) at P8 by immunohistochemistry for vGLUT2 on tangential sections of flattened cortices; we observed that the general topographic organization of the TCA projecting to the S1 area was affected in the mutant cortex; not only was vGLUT2 staining less intense but the number of barrel fields, as outlined by vGLUT2 staining, was also reduced compared to controls (Fig. 7B-B").

A similar phenotype was observed by immunohistochemistry for SERT, Serotonin and vGLUT2 on coronal sections at P8 (Fig. 7C-E'); in particular, cortical barrel fields were less defined and weakly stained (Fig. 7C-E').

Interestingly, the expression of the Efna5, SERT and vMAT2 genes, that we had found downregulated in the mutant dLGN, is concomitantly

downregulated also in the mutant VP (Fig. 5F-H", Fig. 6, Fig. S3I-J"). These findings suggest that at least some of the Sox2-dependent gene regulatory network in the thalamus is shared between different thalamic nuclei.

Discussion

Severe defects of vision are a hallmark of Sox2 deficiency in humans. Known mechanisms underlying the severe visual defects in SOX2-deficiency included, so far, the recognition of the functional importance of SOX2 in the development of retina and crystallin, as revealed by eye-specific mouse conditional knockouts (see Introduction). The importance of SOX2 for the development of dLGN and for its retinal/cortical connections demonstrated in this paper provides a new, important site of Sox2 function in the visual system, and an additional potential explanation for the visual impairment in SOX2-mutant patients.

The strong expression of SOX2 in postmitotic dLGN projection neurons (Fig. 1) was unexpected. In fact, Sox2 functions are critical in stem cells of various types, in particular embryonic, neural, and others, in which it is necessary to preserve stemness (Avilion et al., 2003, Bertolini, 2016, Favaro et al., 2009, Kondoh H, 2016, Bertolini et al., 2019), and in the reprogramming of differentiated cells to stem cells (Takahashi and Yamanaka, 2016). In contrast, in several neural cell types such as differentiated neurons and glia, Sox2 is either not expressed, or important in very specific cell types, such as retinal Müller glia (Taranova et al, 2006) or cerebellar Bergmann glia (Cerrato et al., 2018).

The development of connectivity between retinal, dLGN and visual cortex neurons is the result of complex interactions between developing neurons and their environment, involving signaling molecules and their receptors, which are often co-expressed in the growth cones of outgrowing neurons as well as on the target neurons. The possibility to selectively knock out Sox2 in the dLGN (and not the cortex, nor the retina) with RORα-Cre allowed us to unambiguously attribute the defects observed in mutants in the development of visual connectivity to defects arising, at least primarily, in thalamic neurons, as a result of Sox2 loss.

One important defect consists in a reduction, and a mis-patterning, of neuronal afferents from the retina that reach the dLGN (Fig. 3, S2). As Sox2 was not deleted in the developing eye, these defects must primarily depend on defective Sox2 function in the thalamus itself. It is known that retinal innervation plays an important trophic role in dLGN development, particularly in the early postnatal phase (El-Danaf et al., 2015, Guido, 2018), at a time when the Sox2-mutant thalamus fails to continue growing in size as seen in controls (Fig. 2, S2). Thus, the reduced retino-thalamic innervation may contribute to the reduced dLGN size seen postnatally in thalamic Sox2 mutants. Knockout experiments identified signaling molecules, and their receptors, important for the directional development of axons, and their appropriate targeting. Among these, we find ephrin-A5 to be importantly downregulated in the mutant dLGN (Fig. 5). Of note, Efna5 is expressed in both thalamus and retina (Pfeiffenberger et al., 2005), and the knockouts that demonstrated the importance of ephrin-A5 for

the correct patterning of ipsi- and contra-lateral eye fibres (Pfeiffenberger et al., 2005) ablated the *Efna5* gene throughout the brain (including thalamus and retina); our results are in agreement with the hypothesis that the *Efna5* gene, regulated by Sox2, plays at least part of its function in retinal axon guidance by acting specifically in the thalamus.

Our finding that SOX2 can directly bind the *Efna5* gene (Fig. 5) yields a potential direct Sox2 target within dLGN neurons, and potential regulatory regions for the *Efna5* gene, whose future molecular study could provide insight into dLGN neurons gene regulatory networks.

Sox2-mutant thalamic neurons of the sensory nuclei dLGN (and VP) fail to undergo normal post-natal development, and to generate normal axon outgrowths providing appropriate connections with the cortex (visual and somatosensory, respectively) (Fig. 4, 5, 7). Importantly, these two nuclei are the only ones (with the auditory nucleus) among the many thalamic nuclei, which express high levels of Sox2 in neurons. In addition, in Sox2 mutants, both nuclei show decreased expression of genes known to control axon connectivity (ephrin-A5, and SERT) (Fig. 5, 6, S3). In particular, it is known that the knock-out of SERT affects VP-originating fibres reaching the somatosensory cortex (Gaspar et al., 2003, Persico et al., 2001, Chen et al., 2015, Teissier et al., 2017); studies of the TCA connecting the dLGN to the visual cortex in SERT mutants were not reported. In Sox2 mutants, the connectivity defects between VP and somatosensory cortex mirror the defect seen in SERT-knockout mice (Fig. 7) (Gaspar et al., 2003, Persico et al., 2001); hence, the reduction of SERT and 5-HT expression in Sox2 mutants, together with the altered connections between dLGN with cortical visual areas,

and of VP with somatosensory areas, is in agreement with the hypothesis that Sox2-dependent regulation of serotonin transport/metabolism may contribute to sensory TCA connectivity.

It should be noted that additional molecular/cellular defects may be relevant to the abnormal connectivity of thalamic nuclei to the cortex. The observed reduced size of the dLGN (Fig. 2), implies a reduction of the number of projections to the cortex (Fig. 4). However, the size of the VP nucleus is not, or much less, reduced in mutants, as compared to the dLGN (see Figs. 2A-D', 6A-B''), yet thalamic afferents connecting the VP nucleus to the somatosensory cortex (normally forming the barrel fields, see Fig. 7, controls) are severely abnormal and disorganized in mutants (Fig. 7B-E'). In addition, the distribution of afferents from the periphery to the VP (forming the barreloids) also appears abnormal (Fig. 7A-A"). Hence, overall, factors other than thalamic nuclear size, specifically conditioning the patterning of neuronal afferents to and from the thalamus, appear to be involved in the observed defects.

Many other defects, such as altered expression of additional signaling molecules, and/or their receptors, in thalamic neurons, may likely contribute to the alterations observed in Sox2 mutants, and remain to be identified. Future studies of gene expression in mutant thalamic neurons at the genome-wide level (Kalish et al., 2018), will allow to investigate this point in more detail.

A cortical patterning defect in thalamic Sox2 mutants, i.e. the poor definition of V1 and V^{HO} regions of the visual cortex, first pointed to the existence of abnormal TCA in mutants (Fig. 4).

Very similar defects were described following thalamic ablation, via RORα-Cre, of *Nr2f1*, a gene whose mutation in humans leads to cerebral visual impairment (Bosch et al., 2015, Bosch et al., 2014), raising the question of whether they may functionally interact. We find wide co-expression of SOX2 and NR2F1 in dLGN neurons (not shown); however, we do not detect major alterations in Nr2f1 levels in the mutant dLGN (Fig. 5), ruling out that the failure to activate Nr2f1 in dLGN is a key mechanism underlying the defects in Sox2 mutants. The similarities in the phenotype of the two mutants might be due either to a general biological process, i.e. a reduction of TCA will always result in V^{HO} patterning defects, or to deregulation of a set of common critical Sox2/Nr2f1 targets, controlling TCA development, or to a combination of both mechanisms. Future combined studies of Sox2 and Nr2f1 targets will clarify this point.

The identification of Sox2 targets, such as Efna5, SERT and vMAT2 that are downregulated not only in homozygous Sox2 mutants, but also in heterozygotes (Fig. 5, 6D, S3, S4), points to potential candidates for roles in mediating Sox2 function in human visual defects; interestingly, in human patients, heterozygous Sox2 mutation is sufficient to cause blindness, pointing to dosage-sensitive gene regulation by SOX2 as an important phenomenon in the pathogenesis of these defects.

Genetic defects of vision are often polygenic in nature; importantly, some of these defects are dependent on brain, rather than eye, abnormalities (Williamson and FitzPatrick, 2014), but so far SOX2 has only been considered a gene responsible for anophthalmia and microphthalmia, i.e. congenital defects that primarily affect the eye. Our findings raise the possibility that genetically altered Sox2 levels in

the thalamus (as obtained by regulatory mutations, or by mutations in Sox2-controlling transcription factors) may play roles also in brain-related visual defects. The importance of Sox2 for gene regulatory networks in the thalamus could allow to identify overlaps with the gene regulatory networks controlled, in the thalamus, by different genes, whose mutation also causes visual disease (as hypothesized for Nr2f1, see above). A better understanding of these networks has the potential to generate new, unifying hypotheses for therapy approaches.

Acknowledgements

We are grateful to Dr. D. O'Leary for providing the RORα-Cre mouse, Dr. J. Flanagan, Dr. D. Feldheim, Dr. P. Gaspar, Dr. L. Muzio, Dr. V. Broccoli for ISH probes, and to all members of the Nicolis laboratory and ImprovVision consortium for insightful discussion. Work in the S.K.N. laboratory was funded from the EEC ERANET-NEURON ImprovVision project (also supporting C.F., P.B. and M.S.), Telethon (GGP12152), AIRC (IG-2014), and Cariplo. L.S. was supported by a VINCI PhD fellowship from the Università Italo-Francese/Université Franco-Italienne. P.B. also acknowledges the support of MINECO PCIN-2015-176-C02-01 and BFU2016-75412-R (with FEDER funds). C.F. thanks The Italian Ministry of Health, Mrs. M.C. Regondi for technical support, and Dr. P. Pennacchio for his contribution to early phase of this study.

Figures

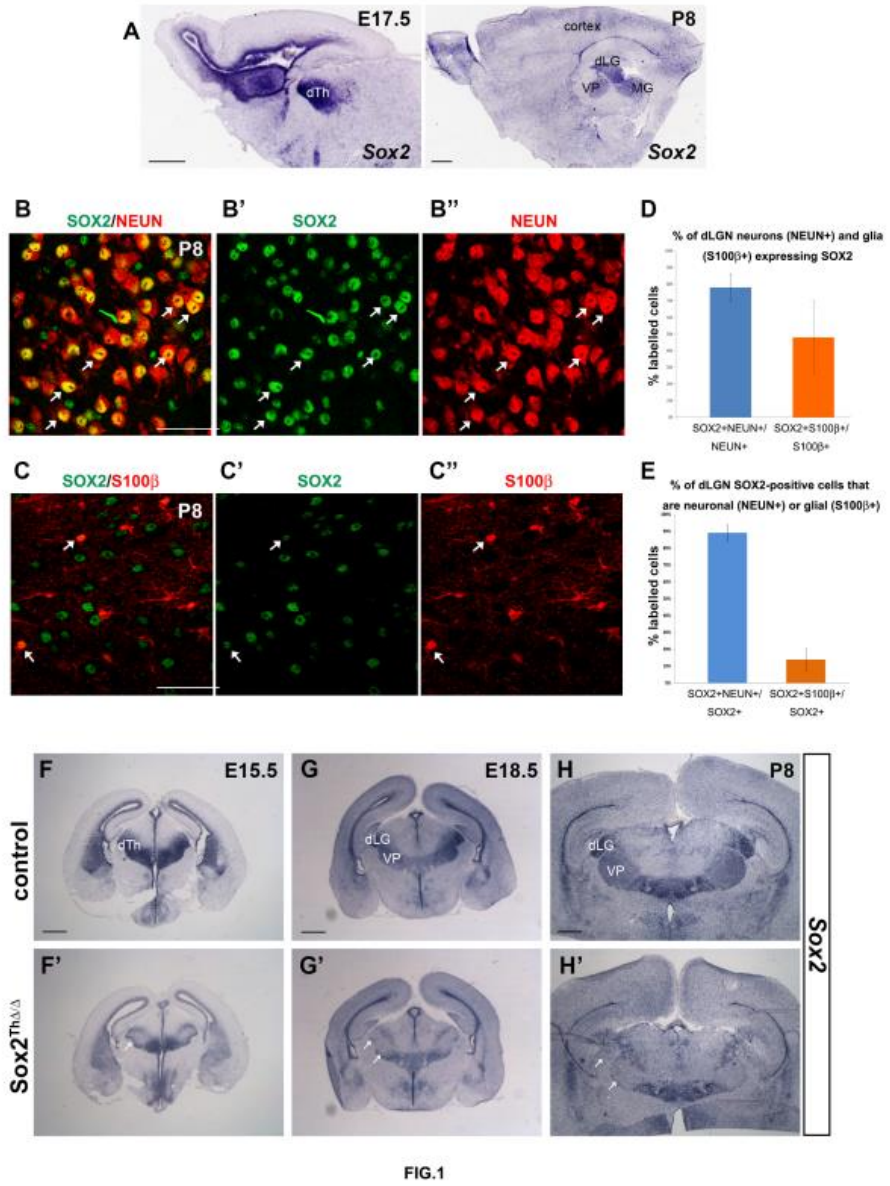

FIG.1

Figure 1. Sox2 thalamic expression and its thalamic ablation

(A) In situ hybridization with a Sox2 probe on sagittal section of mouse brain at E17.5 and P8. Sox2 thalamic expression in the dorsal thalamus (dTh) at E17.5 and in the thalamic nuclei MG, dLG and VP at P8 can be observed. (B-

C’’) Immunofluorescence on coronal sections of dLG of mouse brain at P8 with anti-SOX2 (green) and anti-NEUN (red), a neuronal marker, antibodies in B-B’’ and with anti-SOX2 (green) and anti- S100β (red), an astroglial marker, antibodies in C-C’’. Arrows indicate cells co-expressing SOX2 and NEUN (B-B”) or SOX2 and S100β (C-C”), (n=3). (D) Quantification of the number of cells in the dLG at P8 positive for both SOX2 and NEUN out of the total number of NEUN-positive cells (blue) and of the number of cells positive for both SOX2 and S100β out of the total number of S100β-positive cells (orange). Around 80% of NEUN positive neurons express SOX2. Data are represented as mean ± standard deviation. (E) Quantification of the number of SOX2- and NEUN-positive cells in the dLG at P8 out of the total number of SOX2-positive cells (blue), and of the number of SOX2- and S100β-positive cells out of the total number of SOX2-positive cells (orange). Around 90% of SOX2 positive cells are neurons (n=3). Data are represented as mean ± standard deviation. (F-H’) In situ hybridization with a Sox2 probe on coronal sections of mouse brains at E15.5 (F,F’), E18.5 (G,G’) and P8 (H,H’) of Sox2 thalamic mutants Sox2ThΔ/Δ (F’,G’,H’) and control littermates (Sox2ThΔ/+ or Sox2Th+/+) (F,G,H). A clear ablation of Sox2 expression in the dorsal thalamus of Sox2 thalamic mutants (arrows) is observed at all stages compared to controls, (E15.5 control n=2, mutant n=2; E18.5 control n=3, mutant n=2; P8 control n=2, mutant n=2). Scale bars: 600µm (A,F-H’), 50µm (B-C”).

dTh, dorsal thalamus; MG, medial geniculate nucleus; dLG, dorso lateral geniculate nucleus; VP, ventroposterior nucleus

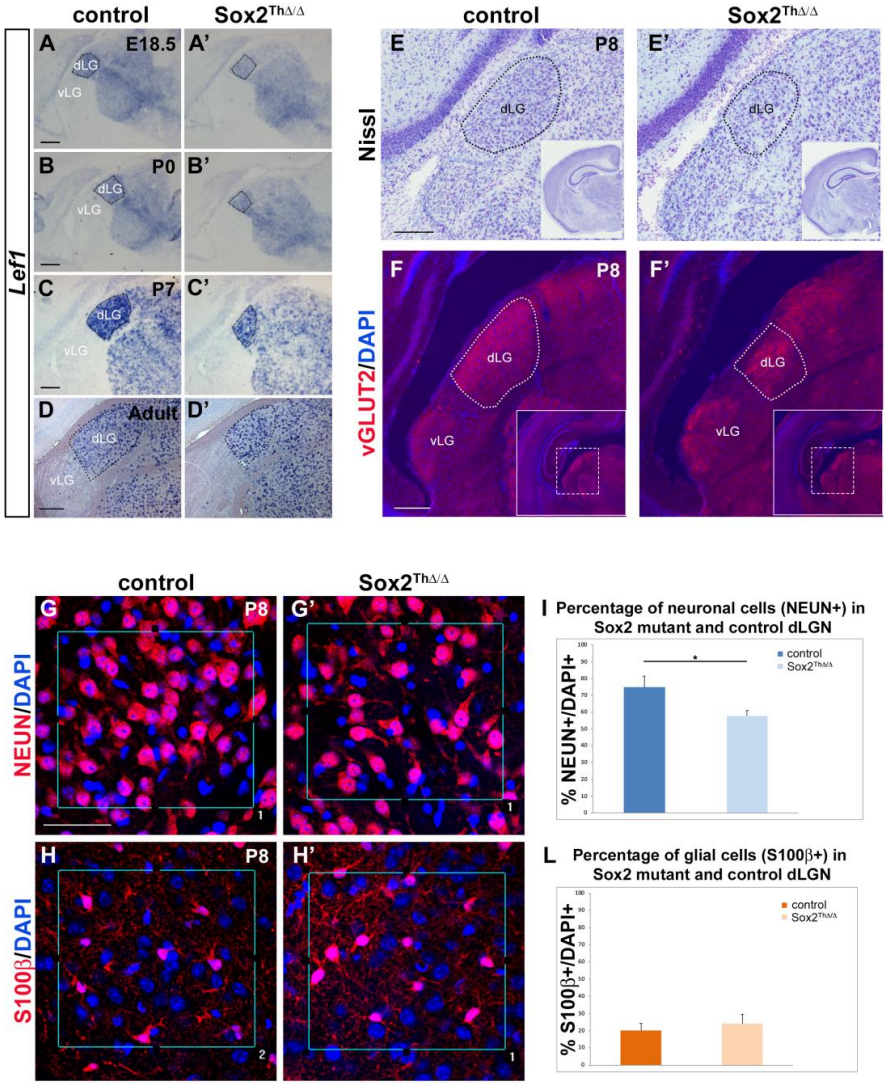

Figure 2. The dLG nucleus is reduced in size in Sox2 thalamic mutants

(A-D') In situ hybridization with a Lef1 probe on coronal sections of mouse brains at E18.5 (A,A'), P0 (B,B'), P7 (C,C') and adults (D,D') of Sox2 thalamic mutants (A',B',C',D') and control littermates (A,B,C,D). The dLG, marked by Lef1 expression, is reduced in size in the mutants starting at P0 (E18.5 control n=6, mutant n=6; P0 control n=4, mutant n=4; P7 control n=5, mutant n=3; adult control n=2, mutant n=2). (E,E') Nissl staining of coronal sections of mouse brains at P8 of Sox2 thalamic mutants (E') and control

littermates (E). The dLG is reduced in size in mutants compared to controls (control n=2, mutant n=2). (F,F') Immunofluorescence with an anti-vGLUT2 antibody (in red) on coronal sections of dorsal thalamus at P8 of Sox2 thalamic mutants (F') and control littermates (F). Nuclei are marked by DAPI (blue). The mutant dLG marked by vGLUT2 expressing retinal fibers appears reduced in size compared to controls. (control n=4, mutant n=2). Dotted lines outline the dLG. (G-H') Immunofluorescence on coronal sections of mouse dLG at P8 of Sox2 thalamic mutants (G',H') and control littermates (G,H) with antibodies anti-NEUN (a neuronal marker, in red) (G,G') and anti-S100 (an astroglial marker, in red) (H,H'). Nuclei are marked by DAPI (blue) (control n=3, mutant n=3). (I) Quantification of the percentage of NEUN positive cells out of DAPI positive cells in control and mutant dLG nuclei. (L) Quantification of the percentage of S100β positive cells out of total DAPI-positive cells in control and mutant dLG nuclei. A slight reduction of NEUN positive neurons in the mutant dLG is observed. Error bars represent the standard deviation, * denotes a statistically significant difference $p<0.05$ ($p= 0.01308$). Scale bars: 200µm (A-F'), 50 µm (G-H').

dLG, dorso-lateral geniculate nucleus; vLG, ventro-lateral geniculate nucleus

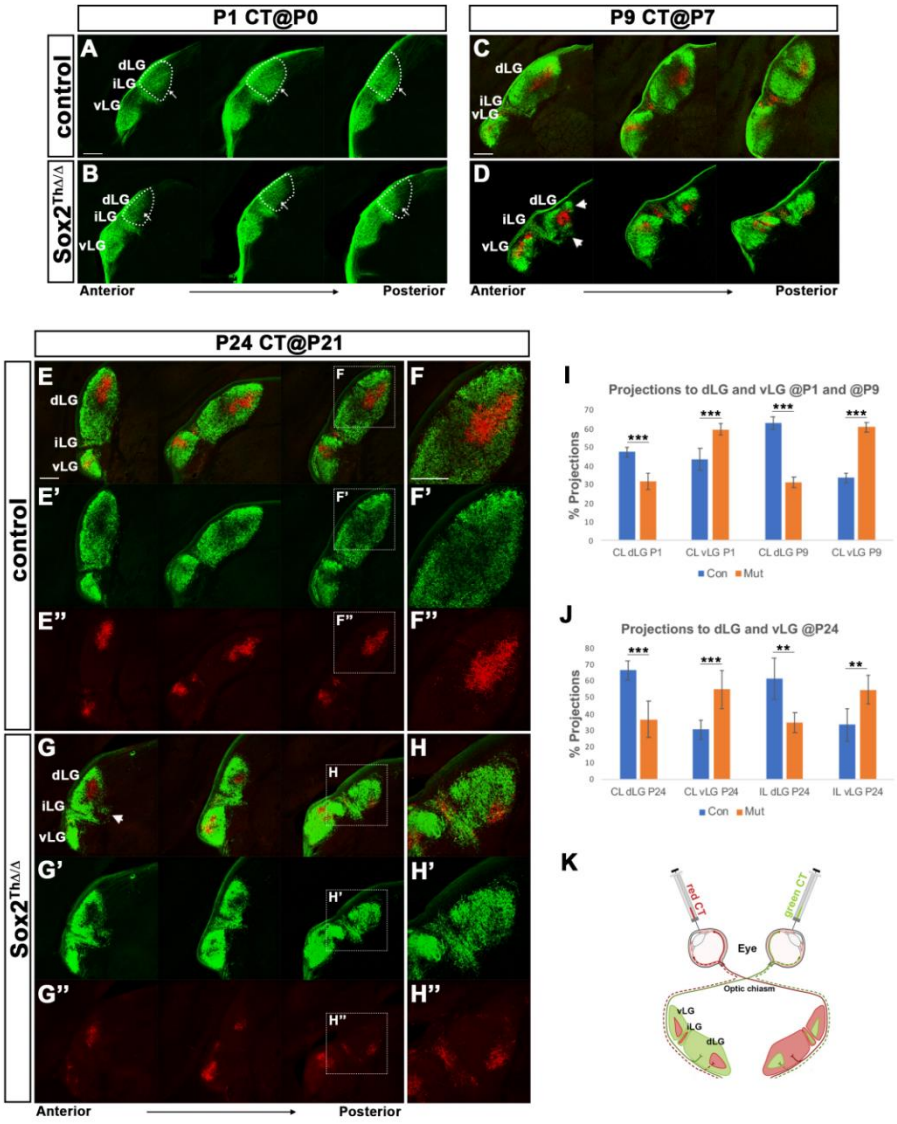

Figure 3. **Defects in retinal projections to the dLG are found in Sox2 thalamic mutants**

(A-H'') Cholera-toxin subunit B (CTB) – Alexa488 (green) and CTB – Alexa 594 (red) were injected respectively in the right and left eye and contralateral (green) and ipsilateral (red) axons to the left dLG and vLG are shown (see scheme of injection in K modified from (Seabrook et al., 2017)). Series of coronal sections of the dLG from anterior (left) to posterior (right) of

representative Sox2 thalamic mutants (B,D,G,H) and littermate controls (A,C,E,F) are shown. (A,B) CT was injected at P0 and brains were analysed at P1. Less retinal axons are observed in the mutant dLG. Arrows mark the medial border of contralateral projections. (C,D) CT was injected at P7 and brains were analysed at P9. Retinal axons arrive to a smaller dLG in mutants and projections are often fragmented (arrowheads). (E-H") CT was injected at P21 and brains were analysed at P24. Retinal projections in mutants arrive to a smaller dLG and are sometimes fragmented (arrowheads) compared to controls (P1 control n=4, mutant n=4; P9 control n=3, mutant n=4; P24 control n=3, mutant n=3). (I) Quantification of the percentage of contralateral (CL) retinal axons that reach the dLG or vLG in mutants and controls at P1 and P9 (*** $p<0.005$, unpaired Student's T-test). (J) Quantification of the percentage of retinal axons, contralateral (CL) or ipsilateral (IL), that reach the dLG or vLG in mutants and controls at P24 (P1 control n=4, mutant n=3; P9 control n=2, mutant n=4; P24 control n=3, mutant n=3). Error bars represent standard deviation; * denotes a statistically significant difference with unpaired Student's T-test, ** $p<0.01$, *** $p<0.005$. Scale bars 200µm.

dLG, dorso lateral geniculate nucleus; iLG, intermediate lateral geniculate nucleus; vLG ventro lateral geniculate nucleus

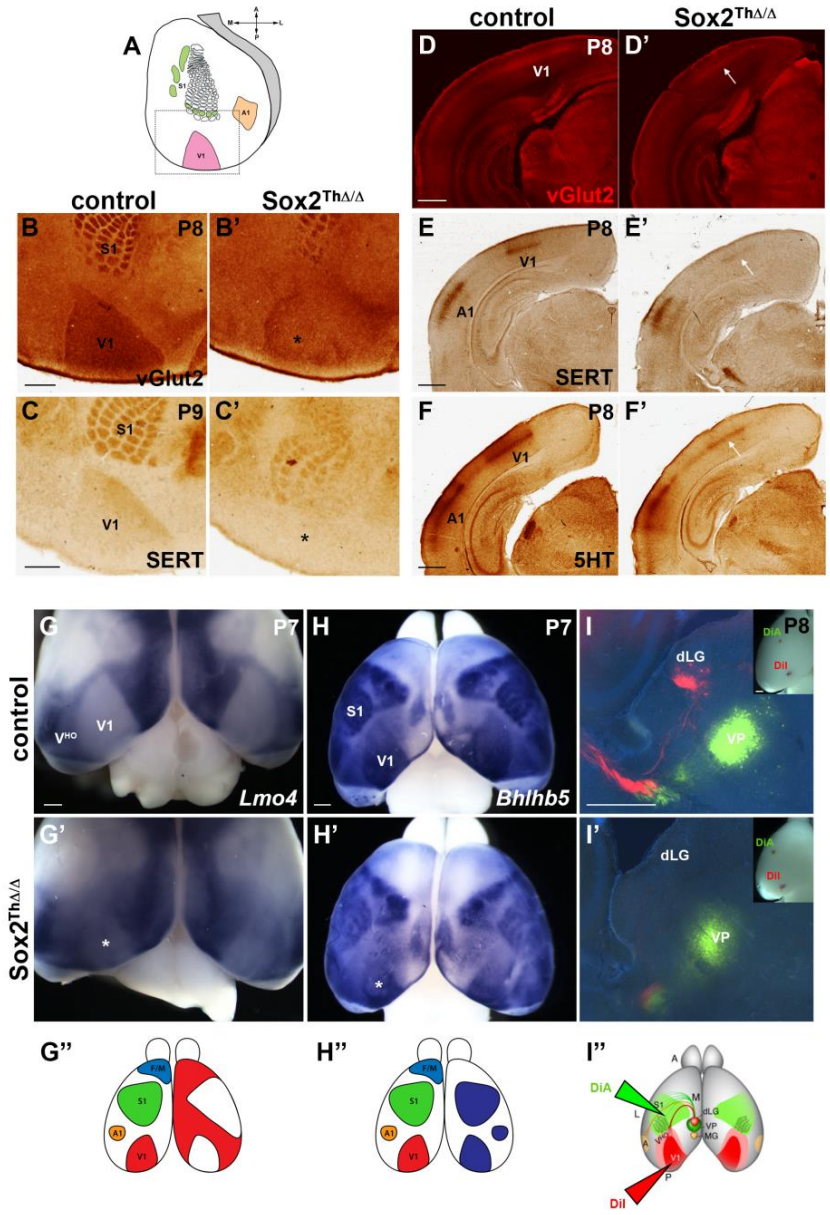

Figure 4. Thalamo-cortical connectivity and cortical patterning are abnormal in Sox2 thalamic mutants

(A) Representation of a cortical flat mount. (B-C') Immunohistochemistry on tangential sections of cortical flat mounts at P8 of Sox2 thalamic mutants

(B',C') and controls (B,C) with vGLUT2 (B,B') and serotonin transporter (SERT) (C,C') both expressed by thalamic projections to the cortex. Staining in the mutant visual cortex is reduced (*) with both markers compared to controls (vGLUT2 control n=16, mutant n=7; SERT control n=6, mutant n=3). (D,D') Immunofluorescence with vGLUT2 on coronal sections of mouse brains at P8. vGLUT2-positive thalamo-cortical projections to V1 are reduced in Sox2 mutants (D') compared to controls (D) (white arrow). (control n=4, mutant n=2). (E-F') Immunohistochemistry on coronal sections of mouse brains at P8 of Sox2 thalamic mutants (E',F') and controls (E,F) with SERT (E,E') and serotonin (5HT) (F,F'). Staining in the mutant V1 is reduced with both markers (white arrows) (SERT control n=4, mutant n=2; 5HT control n=5, mutant n=3). (G-H') Whole mount in situ hybridization for the cortical markers, Lmo4 (G-G') and Bhlhb5 (H-H') (schematic expression pattern in G" and H") on Sox2 thalamic mutants and littermate controls. The mutant visual area (V1) is not clearly distinguished from the neighbouring higher order visual areas (VHO) compared to control V1 (see *) (Lmo4 control n=6, mutant n=3; Bhlhb5 control n=11, mutant n=5). (I-I') Coronal sections at P8 after insertion of DiI crystals (scheme in I'' modified from Chou et al., 2013) in the primary visual cortex (V1) (red) and DiA in the somatosensory cortex (S1) (green) showing axons projecting to the dLG in controls and not in Sox2 thalamic mutants (control hemispheres n=28, mutant hemispheres n=15). Scale bars 600µm.

V1, primary visual area; VHO, higher order visual area; S1, primary somatosensory area; A1, primary auditory area; dLG, dorso lateral geniculate nucleus; VP, ventroposterior nucleus; MG, medial geniculate nucleus; F/M, motor cortex

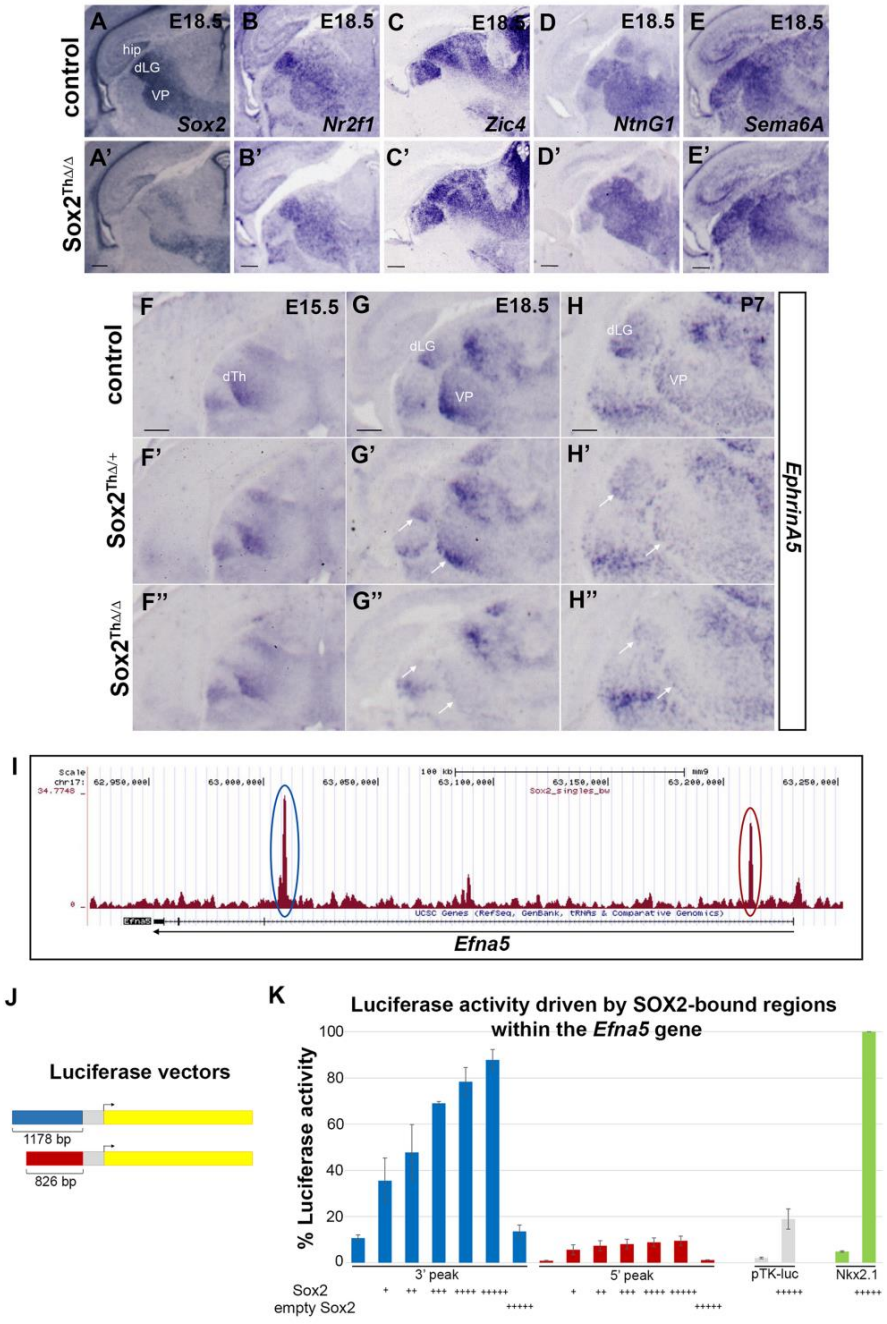

Figure 5. Efna5 expression is reduced in the dLG of Sox2 thalamic mutants and a DNA region within the Efna5 locus is bound and activated by SOX2

(A-E') In situ hybridization on coronal sections of mutant (A',B',C',D',E') and control (A,B,C,D,E) mouse forebrain at E18.5 with Sox2 (A,A'), Nr2f1 (B,B'), Zic4 (C,C'), Netrin G1 (NtnG1; D,D') and Semaphorin 6A (Sema6A; E,E') probes. Sox2 expression is clearly ablated in the mutant thalamus (A' compared to A) while the expression of the other markers appears unchanged (at least 3 controls and 3 mutants were analysed for each probe). (F-H") Time-course of Ephrin-A5 (Efna5) expression by in situ hybridization on coronal sections of controls, heterozygotes and homozygote Sox2 thalamic mutant forebrains at E15.5 (F-F"), E18.5 (G-G") and P7 (H-H"). Efna5 is specifically downregulated in the dLG and VP of Sox2 homozygote thalamic mutants (white arrows), while it remains unchanged in other domains of expression both at E18.5 (G-G") and P7 (H-H"). A mild Efna5 downregulation is also observed in Sox2 heterozygotes (G',H') (E15.5 wild type n=3, heterozygote n=3, mutant n=4; E18.5 wild type n=8, heterozygote n=7, mutant n=8; P7 wild type n=3, heterozygote n=3, mutant n=5). (I) Sox2 ChIPseq profile across the Efna5 locus from neurosphere cultures derived from postnatal mouse telencephalon showing two Sox2 peaks (5', red circle; 3', blue circle) within the first intron of the Efna5 gene. (J) Schematic representation of plasmids containing the 3' and 5' Sox2 bound regions upstream of a minimal promoter and luciferase reporter gene. (K) Co-transfection in Neuro-2a cells of the constructs in (J) with increasing amount of SOX2-expressing vector or with the corresponding empty vector (+, 1:0.06; ++, 1:0.125; +++, 1:0.187; ++++, 1:0.25; +++++, 1:0.5 reporter:transactivator molar ratio). The previously known activation of the Nkx2.1 promoter by the SOX2 expressing vector was used as a positive control of transactivation (Ferri et al., 2013). Results are the mean of three independent transfections, each performed in triplicate. Error bars represent standard deviation. Scale bars 200µm. hip, hippocampus; dLG, dorso lateral geniculate nucleus; VP, ventroposterior nucleus; dTh, dorsal thalamus

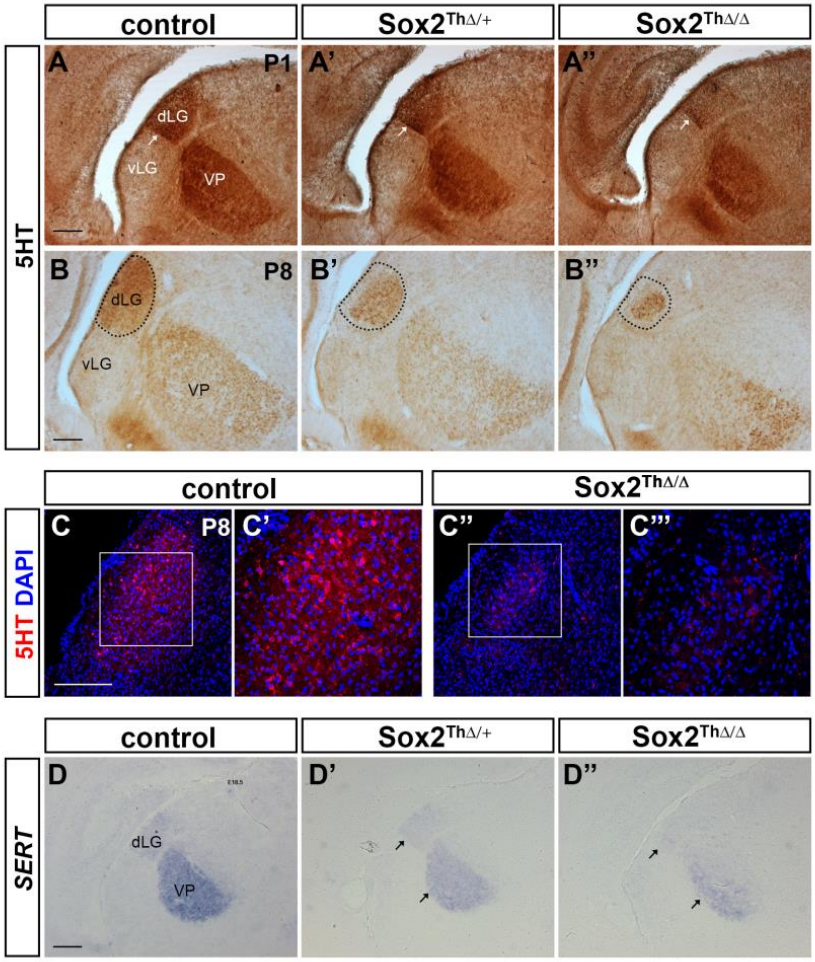

Figure 6. Serotonin levels in mutant dLG are reduced

(A-B") Immunohistochemistry for serotonin (5HT) on coronal sections of Sox2 mutant (A",B"), Sox2 heterozygote (A',B') and control (A,B) mouse brains at P1 (A-A") and P8 (B-B"). The level of serotonin in the dLG is dependent on the number of copies of the Sox2 gene. White arrows indicate the ventral border of the dLG, dotted lines outline the dLG. (C-C"') Immunofluorescence for 5HT (red) on coronal sections of dLG of Sox2 thalamic mutants (C",C"') and controls (C,C') at P8. 5HT levels in the mutant dLG are greatly reduced. Nuclei are marked by DAPI (blue). Note perinuclear

5HT in controls. C',C"' are magnifications of details in C,C" respectively (P1 wild type n=4, heterozygote n=3, mutant n=3; P8 wild type n=3, heterozygote n=2, mutant n=3). (D-D") In situ hybridization on coronal sections of E18.5 forebrains of Sox2 homozygote mutant (D"), Sox2 heterozygote (D') and control (D) with a SERT probe. SERT is downregulated in the Sox2 mutant thalamus compared to control (black arrows). A mild downregulation is also observed in Sox2 heterozygous thalami indicating a dose dependent effect of Sox2 loss (wild type n=5, heterozygote n=3, mutant n=4). Scale bars 200µm. dLG, dorso lateral geniculate nucleus; vLG, ventro lateral geniculate nucleus; VP, ventroposterior nucleus

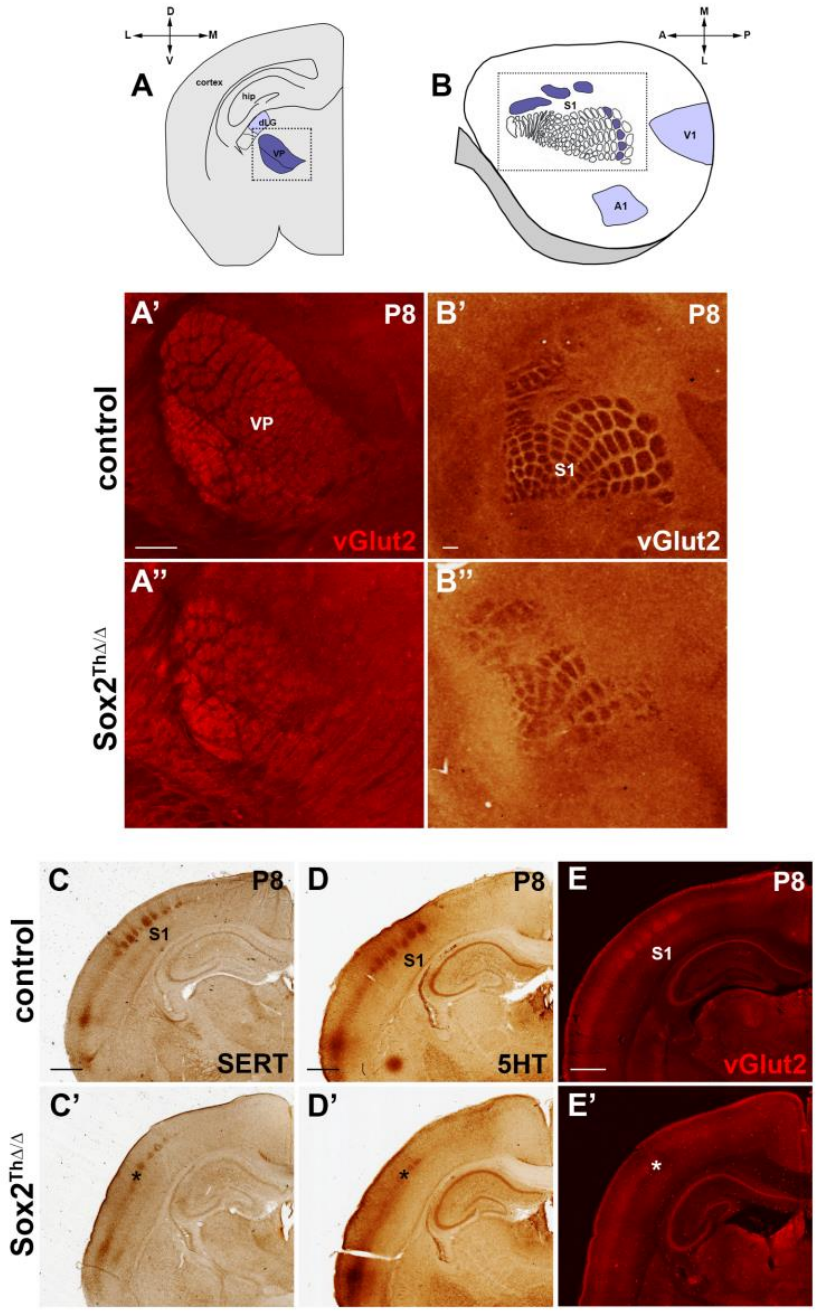

Figure 7. Thalamo-cortical somatosensory afferents and the somatosensory thalamic nucleus (VP) are affected

(A-A") Immunofluorescence for vGLUT2 at P8 on coronal section of the VP thalamic nucleus of controls (A') and Sox2 thalamic mutants (A"). Drawing of a typical coronal section through the thalamus in A. (control n=4, mutant n=2). (B-B") Immunohistochemistry for vGLUT2 of tangential sections of cortical flat mounts (drawing in B) of controls (B') and Sox2 thalamic mutants (B") (control n=16, mutant n=7). (C-E') Immunohistochemistry on coronal sections of mutant and control forebrain at P8 with SERT (C,C'), serotonin (5HT; D,D') and vGLUT2 (E,E') antibodies. Barrel fields are not detected in mutant cortex (see *) (SERT control n=4, mutant n=2; 5HT control n=5, mutant n=3; vGLUT2 control n=4, mutant n=2).
Scale bars: 200µm (A'-B"), 600µm (C-E').
VP, ventroposterior nucleus; S1, primary somatosensory cortex; V1, primary visual cortex; A1, primary auditory cortex; dLG, dorso lateral geniculate nucleus; hip, hippocampus

References

Arnold, K., Sarkar, A., Yram, M. A., Polo, J. M., Bronson, R., Sengupta, S., Seandel, M., Geijsen, N. & Hochedlinger, K. 2011. Sox2(+) adult stem and progenitor cells are important for tissue regeneration and survival of mice. Cell Stem Cell, 9, 317-29.

Avilion, A. A., Nicolis, S. K., Pevny, L. H., Perez, L., Vivian, N. & Lovell-Badge, R. 2003. Multipotent cell lineages in early mouse development depend on SOX2 function. Genes & development, 17, 126-40.

Bertolini, J., Mercurio, S., Favaro, R., Mariani, J., Ottolenghi, S., Nicolis, S.K. 2016. Sox2-dependent regulation of neural stem cells and CNS development.

In: Kondoh, H., Lovell-Badge, R. (ed.) Sox2, Biology and role in development and disease. Elsevier.

Bertolini, J. A., Favaro, R., Zhu, Y., Pagin, M., Ngan, C. Y., Wong, C. H., Tjong, H., Vermunt, M. W., Martynoga, B., Barone, C., Mariani, J., Cardozo, M. J., Tabanera, N., Zambelli, F., Mercurio, S., Ottolenghi, S., Robson, P., Creyghton, M. P., Bovolenta, P., Pavesi, G., Guillemot, F., Nicolis, S. K. & Wei, C. L. 2019. Mapping the Global Chromatin Connectivity Network for Sox2 Function in Neural Stem Cell Maintenance. Cell Stem Cell, 24, 462-476 e6.

Bosch, D. G., Boonstra, F. N., De Leeuw, N., Pfundt, R., Nillesen, W. M., De Ligt, J., Gilissen, C., Jhangiani, S., Lupski, J. R., Cremers, F. P. & De Vries, B. B. 2015. Novel genetic causes for cerebral visual impairment. Eur J Hum Genet.

Bosch, D. G., Boonstra, F. N., Gonzaga-Jauregui, C., Xu, M., De Ligt, J., Jhangiani, S., Wiszniewski, W., Muzny, D. M., Yntema, H. G., Pfundt, R., Vissers, L. E., Spruijt, L., Blokland, E. A., Chen, C. A., Baylor-Hopkins Center For Mendelian, G., Lewis, R. A., Tsai, S. Y., Gibbs, R. A., Tsai, M. J., Lupski, J. R., Zoghbi, H. Y., Cremers, F. P., De Vries, B. B. & Schaaf, C. P. 2014. NR2F1 mutations cause optic atrophy with intellectual disability. Am J Hum Genet, 94, 303-9.

Braisted, J. E., Catalano, S. M., Stimac, R., Kennedy, T. E., Tessier-Lavigne, M., Shatz, C. J. & O'leary, D. D. 2000. Netrin-1 promotes thalamic axon growth and is required for proper development of the thalamocortical projection. J Neurosci, 20, 5792-801.

Cerrato, V., Mercurio, S., Leto, K., Fuca, E., Hoxha, E., Bottes, S., Pagin, M., Milanese, M., Ngan, C. Y., Concina, G., Ottolenghi, S., Wei, C. L., Bonanno, G., Pavesi, G., Tempia, F., Buffo, A. & Nicolis, S. K. 2018. Sox2 conditional mutation in mouse causes ataxic symptoms, cerebellar vermis hypoplasia, and postnatal defects of Bergmann glia. Glia.

Chen, X., Ye, R., Gargus, J. J., Blakely, R. D., Dobrenis, K. & Sze, J. Y. 2015. Disruption of Transient Serotonin Accumulation by Non-Serotonin-Producing Neurons Impairs Cortical Map Development. Cell Rep.

Chou, S. J., Babot, Z., Leingartner, A., Studer, M., Nakagawa, Y. & O'leary, D. D. 2013. Geniculocortical input drives genetic distinctions between primary and higher-order visual areas. Science, 340, 1239-42.

El-Danaf, R. N., Krahe, T. E., Dilger, E. K., Bickford, M. E., Fox, M. A. & Guido, W. 2015. Developmental remodeling of relay cells in the dorsal lateral geniculate nucleus in the absence of retinal input. Neural Dev, 10, 19.

Fantes, J., Ragge, N. K., Lynch, S. A., Mcgill, N. I., Collin, J. R., Howard-Peebles, P. N., Hayward, C., Vivian, A. J., Williamson, K., Van Heyningen, V. & Fitzpatrick, D. R. 2003. Mutations in SOX2 cause anophthalmia. Nature genetics, 33, 461-3.

Favaro, R., Valotta, M., Ferri, A. L., Latorre, E., Mariani, J., Giachino, C., Lancini, C., Tosetti, V., Ottolenghi, S., Taylor, V. & Nicolis, S. K. 2009. Hippocampal development and neural stem cell maintenance require Sox2-dependent regulation of Shh. Nature neuroscience, 12, 1248-56.

Ferri, A., Favaro, R., Beccari, L., Bertolini, J., Mercurio, S., Nieto-Lopez, F., Verzeroli, C., La Regina, F., De Pietri Tonelli, D., Ottolenghi, S., Bovolenta, P. & Nicolis, S. K. 2013. Sox2 is required for embryonic development of the

ventral telencephalon through the activation of the ventral determinants Nkx2.1 and Shh. Development, 140, 1250-61.

Garel, S. & Lopez-Bendito, G. 2014. Inputs from the thalamocortical system on axon pathfinding mechanisms. Curr Opin Neurobiol, 27, 143-50.

Gaspar, P., Cases, O. & Maroteaux, L. 2003. The developmental role of serotonin: news from mouse molecular genetics. Nat Rev Neurosci, 4, 1002-12.

Gezelius, H. & Lopez-Bendito, G. 2017. Thalamic neuronal specification and early circuit formation. Dev Neurobiol, 77, 830-843.

Graham, V., Khudyakov, J., Ellis, P. & Pevny, L. 2003. SOX2 functions to maintain neural progenitor identity. Neuron, 39, 749-65.

Guido, W. 2018. Development, form, and function of the mouse visual thalamus. J Neurophysiol, 120, 211-225.

Horng, S., Kreiman, G., Ellsworth, C., Page, D., Blank, M., Millen, K. & Sur, M. 2009. Differential gene expression in the developing lateral geniculate nucleus and medial geniculate nucleus reveals novel roles for Zic4 and Foxp2 in visual and auditory pathway development. J Neurosci, 29, 13672-83.

Huberman, A. D., Murray, K. D., Warland, D. K., Feldheim, D. A. & Chapman, B. 2005. Ephrin-As mediate targeting of eye-specific projections to the lateral geniculate nucleus. Nat Neurosci, 8, 1013-21.

Kalish, B. T., Cheadle, L., Hrvatin, S., Nagy, M. A., Rivera, S., Crow, M., Gillis, J., Kirchner, R. & Greenberg, M. E. 2018. Single-cell transcriptomics

of the developing lateral geniculate nucleus reveals insights into circuit assembly and refinement. Proc Natl Acad Sci U S A, 115, E1051-E1060.

Kamachi, Y., Uchikawa, M., Tanouchi, A., Sekido, R. & Kondoh, H. 2001. Pax6 and SOX2 form a co-DNA-binding partner complex that regulates initiation of lens development. Genes Dev, 15, 1272-86.

Kania, A. & Klein, R. 2016. Mechanisms of ephrin-Eph signalling in development, physiology and disease. Nat Rev Mol Cell Biol, 17, 240-56.
Kondoh H, L.-B. R. E. B. 2016. Sox2, Biology and Role in Development and Disease, Elsevier, Associated Press.

Lebrand, C., Cases, O., Adelbrecht, C., Doye, A., Alvarez, C., El Mestikawy, S., Seif, I. & Gaspar, P. 1996. Transient uptake and storage of serotonin in developing thalamic neurons. Neuron, 17, 823-35.

Lee, K. E., Seo, J., Shin, J., Ji, E. H., Roh, J., Kim, J. Y., Sun, W., Muhr, J., Lee, S. & Kim, J. 2014. Positive feedback loop between Sox2 and Sox6 inhibits neuronal differentiation in the developing central nervous system. Proc Natl Acad Sci U S A, 111, 2794-9.

Little, G. E., Lopez-Bendito, G., Runker, A. E., Garcia, N., Pinon, M. C., Chedotal, A., Molnar, Z. & Mitchell, K. J. 2009. Specificity and plasticity of thalamocortical connections in Sema6A mutant mice. PLoS Biol, 7, e98.

Mariani, J., Favaro, R., Lancini, C., Vaccari, G., Ferri, A. L., Bertolini, J., Tonoli, D., Latorre, E., Caccia, R., Ronchi, A., Ottolenghi, S., Miyagi, S., Okuda, A., Zappavigna, V. & Nicolis, S. K. 2012. Emx2 is a dose-dependent negative regulator of Sox2 telencephalic enhancers. Nucleic Acids Res, 40, 6461-76.

Miyashita-Lin, E. M., Hevner, R., Wassarman, K. M., Martinez, S. & Rubenstein, J. L. 1999. Early neocortical regionalization in the absence of thalamic innervation. Science, 285, 906-9.

Panaliappan, T. K., Wittmann, W., Jidigam, V. K., Mercurio, S., Bertolini, J. A., Sghari, S., Bose, R., Patthey, C., Nicolis, S. K. & Gunhaga, L. 2018. Sox2 is required for olfactory pit formation and olfactory neurogenesis through BMP restriction and Hes5 upregulation. Development, 145.

Persico, A. M., Mengual, E., Moessner, R., Hall, F. S., Revay, R. S., Sora, I., Arellano, J., Defelipe, J., Gimenez-Amaya, J. M., Conciatori, M., Marino, R., Baldi, A., Cabib, S., Pascucci, T., Uhl, G. R., Murphy, D. L., Lesch, K. P. & Keller, F. 2001. Barrel pattern formation requires serotonin uptake by thalamocortical afferents, and not vesicular monoamine release. J Neurosci, 21, 6862-73.

Pevny, L. H. & Nicolis, S. K. 2010. Sox2 roles in neural stem cells. Int J Biochem Cell Biol, 42, 421-4.

Pfeiffenberger, C., Cutforth, T., Woods, G., Yamada, J., Renteria, R. C., Copenhagen, D. R., Flanagan, J. G. & Feldheim, D. A. 2005. Ephrin-As and neural activity are required for eye-specific patterning during retinogeniculate mapping. Nat Neurosci, 8, 1022-7.

Seabrook, T. A., Burbridge, T. J., Crair, M. C. & Huberman, A. D. 2017. Architecture, Function, and Assembly of the Mouse Visual System. Annu Rev Neurosci, 40, 499-538.

Smith, A. N., Miller, L. A., Radice, G., Ashery-Padan, R. & Lang, R. A. 2009. Stage-dependent modes of Pax6-Sox2 epistasis regulate lens development and eye morphogenesis. Development, 136, 2977-85.

Sur, M. & Rubenstein, J. L. 2005. Patterning and plasticity of the cerebral cortex. Science, 310, 805-10.

Takahashi, K. & Yamanaka, S. 2016. A decade of transcription factor-mediated reprogramming to pluripotency. Nat Rev Mol Cell Biol, 17, 183-93.

Taranova, O. V., Magness, S. T., Fagan, B. M., Wu, Y., Surzenko, N., Hutton, S. R. & Pevny, L. H. 2006. SOX2 is a dose-dependent regulator of retinal neural progenitor competence. Genes & development, 20, 1187-202.

Teissier, A., Soiza-Reilly, M. & Gaspar, P. 2017. Refining the Role of 5-HT in Postnatal Development of Brain Circuits. Front Cell Neurosci, 11, 139.

Vanderhaeghen, P., Lu, Q., Prakash, N., Frisen, J., Walsh, C. A., Frostig, R. D. & Flanagan, J. G. 2000. A mapping label required for normal scale of body representation in the cortex. Nat Neurosci, 3, 358-65.

Williamson, K. A. & Fitzpatrick, D. R. 2014. The genetic architecture of microphthalmia, anophthalmia and coloboma. Eur J Med Genet, 57, 369-80.

Supplemental information

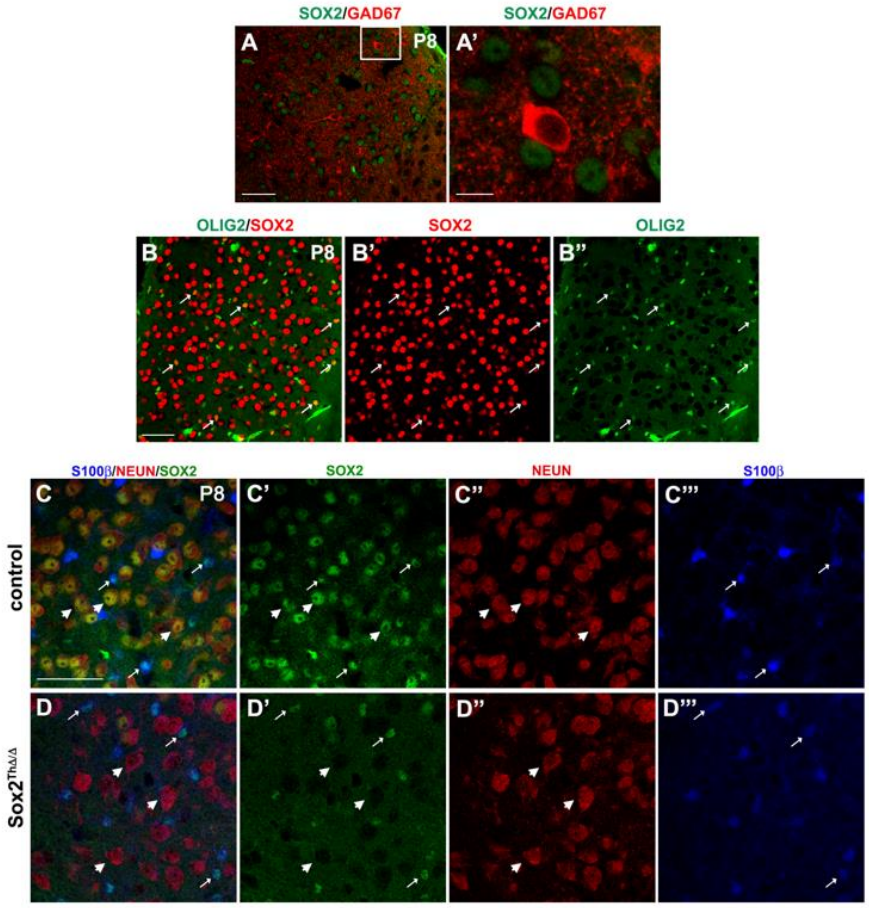

Figure S1. Related to Figure 1. SOX2 is not expressed in GABAergic interneurons and in the large majority of oligodendrocytes in dLG. (A-A') Immunofluorescence on coronal sections of dLG of mouse brain at P8 with anti-SOX2 (green) and anti-GAD67 (red) (a GABAergic interneuron marker), antibodies. SOX2 is not expressed in GABAergic interneurons in dLG (n=3). (B-B'') Immunofluorescence on coronal sections of dLG of mouse brain at P8 with anti-SOX2 (red) and anti-OLIG2 (green) (an oligodendroglial marker), antibodies. Sox2 is expressed in a few oligodendrocytes (arrows). (n=3). (C-D''') Immunofluorescence on coronal

sections of dLG at P8 of controls and Sox2 thalamic mutants with anti-SOX2 (green; C',D'), anti-NEUN (red; C",D") and anti-S100β (blue; C"',D"'). SOX2 expression in the mutant dLG is ablated in neurons (arrow heads) but remains in some S100β-positive cells (arrows) (control n=3, mutant n=3). Scale bars: 50μm (A,B-D"'), 10μm (A'). dLG, dorso lateral geniculate nucleus.

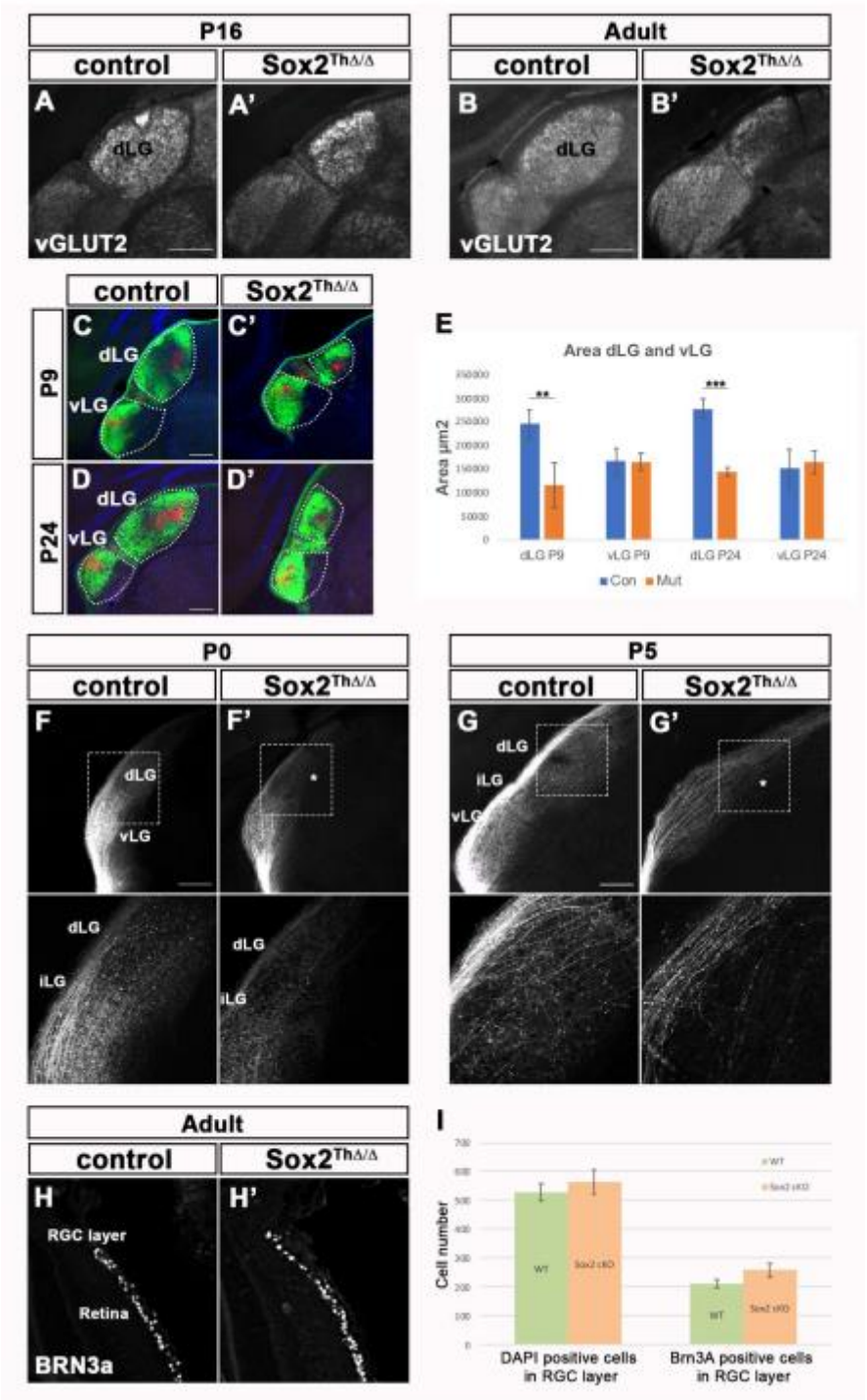
P16
control
Sox2ThΔ/Δ
A
A'
dLG
vGLUT2
Adult
control
Sox2ThΔ/Δ
B
B'
dLG
vGLUT2
control
Sox2ThΔ/Δ
P9
P24
C
C'
D
D'
dLG
vLG
E
Area dLG and vLG
Area µm2
**
***
dLG P9
vLG P9
dLG P24
vLG P24
Con
Mut
P0
control
Sox2ThΔ/Δ
F
F'
dLG
vLG
iLG
P5
control
Sox2ThΔ/Δ
G
G'
dLG
iLG
vLG
Adult
control
Sox2ThΔ/Δ
H
H'
RGC layer
Retina
BRN3a
I
Cell number
WT
Sox2 cKO
DAPI positive cells in RGC layer
Brn3A positive cells in RGC layer

Figure S2. Related to Figure 2 and Figure 3. Sox2 thalamic ablation affects the development of the dLG and retino-geniculate projections but not the final number of adult RGC. (A-B') Anti-vGLUT2 immunofluorescence on coronal sections of control and mutant dLG at P16 (control n=2, mutant n=2) (A,A') and in adult (control n=2, mutant n=2) (B,B') shows a reduction of retinal afferents and of the dLG size in Sox2 mutants. (C-E) Representative coronal vibratome sections used to measure dLG and vLG size at P9 and P24 in which retinal afferents had been marked with CTB. Dotted lines outline the dLG and vLG nuclei total area. (E) Histogram comparing the quantification of dLG and vLG areas in mutants and controls. The dLG size was reduced in Sox2 thalamic mutants at P9 (** $p<0.01$, unpaired Student's T-test, control n=3, mutant n=4) and P24 (*** $p<0.005$, unpaired Student's T-test, control n=3, mutant n=3), while vLG appears unchanged. Error bars represent standard deviation. (F-G') Tracing experiment by inserting DiI crystal in the eye at P0 (control n=3, mutant n=3) (F,F') and P5 (control n=2, mutant n=2) (G,G') shows a reduction and defasiculation of retinal axons (indicated by *) reaching the dLG in mutants (F',G') compared to controls (F,G). (H-I) Anti-BRN3A immunofluorescence on coronal sections of adult mutant and control retina marking retinal ganglion cells (RGC). (I) Quantification of RGC does not show any difference in number between controls and Sox2 mutants (n=3). Error bars represent standard deviation. Scale bars: 250µm (A-B', F-G'), 200 µm (C-D').

dLG, dorso lateral geniculate nucleus; vLG, ventro lateral geniculate nucleus; iLG, intermediate lateral geniculate nucleus; RGC, retinal ganglion cell.

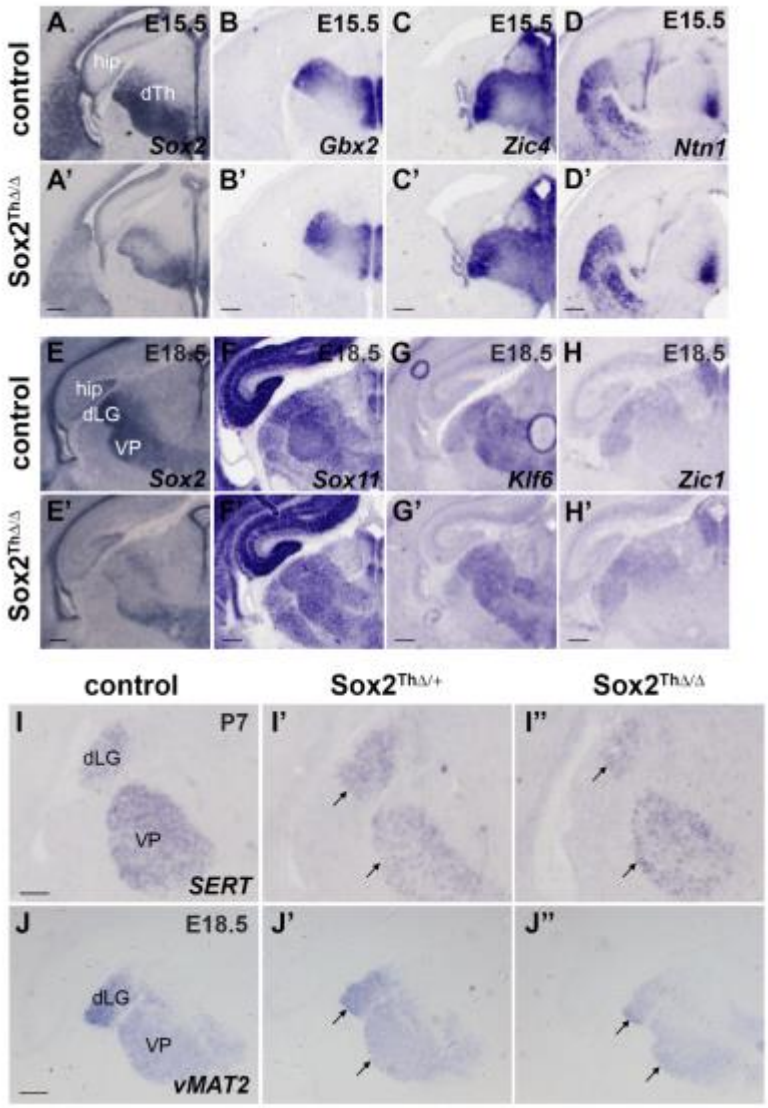

Figure S3. Related to Figure 5 and Figure 6. Expression of key regulators of the development of the visual system. (A-D') In situ hybridization on coronal sections of mutant and control mouse forebrains at E15.5 with Sox2, Gbx2, Zic4 and Netrin1 probes. (At least 3 controls and 2 mutants were analysed for each probe). (E-H') In situ hybridization on coronal sections of mutant and control mouse forebrains at E18.5 for Sox2, Sox11, Klf6 and Zic1 expression (At least 3 controls and 2 mutants were analysed for each probe).

(I-J") In situ hybridization on coronal sections of forebrains of Sox2 homozygote mutants, Sox2 heterozygotes and controls at P7 and E18.5 with the serotonin transporters SERT (control n=2, mutant n=3) (I-I") and vMAT2 (control n=9, mutant n=5) (J-J"). Arrows indicate SERT and vMAT downregulation in dLG (and VP). Scale bars 200µm. hip, hippocampus; dLG, dorso-lateral geniculate nucleus; VP, ventroposterior nucleus; dTh, dorsal thalamus

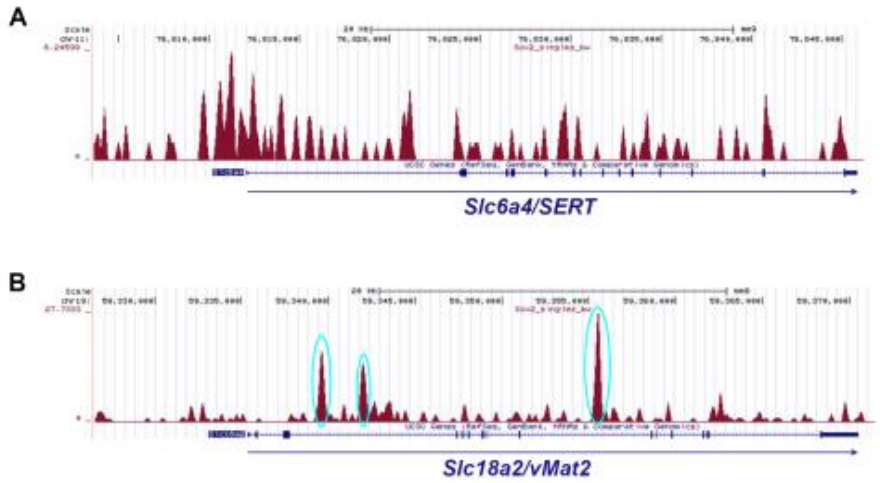

Figure S4. Related to Figure 6. SOX2 ChIPseq detects SOX2 binding to the SERT- and vMAT2-encoding genes. SOX2 ChIPseq profile from neurosphere cultures derived from postnatal mouse telencephalon across the Slc6a4/SERT locus (A) and the Slc18a2/vMAT2 locus (B) showing 3 SOX2 peaks in the Slc18a2/vMAT2 locus (blue circles). N.B. SOX2 binding to the Slc6a4/SERT locus was not detected by the peak calling algorithm. Note the different scale of the Y axis in A and B.

Transparent Methods

Mouse strains

Mutant mice (sex was indifferent) were obtained by crossing the following mouse lines: $Sox2^{Flox}$ (Favaro et al., 2009) with Rorα-Cre (Chou et al., 2013). The day of vaginal plug was defined as embryonic day 0 (E0) and the day of birth as postnatal day 0 (P0). Genotyping was performed with the following primers: Rorα-Cre IRES Forward: 5'AGGAATGCAAGGTCTGTTGAAT 3'; Rorα-Cre IRES Reverse: 5' TTTTTCAAAGGAAAACCACGTC 3'; Sox2 Flox Forward: 5'AAGGTACTGGGAAGGGACATTT 3'; Sox2 Flox Reverse: 5'AGGCTGAGTCGGGTCAATTA 3'

All procedures were in accordance with the European Communities Council Directive (2010/63/EU and 86/609/EEC) regulating animal research, and the Italian Law for Care and Use of Experimental Animals (DL26/14). They were approved by the Italian Ministry of Health (authorization no. 189/2016-PR to Prot. 29C09.4) and the Bioethics Subcommittee of Consejo Superior de Investigaciones Científicas (CSIC, Madrid, Spain) and the Comunidad de Madrid (protocol approval number PROEX 100/15; RD 53/2013).

In situ hybridization

In situ hybridization on sections was performed essentially as in (Cerrato et al., 2018). Briefly, embryonic brains and P0 brains were dissected and fixed overnight in paraformaldehyde 4% in PBS (Posphate Buffered Saline) (PFA 4%). For P1 brains and older, animals were first perfused with PFA 4% and brains were then extracted and fixed as above. The fixed tissue was cryoprotected in a series of sucrose

solutions in PBS (15%, 30%) and then embedded in OCT (Killik, Bio-Optica) and stored at -80°C. Brains were sectioned (20 µm) with a cryostat, placed on a slide (Super Frost Plus 09-OPLUS, Menzel) and stored at -80°C. Slides were then defrosted, fixed in formaldehyde 4% in PBS for 10 minutes (min), washed 3 times for 5 min in PBS, incubated for 10 min in acetylation solution (for 200 ml: 2.66 ml triethanolamine, 0.32 ml HCl 37%, 0.5 ml acetic anhydride 98%) with constant stirring and then washed 3 times for 5 min in PBS. Slides were placed in a humid chamber and covered with prehybridization solution (50% formamide, 5X SSC, 0.25 mg/ml tRNA, 5X Denhardt's, 0.5 µg/ml salmon sperm) for at least 2 hours (h) and then incubated in hybridization solution (fresh prehybridization solution containing the digoxygenin (DIG)-labelled RNA probe of interest) overnight at 65°C. Slides were washed 5 min in 5X SSC, incubated 2 times in 0.2X SSC for 30 min at 65°C, washed 5 min in 0.2X SSC at room temperature and then 5 min in Maleic Acid Buffer (MAB, 100 mM maleic acid, 150 mM NaCl pH 7.5). The slides were incubated in blocking solution (10% sheep serum, 2% blocking reagent (Roche), 0.3% Tween-20 in MAB) for at least 1 h at room temperature, then covered with fresh blocking solution containing anti-DIG antibody Roche © 1:2000 and finally placed overnight at 4°C. Slides were washed in MAB 3 times for 5 min, in NTMT solution (100 mM NaCl, 100 mM Tris-HCl pH 9.5, 50 mM MgCl2, 0.1% Tween-20) 2 times for 10 min and then placed in a humid chamber, covered with BM Purple (Roche), incubated at 37°C until desired staining was obtained (1-6 h), washed in water for 5 min, air dried and mounted with Eukitt (Sigma).

For in situ hybridization on whole mounts (WM), brains were dissected and fixed, after removing the meninges, in PFA 4% overnight at 4°C. Brains were dehydrated in a methanol series (25%, 50% in PBS, followed by 75% in water, 100%), and stored at -20°C until used. Brains were rehydrated at room temperature, and incubated in 6% H2O2 in PTW (1% Tween-20 in PBS) for 1 h at room temperature; they were washed two times for 15 min in PTW and then incubated with proteinase K (20 µg/ml) for 1 h. Brains were further washed two times quickly in PTW, post-fixed in 0.2% glutaraldehyde, 4% formaldehyde in PTW for 20 min at room temperature. Prehybridization (prehyb, 1 ml/brain) WM was then performed by incubating in prehyb WM solution (50% formamide, 5X SSC pH 4.5, 20% SDS, 500 µg/ml tRNA, 200 µg/ml BSA, 50 µg/ml heparin) for 2-3 h at 70°C (individually in closed glass or plastic vials in an oven). Solution was changed to 1 ml/brain hybridization WM solution (prehyb WM solution with added DIG-labelled RNA probe, final dilution of 1:50-1:100 starting from a 120 µl probe solution [20 µl standard probe synthesis reaction + 100 µl prehyb solution]) and incubated for 16-20 h at 70°C. Brains were then washed in solution X (2X SSC pH 4.5, 50% formamide, 1% SDS) at 70°C 4 times for 45 min each, then in MABT (Maleic Acid Buffer –see above- + 1% Tween 20), 3 times (10 min each) at room temperature. The buffer was then changed to blocking solution (10% sheep serum, 2% Roche © blocking reagent in MABT), and incubated for 2 h at room temperature. This was then replaced with anti-DIG solution (anti-DIG antibody Roche © 1:4000 in blocking solution) and incubated overnight at 4°C. Brains were transferred to 12-well plates (1 brain/well) and washed in MABT (3 washes of 10 min each, then 5 washes of 1h each,

and one overnight wash at 4°C), followed by incubation in NTMT WM buffer (100 mM NaCl, 100 mM Tris-HCl pH 9.5, 50 mM MgCl2, 1% Tween 20) at room temperature for two washes of 10 minutes each, and incubation at room temperature in the dark in NBT-BCIP colour reaction solution (3.5 µl NBT, 3.5 µl BCIP, per each ml of NTMT WM; about 3 ml per well), until signal appearance (usually about 2-6 h). The reaction was then blocked with TE stop buffer (10 mM TrisHcl pH 7.5, 10 mM EDTA pH 8), by 2 washes of at least 2 h at room temperature. To improve the signal/background ratio, brains were then cleared in glass vials with a sequence of the following solutions: PBS 2 times quickly, 50% methanol in PBS for 1 h, 100% methanol for 1 h 3 times, 1:1 volume methanol:clearing solution (1:2 volume benzyl alcohol, benzyl benzoate) for 1 h at room temperature, and finally in clearing solution overnight to one week, when tissue should show a clear and clean signal; then, the same washes were performed in reverse, until PBS. Brains were then photographed under a stereomicroscope.

The following DIG-labelled probes were used: *Sox2* (Favaro et al., 2009), *Lef1* (Muzio et al., 2005), *Efna5* (Huberman et al., 2005, Pfeiffenberger et al., 2005) (a gift from J. Flanagan and D. Feldheim, giving equivalent results), *Bhlhb5* (Alfano et al., 2014), *Lmo4* (Chou et al., 2013), *Nr2f1* (Armentano et al., 2007), *Sox11* (a gift from P. Sharpe), *SERT/Slc6a4* (Lebrand et al 1996) (a gift from P. Gaspar), *Semaphorin6A* (Kerjan et al., 2005), *Gbx2* (Li et al., 2002), Netrin1 (Livnat et al., 2010) and we cloned from brain cDNAs (E14.4 or P30 telencephalon) of *Zic1* (using primers from (Gaston-Massuet et al., 2005), *Zic4* (using primers from (Horng et al., 2009)), *NetrinG1, Klf6*

and *vMAT2/Slc18a2* (using the primers provided from http://portal.brain-map.org/).

Immunohistochemistry and cell counting

Immunohistochemistry with anti-vGLUT2 (rabbit polyclonal, Synaptic systems cat. no.135402, lot no. 135402/25, 1:1000), anti-serotonin (5HT) (rabbit polyclonal, Immunostar cat. no. 20080, 1:2000), and anti-SERT (rabbit polyclonal, Immunostar cat. no. 24330, 1:2000) antibodies on P1 and P8 brains was carried out on coronal cryostat sections (40 µm for P1 and 50 µm for P8) collected in 24-well plates filled with PBS. Immunohistochemistry with anti-vGLUT2 and anti-SERT antibodies was also carried out on tangential cryostat sections of P8 flattened cortices (50 µm) also collected in 24-well plates filled with PBS. Sections were washed in H2O2 3% in PBS for 15 min after quick washes in PBS they were incubated in PBS+ (PBS, gelatin 0.2%, Triton X-100 0.25%) for at least 1 h. PBS+ was replaced with PBS+ containing the antibody of interest and sections were incubated overnight at room temperature. Sections were washes 4 times in PBS+, 15 minutes each, and then incubated in PBS+ containing the biotinylated secondary antibody 1:200 (ABC Vector Kit Vectastain) 2 h at room temperature. Sections were washed 4 times, 15 min each, in PBS+, incubated with ABC working solution (ABC Vector Kit Vectastain) 1 h and 30 min at room temperature and then washed in PBS containing Triton X-100 0.25% 3 times, 15 min each and then left washing overnight at 4°C. They were washed in PBS, Triton X-100 0.25% for 15 min, then washed twice in PBS and finally incubated in Tris-HCl 0.05M pH 7.5 for 10 minutes. Sections were placed in DAB (3,3'-diamiobenzidine

tetrahydrochloride, Sigma) staining solution (DAB 0.075%, H2O2 0.002% in Tris-HCl 0.05M pH 7.5). When desired staining was obtained (usually after 10-30 min) the reaction was blocked with PBS washes. Sections were placed on slides (Super Frost Plus 09-OPLUS, Menzel), dried and mounted with Eukitt (Sigma). Immunofluorescence with anti-vGLUT2 and anti-5HT on P8 and P16 coronal cryostat sections was carried out essentially as above with the following alterations: the H2O2 treatment was skipped, sections were incubated with anti-rabbit Alexa 546 secondary antibody (Invitrogen 1:800) and after the PBS washes sections were directly mounted on slides with Fluormount (Sigma) containing DAPI. Retinal ganglion cell (RGC) counting was performed on cryostat sections (20µm) from enucleated eyes. Animals were perfused as described above and then eyes were enucleated maintaining a piece of the eye lid for orientation, post-fixed overnight at 4°C and cryoprotected in sucrose solutions and embedded in OCT, as described above. Sections were subjected to immunohistochemistry as described above using the RGC marker BRN3a (Santa Cruz; cat. no. SC-31984, lot no. D2915, 1:1000).

Selected free-floating P8 coronal vibratome sections (50µm thick) were blocked in PBS containing 1% bovine adult serum (BSA, Sigma) and 0.2% Triton-X 100 for 2 h and, subsequently, incubated overnight at 4°C with mouse or goat anti-Sox2 (R&D MAB 2018, 1:50 or R&D AF2018, 1:200) combined with one of the following antibodies: guinea pig anti-NEUN (Chemicon, Temecula, CA, USA,1:2000), rabbit anti-S100β (Dako, Glostrup, Denmark. 1:1000), goat anti-GAD67 (R&D, 1:200), mouse anti-OLIG2 (Merk Millipore, Billerica, Mass, USA;1:500). After PBS washes, sections were incubated for 2 h in a

mixture of the corresponding indo-carbocyanine Cy3 or Cy2-conjugated secondary antibodies (Jackson ImmunoResearch Laboratories, West Grove, Pa., USA; 1:600). Sections were then counterstained with 4,6-diamidino-2-phenylindole (DAPI; Molecular Probes, Eugene, OR, USA; 1:1000), mounted with Fluorsave (Calbiochem, San Diego, CA, USA), and imaged with a confocal microscope D-Eclipse C1 (Nikon, Tokyo, Japan). Confocal images were acquired using small pinhole aperture size and low gain and offset to prevent saturation and imported into Adobe Photoshop CS5 (Adobe Systems Incorporated, San Jose, CA, USA) after adjustment of contrast and brightness. The number of dLGN NEUN-positive neurons and S100β-positive glial cells and those double stained with SOX2 was counted using images taken at 40X magnification from 3 sections along rostro-caudal extent of dLGN from each mouse (3 control and 3 mutant mice). Data were statistically analysed using two sample t-test ($p<0,05$) or Mann-Whitney test ($p<0,001$), after applying Shapiro-Wilk normality test.

Labelling of retino-geniculate projections

$Sox2^{Th\Delta/\Delta}$ mutants and controls were perfused (P0, P5), heads were post-fixed in PFA4% overnight at 4°C and then washed 3 times in PBS. DiI crystals (Invitrogen) were inserted in the optic disc in one eye and then incubated at 37°C in PBS containing PFA 0.1% for 1-2 weeks essentially as described in (Sanchez-Arrones et al., 2013). Brains were dissected, embedded in 4% agarose, sectioned with a vibratome (70µm), mounted on glass slides with Fluormount (Sigma) containing DAPI and imaged with an epifluorescence microscope (Nikon).

To label retino-geniculate projection with a different, more rapid method, $Sox2^{Th\Delta/\Delta}$ mutants and controls (P0, P7 and P21) were anesthetized and cholera-toxin subunit B (CTB) conjugated to a fluorochrome (Life Technologies) was injected in each eye, CTB-Alexa 488 (green) in the right and CTB-Alexa 594 (red) in the left eye as described in (Sanchez-Arrones et al., 2013). After 24-72 h mice were perfused, brains were dissected, embedded in 4% agarose, sectioned with a vibratome (70µm), mounted on glass slides with Fluormount (Sigma) containing DAPI and imaged with an epifluorescence or confocal microscopy (Nikon).

Labelling of cortico-thalamic projections

$Sox2^{Th\Delta/\Delta}$ mutants and controls were perfused at P8, brains were dissected, fixed in PFA 4% overnight at 4°C and then washed 3 times in PBS. DiI and DiA crystals (Invitrogen) were inserted in the primary visual and primary somatosensory area, respectively. Brains were incubated at 37°C in PFA 4% for 4 weeks and then embedded in 4% agarose, sectioned with a vibratome (70µm), mounted on slides with Fluormount (Sigma) containing DAPI and imaged with an epifluorescence microscope (Nikon). DiA staining in the VP was observed in 100% of controls and mutants while DiI staining in the dLG was observed in 60% of controls and 10% of mutants.

Quantification of projections to LG

Images were taken with a confocal microscope (Nikon), two or three central sections of each brain were analysed, stacks of 30 µm were generated for each section and Image J was used to reduce background

with a rolling ball filter of 250 pixels. The LG (lateral geniculate) was thresholded in an unbiased way, using the default function of ImageJ, to generate a binary image that resembles the original unthresholded contralateral (CL) and ipsilateral (IL) projections. The percentage of CL or IL projections reaching the dLG or vLG was calculated on the thresholded images (es. area CL projections in dLG/area total CL projections in LG x 100). DAPI staining of each section was used to help define the borders of the dLG and vLG. The area of the dLG and vLG was measured on these sections with ImageJ. Data are represented as mean ± standard deviation and were statistically analyzed using unpaired Student's T-test, ** $p<0.01$, *** $p<0.005$, after applying Shapiro-Wilk normality test.

ChIP-seq

ChIPseq was performed on neural stem/progenitor cell cultures (neurospheres) obtained from six P0 forebrains (Favaro et al., 2009, Zhang et al., 2013). Briefly, cells were collected as small neurospheres and fixed sequentially with di(N-succimidyl) glutarate and 1% formaldehyde in phosphate-buffered saline and then lysed, sonicated and immunoprecipitated as described previously (Mateo et al., 2015). SOX2 was immunoprecipitated with 3 mg of goat anti-SOX2 (Santa Cruz sc-17320). DNA libraries were prepared from 10 ng of immunoprecipitated DNA and 10 ng of input DNA control, according to the standard Illumina ChIP-seq protocol. Libraries were sequenced with the Genome Analyzer IIx (Illumina). The raw reads were mapped to the mouse genome (mm9 including random chromosomes) with Bowtie version 0.12.5. We used MACS (Zhang et al., 2008) version

2.0.9 to define Sox2 bound regions (peaks). The details and global features of this SOX2 ChIPseq analysis are reported in (Bertolini et al., 2019)

Luciferase constructs

The Efna5 SOX2-bound 3' region (1178 bp) was amplified by PCR from genomic DNA with the following primers: Forward (XhoI) 5' ATATCTCGAGTGAAACCAAATAACGGCAGACT 3' (added XhoI site underlined); Reverse (SacI) 5' ATATGAGCTCTGTAAGTCATCTAGGCATGGAGA 3' (added SacI site underlined). The Efna5 SOX2-bound 5' region (826 bp) was amplified by PCR with the following primers: Forward (XhoI) ATATCTCGAGGGGAGAGCGGTTATTCTGGAAC (added XhoI site underlined) Reverse (SacI) ATATGAGCTCCTGCAATGACATTCTGGGCAGA (added SacI site underlined). The 3' and 5' Sox2-bound regions of Efna5 were cloned upstream of the minimal TK promoter into the SacI and XhoI-digested TK-LUC vector (Mariani et al., 2012) to generate 3' peak-luciferase and 5' peak-luciferase plasmids respectively.

Transfections

Transfections were performed essentially as described in (Panaliappan et al., 2018). Neuro-2a cells (1.5x105 cells/well) were plated in 12-well plates in 1 ml of MEM (Sigma) supplemented with 10% foetal bovine serum, 1% L-glutamine, 1% penicillin and streptomycin, and transfected after 24 h with LipofectamineR 2000 Reagent (Invitrogen). Medium in each well was replaced with 1 ml of MEM medium (with

no additions) mixed with 2 µl of Lipofectamine 2000 and DNA. We used a fixed amount of 300 ng of luciferase reporter plasmids (3'peak-Luciferase, or 5'peak-Luciferase) and increasing amounts of Sox2-expressing vector (Favaro et al., 2009). pBluescript was added to each transfection to equalize total DNA to 800 ng. We used the Nkx2.1-luciferase construct (Ferri et al., 2013) as a positive control of Sox2 activation. We used the following molar ratios of peak-luciferase vector: Sox2 expressing vector: 1: 0.06 (+), 1:0.125 (++), 1:0.187 (+++), 1:0.250 (++++), 1:0.50 (+++++). After 24 h cells were washed with PBS and lysed with Lysis Buffer 1x (Promega) for 20 min on a rocker. The cells were then subjected to a freeze-thaw cycle (20 min at -80°C and 20 min at 37°C) and lysates were collected and centrifuged at 4°C for 1 min at 13000 rpm. Luciferase activity was measured with the Dual LuciferaseR Reporter Assay System (Promega) according to the provided instructions by using the Glomax luminometer. Results, represented in histograms as percentage of luciferase activity, are the mean of three independent transfections in triplicate. Error bars represent standard deviation. The activity of Nkx2.1-luciferase co-transfected with Sox2 was set = 100%.

References

Alfano, C., Magrinelli, E., Harb, K. & Studer, M. 2014. The nuclear receptors COUP-TF: a long-lasting experience in forebrain assembly. Cell Mol Life Sci, 71, 43-62.

Armentano, M., Chou, S. J., Tomassy, G. S., Leingartner, A., O'leary, D. D. & Studer, M. 2007. COUP-TFI regulates the balance of cortical patterning between frontal/motor and sensory areas. Nature neuroscience, 10, 1277-86.

Bertolini, J. A., Favaro, R., Zhu, Y., Pagin, M., Ngan, C. Y., Wong, C. H., Tjong, H., Vermunt, M. W., Martynoga, B., Barone, C., Mariani, J., Cardozo, M. J., Tabanera, N., Zambelli, F., Mercurio, S., Ottolenghi, S., Robson, P., Creyghton, M. P., Bovolenta, P., Pavesi, G., Guillemot, F., Nicolis, S. K. & Wei, C. L. 2019. Mapping the Global Chromatin Connectivity Network for Sox2 Function in Neural Stem Cell Maintenance. Cell Stem Cell, 24, 462-476 e6.

Cerrato, V., Mercurio, S., Leto, K., Fuca, E., Hoxha, E., Bottes, S., Pagin, M., Milanese, M., Ngan, C. Y., Concina, G., Ottolenghi, S., Wei, C. L., Bonanno, G., Pavesi, G., Tempia, F., Buffo, A. & Nicolis, S. K. 2018. Sox2 conditional mutation in mouse causes ataxic symptoms, cerebellar vermis hypoplasia, and postnatal defects of Bergmann glia. Glia.

Chou, S. J., Babot, Z., Leingartner, A., Studer, M., Nakagawa, Y. & O'leary, D. D. 2013. Geniculocortical input drives genetic distinctions between primary and higher-order visual areas. Science, 340, 1239-42.

Favaro, R., Valotta, M., Ferri, A. L., Latorre, E., Mariani, J., Giachino, C., Lancini, C., Tosetti, V., Ottolenghi, S., Taylor, V. & Nicolis, S. K. 2009. Hippocampal development and neural stem cell maintenance require Sox2-dependent regulation of Shh. Nature neuroscience, 12, 1248-56.

Ferri, A., Favaro, R., Beccari, L., Bertolini, J., Mercurio, S., Nieto-Lopez, F., Verzeroli, C., La Regina, F., De Pietri Tonelli, D., Ottolenghi, S., Bovolenta, P. & Nicolis, S. K. 2013. Sox2 is required for embryonic development of the

ventral telencephalon through the activation of the ventral determinants Nkx2.1 and Shh. Development, 140, 1250-61.

Gaston-Massuet, C., Henderson, D. J., Greene, N. D. & Copp, A. J. 2005. Zic4, a zinc-finger transcription factor, is expressed in the developing mouse nervous system. Dev Dyn, 233, 1110-5.

Horng, S., Kreiman, G., Ellsworth, C., Page, D., Blank, M., Millen, K. & Sur, M. 2009. Differential gene expression in the developing lateral geniculate nucleus and medial geniculate nucleus reveals novel roles for Zic4 and Foxp2 in visual and auditory pathway development. J Neurosci, 29, 13672-83.

Huberman, A. D., Murray, K. D., Warland, D. K., Feldheim, D. A. & Chapman, B. 2005. Ephrin-As mediate targeting of eye-specific projections to the lateral geniculate nucleus. Nat Neurosci, 8, 1013-21.

Kerjan, G., Dolan, J., Haumaitre, C., Schneider-Maunoury, S., Fujisawa, H., Mitchell, K. J. & Chedotal, A. 2005. The transmembrane semaphorin Sema6A controls cerebellar granule cell migration. Nat Neurosci, 8, 1516-24.

Li, J. Y., Lao, Z. & Joyner, A. L. 2002. Changing requirements for Gbx2 in development of the cerebellum and maintenance of the mid/hindbrain organizer. Neuron, 36, 31-43.

Livnat, I., Finkelshtein, D., Ghosh, I., Arai, H. & Reiner, O. 2010. PAF-AH Catalytic Subunits Modulate the Wnt Pathway in Developing GABAergic Neurons. Front Cell Neurosci, 4.

Mariani, J., Favaro, R., Lancini, C., Vaccari, G., Ferri, A. L., Bertolini, J., Tonoli, D., Latorre, E., Caccia, R., Ronchi, A., Ottolenghi, S., Miyagi, S.,

Okuda, A., Zappavigna, V. & Nicolis, S. K. 2012. Emx2 is a dose-dependent negative regulator of Sox2 telencephalic enhancers. Nucleic Acids Res, 40, 6461-76.

Mateo, J. L., Van Den Berg, D. L., Haeussler, M., Drechsel, D., Gaber, Z. B., Castro, D. S., Robson, P., Crawford, G. E., Flicek, P., Ettwiller, L., Wittbrodt, J., Guillemot, F. & Martynoga, B. 2015. Characterization of the neural stem cell gene regulatory network identifies OLIG2 as a multifunctional regulator of self-renewal. Genome Res, 25, 41-56.

Muzio, L., Soria, J. M., Pannese, M., Piccolo, S. & Mallamaci, A. 2005. A mutually stimulating loop involving emx2 and canonical wnt signalling specifically promotes expansion of occipital cortex and hippocampus. Cereb Cortex, 15, 2021-8.

Panaliappan, T. K., Wittmann, W., Jidigam, V. K., Mercurio, S., Bertolini, J. A., Sghari, S., Bose, R., Patthey, C., Nicolis, S. K. & Gunhaga, L. 2018. Sox2 is required for olfactory pit formation and olfactory neurogenesis through BMP restriction and Hes5 upregulation. Development, 145.

Pfeiffenberger, C., Cutforth, T., Woods, G., Yamada, J., Renteria, R. C., Copenhagen, D. R., Flanagan, J. G. & Feldheim, D. A. 2005. Ephrin-As and neural activity are required for eye-specific patterning during retinogeniculate mapping. Nat Neurosci, 8, 1022-7.

Sanchez-Arrones, L., Nieto-Lopez, F., Sanchez-Camacho, C., Carreres, M. I., Herrera, E., Okada, A. & Bovolenta, P. 2013. Shh/Boc signaling is required for sustained generation of ipsilateral projecting ganglion cells in the mouse retina. J Neurosci, 33, 8596-607.

Zhang, Y., Liu, T., Meyer, C. A., Eeckhoute, J., Johnson, D. S., Bernstein, B. E., Nusbaum, C., Myers, R. M., Brown, M., Li, W. & Liu, X. S. 2008. Model-based analysis of ChIP-Seq (MACS). Genome Biol, 9, R137.

Zhang, Y., Wong, C. H., Birnbaum, R. Y., Li, G., Favaro, R., Ngan, C. Y., Lim, J., Tai, E., Poh, H. M., Wong, E., Mulawadi, F. H., Sung, W. K., Nicolis, S., Ahituv, N., Ruan, Y. & Wei, C. L. 2013. Chromatin connectivity maps reveal dynamic promoter-enhancer long-range associations. Nature, 504, 306-10.

CHAPTER 3

Characterization of Sox2 and COUP-TF1 targets in the dLGN

Linda Serra[1], Federico Zambelli[3], Giulio Pavesi[3], Michèle Studer[2], Silvia Nicolis[1], Sara Mercurio[1]

[1]Department of Biotechnology and Biosciences, University of Milano-Bicocca, piazza della Scienza 2, 20126 Milano, Italy

[2]Université Côte d'Azur, CNRS, Inserm, iBV, Nice, France

[3]Department of Biosciences, University of Milano, 20133 Milano, Italy

Ongoing work

Introduction

As shown in Chapter 2, Sox2 is required for the correct development of the visual system. In fact, *Sox2* conditional ablation in specific nuclei of the dorsal thalamus (dLGN, VPN and MGN), when thalamic neurons are already post-mitotic, strongly affects the development of the dLGN, neuronal projections that connect the eye, the thalamus and the visual cortex and, consequently, visual cortical patterning. We identified, by candidate gene approach, the axon guidance molecule *EphrinA5* and the two serotonin transporters *SERT* and *V-MAT2* to be downregulated in the dLGN when Sox2 is deleted.

Interestingly, the phenotype we observed in *Sox2* thalamic mutants is highly similar to that described in *COUP-TF1* thalamic mutants, where *COUP-TF1* gene is specifically ablated in post-mitotic neurons of the dLGN with the same Cre recombinase (Chou et al., 2013). Therefore, I started to investigate if these two transcription factors are expressed in the same post-mitotic thalamic neurons and if they could belong to the same genetic pathway and potentially regulate each others' expression. Finally, we investigated by a genome wide approach the gene expression profile of *Sox2*-ablated dLGNs to elucidate how Sox2 regulates the establishment of the visual axis.

Results

Sox2 and COUP-TF1 are co-expressed in the same cells of the dLGN but they don't regulate each other's expression

Sox2 and *COUP-TF1* are expressed in the three components of the visual system (the eye, the dLGN and the cortex) and their individual thalamic conditional knock-out leads to similar developmental defects

in the formation of the visual axis. To understand if the two transcription factors are expressed in the same cells of the dLGN we analysed SOX2 and COUP-TF1 expression in the dLGN by immunohistochemistry. We interestingly found that SOX2 and COUP-TF1 are localized in the same neurons already at birth (P0) (Figure 1A) and that they keep being co-expressed in the dLGN also at postnatal day 8 (P8) (Figure 1B) (in collaboration with Dr. Carolina Frassoni at the Istituto Neurologico Carlo Besta).

This observation raised the hypothesis that Sox2 and COUP-TF1 could regulate each other's expression during the development of the visual thalamus. In particular, we first hypothesized that Sox2 could be upstream of COUP-TF1 in the dLGN and that, after Sox2 loss, COUP-TF1 deregulation at the RNA level could lead to the observed defects. Thus, we looked, by in situ hybridization, at the expression of *COUP-TF1* in Sox2 thalamic mutants at embryonic day 18.5 (E18.5), a stage in which the dLGN size is still comparable between control and mutant mice. Surprisingly, no changes in *COUP-TF1* expression were detected in the dLGN when *Sox2* is ablated (Figure 2A). We then hypothesized that COUP-TF1 could be upstream of Sox2 during the development of the dLGN, but when we analysed the expression of *Sox2* in *COUP-TF1* thalamic mutants by in situ hybridization, at the same developmental stage, we did not observe any significant change in its expression (Figure 2B).

Could genes downregulated in *Sox2* thalamic mutant be also downregulated in *COUP-TF1* thalamic mutants?

On the basis of these observations, it is plausible that the two transcription factors co-regulate target genes during the development of the visual system.

Therefore, I analyzed in *COUP-TF1* thalamic mutants the expression of *EphrinA5* and *V-MAT2* genes, that are downregulated in *Sox2* thalamic mutants (see Chapter 2). We observed that *EphrinA5* and *V-MAT2* expression is not reduced in *COUPTF1* mutants. On the contrary, their expression appears upregulated in the mutant dLGN (Figure 2C).

These observations could be consistent with the idea that SOX2 and COUP-TF1 regulate common target genes, but in an opposite manner; thus, Sox2 positevely regulates the expression of the two genes analysed, while COUP-TF1 seems to negatively regulate them, in fact their expression is increased when *COUP-TF1* is ablated.

RNA sequencing from *Sox2* thalamic mutants reveals a wide set of deregulated genes.

To shed light on the developmental defects observed in the two different mutants we need to understand what happens to dLGN neurons' gene expression patterns, when *Sox2* and *COUP-TF1* are ablated, from an unbiased point of view.

We started with gene expression analyses on *Sox2* thalamic mutants. As shown in Chapter 2 we found *Efna5*, *SERT* and *V-MAT2* genes to be downregulated in the dLGN by candidate gene approach, looking for genes whose knock-out leads to phenotypes similar to the ones we observe in our Sox2 mutants. However, these three downregulated genes do not tell the whole story. Therefore, we looked at gene

expression in differentiated neurons of the dLGN of *Sox2* mutants and control siblings by a genome-wide approach. Indeed, we performed whole-tissue RNA sequencing at postnatal day 0 (P0), when dLGN size is still comparable between control and mutant mice; in this way we can identify deregulated genes before the phenotype appears and that, consequently, can be responsible of the developmental defects observed.

Differential analyses of cellular transcripts revealed several deregulated genes in the mutant dLGN, both downregulated and upregulated compared to control mice. *COUP-TF1* is highly expressed in the dLGN but it is not differentially expressed in *Sox2* mutants as we observed by in situ hybridization. Instead, *Efna5*, *SERT* and *V-MAT2* are among the most downregulated genes, confirming what we observed by in situ hybridization on brain sections and indicating that the experiment perfectly worked (Figure 3). Among the most downregulated genes we found also *Gbx2*, a transcription factor known to have a crucial role in the development and organization of the thalamus and *Lef1*, a downstream mediator of the Wnt/β-catenin signalling pathway (Figure 3).

We found several categories enrinched within genes downregulated in the mutant dLGN, for example glutamatergic synapse, axon guidance, calcium signalling pathway, dopaminergic-colinergic-GABAergic-serotonergic synapses, as shown in Figure 4. In addition, downregulated genes are involved in several important biological processes such as neurogenesis, neuronal differentiation, cell projection organization, cell-cell signalling and synapse signalling. Importantly, among the most downregulated genes are a lot of members of the Eph-Ephrins family,

indicating strong defective guidance cues pathways and several glutamate receptors, indicating that synaptic transmission activity is highly affected.

We also identified genes whose expression is significantly upregulated in the mutants. Some of the categories enrinched within genes upregulated in the mutant dLGN are for example the calcium signalling pathway, neuroactive ligand-receptor interaction and axon guidance, as shown in Figure 5.

Thus, RNA sequencing revealed several genes related to axon guidance and connectivity but many others that, until now, are not involved in these processes. The identification of genes whose activity is not previously related to these processes could allow us to discover something new about the development and connectivity of the different components of the visual system.

Conclusions

Our gene expression analyses reveals that the transcription factors Sox2 and COUP-TF1, in the visual thalamus, don't regulate each other and suggest that they could regulate common targets but maybe in opposite ways. RNA sequencing from *Sox2* mutant dLGN revealed many deregulated genes that will help us to deeply understand what happens in the visual system development when it is ablated. Currently, we are performing RNA sequencing also on *COUP-TF1* thalamic mutants, in order to identify deregulated genes that we will compare to Sox2 RNA sequencing data. The combination of the two datasets will identify potential common target genes in the development of the visual system.

Moreover, we generated double mutant mice, lacking both *Sox2* and *COUP-TF1* genes in the dorsal thalamus, in order to see what happens to the dLGN, the neuronal projections between the eye-thalamus-cortex, and to the visual cortex itself when both transcription factors are deleted in the dLGN.

Materials and methods

Mouse strains

Sox2 mutant mice were obtained by crossing the following mouse lines: Sox2Flox (Favaro et al., 2009) with Rorα-Cre (Chou et al., 2013). Genotyping was performed with the following primers: Rorα-Cre IRES Forward: 5'AGGAATGCAAGGTCTGTTGAAT 3'; Rorα-Cre IRES Reverse: 5' TTTTTCAAAGGAAAACCACGTC 3'; Sox2 Flox Forward: 5'AAGGTACTGGGAAGGGACATTT 3'; Sox2 Flox Reverse: 5'AGGCTGAGTCGGGTCAATTA 3'.

COUP-TF1 mutant mice were generated by crossing the following mouse lines: COUP-TF1Flox (Armentano et al., 2007) with Rorα-Cre (Chou et al., 2013). Genotyping was performed with the following primers: Rorα-Cre IRES Forward: 5'AGGAATGCAAGGTCTGTTGAAT 3'; Rorα-Cre IRES Reverse: 5' TTTTTCAAAGGAAAACCACGTC 3'; COUP-TF1 Flox Forward 5'-CTGCTGTAGGAATCCTGTCTC-3'; COUP-TF1 Flox Reverse: 5'-AATCCTCCTCGGTGAGAGTGG-3' and 5'–AAGCAATTTGGCTTCCCCTGG-3'

The day of vaginal plug was defined as embryonic day 0 (E0) and the day of birth as postnatal day 0 (P0).

In situ hybridization on cryostat sections

In situ hybridization on cryostat sections of COUP-TF1 controls and thalamic mutants was performed by using the same protocol described in detail in Chapter 2. The following DIG-labelled probes were used: *Sox2* (Favaro et al., 2009), *Efna5* (Huberman et al., 2005, Pfeiffenberger et al., 2005), *Nr2f1* (Armentano et al., 2007), and we cloned from brain cDNA (E14.4 or P30 telencephalon) *vMAT2/Slc18a2* (using the primers provided from http://portal.brain-map.org/).

Immunohistochemistry on cryostat sections

Slides were washed 2x 10 minutes in PBS1x and then unmasked in Na Citrate 0.1M-Citric acid 0.1M pH6 solution for 2 minutes. Sections were washed in PBS1x for 10 minutes and incubated for at least 1 h with pre-blocking solution (Sheep serum 5%, Tween-20 0,3% in PBS1x) at room temperature. Sections were then incubated over night at 4°C in blocking solution (Sheep serum 1%, Tween-20 0,1% in PBS1x) in which primary antibodies were diluted. I used the following primary antibodies: anti-Sox2 diluted 1:500 (R&D AB2018, mouse) and anti-COUPTF1 diluted 1:1000 (Abcam Ab181137, rabbit). Sections were then washed 2x 10 minutes in PBS1x and incubated for at least 1h at room temperature with blocking solution in which I diluted the following fluorescent secondary antibodies: anti-mouse IgG Alexa Fluor 488 and anti-rabbit IgG Alexa Fluor 594 (Termo Fisher scientific) diluted 1:500. Slides were then washed 2x 10 minutes in PBS1x and mounted.

Brain extraction and dissection for RNA-sequencing Brains from Sox2 control and mutant puppies at postnatal day 0 (P0) were removed from the skulls in ice-cold PBS1x, coronally embedded in low melt agarose 4%/PBS1x and kept on ice. Brains were then sectioned in ice-cold and sterile PBS1x by using the vibratome (Leica VT1000s) keeping the ice all around, and we obtained 200µm brain sections that we collected in ice cold PBS1x. We selected the sections in which we could see by morphology the dLGN under a stereoscopic microscope, we placed them on a glass slides on drops of ice cold PBS1x and quickly dissected dLGNs with sterile chirurgic scalpels (Paragon 15T). We dissected dLGNs from two sequencial sections. Excised dLGNs were picked up with a pipette, collected in sterile tubes, snap-frozen in liquid nitrogen and stored at -80°C until RNA extraction. We took pictures of all the sections before and after the dissection of dLGNs.

RNA extraction and RNA sequencing

To obtain high quality RNA from small amounts of fresh brain tissue (each dLGN has a total weight of about 0,3 mg) total RNA from snap-frozen dLGNs was extracted with the RNeasy Micro Kit (QIAGEN) with some precautions. dLGNs samples were taken out from the -80°C and left a few seconds on the bench before tissue homogenization. Each dLGN sample was homogenized in 350 µl of RLT buffer, containing β-mercaptoethanol (β-ME) as indicated by the kit protocol (10 µl of β-ME per 1 ml of RLT buffer). The homogenization of the tissue was carried out trough sequential passages in syringe and needles of descending diameter. Precisely, we used a 1cc syringe and three different sterile needles: 18G, 22G and 26G. First, the tissue was passed

10 times through the larger diameter needle (18G), then 10 times through the intermediate diameter needle (22G) and finally 10-12 times through the thinnest one (26G), in order to correctly lysate and disrupt the tissue. Subsequently, the homogenized sample was vortexed for 30 seconds and centrifuged for 3 minutes at 13200 rpm to pellet the debris. An equal volume of fresh ethanol 70% was added to the homogenized supernatant. The sample was well mixed and quickly applied to the RNeasy MinElute Spin Column provided by the kit. The column was then centrifuged for 1 minute at 13000 rpm at room temperature to let the RNA bind the column membrane, and the eluate was discarded by pipetting. The column was then washed with 350 µl of RW1 buffer (by turning it between the fingers) and then centrifuged for 15 seconds at 13000rpm. After discarding the flow-through with a pipette, the sample was incubated with 80 µl DNase I digestion mix (10 µl of DNAse I + 70 µl of buffer RRD) for 15 minutes at room temperature. After that the column was washed with 350 µl of RW1 buffer (by turning it between the fingers) and then centrifuged for 15 seconds at 13000rpm. 500 µl of RPE buffer was pipetted onto the membrane where the RNA is still bound, and the column was rotated between the fingers for 2 minutes, in order to properly remove all the potential contaminants from the tube walls. After 1minute spin at 13000 rpm, the column was washed again with 500 µl of RPE buffer and centrifuged for 1 minute at the same speed; subsequently it was washed with fresh ethanol 80% (turning the column between the fingers) and centrifuged for 2 minutes at 13000 rpm. The column was centrifuged with the cap open for 5 minutes at maximum speed, to let the ethanol completely evaporate. Finally, 14 µl of RNase-free water were pipetted on the membrane and, after 1 minute

on the bench, the sample was centrifuged for 1 minute at 13200 rpm to elute the RNA.

RNA sequencing experiment was performed on triplicates for the two genotypes studied - controls and Sox2 thalamic mutants – and each sample was composed of dLGNs coming from three animals of the same genotype pulled together. For each sample sequenced we obtained at least 150 ng of high quality total RNA (RIN ≥ 8), and thus 150 ng were used for library preparation. Library preparation was performed with Nugen Universal + mRNAseq kit, followed by sequencing in a HiSeq 4000 (Illumina), paired-reads 2x 75 bp.The KEGG 2019 Mouse database was used to analyse RNA-sequencing data.

Figures

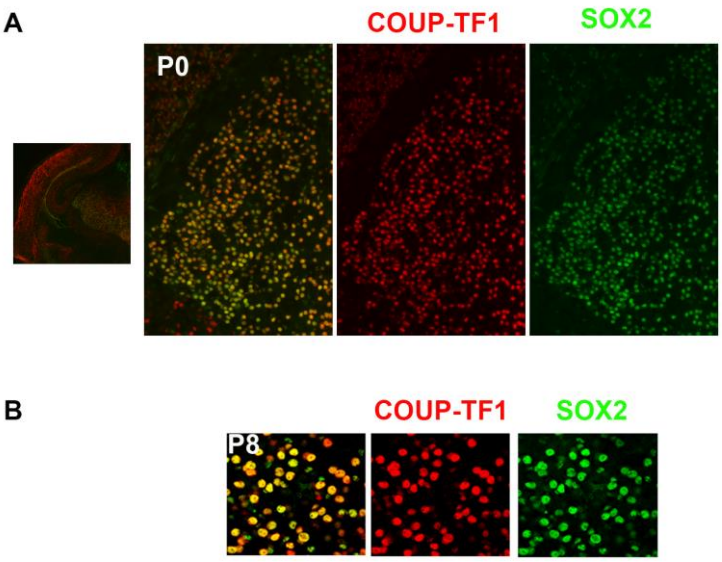

Figure 1. SOX2 and COUP-TF1 are largely co-localized in the same cells of the dLGN. A) Immunohistochemistry on mouse brain section at P0 show that COUP-TF1 (red) and SOX2 (green) are co-expressed in the majority of dLGN cells. B) Immunohistochemistry on mouse brain section at P8 show that SOX2 (green) and COUP-TF1 (red) are still co-expressed in the dLGN.

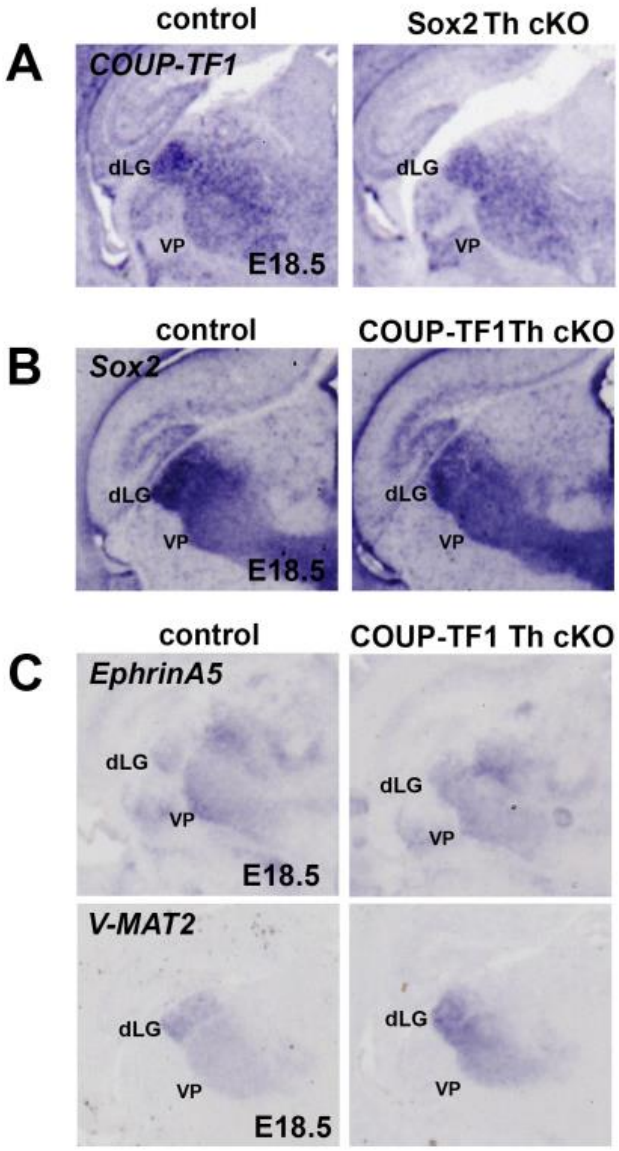

Figure 2. Sox2 and COUP-TF1 don't regulate each other. A) ISH on brain sections at E18.5 reveals that *COUP-TF1* expression is unchanged in *Sox2* thalamic mutants (Sox2 Th cKO). B) ISH on brain sections at E18.5 reveals tha *Sox2* expression is unchanged in *COUP-TF1* thalamic mutants (COUP-TF1 Th cKO). C) ISH for *EhprinA5* and *V-MAT2* on controls and *COUP-TF1*

thalamic mutants reveals that the two genes are upregulated in mutants at embryonic day 18.5 (E18.5) compared to controls.

Gene	Average expression	Log fold change	P value	FDR
Sox2	216,1467	-1,638069788	2E-33	7,544E-31
vMAT2	141,5283	-2,861570057	4E-70	1,71E-66
Efna5	24,8133	-2,044844104	3E-45	2,517E-42
SERT	39,9333	-1,399855218	2E-24	3,292E-22
Gbx2	38,6117	-1,333927794	6E-23	1,039E-20
Lef1	111,1667	-1,189744934	1E-19	1,774E-17

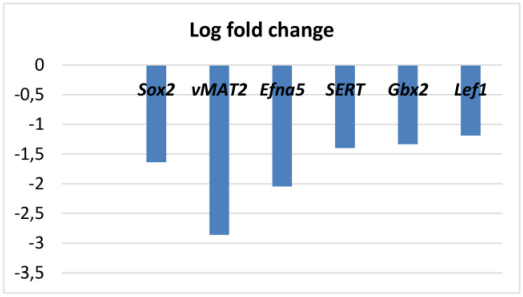

Figure 3. *V-MAT2, SERT* and *EphrinA5* are found downregulated in Sox2 thalamic mutants by RNA sequencing. In the table the gene average expression between controls and mutants, the differential expression (log fold change) and the statistical significance are reported.

Index	Name	P-value	Adjusted p-value	Odds Ratio	Combined score
1	Glutamatergic synapse	1.153e-9	3.493e-7	4.29	88.34
2	Axon guidance	7.610e-7	0.0001153	2.94	41.49
3	Calcium signaling pathway	0.000001952	0.0001971	2.80	36.87
4	MAPK signaling pathway	0.000003236	0.0002451	2.36	29.80
5	Dopaminergic synapse	0.000009530	0.0004125	3.02	34.92
6	Glycosaminoglycan biosynthesis	0.000007498	0.0004544	4.62	54.47
7	Cholinergic synapse	0.000009476	0.0004785	3.25	37.56
8	Oxytocin signaling pathway	0.00002113	0.0008003	2.78	29.93
9	Circadian entrainment	0.00009304	0.003132	3.09	28.67
10	GABAergic synapse	0.0001183	0.003583	3.17	28.68
11	Serotonergic synapse	0.0002533	0.006976	2.63	21.74
12	Dilated cardiomyopathy (DCM)	0.0004328	0.01093	2.94	22.81
13	Arrhythmogenic right ventricular cardiomyopathy (ARVC)	0.0007255	0.01570	3.11	22.52
14	Mannose type O-glycan biosynthesis	0.0006740	0.01571	5.32	38.84
15	Insulin secretion	0.0009730	0.01843	2.84	19.73
16	Hypertrophic cardiomyopathy (HCM)	0.0009730	0.01965	2.84	19.73
17	Retrograde endocannabinoid signaling	0.001118	0.01992	2.31	15.70
18	Morphine addiction	0.001766	0.02816	2.66	16.86
19	Amphetamine addiction	0.001684	0.02834	3.00	19.15
20	Adrenergic signaling in cardiomyocytes	0.002514	0.03809	2.20	13.19
21	Gap junction	0.003156	0.04346	2.61	15.02
22	Nicotine addiction	0.003014	0.04349	3.57	20.71
23	Long-term potentiation	0.005252	0.06919	2.74	14.38
24	Glycosphingolipid biosynthesis	0.005936	0.07495	3.17	16.26
25	Type II diabetes mellitus	0.008486	0.09523	2.97	14.18

Figure 4 Gene Ontology (GO) categories enriched within genes downregulated in Sox2-mutant dLGNs. The KEGG 2019 Mouse database was used to perform the analyses.

Index	Name	P-value	Adjusted p-value	Odds Ratio	Combined score
1	Lysosome	9.988e-12	3.026e-9	4.10	103.72
2	Pathways in cancer	1.250e-9	1.894e-7	2.14	43.93
3	Calcium signaling pathway	1.393e-7	0.00001407	2.77	43.78
4	Rap1 signaling pathway	4.760e-7	0.00003606	2.59	37.65
5	Fc gamma R-mediated phagocytosis	9.648e-7	0.00005847	3.58	49.55
6	Neuroactive ligand-receptor interaction	0.000003725	0.0001612	2.07	25.89
7	Regulation of actin cytoskeleton	0.000003229	0.0001630	2.42	30.54
8	Proteoglycans in cancer	0.000006202	0.0002349	2.42	29.03
9	Signaling pathways regulating pluripotency of stem cells	0.000008938	0.0003009	2.75	31.97
10	Focal adhesion	0.00001159	0.0003511	2.39	27.13
11	Glutamatergic synapse	0.00001736	0.0004783	2.87	31.50
12	Amino sugar and nucleotide sugar metabolism	0.00002843	0.0007177	4.01	41.99
13	Axon guidance	0.00003765	0.0007605	2.37	24.10
14	Bacterial invasion of epithelial cells	0.00003378	0.0007874	3.32	34.18
15	Fatty acid elongation	0.00003759	0.0008136	5.08	51.79
16	Platelet activation	0.00006818	0.001291	2.62	25.14
17	cAMP signaling pathway	0.00008986	0.001361	2.17	20.25
18	Ras signaling pathway	0.00008974	0.001431	2.11	19.65
19	beta-Alanine metabolism	0.00008916	0.001501	4.61	42.96
20	Breast cancer	0.00008502	0.001515	2.45	22.98
21	Starch and sucrose metabolism	0.0001160	0.001674	4.47	40.48
22	ECM-receptor interaction	0.0001345	0.001853	2.96	26.39
23	Chemokine signaling pathway	0.0001725	0.002273	2.16	18.73
24	Human papillomavirus infection	0.0001863	0.002352	1.82	15.63
25	Gap junction	0.0002029	0.002459	2.86	24.29

Figure 5. Gene Ontology (GO) categories enriched within genes upregulated in Sox2-mutant dLGNs. The KEGG 2019 Mouse database was used to perform the analyses.

References

Armentano, M., Chou, S. J., Tomassy, G. S., Leingartner, A., O'leary, D. D. & Studer, M. 2007. COUP-TFI regulates the balance of cortical patterning between frontal/motor and sensory areas. Nature neuroscience, 10, 1277-86.

Chou, S. J., Babot, Z., Leingartner, A., Studer, M., Nakagawa, Y. & O'leary, D. D. 2013. Geniculocortical input drives genetic distinctions between primary and higher-order visual areas. Science, 340, 1239-42.

Favaro, R., Valotta, M., Ferri, A. L., Latorre, E., Mariani, J., Giachino, C., Lancini, C., Tosetti, V., Ottolenghi, S., Taylor, V. & Nicolis, S. K. 2009. Hippocampal development and neural stem cell maintenance require Sox2-dependent regulation of Shh. Nature neuroscience, 12, 1248-56.

Huberman, A. D., Murray, K. D., Warland, D. K., Feldheim, D. A. & Chapman, B. 2005. Ephrin-As mediate targeting of eye-specific projections to the lateral geniculate nucleus. Nat Neurosci, 8, 1013-21.

Pfeiffenberger, C., Cutforth, T., Woods, G., Yamada, J., Renteria, R. C., Copenhagen, D. R., Flanagan, J. G. & Feldheim, D. A. 2005. Ephrin-As and neural activity are required for eye-specific patterning during retinogeniculate mapping. Nat Neurosci, 8, 1022-7.

During my PhD, I spent a few months in the laboratory of Michèle Studer, my thesis Co-director, in Nice and I was involved in the characterization of the thalamus in *COUP-TF1 null* mice. In particular, I performed Nissl stainings of the forebrain in mutants and control siblings at P0 and P8 to visualize the different thalamic nuclei. These staining were included in the paper described in Chapter 4 that investigates defects in the mouse retina and optic nerve in *COUP-TF1 null* mice. Note that COUP-TF1 is also called Nr2f1 and this is the name used in Chapter 4.

CHAPTER 4

Mouse *Nr2f1* haploinsufficiency unveils new pathological mechanisms of a human optic atrophy syndrome

Michele Bertacchi[1,2]*, Agnès Gruart[3], Polynikis Kaimakis[4,5], Cécile Allet[6,7], Linda Serra[1,8], Paolo Giacobini[6,7], José M. Delgado-García[3], Paola Bovolenta[4,5] and Michèle Studer[1]*

[1]Université Côte d'Azur, CNRS, Inserm, iBV, Nice, France ;
[2]Fondazione IRCCS Istituto Neurologico Carlo Besta, Milan, Italy;
[3]Division of Neurosciences, Pablo de Olavide University, Seville, Spain;
[4]Centro de Biología Molecular "Severo Ochoa", CSIC-UAM;
[5]CIBER de Enfermedades Raras (CIBERER), Campus de la Universidad Autónoma de Madrid, Madrid, Spain;
[6]Jean-Pierre Aubert Research Center (JPArc), Laboratory of Development and Plasticity of the Neuroendocrine Brain, Inserm, UMR-S 1172, Lille, France;
[7]University of Lille, FHU 1,000 Days for Health, Lille, France.

[8]Department of Biotechnology and Biological Sciences, University of Milano-Bicocca, Milano, Italy.
Published in EMBO Mol Med. 2019 Aug;11(8):e10291.
doi: 10.15252/emmm.201910291.

Abstract

Optic nerve atrophy represents the most common form of hereditary optic neuropathies leading to vision impairment. The recently described Bosch-Boonstra-Schaaf optic atrophy (BBSOA) syndrome denotes an autosomal dominant genetic form of neuropathy caused by mutations or deletions in the *NR2F1* gene. Herein, we describe a mouse model recapitulating key features of BBSOA patients -optic nerve atrophy, optic disc anomalies, and visual deficits- thus representing the only available mouse model for this syndrome. Notably, *Nr2f1*-deficient optic nerves develop an imbalance between oligodendrocytes and astrocytes leading to postnatal hypomyelination and astrogliosis. Adult heterozygous mice display a slower optic axonal conduction velocity from the retina to high order visual centers together with associative visual learning deficits. Importantly, some of these clinical features, such the optic nerve hypomyelination, could be rescued by chemical drug treatment in early post-natal life. Overall, our data shed new insights into the cellular mechanisms of optic nerve atrophy in BBSOA patients and open a promising avenue for future therapeutic approaches.

Introduction

Optic atrophy denotes the loss of part or all the nerve fibers in the optic nerve (ON), often leading to widening of the optic cup, and represents

an important sign of advanced ON disease frequently associated with gradual vision loss or reduced visual acuity. Optic neuropathies may range from non-syndromic genetic diseases to rare syndromic multisystemic disorders. The most common forms of inherited optic atrophies, described so far, are the Leber's optic neuropathy (LHON) and the dominant optic atrophy (DOA) caused by mutations in the nuclear gene OPA1 (Carelli et al, 2017; Chun & Rizzo, 2017). Recently, patients carrying deletions or missense point mutations in the *NR2F1* locus have also been diagnosed with optic atrophy associated with developmental delay and intellectual disability (Al-Kateb et al, 2013; Bosch et al, 2014; Chen et al, 2016; Kaiwar et al, 2017). This autosomal dominant disorder resulting from *NR2F1* haploinsufficiency is currently named as Bosch-Boonstra-Schaaf optic atrophy (BBSOA) syndrome (OMIM: 615722). BBSOA patients display a variable array of clinical deficits, both visual and cognitive, where malformed optic disc (OD), ON atrophy, decreased visual acuity, developmental delay, epilepsy and mild to moderate intellectual disability are among the most common deficiencies (reviewed in (Bertacchi et al, 2018)). The clinical features of BBSOA syndrome are still evolving, as the number of reported cases is continuously increasing since 2014, when the first patients with missense mutations were reported (Bosch et al, 2014; Chen et al, 2016; Kaiwar et al, 2017; Martin-Hernandez et al, 2018). This suggests that the prevalence of BBSOA syndrome might be still underestimated, which prompted us to further understand the mechanisms of this newly identified neurodevelopmental disease.

NR2F1, also known as COUP-TFI, is an orphan nuclear receptor belonging to the superfamily of steroid/thyroid hormone receptors and

acting as a strong transcriptional regulator (Alfano et al, 2013; Bertacchi et al, 2018). Two major homologs of this family have been identified in vertebrates: NR2F1 and NR2F2 (also named COUP-TFII) (Alfano et al, 2013; Ritchie et al, 1990; Wang et al, 1991). Their molecular structure encompasses two highly conserved domains, the DNA-binding domain (DBD) and the ligand-binding domain (LBD). Most of the pathogenic mutations causing BBSOA syndrome are located in the NR2F1 DBD, hence disrupting its activity as a transcription factor, but some have been reported also in the LBD or in the start codon (ATG) (Bertacchi et al, 2018; Bosch et al, 2014; Chen et al, 2016). The mouse Nr2f1 and human NR2F1 proteins are very well conserved during evolution and share 98-100% of sequence homology in both DBDs and LBDs (Bertacchi et al, 2018). Nr2f1 is widely and dynamically expressed in several mouse brain regions (Alfano et al, 2013; Armentano et al, 2006; Bertacchi et al, 2018; Flore et al, 2017; Lodato et al, 2011b; Parisot et al, 2017; Qiu et al, 1995; Tripodi et al, 2004; Wang et al, 1991) and its expression pattern seems to be well conserved in human embryos and fetuses, as recently shown (Alzu'bi et al, 2017a; Alzu'bi et al, 2017b). Thus, structural and expression similarities between mouse and humans strongly suggest a conserved role of NR2F1 during development of the central nervous system (CNS).

Multiple data in mice have highlighted the multi-faceted functions of Nr2f1 in the development of several mouse brain structures (Alfano et al, 2013; Bertacchi et al, 2018), but its exact role during eye development is still vague. Indeed, there is still inconsistency between the ocular phenotype obtained in mouse and the clinical features

described in BSSOA patients, as the ON atrophy and cerebral visual deficits identified in several patients have not been reproduced in mice lacking solely Nr2f1 (Bertacchi et al, 2018; Tang et al, 2015). Only the combined inactivation of both homologs, *Nr2f1* and *Nr2f2*, produced severe early ocular defects, such as coloboma and microphtalmia, suggesting a genetic compensation in the mouse (Tang et al, 2015; Tang et al, 2010). This is surprising since BBSOA patients are haploinsufficient for *NR2F1*, i.e. lack only one copy of the gene, but develop ocular impairments with high prevalence (Bertacchi et al, 2018; Chen et al, 2016). This discrepancy could depend either on species-specific functional differences or on the conditional mouse model used by Tang and colleagues (Swindell et al, 2006; Tang et al, 2010). Since genetically-modified mice still offer a unique opportunity to decipher the mechanisms underlying eye development and assembly of the visual pathway, we investigated the role of Nr2f1 during visual development from the retina to the visual cortex, using heterozygotes (*HET*) and homozygotes (*KO or null*) of the constitutive mouse knock-out (*KO*) model (Armentano et al, 2006). We reasoned that constitutive loss of one *Nr2f1* allele would better reproduce the human disease condition, in which Nr2f1 dosage is decreased in all cells and from the earliest stages of development.

In this study, we report that Nr2f1/NR2F1 is expressed in the peripheral visual system in both mice and humans, particularly in cell types involved in the development and maturation of the ON, such as neural retina cells, ON astrocytes and oligodendrocytes. Furthermore, we show that *Nr2f1 HET* and *KO* mice have clear ocular abnormalities, from OD malformations, delayed retinal ganglion cell (RGC)

differentiation and apoptosis to decreased ON myelination and increased astrogliosis, resulting in reduced axonal conduction velocity from the retina to higher order centers. At adult stages, *Nr2f1 HET* mice have visual and associative learning deficits, reproducing in some ways the cerebral visual impairment described in patients (Bosch et al, 2014; Chen et al, 2016). Notably, Miconazole treatment in early postnatal pups rescues the ON demyelination defect, by restoring appropriate levels of oligodendrocytes, but has little effect on astrogliosis, indicating that the two events are independently controlled in this optic atrophy syndrome. Overall, we show that *Nr2f1* mutant mice can be used as a model to reproduce the BBSOA syndrome and, more broadly, could serve as a tool to test possible therapeutic approaches aimed at counteracting ON neuropathies.

Results

NR2F1 is dynamically expressed in the mouse and human neural retina (NR) and optic nerve

As most BBSOA patients develop ON atrophy, we carefully assessed NR2F1 expression in both the mouse and human developing eye and ON. As previously reported (Tang et al, 2010), the murine Nr2f1 protein is strongly expressed in both the presumptive dorsal and ventral optic stalk (OS), the precursor of the ON at embryonic day (E) 10.5 and shows a ventral-high to dorsal-low gradient in NR progenitors (Fig. 1A). At E12.5, when the optic vesicle invaginates forming a bi-layered optic cup, Nr2f1 graded expression is maintained in the ventral retina, in the OS and in the optic disc (OD) (Fig. 1B-B”). Nr2f1 co-localizes with virtually all Sox2+ retinal progenitors at E13.5 (Fig. 1C-C”) and

with Brn3a+ early differentiating RGCs (Fig. 1D-D"), even if at lower levels when compared to progenitors (Fig. 1C'-D"). At E18.5 and postnatal (P) stages, Nr2f1 is still expressed in both Brn3a+ RGC neurons forming long-distance projections constituting the ON (Fig. 1E-F"), and in residual progenitors (Sox2+ cells; Fig. 1G,G'). Beside retinal neurons, Nr2f1 is also localized in astrocytes and oligodendrocytes of the ON. Between E13.5 and E18.5, Nr2f1 is expressed in virtually all Glast+/NF1A+ astrocytes of the OS/ON (Fig. 1H-I" and Appendix. Fig. 1A-A"), then maintained in 70% of Glast+/NF1A+ astrocytes at P7 and P28 (Appendix Fig. 1B), and in around 80% of Sox10+ oligodendrocytes at post-natal stages (Fig. 1J-K" and Appendix Fig. 1C). In summary, Nr2f1 is highly expressed in both retinal and optic nerve components of the peripheral visual system in mouse.

Staining of NR2F1 on human embryonic sections of gestational week (GW) 11 confirmed expression conservation in both the developing neural retina (identified by the retinal marker PAX6) and the ON (Fig. 1L-L"). Notably, NR2F1 is highly expressed in progenitors (SOX2+) as well as in post-mitotic differentiated retinal cells (SOX2-) (Appendix Fig. 1D-D"). Along the ON, from the optic disc (distal) to the chiasm (proximal) regions, almost all cells are positive for NR2F1 and 93% of them co-express the astrocytic marker S100β (Fig. 1M-N"). High co-expression of NR2F1 with SOX2 and S100β (Fig. 1O-P' and Appendix Fig 1E-E"), as well as with BRN3a in the ganglion cell layer (GCL) of the neural retina (Fig. 1Q-Q"') is maintained at GW14, indicating that NR2F1 expression follows cell differentiation in both the NR (from progenitor to post-mitotic RGCs) and the ON. Moreover,

oligodendrocytes have not reached the ON at these early stages, but can be distinguished in the preoptic area, where they are generated and co-express NR2F1 (93% double-positive cells; Appendix Fig 1F-F"'). The high expression of NR2F1 in the human and mouse NR, OD and ON suggests a conserved role for this gene in the development of the peripheral visual system. We observed that along the human ON, NR2F1 expression levels seem even higher than in mouse (compare Fig. 1I-I" with Fig. 1L-L"), suggesting an important role for NR2F1 in human ON development.

Optic disc malformations in *Nr2f1* mutant mice

In light of the early *Nr2f1* expression gradient in the developing optic vesicle, key markers of proximo-distal (P-D) eye patterning, such as Pax6 and Pax2 (Schwarz et al, 2000), were first analyzed in *WT*, *HET* and *KO* embryos. We found ectopic Pax6 expression in the presumptive ventral OS of *HET* and *KO* E10.5 embryos (Appendix Fig. 2A-F), as well as Pax2 downregulation and reciprocal Pax6 upregulation in invaginating E11.5 mutant optic cups (Appendix Fig. 2G-M"). Thus, differently from previously reported (Tang et al, 2015; Tang et al, 2010), loss of *Nr2f1* alone is sufficient to affect early patterning of the developing optic vesicle, indicating that Nr2f1 can control key molecular regulators of early identity acquisition during eye development.

The refinement of P-D marker expression is essential for the establishment of a structural border between OS and neural retina (NR), called the optic disc (OD), which forms at the most proximal region of the optic cup. In light of the ventral shift of the presumptive OS/NR

border in *Nr2f1* mutants, and of BBSOA patients displaying OD abnormalities (Bosch et al, 2014; Chen et al, 2016), we decided to closely follow the morphological and molecular development of the OD in *Nr2f1 HET* and *KO* eyes. Abnormal positioning and aberrant morphology of the presumptive OD was found in E12.5 *Nr2f1* mutants (Fig. 2A-B"), particularly in *Nr2f1 KO* optic vesicles, in which Pax2 expression is lost in the proximal OS region and ectopic Pax6+ cells appear to differentiate into Tuj1+ neurons *in loco* (arrowheads and inset in Fig. 2C-D"). Cells positive for Pax2 remain abnormally low in the OD domain of *Nr2f1 HET* and *KO* mutants until E18.5 (Fig. 2E-F) and fail to properly surround and constrain the extension of Tuj1+ axons already at E15.5 (Fig. 2G-G'"). Early tissue patterning defects ultimately impinge on the final morphology and cell organization of the OD at later stages, in which Tuj1+ fibers and Brn3a+ RGC bodies remain severely misplaced in E18.5 *KO* fetuses (Fig. 2H-I'). Together, our data show that reduced Nr2f1 expression levels affect P-D molecular patterning and lead to an abnormal OD organization from which RGC axons exit and form the ON. Interestingly, these defects are reminiscent of various OD abnormalities described in BBSOA patients, including small discs, pale discs, and disc excavations (Bosch et al, 2014; Chen et al, 2016).

Pre- and early postnatal optic nerve defects in *Nr2f1* mutants

Since Nr2f1 promotes cell differentiation in different regions of the CNS (Bertacchi et al, 2018; Faedo et al, 2008; Lodato et al, 2011a; Parisot et al, 2017), we asked whether partial or complete loss of Nr2f1 function in the NR would affect cell proliferation and/or RGC

differentiation (Fig 2J-V). Retinal neurons start to be generated around E11.5 in the mouse eye and express the neuron-specific ß-tubulin marker Tuj1 and the RGC marker Brn3a (Heavner & Pevny, 2012). A reduction of Tuj1+ differentiating cells in the ventral but not dorsal retina was detected in E13.5 *HET* and *KO* optic cups (Fig. 2J-L), and consequently fewer axons entered the OS (arrowheads in Fig. 2K,K'). Reduced rates of differentiation were most probably due to an increased number of proliferative EdU+/Ki67+ cells resulting in tissue expansion and bending (arrowhead in Fig. 2J' and Appendix Fig. 3A-B'). Even if these morphological deformations might resemble a coloboma (Appendix Fig. 3C-D'"), which normally results from a failure in ventral fissure closure (Patel & Sowden, 2017), transverse sections of the optic vesicle depict proper fusion of the ventral fissures in E13.5 *Nr2f1* mutants (Appendix Fig. 3E-J). Therefore, abnormal optic vesicle morphology observed in *Nr2f1* mutants arises most probably from tissue bending due to excessive proliferation and delayed cell differentiation.

A delay in RGC ventral differentiation was further confirmed by Brn3a staining, which results particularly reduced in malformed NR areas in E13.5 mutant embryos (Fig. 2M-N'). However, *HET* and *KO* animals gradually recover their initial differentiation defect, since a comparable number of RGCs was quantified at E15.5 and E18.5 (Fig. 2P). Accordingly, the diameter of the ON encompassing retinal fibers was only slightly reduced in *KO* animals at birth and not affected in *HETs* (P0; Fig. 2Q-Q",S). However, the number of RGCs decreased again in P7 *KO* and *HETs* (Fig. 2P) and remained low at P28 (Fig. 2O-P), in line with the affected ON size (Fig. 2R-S; note that *KO* animals do not

survive past P8). To assess whether RGC death could explain this postnatal defect, we stained *KO* and *HET* retinae with Brn3a and Caspase3, a marker for apoptotic cells. The number of apoptotic Brn3a+ RGCs was increased in both E18.5 *HET* and *KO* retinae compared with *WT* (Fig. 2T-U'), but only slightly changed at P5 and no more detected at P7 (Fig. 2V, and data not shown). Together our data show that reduced dosage of *Nr2f1* not only delays RGC differentiation prenatally, but also induces acute RGC death around birth resulting in progressive ON hypoplasia at early postnatal stages.

Altered astroglia/oligodendroglia balance in *Nr2f1*-deficient optic nerves

The observation that ON atrophy worsens postnatally in mutant mice suggests that additional defects other than reduced RGC number and perinatal cell death might contribute to ON degeneration. Astrocytes and oligodendrocytes are two key glial populations supporting the stability and function of axonal fibers in the ON (Hernandez et al, 2008; Tsai & Miller, 2002). While primary astrocytes are mainly generated *in loco* from Pax2+ cells of the OS inner layer and express NF1A and S100β (Sun et al, 2017; Tsai & Miller, 2002), mouse oligodendrocyte precursors originate from the preoptic area of the ventral forebrain and enter the ON at the chiasm region around E18.5. They subsequently migrate, proliferate and differentiate along the ON until P28, when myelination is accomplished (Ono et al, 2017). Oligodendrocytes can be labeled by Sox10 and Myelin Basic Protein (MBP) expression. MBP is exclusive of fully differentiated oligodendrocytes that actively embed axonal fibers in myelin sheets to allow for efficient signal transmission

(Stolt et al, 2004; Stolt et al, 2002). NF1A and Sox10 mutually antagonize each other to control glial sub-lineage differentiation (Glasgow et al, 2014); hence, these markers are specific for their lineages (astrocytes *vs* oligodendrocytes, respectively) and virtually never overlap.

Since Nr2f1 is expressed at high levels in both astro- and oligodendrocyte cell populations of the developing ON (Fig. 1 and Suppl. Fig. 1), we analyzed the effects of Nr2f1 reduced dosage on the differentiation of both lineages at different developmental times. We found an increase of Pax2+ astrocytic progenitors and NF1A+ precursors in the inner layer of the OS in *Nr2f1* mutants at E13.5, and in the retinal, medial and chiasmal regions of the ON at E15.5 and E18.5/P0 (Fig. 3A-I). An increased NF1A+ astrocyte production is still maintained at P7 and leads to an over-represented astrocytic population in both *HET* and *Null* animals (Fig. 3J-L). Strikingly, this abnormal astrocytic pool, intermingled between Tuj1+ fibers, shows a hypertrophic morphology (Fig. 3M-O''). This is confirmed by the presence of expanded astrocytic processes containing large bundles of intermediate filaments in P8 *KO* transmission electron microscopic (TEM) thin sections (arrowheads and red dotted lines in Fig. 3P,Q). Astrocytes appear to form a tight network, and to display stress granules and a more heavily stained cytoplasm in mutants, not detected in *WT*, and compatible with a "reactive" state observed during neuroinflammation (Appendix Fig. 4A-D'). Although there was a clear difference between *WT* and mutant ON astrocytes prenatally, they seem to acquire a hypertrophic phenotype right around the first week of age, as described in other cases (Bovolenta et al, 1987). We thus assessed

the presence of reactive astrocytes at P28, when their development was over, using Sox2, which is upregulated by pro-inflammatory signals triggering astrocytic proliferation (Bani-Yaghoub et al, 2006). P28 *Nr2f1 HET* ONs show a 25% increase of high-expressing Sox2+ astrocytes with abnormal morphology compared with *WT* Sox2-expressing cells (Fig. 3R-T). This was confirmed by TEM analysis illustrating enlarged astrocytic processes in *HET* ONs (Fig. 3U,V). Interestingly, astrocyte inflammation was associated to abnormal mitochondrial morphology (Appendix Fig. 5), in line with a recently described mitochondrial involvement in BBSOA pathogenesis (Martinez-Hernandez et al., 2018). At P8, astrocyte mitochondria became hypertrophic (1.78±0.15 times larger than WT ones) with disorganized cristae, whereas RGC axonal mitochondria had a normal size (Appendix Fig. 5A-F). However, RGC somata showed increased ATPIF1 staining at later stages (Appendix Fig. 5G-H'), suggesting that mitochondrial biogenesis and function could be altered also in RGC cells. Together, these data show that reduced Nr2f1 dosage promotes an inflammatory process starting at early postnatal stages and possibly involving mitochondrial dysfunction.

Miconazole treatment rescues improper oligodendrocyte differentiation and myelin lamination found in *Nr2f1* deficient mice

While the astrocytic population is overrepresented in Nr2f1-deficient P8 ONs, the Sox10+ oligodendrocyte population shows a dose-dependent opposite trend (Fig. 4A-C), in a way that the glial population is imbalanced with astrocytes outnumbering oligodendrocytes (Fig. 4C). Thus, we evaluated the proportion of proliferating, migrating and

differentiating oligodendrocytes by co-labeling Sox10+ cells with the proliferative marker Ki67, the apoptotic marker Caspase3, and the terminal differentiation protein MBP in normal and mutant ONs (Appendix Fig. 6). While there was no difference in proliferation or apoptosis between *Nr2f1* mutants and *WT* littermates, the ratio of undifferentiated (Sox10+/MBP-) *versus* differentiated (Sox10+/MBP+) oligodendrocytes was significantly increased in *HET* and *KO Nr2f1* mutant ONs (Appendix Fig. 6A-I), indicating failed oligodendrocyte maturation upon reduced *Nr2f1* expression. More Sox10+ oligodendrocytes are present in the proximal *versus* distal ON portions in both *HET* and *KO* animals (Appendix Fig. 6H), suggesting also a defective migration along the nerve. Thus, deficiency in *Nr2f1* genetic dosage affects migration and differentiation of developing oligodendrocytes (summarized in Appendix Fig. 6J).

Next, we asked whether impaired oligodendrocyte development would affect fiber myelination using MBP as a late marker. At P8, the proximal and distal ON ends of both *HET* and *KO* animals present a drastic reduction of MBP immunostaining compared to *WT* (Fig. 4D-J). Notably, *Nr2f1 HET* mice have impaired myelination at the proximal end to an extent similar to that of *KO* animals (Fig. 4E,F,J), indicating that fine regulation of gene dosage is essential for proper oligodendrocyte differentiation. TEM analysis confirmed a lower amount of myelinated fibers in both *HET* and *KO* ONs, although with different severity (Fig. 4K-N). The few myelinated fibers in P8 *KO* animals display thin and incomplete sheets (Fig. 4M, inset). Poor myelination is still maintained in P28 *HET* animals (Fig. 4O-Q), excluding a transient defect. Indeed, high magnification EM images

show that several *HET* fibers are surrounded by disorganized and poorly compacted myelin sheaths (g-Ratio: 0.63±0.04), when compared with the dense myelin layer of *WT* animals (g-Ratio: 0.74±0.02) (Fig. 4R,S). Together, our findings show that *Nr2f1*-deficient oligodendrocytes fail to properly migrate and differentiate during development, ultimately leading to reduction of myelin surrounding optic nerve fibers in juvenile mutant mice.

Miconazole and Clobetasol act as two potent inducers of oligodendrocyte differentiation, as they trigger fast maturation of MBP+ cells in both physiological and pathological conditions (Najm et al, 2015; Su et al, 2018). Given our observations, we asked whether this treatment could be of use in the BBSOA mouse model of optic neuropathy. Using previous treatment protocols (Najm et al, 2015), we injected Miconazole or Clobetasol daily in control and *Nr2f1 HET* pups from P2 to P8 (Fig. 5A). Miconazole, but not Clobetasol, which resulted toxic for the pups (M.B., M.S. unpublished observations), increased the number of Sox10+ precursors in *Nr2f1 HET* ONs and improved fiber myelination to a level comparable to that of *WT* littermates (Fig. 5B-E). Miconazole has been showed to specifically enhance ERK1/2 activity. Consistently, the phosphorylated (i.e. activated) form of ERK was upregulated upon Miconazole treatment (Fig. 5F,G), as quantified in whole ON (Fig. 5H) and specifically in the cytoplasm of Sox10+ oligodendrocytes (Fig. 5I). To understand whether the short Miconazole treatment was enough to sustain fiber myelination even at later stages, we analyzed P2- to P8-treated animals at P28 (Appendix Fig. 7A-H). Notably, treated ONs maintain oligodendrocyte number and myelination recovery at later postnatal stage (Appendix Fig. 7A-

D). Increased levels of Sox10+ oligodendrocytes in treated pups were also maintained at P28 compared to untreated *HETs* (Appendix Fig. 7E-H). However and interestingly, the number of Sox2+ reactive astrocytes and their aberrant morphology were not modified in treated pups and remained similar to untreated ones (Fig. 5N-Q), strongly suggesting that astrocyte alterations are not secondary to defects in myelination in *Nr2f1*-deficient animals.

Thalamic and cortical visual regions are reduced in *Nr2f1*-deficient mice

Since Nr2f1 is also expressed in the visual thalamus and cortex (Armentano et al, 2006; Chou et al, 2013), we wondered whether the thalamic relay of RGC visual fibers, the dorsal lateral geniculate nucleus (dLGN), was altered in *Nr2f1*-deficient animals (Appendix Fig. 8). At both P0 to P8, the size of the dLGN, measured in Nissl-stained sections, was progressively and significantly reduced in both *HET* and *KO* animals when compared with *WT* (Appendix Fig. 8A-F), as also reported in thalamic-specific conditional *Nr2f1 KO*s (Chou et al, 2013). Furthermore, and possibly related to the reduction of both the RGC number and the dLGN size, DiI labelled E18.5 RGC axons were less efficient in invading the dLGN as compared with their *WT* counterparts (Appendix Fig. 8G-I). Moreover, since *Nr2f1* is one of the major genes orchestrating cortical arealization (Alfano et al, 2013; Armentano et al, 2007; Zhou et al, 2001), we wondered whether reduced *Nr2f1* expression would also affect the size of neocortical areas, particularly sensory areas (including the visual cortex).Consistently, the *Lmo4*-expressing visual cortex of *HET* animals was slightly reduced, even if

not as severely as observed in *KO* brains (Appendix Fig. 9A-D). Together, our data indicate that *Nr2f1* haploinsufficiency affects the development of the entire visual system, from the retina to the visual cortex.

Reduced axonal conduction velocity in the visual pathway of *Nr2f1* mutant adults

To test whether the clear alterations in the visual system of *Nr2f1* heterozygotes had functional consequences, we quantified the conduction velocity of nerve impulses along the visual pathway by implanting recording electrodes into their dLGN, superior colliculus, and visual cortex (Fig. 6A,B). Alert-behaving *WT* and *HET* adults were stimulated with light flashes presented bilaterally 40 times per session at a rate of 6/min. As previously described (Meeren et al, 1998; Sanz-Rodriguez et al, 2018; Wiggins et al, 1982), flash stimulations evoke an early positive-negative-positive field potential followed by some late oscillatory components in the dLGN (Fig. 6C). The latency values for the first positive component in *WT* mice are in line with reported mouse field potentials and unitary recordings evoked by photic stimulation (Lintas et al, 2013; Sanz-Rodriguez et al, 2018). Notably, *HET* animals displayed a significantly ($t = -6.385$ with 22 degrees of freedom; $P < 0.001$) longer mean conduction velocity (15.79 ± 048 ms) for the first component of the evoked field potential than *WT* mice (12.38 ± 0.25 ms) (Fig. 6C,D), suggesting decreased transmission of retinal impulses upon *Nr2f1* reduced dosage. At the level of the superior colliculus, field potentials present a succession of negative-positive components that lasted for > 80 ms. In this case, the latency to the initiation of the first

negative component was also significantly longer (t = -2.148 with 18 degrees of freedom; *P* = 0.046) in *Nr2f1 HET* (17.60 ± 0.58 ms) than in *WT* (15.95 ± 0.50 ms) mice (Fig. 6C,D). Finally, field potentials evoked in the primary visual cortex produced an early and noticeable positive-negative-positive component followed for a long-lasting (>80 ms) succession of negative waves sometimes riding on the top of a slow positive wave (Fig. 6C)(Meeren et al, 1998; Ridder & Nusinowitz, 2006; Wiggins et al, 1982). The latency to the first positive component is again significantly longer (t = -3.073 with 26 degrees of freedom; *P* = 0.005) for *Nr2f1 HET* (16.75 ± 0.41 ms) than for *WT* (14.64 ± 0.55 ms) mice (Fig. 6D). Taken together, these data show that *Nr2f1*-deficient mice exhibit a significant defect in the transmission of visual stimuli from the retina to the visual cortex. Since these differences were similar (≈2 ms) among the three recording sites, we can assume that the deficits in axonal conduction velocity are mainly restricted to the optic nerve.

Visual and associative learning deficits in *Nr2f1* heterozygous mice

BBSOA patients have been diagnosed with cerebral visual impairments (CVI)(Bosch et al, 2014; Chen et al, 2016), a condition in which visual stimuli are not properly interpreted and associated, and which relates to damage or malfunction of the visual pathway or visual centers in the brain. To understand whether *Nr2f1* heterozygotes encountered similar associative visual and learning disorders, we tested their performance firstly in a light-dependent operant conditioning task (Fig. 6E, top panel) and later in the same box, but with a cue depending on a small light bulb switched on or off (Fig. 6E, bottom panel). *WT* (n = 13) and

Nr2f1 heterozygous (*HET*; n = 18) mice where trained in a Skinner box to obtain a food pellet every time they press a lever in 10 daily sessions of 20 min each. In this preliminary training, the two groups reached the selected criterion (Fig. 6F) at the same time (U = 142.000; *P* = 0.703; Mann-Whitney rank sum test). In addition, they performed similar numbers of lever presses (t = -0.733 with 18 degrees of freedom; *P* = 0.473) (Fig. 6G). After this pre-training, mice were subjected to a more complex task, where pressing the lever was only rewarded with a pellet during those periods (20 s) in which a small light bulb located above the lever was switched on (light on/light off protocol, Fig. 6E, bottom panel). In this case, the *WT* group reached the selected criterion by the 6th conditioning session, while *Nr2f1 HETs* were unsuccessful in completing this task (Fig. 6H). Values collected for the light on/light off coefficient (see Methods) were significantly higher for *WT* mice compared to *HETs* [$F_{(1, 135)} = 6.129$; *P* = 0.026]. A best linear fit to the collected data points indicates that *WT* mice increased their performance across training (slope = 0.0632; r = 0.75; *P* = 0.046), whereas *HET* animals failed to show any sign of improvement (slope = - 0.0118; r = 0.199; *P* = 0.809) (Fig. 6H). A further analysis indicated that *Nr2f1* heterozygous mice were unaware of the working code indicated by the light bulb. Indeed, and as shown in Fig. 6I, while *WT* mice learned to press the lever preferentially (t = 5.272 with 24 degrees of freedom; *P* < 0.001) during the light-on (≈75%) *versus* the light-off (≈25%) periods, *HETs* pressed the lever equally (≈50% each) during these two periods (t = 0.091 with 16 degrees of freedom; *P* = 0.929). In conclusion, *Nr2f1* heterozygous mice show a significant deficit in associating the dim visual cue with the operant task. Although the

negative slope value of the regression line illustrated in Fig. 6H suggest the possibility of a learning deficit in *Nr2f1* mice not necessarily related to visual limitations, the fact that *HETs* acquired the initial training in a well illuminated box similarly to controls support the presence of a relevant deficit in the acquisition/processing of visual cues.

Discussion

BBSOAS, a new pathogenic model for optic atrophy

Dominant optic atrophy is the most common form of autosomically inherited (non-glaucomatous) optic neuropathy characterized by optic nerve pallor and reduced visual acuity. RGC alterations have been proposed as the main cause of optic neuropathy. RGCs are long projection neurons with an initial long unmyelinated intraretinal segment that is thought to be particularly vulnerable to insults, at least in cases of LHON and OPA1 mutations, the major forms of optic atrophy described so far (Chun & Rizzo, 2017; Jurkute & Yu-Wai-Man, 2017; Lenaers et al, 2012). The underlying mechanisms that mediate RGC death and progressive ON degeneration are still not completely elucidated in the various forms of neuropathies. Our study now offers different mechanisms to explain optic atrophies of the BBSOA type (schematized in Fig. 7).

First, *Nr2f1* heterozygous mice, analogous to *NR2F1* haploinsufficient patients, recapitulate important features of BBSOA patients, such as OD malformations and ON atrophy, and could serve as a model to study the pathogenesis of optic neuropathies and visual impairments. Furthermore and in contrast to what previously reported (Tang et al,

2015; Tang et al, 2010), we demonstrate that *Nr2f1* deletion alone is sufficient to induce major optic abnormalities in mouse that, as in humans, do not seem to be compensated by its homolog *Nr2f2*. This contention is also supported by our novel observation that the expression pattern of *NR2F1* is strongly conserved between human and mouse, at least in the developing eye. In humans, *NR2F1* point mutations cause visual deficits with high penetrance, apparently in the absence of any additional gene mutation, indicating that our mouse model can be used to unravel the molecular/cellular mechanisms leading to human BSSOA syndrome, and more generally to understand the pathogenesis of ON neuropathy and/or degeneration. Why our findings differ from those reported by Tang and colleagues (Tang et al, 2012; Tang et al, 2015) is unclear; however, the most likely explanation reside in the use of a conditional mutant (*Rax-Cre Nr2f1*), in which the removal of the gene occurs either too late or less efficiently than in our model based on constitutive gene loss. We thus consider that mice heterozygous for *Nr2f1* well replicate the pathology of patients haploinsufficient for *NR2F1*.

Second, Nr2f1 seems to directly act on the migration and differentiation of oligodendrocytes and ultimately on the myelination degree of the ON. Oligodendrocyte precursors appear in the preoptic area of the ventral telencephalon around E12.5 in the mouse and migrate caudally toward the ON, where they form myelin sheaths wrapping axons (Ono et al, 2017). *Nr2f1* is highly expressed in the preoptic area (Armentano et al, 2006; Lodato et al, 2011b) and co-localizes with Sox10 in ON oligodendrocytes, suggesting that *Nr2f1* expression follows oligodendrocyte development from its source to its target. Our data

show a progressively reduced number of Sox10+ from the proximal to the distal ON portions in both *Nr2f1 HET* and *KO* mutants indicating a delay of migrating oligodendrocytes in reaching more distal parts of the ON. This is in accordance with ON hypomyelination at P8, although with different severities between *HET* and *KO,* and in *HET* mutants at P28. Strikingly, postnatal treatment with Miconazole, a potent inducer of oligodendrocyte differentiation in several brain regions (Najm et al, 2015; Su et al, 2018), efficiently rescues the myelination grade of *Nr2f1* mutants *via ERK* signaling activation, showing that this chemical drug can counteract hypomyelination in the context of our BBSOA mouse model. This is a first step not only in understanding the pathological features of a complex syndrome, but also in proposing possible therapeutic approaches. If proved efficient and safe in humans, Miconazole could be used in the future as a treatment to trigger oligodendrocyte maturation/differentiation and eventually improve ON signal conductance in BBSOA patients.

Third, our data show increased astrogliosis in the postnatal ON of *Nr2f1*-deficient mice. Differently from late-generated cells such as oligodendrocytes, astrocyte precursors are already present in the OS and ON at early stages and constitute the principal glial population at E18.5. Later on, they still represent the major glial cell type in the non-myelinated ON heads in most mammals (Hernandez et al, 2008) and respond to damage by changing from a quiescent to an activated state. During development, Pax2+ astrocyte precursor cells express guidance molecules at the OD through which RGC axons exit (Chu et al, 2001). At later stages, NF1A- and S100ß-expressing astrocytes are intermingled with oligodendrocytes along the ON providing structural

support and nutrients to axons, as well as forming a scaffold around endothelial cells to help maintaining the integrity of the blood–brain barrier. Astrocytes become reactive and re-express the progenitor marker Sox2 in response to a range of pathological conditions, from acute traumatic injury to chronic neurodegenerative diseases (Bani-Yaghoub et al, 2006). In the eye, glial cell proliferation and/or activation (gliosis) usually occur as a reactive change associated with ON degeneration and/or glaucoma (Hernandez et al, 2008; Pekny et al, 2014). Reactive astrocytes are generally identified by morphological changes (hypertrophy, thicker cell processes, larger, more vesicular nuclei, and in this case larger mitochondria), and tend to form a mesh (or glial scar) that alters the microenvironment of fibers likely contributing to Wallerian degeneration and thus RGC cell death (Conforti et al, 2014; Sofroniew, 2009).

We found that Nr2f1 protein is expressed in the astrocytic population at early stages in mice as well as in humans, and that already at E13.5 the Pax2+ astrocyte precursors are over-represented along the ON of mutants. Abnormally high production of astrocytes continues at later stages in both *HET* and *KO* animals, suggesting that Nr2f1 might play an intrinsic role in modulating the generation of astrocytes during ON development. This is supported by the finding that Nr2f1 cell-intrinsically drives progenitors toward neurogenesis by repressing astrogliogenesis in adult neural stem cells of the hippocampus (Bonzano et al, 2018). In its absence, neurogenesis is reduced at the expense of astrocyte production and, conversely, high Nr2f1 protein levels can rescue the hippocampal neurogenesis-astrogliogenesis imbalance due to neuroinflammation (Bonzano et al, 2018). Thus,

Nr2f1 might finely modulate astrocyte production/proliferation not only during adult neurogenesis, but also, as shown in this study, during ON development. We propose that the appearance of reactive astrocytes along the ON at P8 and P28 is a consequence of astrocyte over-proliferation occurring at early pre-natal stages, which might progressively impact on ON physiology and ultimately lead to neurodegeneration, as observed in other optic neuropathies (Carelli et al, 2017). This is also supported by the fact that ON demyelination but not gliosis can be rescued by Miconazole treatment in early post-natal life, suggesting that the two processes develop separately in this syndrome.

Our data disclose that gradual gliosis coupled to hypomyelination contribute to the optic atrophy phenotype characterized in mutant mice and described in BBSOAS patients. However, we cannot exclude that this atrophy might also be due to the altered ratio between proliferation and differentiation of RGCs during early development, leading to a reduced number of fibers exiting the retina at the proper developmental time. We believe that the reduced number of differentiating RGCs upon *Nr2f1* down-regulation represents only a delay in differentiation, which is gradually rescued. Indeed, the ON size between *WT*, *HET* and *KO* animals at birth is only slightly affected, even in *KO* animals, but worsen at later stages (20% of reduction found in *HET* animals remains constant over time). We propose that this postnatal atrophy is due to transient RGC apoptosis at peri-natal stages, combined with further axonal damage due to reactive gliosis. Indeed, Miconazole treatment recovers the oligodendrocyte number and myelination defects in *HET* ONs, but does not rescue the overall size of the ON, suggesting that

atrophy is independent of the ON myelination grade. Thus, Nr2f1 is a strong regulator of astrocyte production and reduced dosage of *Nr2f1* results in astrocyte overproduction and gliosis ultimately affecting ON growth and stability.

Fourth, we found abnormal axonal conductance and impaired visual learning upon reduced *Nr2f1* dosage. OD malformation, optic nerve atrophy and defective myelination of axonal fibers might ultimately lead to decreased signal transmission in our BBSOA model. In fact, by directly measuring the conduction velocity along the optic nerve and in following relay points along the visual system, we could demonstrate that *Nr2f1*-deficiency affects normal visual conductance. Notably, in comparison with *WT* mice, *Nr2f1 HET* animals presented more than 20% delay in the latency of field potentials evoked in the dLGN, suggesting a deficit in the transmission velocity of retino-geniculate fibers. The deficit in axonal conduction velocity seems to be restricted to the ON, since the latency to field potentials evoked at the superior colliculus (1.65 ms; 10,6%) and to the visual cortex (2.1 ms; 12.6%) presented similar (not significantly different) delays.

BBSOA patients often display visual acuity and image processing deficits, besides ON atrophy (Bosch et al, 2016; Bosch et al, 2014; Chen et al, 2016). Even if we focused here on the "periphery" of the visual system (the retina and ON), our data on the role of Nr2f1 in structures along the visual pathway, such as the thalamic dLGN and the visual cortex, unveil further abnormalities, possibly contributing to the visual deficits of *HET* mice and suggesting a causative link with patients' CVI. According to the present results, the performance of *Nr2f1 HET* mice in the Skinner box was mostly based on somatosensory and olfactory

cues, since they failed to acquire the visual-dependent operant conditioning task. Nevertheless, the negative slope of their performance in the Skinner box suggests that this learning deficit could be ascribed to more general limitations in the acquisition of complex learning tasks and not (exclusively) to visual difficulties. However, since *Nr2f1*-conditional mice have been proved to be capable of learning complex behavioral tasks (Flore et al, 2017), we preferentially think of a specific deficit in the perception and elaboration of visual stimuli at a neocortical level rather than a general defect in the learning process. Further studies will be necessary to specifically challenge the role of Nr2f1 in the development and functioning of thalamic and neocortical visual structures.

Figures

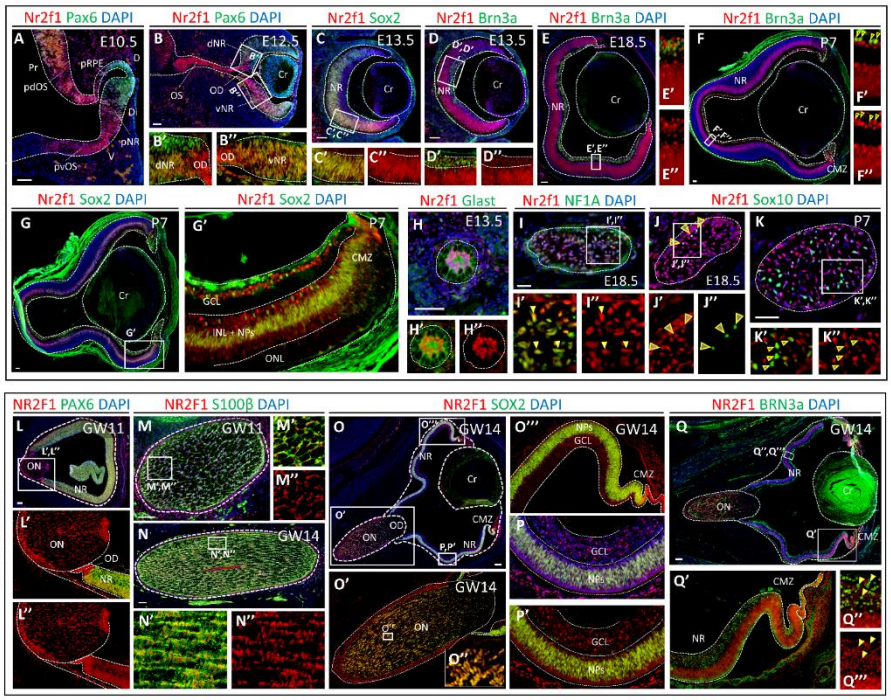

Figure 1. Nr2f1/NR2F1 expression during neural retina and optic nerve development in mice and humans. (A-B'') Nr2f1 (red) and Pax6 (green, retinal progenitors) immunofluorescences (IF) on sagittal sections of E10.5 and E12.5 mouse optic vesicles. Note the high-ventral to low-dorsal Nr2f1 gradient in the presumptive neural retina (pNR), and high Nr2f1 expression in both the presumptive dorsal and ventral optic stalk (pvOS and pdOS). Cr: crystal lens; Di, distal; Pr, proximal; presumptive retinal pigmented epithelium (pRPE). (C-D") IF on E13.5 mouse eye sagittal sections with Nr2f1 (red) and Sox2 (green, progenitors in C,C') or Brn3a (green, RGCs in D,D') showing Nr2f1 expression in NR progenitors and post-mitotic RGCs (insets in C'-D"). (E-F") Nr2f1 (red) and Brn3a (green) IF on E18.5 and P7 mouse eyes depicting Nr2f1 expression in virtually all RGCs in the ganglion cell layer (GCL). (G,G') Nr2f1 (red) and Sox2 (green) IF on P7 mouse retina

illustrating low Nr2f1 expression in the inner nuclear layer (INL) and progenitors (NPs), and high levels in the GCL and ciliary marginal zone (CMZ). No expression in the outer nuclear layer (ONL). (H-K") IF on cross-sections of E13.5 optic stalks (OS), and E18.5 and P7 optic nerves (ONs) with Nr2f1 (red) and Glast (green, astrocytic progenitors in H-H''), NF1A (green, astrocytes in I-I'') or Sox10 (green, oligodendrocyte precursors in J-K'') showing Nr2f1 expression in both astrocytic and oligodendrocytic lineages. Arrowheads point to double labeled cells. See Suppl. Fig. 1B,C for quantification. (L-L") NR2F1 (red) and PAX6 (green; NR domain) IF on sagittal sections of human eye primordia at gestational week (GW) 11 illustrating high NR2F1 expression in both ON and NR cells. (M-N") NR2F1 (red) and S100β (green, astrocytes) IF on cross-sections of human GW11 and GW14 ONs. Higher magnifications (M'-N") show that most of S100β+ astrocytes co-express NR2F1. (O-Q"') NR2F1 (red) and SOX2 (green in O-P') or BRN3a (green in Q-Q''') IF on sagittal sections of human GW14 eyes indicating high NR2F1 expression in virtually all NR progenitors (O''',P,P'), differentiating RGCs (Q-Q''') and in the majority of ON astrocytic progenitors (O'). Nuclei counterstaining (blue) was obtained with DAPI. Scale bars: 50µm or 100µm for mouse and human sections, respectively.

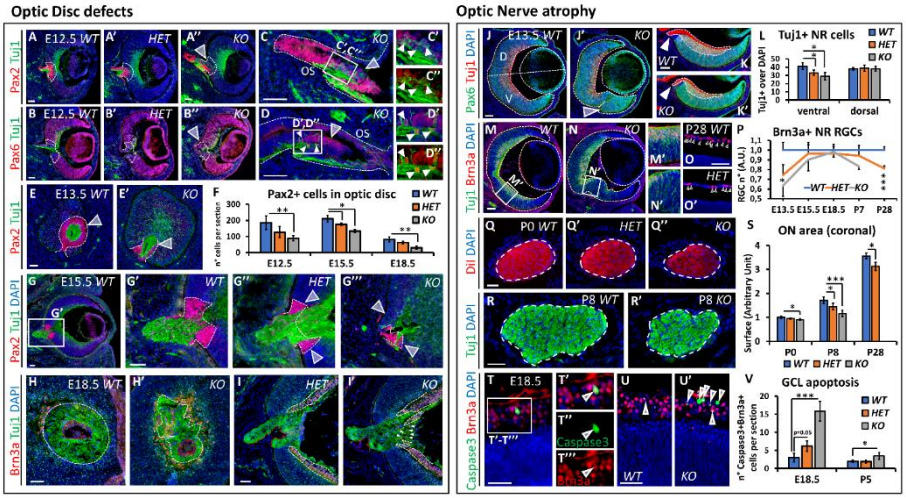

Figure 2. Optic disc (OD) malformations and optic nerve (ON) atrophy in Nr2f1-deficient mice. (A-A'') Pax2 (red, OD) and TujI (green, axons) IF on E12.5 optic cup cross-sections in wild-type (WT), Heterozygous (HET) and knock-out (KO) embryos showing abnormal ODs (white dotted lines and arrowhead). (B-B'') Pax6 (red, retinal progenitors) and Tuj1 (green) IF indicating ectopic Pax6+ retinal tissue in HET (B') and KO embryos (B", arrowhead). (C-D") High magnification views highlight a morphological displacement of Pax2- (C-C") and Pax6+ (D-D") cells. Arrowheads in (D',D") point to ectopic Tuj1/Pax6+ neurons. (E,E') Pax2 (red) and Tuj1 (green) IF on tangential sections of E13.5 optic cups revealing strong OD reduction in KO embryos (dotted line and arrowhead in E'), compared to WT (surrounded by a white dotted line in E). (F) Histogram quantifying the gradual reduction of Pax2+ OD cells in HET and KO at different ages. (G-G''') Low (G) and high (G'-G''') magnifications of E15.5 optic cups stained for Pax2 (red) and Tuj1 (green) confirming Pax2+ reduction in HET and KO ODs and severe morphological malformations in KO (arrowheads in G'''). (H-I') Tangential (H,H') and sagittal (I,I') sections of the OD in E18.5 WT and KO retinae stained for Brn3a (red; RGCs) and Tuj1 (green; axons) highlighting the malformed OD and disorganized arrangement of RGCs in KO. In (H,H')

white dotted line delineate the borders of the OD and in (I,I') the RGC layer; red dotted line surrounds mesodermal cells forming the hyaloid vessel. (J-K') IF on E13.5 optic cup cross-sections in WT and KO embryos showing increased Pax6 (green, retinal progenitors) and decreased Tuj1+ (red, differentiating cells) in the ventral retina of HET and KO embryos. Arrowhead in (J') points to increased thickness and bending of the ventral retina, while arrowheads in (K,K') indicate Tuj1+ axons exiting the OD. (L) Histogram confirming the decreased number of Tuj1+ neurons in the ventral, but not dorsal, retina of Nr2f1 mutants. (M-N') Double Tuj1/Brn3a IF on E13.5 WT and KO optic cup sections revealing decreased numbers of differentiating RGCs in bending ventral retinae of KO embryos (N'). (O,O') Details of P28 WT and HET retinae indicating decreased number of Brn3a+ neurons (arrowheads) in the GCL of HET animals. (P) Graph illustrating the dynamics of RGC differentiation from E13.5 to P28, normalized to WT animals. (Q-Q") Cross-sections of DiI-labelled P0 ONs and (R,R') Tuj1+ P8 ON fibers in WT and KO pups showing a progressive volume loss from P0 to P8. (S) Quantification of the surface occupied by Tuj1+ or DiI+ fibers in different genotypes and ages, as indicated. (T-U') Cleaved-Caspase-3 (green, apoptotic cells) and Brn3a (red, RGCs) IF on transverse sections of E18.5 retinae in WT and KO fetuses. High magnifications (T'-T'") highlight an example of a double-labeled RGC undergoing apoptosis (arrowheads) in the ganglion cell layer (GCL). Apoptotic RGCs are increased in KO animals (arrowheads in U'), compared to WT (U). (V) Histogram quantifying the number of RGC apoptotic cells in WT, HET and KO from E18.5 to P5. Note the significant increase of dying cells at E18.5. Nuclei (blue) were stained with DAPI. In (F,L,P,S,V) data are represented as mean ± SEM; N=3-4 for (F,L,P,V); N=4-5 for (S). Student t-test (*P<0.05, **P<0.01, ***P<0.001). Scale bars: 50µm.

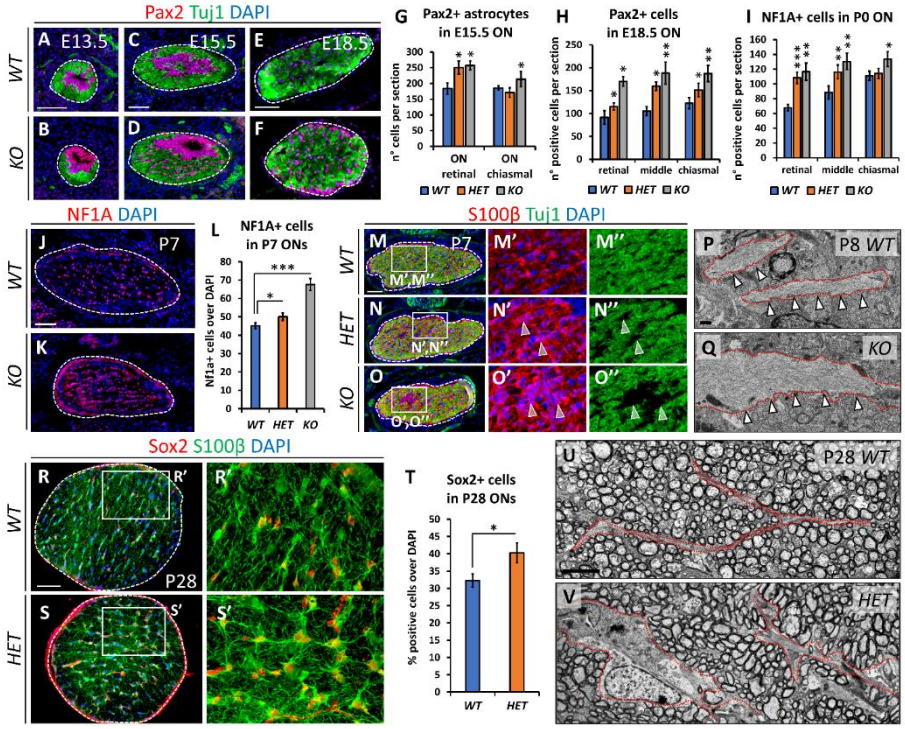

Figure 3. Increased astrocytic population in Nr2f1-deficient optic nerves. (A-F) Pax2 (magenta, astrocytic progenitors) and Tuj1 (green, RGC axons) IF on E13.5, E15.5 and E18.5 OS/ONs cross-sections showing an increase of Pax2-expressing cells within the optic nerve (ON) of KO embryos at all stages. (G-I) Histograms quantifying the average number of Pax2+ (G,H) or NF1A+ (I) cells in WT, HET and KO at different stages and axial length of the ON, as indicated. Astrocytic progenitors are significantly increased along the nerve of mutants. (J,K) NF1A (red, astrocyte precursors) IF on P7 WT and KO ON cross-sections illustrating a high astrocytic density in KO ON (delineated by thin dashed lines). (L) Histogram confirming the increased percentage of NF1A+ astrocytes in HET and KO ONs compared to WT. (M-O") Tuj1 (green, RGC axons) and S100β (red, astrocytes) IF on P7 WT, HET and KO ONs. Arrowheads point to S100β+ astrocyte groups (N',O') and absence of Tuj1+ fibers (N'',O'') in HET and KO ONs. (P.Q) TEM images of WT and KO P8 ONs showing thick astrocytic processes filled with

intermediate filaments (red dotted lines and arrowheads) in KO nerves. (R-S') S100β (green, astrocytes) and Sox2 (red, reactive/inflamed astrocytes) IF on P28 WT and HET ONs illustrating strong Sox2 expression in reactive astrocytes. (T) Graph quantifying the average number of Sox2+ astrocytes per P28 ON section in KO and WT animals. (U,V) EM sections of P28 WT and HET ONs illustrating the expanded astrocytic processes (surrounded by red dotted lines) among myelinated fibers of P28 ONs. In (G,H,I,L,T) data are represented as means ± SEM; N=3-5. Statistical significance was obtained by Student t-test (*P<0.05; **P<0.01; ***P<0.001). Nuclei (blue) were stained with DAPI. Scale bars: 50µm, except (P,Q) (500nm) and (U,V) (4µm).

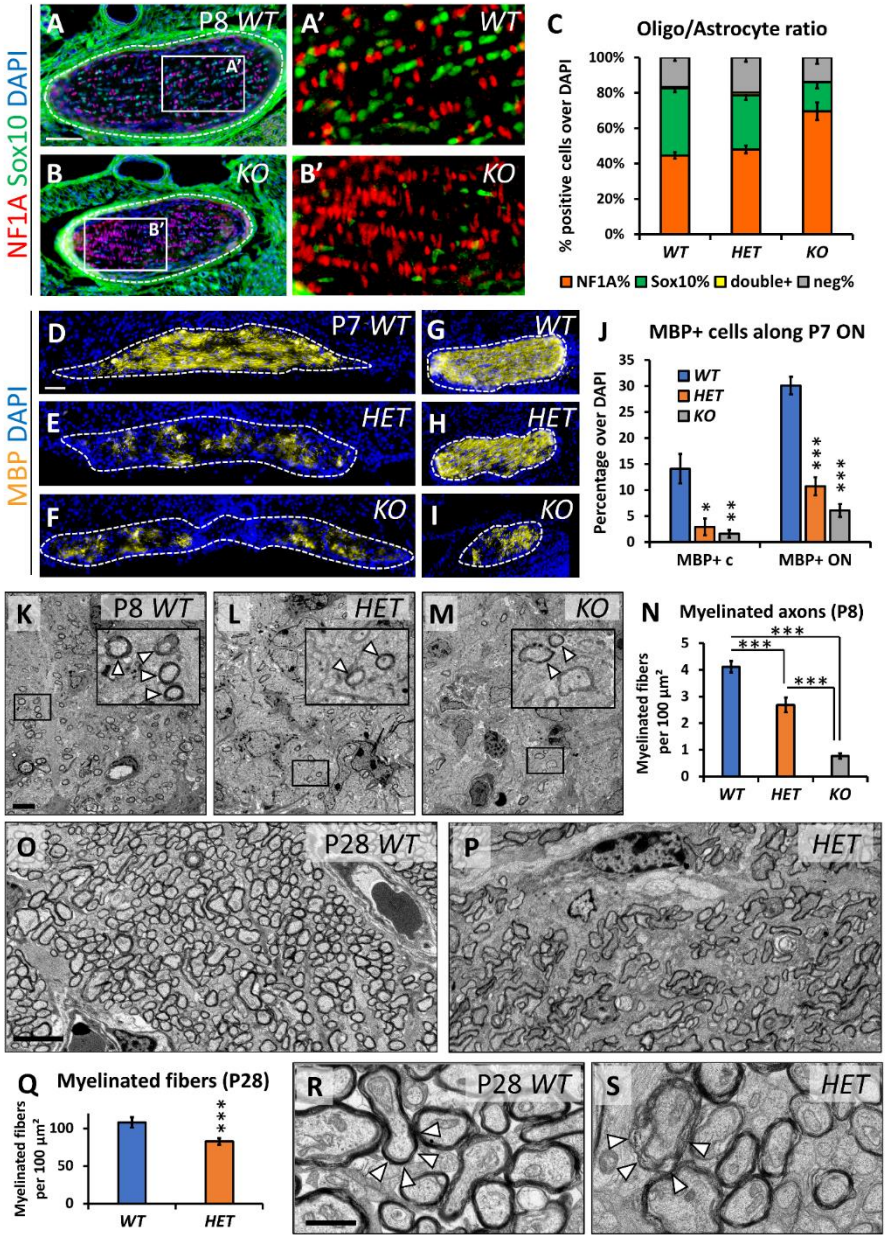

Figure 4: Optic nerve myelination is affected by reduced Nr2f1 dosage. (A-C) NF1A (red, astrocytes) and Sox10 (green, oligodendrocytes) IF on cross-sections of WT and KO P8 ONs showing altered ratio of astrocytes and oligodendrocytes in mutants, particularly in KOs, as quantified in (C). (D-J)

MBP (yellow, fully differentiated oligodendrocytes) IF on cross-sections of WT, HET and KO P7 optic nerves (ONs) at the chiasm (D-F) and between the chiasm and the eye (G-I). Note the dramatic decrease of MBP+ oligodendrocytes at the chiasm in HET and KO, quantified in (J). The ratio of MBP+ cells is calculated over the total DAPI+ cell number per chiasmal/ON section. (K-N) EM thin sections of P8 WT, HET and KO ONs depicting myelin as a dense, dark staining around axonal fibers illustrate a significantly lower number of myelinated fibers in HET and KO, as quantified in (N). Higher magnification images (insets) showing different degrees of myelination in HET and KO ONs. (O-Q) TEM images of P28 WT and HET confirming persistent hypomyelination in mutants at P28, as quantified in (Q). (R,S) High magnification EM images of P28 WT and HET ONs showing the difference in myelin compaction between WT (arrowheads in R) and HET (arrowheads in S). In (C,J,N,Q), data are represented as means ± SEM. N=4-5 for (C,J); N=3 for (N,Q). Statistical significance was obtained by Student t-test or by two-way ANOVA when comparing 2 or multiple conditions, respectively (*P<0.05; **P<0.01; ***P<0.001). Nuclei (blue) were stained with DAPI. Scale bars: 50µm, except (K-P) (4µm) and (R,S) (1µm).

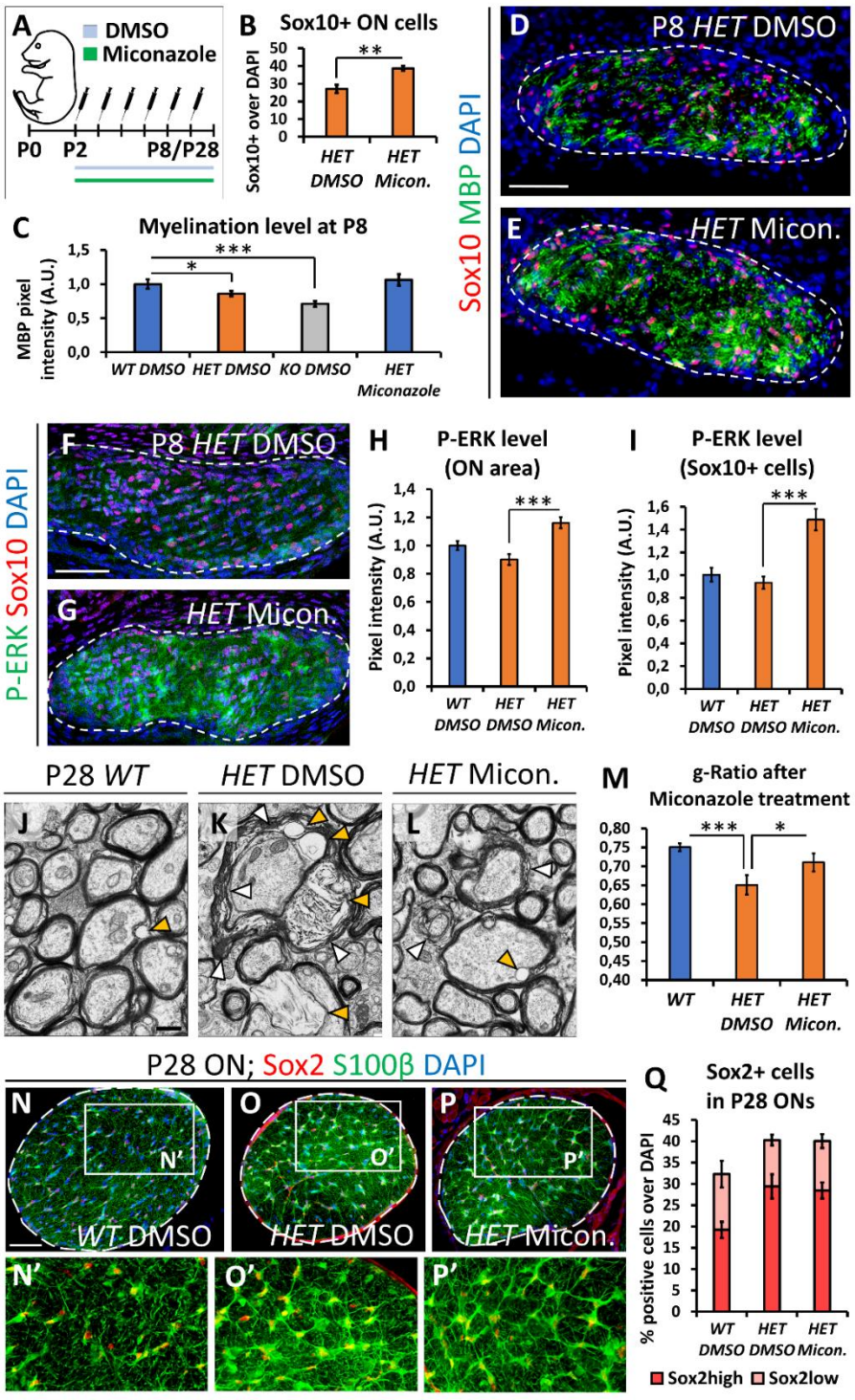
A
DMSO
Miconazole
P0
P2
P8/P28
B
Sox10+ ON cells
Sox10+ over DAPI
HET DMSO
HET Micon.
C
Myelination level at P8
MBP pixel intensity (A.U.)
WT DMSO
HET DMSO
KO DMSO
HET Miconazole
D
P8 HET DMSO
E
HET Micon.
Sox10 MBP DAPI
F
P8 HET DMSO
G
HET Micon.
P-ERK Sox10 DAPI
H
P-ERK level (ON area)
Pixel intensity (A.U.)
I
P-ERK level (Sox10+ cells)
Pixel intensity (A.U.)
P28 WT
HET DMSO
HET Micon.
J
K
L
M
g-Ratio after Miconazole treatment
WT
HET DMSO
HET Micon.
P28 ON; Sox2 S100β DAPI
N
N'
WT DMSO
O
O'
HET DMSO
P
P'
HET Micon.
N'
O'
P'
Q
Sox2+ cells in P28 ONs
% positive cells over DAPI
Sox2high
Sox2low

Figure 5. **Miconazole treatment specifically rescues Nr2f1-dependent hypomyelination in postnatal pups.** (A) Experimental design to treat HET pups from P2 to P8 with Miconazole. DMSO (controls) and Miconazole-treated pups were sacrificed at P8 or at P28 to evaluate the ON myelination. (B-E) Sox10 (red, oligodendrocyte precursors) and MBP (green, fully differentiated oligodendrocytes) IF on cross-sections of P8 HET ONs after 6 days of treatment with DMSO (D) or Miconazole (E). Miconazole increased the number of Sox10+ cells compared to HETs treated with DMSO (quantified in B) and rescued MBP staining pixel intensity of HET pups to level comparable to those of WT pups (quantified in C). (F-I) Sox10 (oligodendrocyte marker, red) and Phospho-ERK (dually phosphorylated forms of active ERK1 and ERK2, green) IF in WT and HET ONs, treated with DMSO (F) or Miconazole (G) between P2 and P8. As previously reported, Miconazole strongly activate ERK signaling pathway (G). Signal intensity quantification in whole ON area is shown in (H), while specific evaluation of pixel intensity around Sox10+ nuclei is shown in (I). (J-M) EM thin sections of P28 WT and HET ONs, treated with DMSO (J,K) or Miconazole (L) between P2 and P8. Different degrees of myelin compaction can be appreciated at high magnification, with HET ONs showing non compacted sheaths (white arrows in K) and vacuoles (yellow arrows). Miconazole treatment rescues almost normal myelin g-ratio, as quantified in M. (N-P') S100β (green, astrocytes) and Sox2 (red, reactive/proliferative astrocytes) IF in the ONs of WT (N,N') and HET (O-P') animals after 6 days of treatment with DMSO (N-O') or Miconazole (P,P'), then sacrificed at P28. Astrocytes undergo remodeling and express Sox2 in Nr2f1 HET animals (O',P'), even after Miconazole treatment. (Q) Histogram showing the average number of S100β+/Sox2+ astrocytes per P28 ON section in WT or HET animals treated with DMSO or Miconazole as indicated, with Sox2 high (magenta columns) and low levels (pink columns). Nuclei (blue) were stained with DAPI. In (B,C,H,I,M,Q), the error bars represent the SEM of the means; N=3 for (B,C);

N=2 for (H,I,M,Q). Statistical significance was obtained by ANOVA (*P<0.05; **P<0.01; ***P<0.001). Scale bars: 50µm, except (J-L) (500nm).

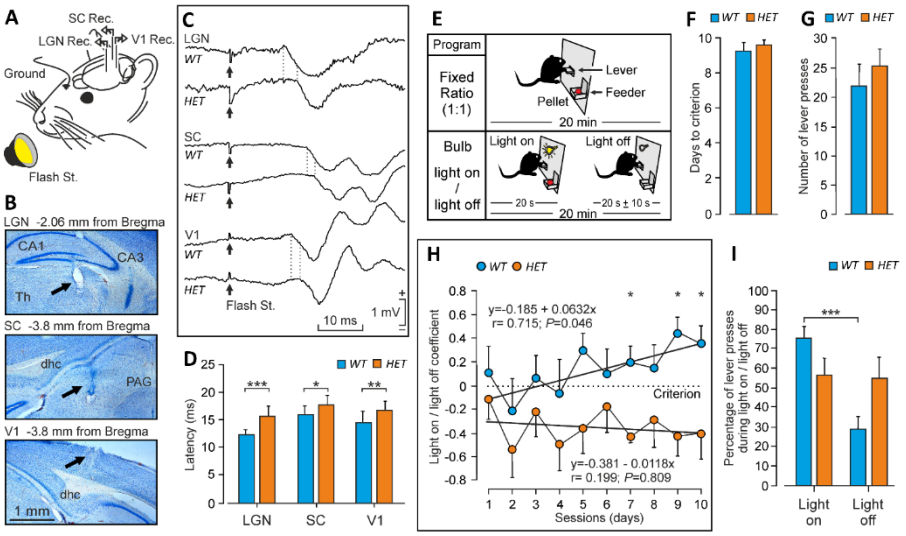

Figure 6. Axonal conduction velocity and visually-dependent operant conditioning are impaired in Nr2f1 HET mice. (A) Animals were implanted with recording electrodes in lateral geniculate nucleus (LGN), superior colliculus (SC), and visual cortex (V1) and stimulated with a flashing stroboscope. (B) Nissl-stained sections illustrating the location of the recording electrodes (arrows). dhc, dorsal hippocampal commissure; PAC, periaqueductal grey; Th, thalamus. (C) Examples of field potentials (averaged ≥ 20 times) evoked by flash stimulation in the recording sites for WT and HET mice. Dotted lines indicate the beginning of evoked field potentials. (D) Latency of evoked field potentials for WT (N=13) and HET (N=18) mice. (E) In a first series of experiments, animals [WT (N=13) and HET (N=18)] were trained to press a lever to obtain a pellet of food in an illuminated Skinner box with a fixed-ratio (1:1) schedule. After ten days of training, they were transferred to a light on/light off protocol where lever presses were only rewarded when a small light bulb located over the lever was switched on.

Lever presses while the bulb was off were punished with a time penalty of ≤ 10 s during which the bulb would not turn on. (F,G) Mean days to criterion (F) and mean number of lever presses during the last two training sessions (G) for the fixed-ratio (1:1) paradigm. No significant differences were observed. (H) Performance of WT (N=13) and HET (N=18) mice in the light on/light off test. Criterion (dotted line) was that the animal had to press the lever more times during the small bulb light on period than during the light off one. WT mice performed better than HET animals and reached the criterion by the 6th session. The HET did not reached criterion for the duration of the test. While a linear fit to WT data increased significantly across training, the same linear fit to HET performance did not present any significant change. (I) The percentage of lever presses during the light on and light off periods for WT and HET mice was also different, because the WT group pressed the lever preferentially during the light period. Data were averaged from the 9th and 10th sessions. For statistical significance, see Materials and Methods (*P<0.05; **P<0.01; ***P<0.001).

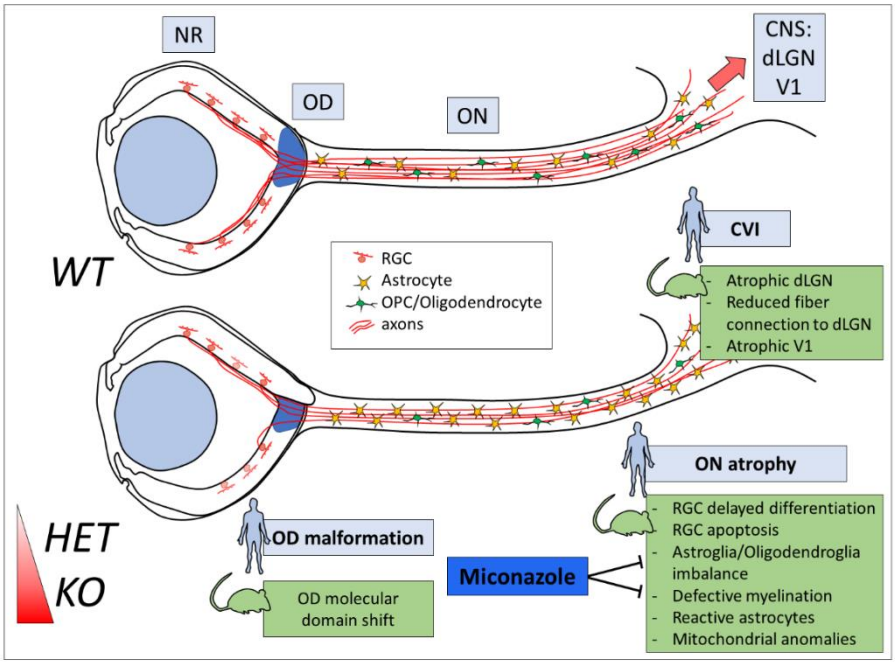

Figure 7. Summary of the defects observed in the visual system of Nr2f1 mutant mice compared to patient features. Schematic overview of the different phenotypes observed in the retina, optic nerve, thalamus and visual cortex of Nr2f1 Heterozygous (HET) and Knock-out (KO) mice. Some of the defects characterized in the mouse model (green boxes) are reminiscent of the major features reported in BBSOA patients (light blue boxes). Nr2f1 haploinsufficiency causes a shift of NR/OS molecular domains (in blue), leading to aberrant positioning of the optic stalk (OS) and ultimately optic disc (OD) malformations at early stages. Pale and abnormal ODs have also been reported in human patients. Optic nerve (ON) atrophy, the most characteristic feature of BBSOA patients, is most probably caused by: (i) delayed RGC differentiation (red cells) at early embryonic stages and increased apoptosis at perinatal stages; (ii) affected oligodendrocyte migration and maturation (green cells) leading to ON fiber demyelination and reduced volume; (iii) reduced axonal innervation and connectivity to the atrophic thalamic dLGN and V1 neocortex; (iv) reactive gliosis consistent with astrocyte inflammation and (v) possible associated mitochondrial dysfunctions. All these defects identified in Nr2f1 mutants contribute to form a reduced and hypomyelinated ON and ultimately affect visual axonal conduction velocity. While the myelination defect could be rescued by Miconazole treatment (blue box), the high proportion of astrocyte precursors and reactive astrocytes (yellow cells) leading to gliosis could not be rescued and might lead to ON degeneration at adult stages. The majority of these defects are already present in HET but further worsened in KO mice, suggesting a gene dosage effect during development of the visual system (red gradient).

Supplementary Figures

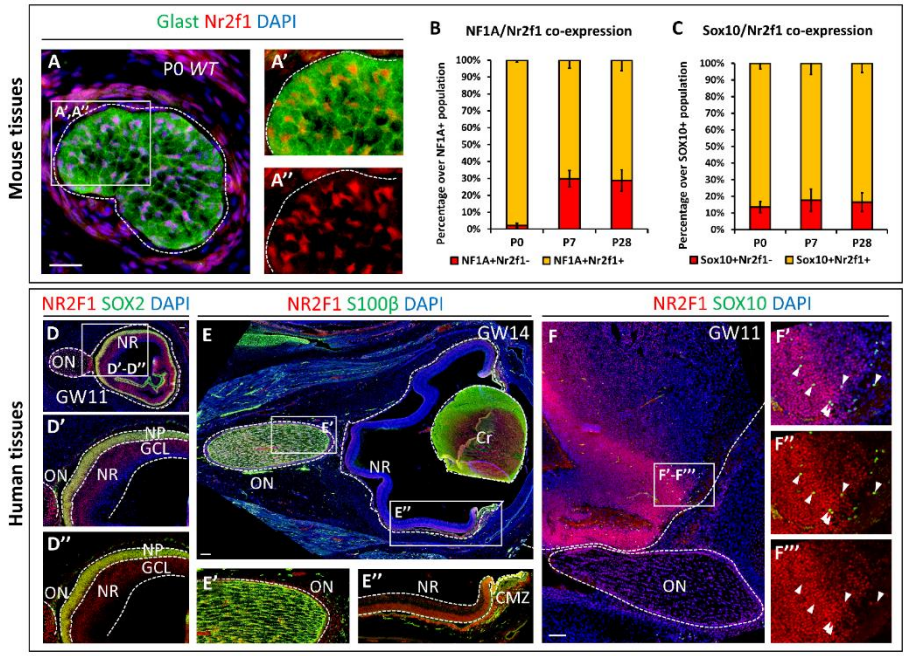

Suppl Figure 1. Nr2f1/NR2F1 expression in mouse and human retina and optic nerve. (A-A'') Nr2f1 (red) and Glast (green, astrocyte precursors) immunofluorescences (IF) in a wild-type (*WT*) P0 mouse optic nerve (ON) showing that almost all Glast+ astrocytes are co-labelled with Nr2f1 (insets A',A''). (B) Graph illustrating the percentage of double NF1A+/Nr2f1+ astrocytes (yellow) over the total NF1A+ population in P0, P7 and P28 mouse ONs. (C) Graph showing the percentage of double Sox10+/Nr2f1+ oligodendrocytes (yellow) over the total Sox10+ population, in P0, P7 and P28 mouse ONs. (D-D'') NR2F1 (red) and SOX2 (green, NR progenitors) IF of gestational week (GW) 11 human eye, showing high NR2F1 expression in all NR progenitors. GCL: ganglion cell layer; NP: neural progenitor layer; NR: neural retina. (E-E'') NR2F1 (red) and S100β (green) IF in a sagittal GW14 eye section showing NR2F1 expression in almost all astrocytes of the ON (E'), in the NR and ciliary marginal zone (CMZ; E''). Cr: lens crystal. (F-

F''') NR2F1 (red) and SOX10 (green, oligodendrocyte precursors) IF in a sagittal GW11 human brain section (proximal ON and basal forebrain region) illustrating the presence of SOX10+ oligodendrocyte progenitors at the ventricular zone and in proximity of the ON (arrows in F'-F'''). Nuclei (blue) were stained with DAPI. In (B,C) data were normalized to the total NF1A+ or Sox10+ cells and represented as mean ± SEM; N=3. Scale bars: 50µm in (A), 100µm in (D-F).

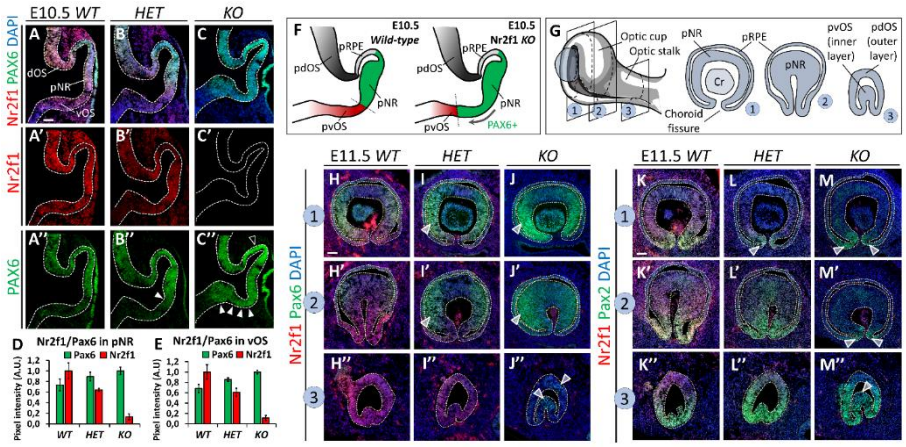

Suppl Figure 2. Nr2f1-dependent control of early OS/NR molecular domains. (A-C") Nr2f1 (red) and Pax6 (green, NR) IF on sagittal sections of E10.5 optic vesicles in *wild-type (WT), Heterozygous (HET)* and *full knock-out (KO)* embryos. (A'-C') Note the progressive reduction of Nr2f1 protein levels from *WT* to *KO*. (A"-C") Full and empty arrowheads point to increased Pax6 expression in the ventral and dorsal regions, respectively, of the optic vesicle. (D,E) Pixel intensity quantification of Pax6 and Nr2f1 IF in presumptive neural retina (pNR; D) and ventral optic stalk (vOS; E) of E10.5 embryos confirming an inverse relationship between Nr2f1 and Pax6 protein levels. Data represent the mean ± SEM; N=4-5. (F) Scheme illustrating the expansion of Pax6+ pNR domain (green) towards the pvOS domain (red) in *Nr2f1 KO* mutants. pdOS, presumptive dorsal optic stalk; pRPE, presumptive retinal pigmented epithelium. (G) Scheme depicting an E11.5 mouse eye

primordium and the structures visible after cross-section at different levels, from distal (1) to middle (2) to proximal (3). (H-J'') Nr2f1 (red) and Pax6 (green, NR) IF on E11.5 *WT, HET* and *KO* optic cups, at the levels indicated above showing the inverse correlation between Nr2f1 and Pax6 expression levels from *WT* to *KO* (arrowheads in I,J,I',J'). Note the presence of Pax6+ cells in the proximal region of the pvOS of *KO* animals (J''), suggesting that pNR cells substitute pvOS cells along the OS axis. (K-M'') Nr2f1 (red) and Pax2 (green) IF on E11.5 *WT, HET* and *KO* optic cups at the levels indicated above and showing reduced Pax2 expression and reciprocal Pax6 is up-regulation in the ventral region of the pNR of *HET* and *KO* animals (arrowheads in L,M,M'). Nuclei (blue) were stained with DAPI. Scale bars: 50µm.

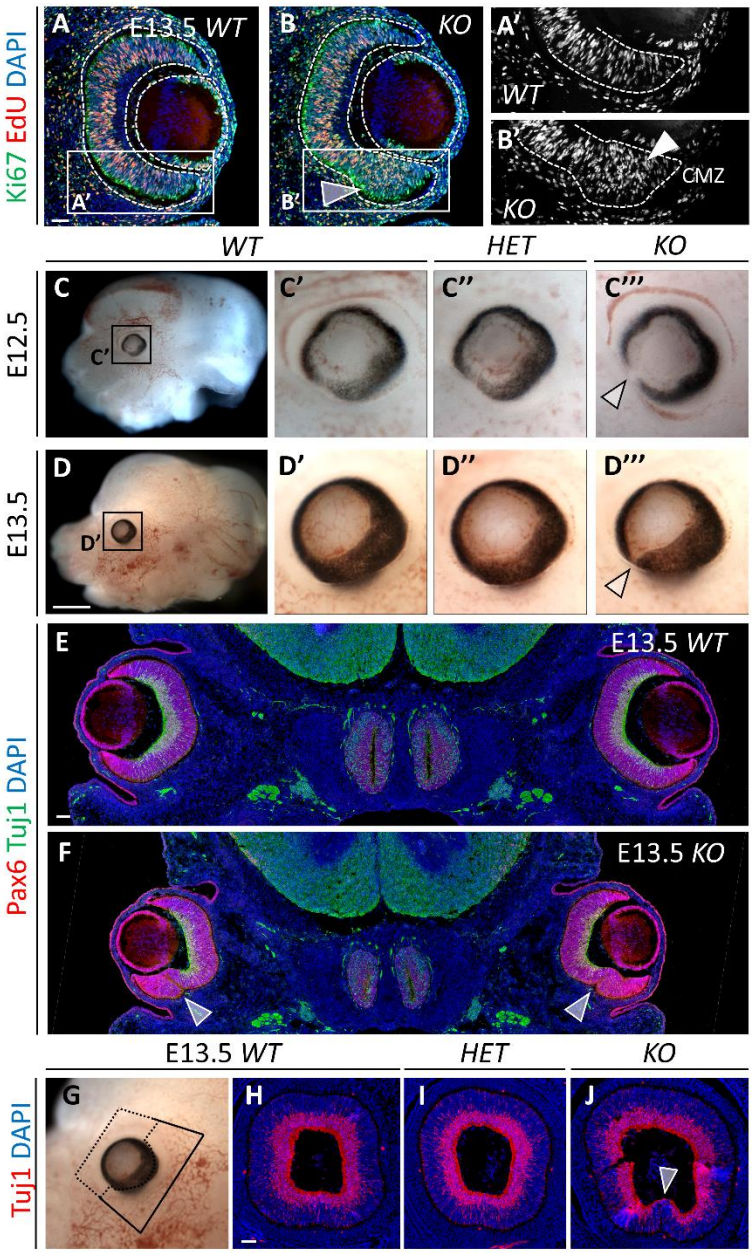

Suppl Figure 3. Nr2f1 reduced levels associated with hyperproliferation and coloboma-like retinal malformations. (A-B') Ki67 (green, proliferative cells) and EdU (red in A,B, grey in A',B'; S-phase proliferating cells) IF on E13.5 *WT* and *KO* optic cup cross-sections showing increased proliferation,

particularly in the ventral ciliary marginal zone (CMZ), where Ki67+/EdU+ cells abnormally accumulate in the *KO* (arrowhead in B,B'). (C-D''') Microphotographs of E12.5 (C-C"') and E13.5 (D-D"') *WT*, *HET* or *KO* mouse embryo heads as indicated. Arrowheads in C"' and D"' point to coloboma-like malformations in the ventral *KO* retinas. (E,F) Pax6 (NR, red) and Tuj1 (differentiating RG cells, green) IF of E13.5 *WT* (E) and *KO* (F) heads showing expanded CMZ and reduced ventral cell differentiation (arrowheads in F) in *Nr2f1 KO* embryos. (G-J) Tuj1 (red) IF of E13.5 eye cross-sections (as schematized in G) of *WT* (H), *HET* (I) and *KO* (J) embryos confirming normal ventral fusion in the *KO* retina. Nuclei (blue) were stained with DAPI. Scale bars: 50µm in IFs (A-B',E-J), 1mm in microphotographs (C,D).

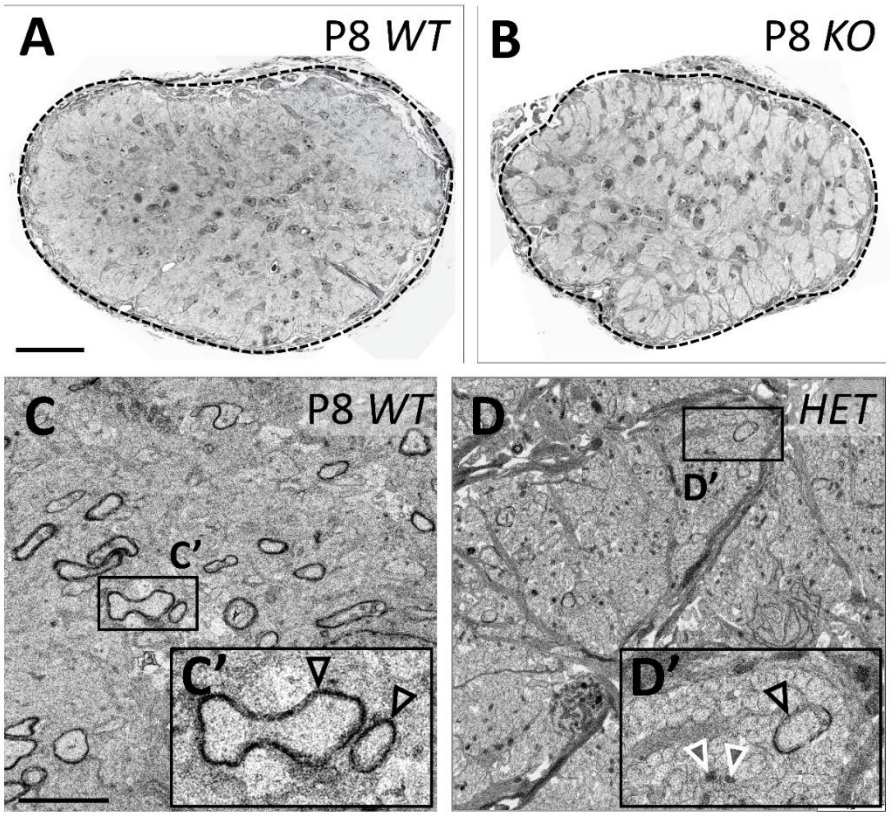

Suppl Figure 4. Reactive gliosis and reduced myelination in P8 *Nr2f1*-deficient nerves. (A,B) Electron microscopy (EM) images of P8 *WT* (A) and *KO* (B) mouse ONs displaying an electron-dense cytoplasm in *Nr2f1 KO* nerves. (C,D) EM images of P8 *WT* (C) and *HET* (D) mouse ONs showing thick electron-dense astrocytic processes and high number of stress granules (white arrowheads in inset D'). The number of myelinated fibers is lower in *HET* animals (D), than in *WT* littermates (C). Laminae of myelin around axons are often thin and discontinuous in *HET* animals (black arrowheads in C',D'). Scale bars: 100µm in (a,b), 5µm in (c,d).

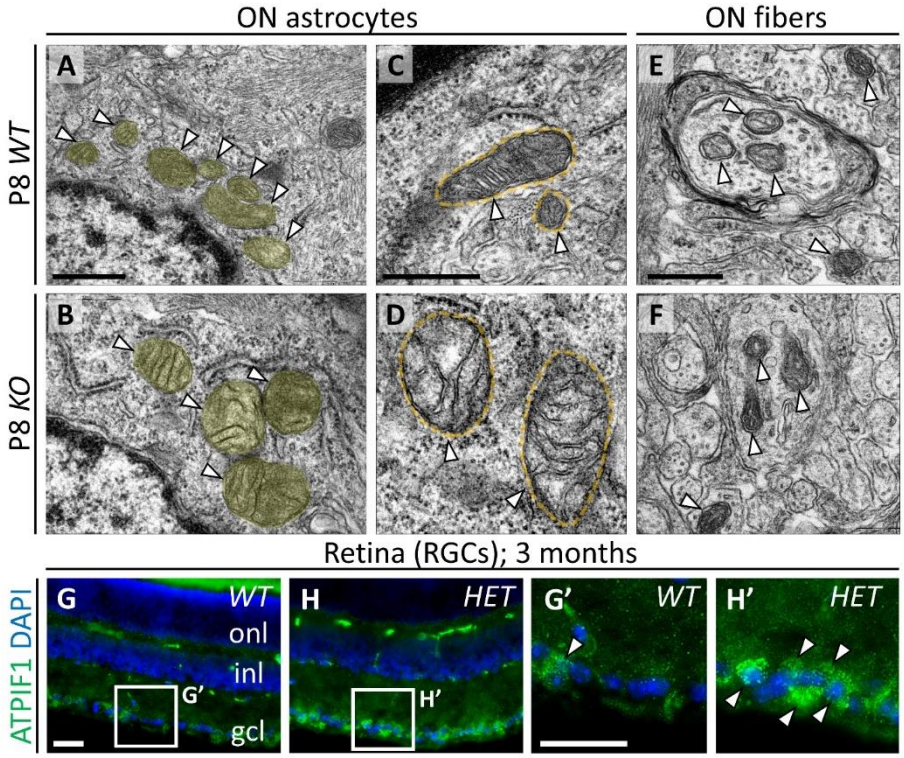

Suppl Figure 5. Mitochondrial hypertrophy in ON astroglia and RGC somata. (A-F) Electron microscopy (EM) images of P8 *WT* (A,C,E) and *KO* (B,D,F) mouse ONs displaying the structure of mitochondria in both astrocyte cytoplasm (A-D) and RGC axons (E,F). The average size of glia mitochondria (white arrowheads in A-D; highlighted in yellow in A,B) is increased in KO

ONs (1.78±0.15 times bigger than WT; p = 0.0018), additionally showing abnormal *cristae* (D). On the contrary, their structure/size seems normal in axons (E,F). (G-H') ATPIF1 (pan-mitochondria OxPhos marker, green) IF in the retina of 3 months-old WT (G,G') and HET (H,H') animals, showing intense staining in HET ganglion cell layer (gcl). High magnification images show increased mitochondrial staining in HET GCL cytoplasm (arrows in H'). Nuclei (blue) were stained with DAPI. Scale bars: 500nm in (A-F), 50µm in (G-H'). onl: outer nuclear layer; inl: inner nuclear layer.

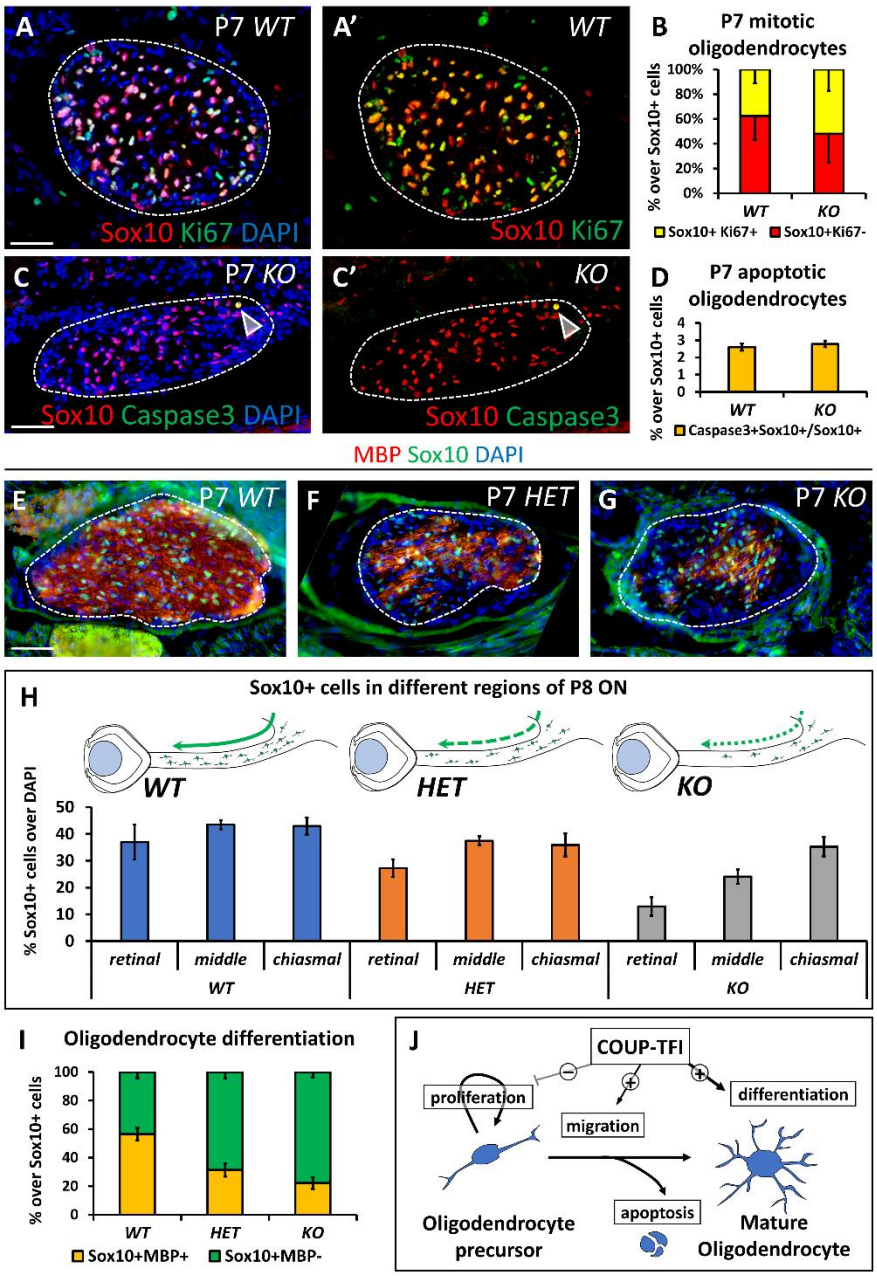

Suppl Figure 6. Oligodendrocyte maturation is defective in *Nr2f1*-deficient nerves. (A-B) Sox10 (oligodendrocyte marker, red) and Ki67 (proliferation marker, green) IF in P7 *WT* and *KO* ONs showing normal proliferation of single Sox10+ (non-proliferative, red) and double

Sox10+/Ki67+ (proliferative, yellow) oligodendrocytes, as quantified in (B). (C-D) Sox10 (oligodendrocyte marker, red) and cleaved-Caspase3 (apoptotic marker, green) IF in P7 *WT* and *KO* ON showing an equivalent number of double Sox10+/Caspase3+ apoptotic oligodendrocytes (arrowheads) in both genotypes, as quantified in (D). (E-I) Sox10 (oligodendrocyte marker, green) and MBP (fully differentiated oligodendrocyte marker, red) IF in P7 *WT* (E), *HET* (F) and *KO* (G) ONs illustrating strong reduction of oligodendrocytes on the retinal side of *HET* and *KO* ON. Percentages of Sox10+ cells and their distribution along the ON are quantified in (H). (I) Ratio of MBP+/MBP- oligodendrocytes. (J) Schematic summary of Nr2f1 role in the Sox10+ oligodendrocyte population. Nr2f1 controls the development of oligodendrocyte precursors, their migration along the ON and their terminal differentiation. Nuclei (blue) were stained with DAPI. In (B,D,H,I) data are represented as mean ± SEM; N=3-4. Scale bars: 50µm.

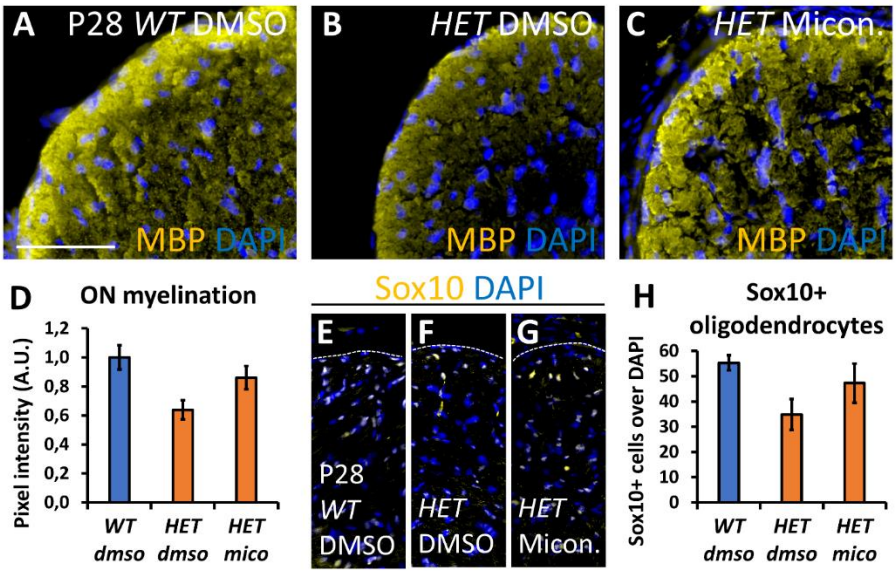

Suppl Figure 7. Long term effects of Miconazole treatment at post-natal age. (A-D) MBP (yellow) IF on P28 WT or HET ONs after 6 days of treatment with DMSO (A,B) or Miconazole (C) during the P2-P8 sensitive window. A

short treatment with Miconazole partially maintains improved myelination 20 days later (C,D), even if levels failed to reach those of WT (A). EM images of similarly treated samples are shown in Figure 5J-L. (E-H) Sox10 (yellow) IF on P28 WT or HET ONs after 6 days of treatment with DMSO (E,F) or Miconazole (G) between P2-P8 showing increased Sox10-expressing cells in treated HET ONs (H). In (D,H), the error bars represent the SEM of the means; N=2. Scale bars: 100µm.

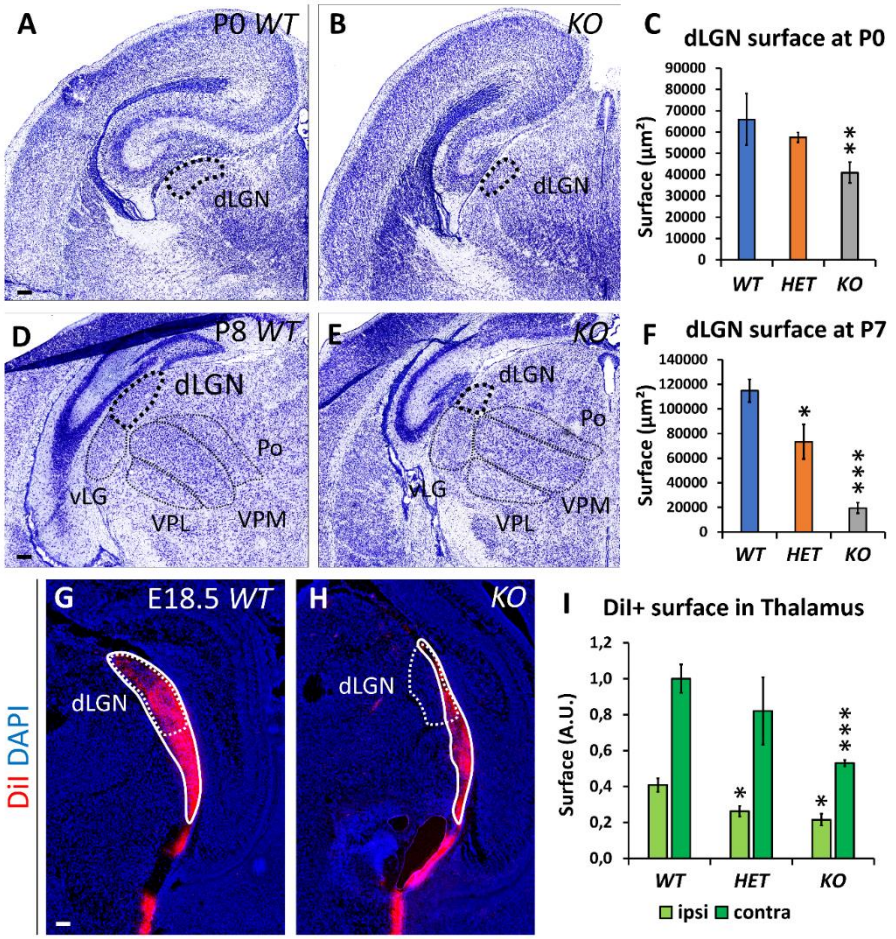

Suppl Figure 8. Visual system impairment in *Nr2f1* mutants at thalamic level. (A-C) Nissl staining of P0 *WT* (A) and *KO* (B) brain coronal sections,

showing strong reduction of the dorsolateral geniculate nucleus (dLGN; dotted black line) in the *Nr2f1 KO* thalamus, compared to *WT*. Area quantification of *WT*, *HET* and *KO* dLGN in P0 brains is shown in Graph (C). (D-F) Nissl staining of P8 *WT* (D) and *KO* (E) brain coronal sections confirming persistent and exacerbated reduction of the dLGN (thicker dotted line) in *KO* brains, as quantified in (F). vLGN: ventrolateral geniculate nucleus; Po: posterior nucleus; VPL: ventral posterolateral nucleus; VPM: ventral posteromedial nucleus. (G,H) Fluorescent axonal labeling (red staining, highlighted by white line) of optic tract fibers after injection of DiI crystals in the eye showing reduced innervation of *KO* fibers in the dLGN. White dotted lines highlight the size of the dLGN. (I) Quantification of the ipsi- (light green) and contra-lateral (dark green columns) fibers reaching the dLGN. Nuclei (blue) were stained with DAPI. In (C,F,I) data are represented as mean ± SEM. Statistical significance was obtained by ANOVA (*P<0.05; **P<0.01; ***P<0.001). N=3-4. Scale bars: 100µm.

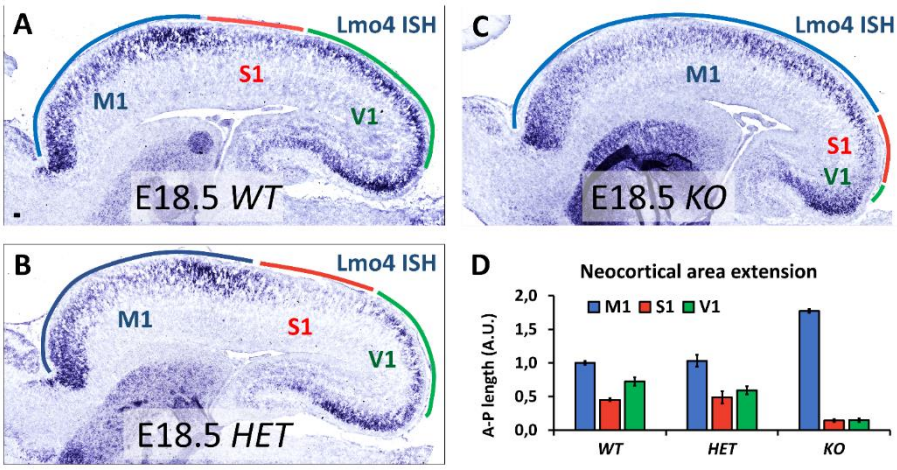

Suppl Figure 9. V1 neocortical area shrinkage in *Nr2f1*-deficient brains. (A-D) *In situ* hybridization of *Lmo4 mRNA* in E18.5 *WT* (A), *HET* (B) and

KO (C) sagittal brain sections. *Lmo4* expression labels the primary motor cortex anteriorly (M1; blue line) and the primary visual cortex posteriorly (V1; green line), leaving the primary somatosensory cortex unlabeled (S1; red line). *Nr2f1* loss shifts neocortical areas, compressing S1 and V1 in the posterior-most region (C); *HET* animals show a slight shift of V1 (B), compared to *WT* (A). Antero-posterior (A-P) length of the different neocortical areas across genotypes is quantified in Graph (D). Data in (D) are represented as mean ± SEM. Scale bars: 100µm.

Materials And Methods

Animal procedures

All mouse experiments were conducted according to national and international guidelines and have been approved by the local ethical committee in France (CIEPAL NCE/2014-209) and Spain (JA/CAPD 06/03/2018/025). *Nr2f1* heterozygous (*HET*) and homozygous (*KO*) mice were generated and genotyped as previously described(Armentano et al, 2006). Littermates of *HET* and *KO* mice with normal *Nr2f1* alleles were used as control mice (herein called *WT*). Midday of the day of the vaginal plug was considered as embryonic day 0.5 (E0.5). Control and mutant mice were bred in a 129S2/SvPas background. Both male and female embryos and pups were used in this study.

Immunofluorescence

Mouse embryonic heads were dissected and fixed in 4% paraformaldehyde (PFA) at 4°C for 3 h in agitation, then washed in PBS 1X and dehydrated in 25% sucrose overnight at 4°C. P8 brains and eyes

were fixed by intra-cardiac perfusion of 4% PFA, then processed as previously described(Armentano et al, 2007; Armentano et al, 2006). Primary antibodies used: NR2F1 (Abcam ab181137, 1:1000, rabbit; R&D H8132, 1:1000, mouse), ATPIF1 (ThermoFisher 5E2D7, 1:500, mouse), Phospho-ERK (Cell signaling #4370, 1:200, rabbit), Sox10 (Santacruz sc-365692, 1:200, mouse), Sox2 (R&D AB2018, 1:500, mouse), NF1a (Abcam ab41851, 1:1000, rabbit), MBP (Abcam ab7349, 1:1000, rat), Brn3a (1:1000, mouse, kind gift of Thomas Lamonerie, IBV, Nice), Caspase-3 (Cell signaling #9661, 1:2000, rabbit), Pax2 (Abcam ab79389, 1:1000, rabbit), Pax6 (Millipore AB2237, 1:500, rabbit), Ki67 (ThermoFisher PA5-16446, 1:1000), GLAST (1:1000, rabbit), GFAP (Dako, 1:200, rabbit), S100β (Dako Cytomation Z0311, 1:200, rabbit) and Tuj1 (β-III TUBULIN, Covance MRB-435P, 1:1000; or Sigma T8660, 1:1000, mouse). Alexa Fluor 488, 555, 594 and 647 anti-mouse, anti-rabbit or anti-rat IgG conjugates (Thermo Fisher scientific, all 1:500) were used as secondary antibodies.

Nissl Staining

Cryostat sections were left to dry for 60 minutes at room temperature. The slides were briefly washed in MilliQ water, post-fixed in 4% PFA 10 minutes at room temperature and then immersed 5 min in the following staining solution: 0.025% thionine acetate (Sigma, T2029-5G), 0.025% Cresyl violet acetate (Sigma, T2029-5G), 100mM sodium acetate, 8mM acetic acid. Slides were then washed in ethanol/acetic acid (80/0.05 %) for a variable time depending on the rate of clarification. Slides were dehydrated by two brief washes in ethanol 100% and finally 2X 5-min washes in xylene. Sections were cover-

slipped using Eukitt mounting medium (KO Kinder GmbH D-79110).

In situ hybridization (ISH)

Netrin1 and *Lmo4 RNA* probes were *in vitro* transcribed from previously used plasmids(Alfano et al, 2014; Deiner et al, 1997). Heads/eyes for ISH were fixed overnight with PFA 4% at 4°C, dehydrated in 25% sucrose, and embedded in OCT resin, then stored at -80°C. ISH was carried out on 14-µm cryosections, as previously described(Armentano et al, 2007).

DiI labelling of mouse optic nerves

E18.5 mouse heads were fixed O/N in 4% PFA at 4°C. Lenses were gently removed from the eyes using sharp forceps, and a DiI crystal (Invitrogen, Life Technologies) was inserted inside the optic nerve head. To help keeping the crystal in position, the lens was placed back inside the eye. Heads were kept in 4% PFA at 37°C for 3 to 4 weeks, allowing for DiI diffusion along the nerve. When ready to be processed, heads were washed in PBS, dehydrated in 25% sucrose, included in OCT and 14µm-thin sections were obtained by cryostat cutting. DAPI counterstaining was performed before slide mounting.

Transmission electron microscopy

Eyes, with their ON attached, from P8 and P28 *WT* and *Nr2f1* mutants were fixed O/N at 4°C with 3% glutaraldehyde in PBS and then washed in PBS. ON were separated from the eye bulb and the surrounding muscle and treated with 1% osmium tetroxide in double-distilled water and 1% potassium ferrocyanide for 1hr at 4°C. After washing, the ONs

were incubated in 0.15% tannic acid in 0.1 m PBS, pH 7.4 followed by staining with 2% uranyl acetate in distilled water for 1hr RT in darkness. After washing, the tissue was dehydrated with an ascending series of EtOH dilutions up to 100% at 4°C, followed by a stepwise incubation in propylene oxide. Tissue was then infiltrated stepwise with Epoxy resin (TAAB 812; TAAB Laboratories) and encapsulated in flat molds taking into accounts the proximo-distal orientation of the nerves. Blocks were polymerized for 48 h at 60°C. Semithin (1 μm) sections were stained with toluidine blue and ultrathin sections (70–80 nm) were collected along three different proximo-distal levels of the ONs, using an ultramicrotome (Leica Ultracut UCT) with a diamond blade (Diatome). Sections were collected on Cu-Pd boutonniere grids covered by Formvar and stained in drops of 2% aqueous uranyl acetate for 7 min, followed by Reynolds's lead citrate for 2 min. Grids were analysed and photographed with a JEM 1010 transmission electron microscope operated at 120 kV and recorded at different magnifications using a CMOS 4K × 4K, F416 of TVIPS camera. Images were taken to cover the entire major and minor axis of the nerve in order to have an equivalent representation of ON.

Miconazole treatment

Miconazole (Sigma, QB-6813-5G) was resuspended in DMSO to a concentration of 200 µg/µl, aliquoted and stored at -20°C. Mouse pups were treated with Miconazole (intra-peritoneal injection; 10 µg/g) between post-natal day (P) 2 and P8. The day of the injection, Miconazole stock was diluted 1.000X in physiological solution, to obtain a 0.2 µg/µl injectable solution.

Collection and processing of human foetuses

Tissues were made available in accordance with French bylaws (Good practice concerning the conservation, transformation and transportation of human tissue to be used therapeutically, published on December 29, 1998). The studies on human foetal tissue were approved by the French agency for biomedical research (Agence de la Biomédecine, Saint-Denis la Plaine, France, protocol n°: PFS16–002). Non-pathological human foetuses (11 and 14 gestational weeks, n = 2) were obtained from voluntarily terminated pregnancies after obtaining written informed consent from the parents (Gynaecology Department, Jeanne de Flandre Hospital, Lille, France). Foetuses were fixed by immersion in 4% PFA at 4 °C for 7 days. The tissues were then cryoprotected in 30% sucrose/PBS for 3 days, embedded in Tissue-Tek OCT compound (Sakura Finetek, USA), frozen in dry ice and stored at -80 °C until sectioning. Frozen samples were cut serially at 20 μm using a Leica CM 3050S cryostat (Leica Biosystems Nussloch GmbH, Germany).

Electrophysiological recordings in behaving animals

Following the associative learning task, the same mice (13 *WT* and 18 *HET)* were prepared for the chronic recording of field potentials evoked at the visual pathway by flashes of light. To this end, animals were anesthetized with 4% chloral hydrate and stereotaxically implanted with two recording electrodes in the left lateral geniculate nucleus (2.06 mm posterior to Bregma, 2.0 lateral to the midline and 2.5 mm depth from brain surface), the right superior colliculus (3.8 mm posterior to Bregma, 1.25 lateral to the midline and 1.5 mm depth from brain

surface), and the left visual cortex (3.8 mm posterior to Bregma, 2.5 lateral to the midline and 0.5 mm depth from brain surface). Electrodes were made from 50µm Teflon-coated tungsten wire (Advent Research Materials, Eynsham, UK). Two bare silver wires were affixed to the skull as ground. Electrodes were connected to two 4-pin sockets (RS-Amidata, Madrid, Spain) that were fixed to the cranium with dental cement. After surgery, animals were allowed 5 days for a proper recovery.

Flashes of light were provided by a xenon arc lamp located 30 cm in front of the animal's eyes, and lasted ≈1 ms (Photic stimulator, Cibertec, Madrid, Spain). Photic stimulations were triggered from a programmable CS-20 stimulator (Cibertec). For recordings, each alert behaving mouse was placed in a transparent box (5 × 5 × 5 cm), dark adapted for 30 min and presented with a total of 40 stimuli at a rate of 6 per min. The recording box was located in the center of a larger (30 × 30 × 30 cm) cage made of polished aluminum and connected to a ground system to avoid unwanted electric interferences. Each animal received two stimulation sessions(Sanz-Rodriguez et al, 2018).

Histology after electrophysiology

At the end of the electrophysiological recording experiments, mice were deeply re-anesthetized and perfused transcardially with saline and 4% PFA. Selected sections (50 µm) including the implanted electrodes were mounted on gelatinized glass slides and stained using the Nissl technique with 0.1% Toluidine Blue, to determine the proper location of stimulating and recording electrodes. Photomicrographs were taken using a Leica DMRE microscope equipped with a Leica DFC550

camera, and with the LAS V4.2 software (Leica Microsystems GmbH, Wetzlar, Germany). Photomicrograph reconstructions were made with the Microsoft Office Professional Plus 2010 and CorelDRAW X4 software.

Behavior - Instrumental conditioning

Operant conditioning took place in commercial Skinner box modules (n = 5) measuring 12.5 × 13.5 × 18.5 cm (MED Associates, St. Albans, VT, USA). The conditioning boxes were housed within sound-attenuating chambers (90 × 55 × 60 cm), which were constantly illuminated (19 W lamp) and exposed to a 45-dB white noise (Cibertec, S.A., Madrid, Spain). Each Skinner box was equipped with a food dispenser from which pellets (MLabRodent Tablet, 20 mg; Test Diet, Richmond, IN, USA) could be delivered by pressing a lever. Each box was also equipped with a small light bulb located over the lever (Fig. 6E). Before training, mice were handled daily for 7 days and food-deprived to 90% of their free-feeding weight(Jurado-Parras et al, 2012; Madronal et al, 2010). In all cases, training sessions lasted for 20 min. The start and end of each session was indicated by a tone (2 kHz, 200 ms, 70 dB) provided by a loudspeaker located in the recording chamber (Fig. 6E).

In a first experimental step, mice (13 *WT* and 18 *HET*) were trained to press the lever to receive pellets from the food tray using a fixed-ratio (1:1) schedule (Fig. 6E, top panel). Animals were maintained on the 1:1 schedule for 10 training sessions. Mice typically reach criterion (pressing the lever ≥ 20 for two successive sessions) after 4-9 days of

training(Jurado-Parras et al, 2012; Madronal et al, 2010), but for the sake of homogeneity, all mice where trained for 10 days.

After this preliminary training, mice were further conditioned using a small bulb light on/light off protocol for 10 additional days. In this program, only lever presses performed during the light period (20 s) were reinforced with a pellet (Fig. 6E, bottom panel). The cued light was provided by the small bulb located over the lever. Lever presses performed during the dark period (20 ± 10 s) were not reinforced and restarted the dark protocol for an additional random (1-10 s) time. The light on/light off coefficient was calculated as follows: (number of lever presses during the light period – number of lever presses during the dark period) / total number of lever presses). In this case, the criterion was to reach a positive performance (i.e., a larger number of lever presses during the light than during the dark periods) for 2 successive sessions. Conditioning programs, lever presses, and delivered reinforcements were controlled and recorded by a computer, using a MED-PC program (MED Associates, St. Albans, VT, USA).

Statistical Analysis

All the data were statistically analyzed and graphically represented using Microsoft Office Excel software. Quantitative data are shown as the mean ± standard error (SEM). For operant conditioning, statistical significance of differences between groups was inferred by two-way ANOVA (sessions by groups) for repeated measures (sessions), with a contrast analysis (Holm-Sidak method) for a further study of significant differences. The best fit for a linear equation was settle for each group across the operant conditioning sessions. Data collected from the

electrophysiological experiments were subjected to normality (Shapiro-Wilk) and equal variance tests and then compared using a Student´s t-test between control and experimental groups. The same test and procedure were used to check differences on the percentage of lever responses between the light and dark periods in both mouse groups.

For cell percentage/number quantification after immunofluorescence (IF), measurements were performed on at least 9 sections coming from 3 to 5 different animals, unless otherwise stated. Microscope images were processed with Photoshop or ImageJ software, by randomly overlapping fixed-width (100µm) rectangular boxes on the area of interest (e.g. the retina), then quantifying positive cells inside the boxes. For ON cross-sections, the whole ON area was considered for the analysis, without placing any box. In the specific case of EM images, the myelination grade was evaluated as the average number of myelinated fibers found inside randomly placed 100µm^2 boxes. When calculating percentages over the total cell number, the latter was quantified by counting DAPI+ nuclei, unless otherwise specified. Data were compared by two-tailed Student's *t*-test (when comparing two data group) or by ANOVA (analysis of variance; for comparison of three or more groups) and statistical significance was set as follows: *= $P \leq 0.05$; **= $P \leq 0.01$; ***= $P \leq 0.001$.

Funding

This work was supported by an ERA-NET Neuron II grant (ImprovVision) ANR-15-NEUR-0002-04 to M.S. and P.B., by ''Investments for the Future'' LabEx SIGNALIFE (grant ANR-11-LABX-0028-01) to M.S. and by a postdoctoral fellowship from the

Ville de Nice, France (‘‘Aides Individuelles aux Jeunes Chercheurs’’) to M.B. Spanish Ministry of Science and Innovation BFU2016-75412-R (with FEDER funds) and PCIN-2015-176-C02-01/ERA-Net NeuronII to P.B. and an Institutional CBMSO Grant from the Fundación Ramón Areces. The electrophysiological and behavioral study was supported by grants from the Spanish Ministry of Science and Innovation (BFU2017-82375-R), the Junta de Andalucía (Spain, BIO-122) and the Spanish Tatiana Pérez de Guzmán el Bueno Foundation to A.G. and J.M.D.-G.

Author Contributions

M.S. and M.B. conceptualized and designed the research study. A.G. and J.D.G. designed, conducted and analyzed the electrophysiological/behavioral experiments. M.B., P.K., C.A., L.S. conducted the experiments and acquired the data. P.G. provided the human samples. M.B., M.S. and P.B. analyzed the data. M.B., M.S. and P.B. wrote the paper.

Acknowledgements

We are grateful to Eya Setti for technical help and to the whole Studer lab for feedback on the study. We thank Simona Casarosa and Federico Cremisi for useful hints during the initial design of the research study. We thank Ms. M. Sanchez-Enciso and Mr. J.M. González-Martín for their help in animal handling and care, as well as for instrumental design for electrophysiology and behavioral experiments. We also thank the iBV PRISM Microscopy facility for their regular support. The help of

Milagros Guerra and M. Teresa Rejas of the CBMSO EM facility is also acknowledged.

References

Al-Kateb H, Shimony JS, Vineyard M, Manwaring L, Kulkarni S, Shinawi M (2013) NR2F1 haploinsufficiency is associated with optic atrophy, dysmorphism and global developmental delay. *Am J Med Genet A* **161A:** 377-381

Alfano C, Magrinelli E, Harb K, Hevner RF, Studer M (2014) Postmitotic control of sensory area specification during neocortical development. *Nature communications* **5:** 5632

Alfano C, Magrinelli E, Harb K, Studer M (2013) The nuclear receptors COUP-TF: a long-lasting experience in forebrain assembly. *Cell Mol Life Sci*

Alzu'bi A, Lindsay S, Kerwin J, Looi SJ, Khalil F, Clowry GJ (2017a) Distinct cortical and sub-cortical neurogenic domains for GABAergic interneuron precursor transcription factors NKX2.1, OLIG2 and COUP-TFII in early fetal human telencephalon. *Brain Struct Funct* **222:** 2309-2328

Alzu'bi A, Lindsay SJ, Harkin LF, McIntyre J, Lisgo SN, Clowry GJ (2017b) The Transcription Factors COUP-TFI and COUP-TFII have Distinct Roles in Arealisation and GABAergic Interneuron Specification in the Early Human Fetal Telencephalon. *Cereb Cortex* **27:** 4971-4987

Armentano M, Chou SJ, Tomassy GS, Leingartner A, O'Leary DD, Studer M (2007) COUP-TFI regulates the balance of cortical patterning between frontal/motor and sensory areas. *Nat Neurosci* **10:** 1277-1286

Armentano M, Filosa A, Andolfi G, Studer M (2006) COUP-TFI is required for the formation of commissural projections in the forebrain by regulating axonal growth. *Development* **133:** 4151-4162

Bani-Yaghoub M, Tremblay RG, Lei JX, Zhang D, Zurakowski B, Sandhu JK, Smith B, Ribecco-Lutkiewicz M, Kennedy J, Walker PR, Sikorska M (2006) Role of Sox2 in the development of the mouse neocortex. *Dev Biol* **295:** 52-66

Bertacchi M, Parisot J, Studer M (2018) The pleiotropic transcriptional regulator coup-tfi plays multiple roles in neural development and disease. *Brain Res*

Bonzano S, Crisci I, Podlesny-Drabiniok A, Rolando C, Krezel W, Studer M, De Marchis S (2018) Neuron-Astroglia Cell Fate Decision in the Adult Mouse Hippocampal Neurogenic Niche Is Cell-Intrinsically Controlled by COUP-TFI In Vivo. *Cell reports* **24:** 329-341

Bosch DG, Boonstra FN, de Leeuw N, Pfundt R, Nillesen WM, de Ligt J, Gilissen C, Jhangiani S, Lupski JR, Cremers FP, de Vries BB (2016) Novel genetic causes for cerebral visual impairment. *European journal of human genetics : EJHG* **24:** 660-665

Bosch DG, Boonstra FN, Gonzaga-Jauregui C, Xu M, de Ligt J, Jhangiani S, Wiszniewski W, Muzny DM, Yntema HG, Pfundt R, Vissers LE, Spruijt L, Blokland EA, Chen CA, Baylor-Hopkins Center for Mendelian G, Lewis RA,

Tsai SY, Gibbs RA, Tsai MJ, Lupski JR, Zoghbi HY, Cremers FP, de Vries BB, Schaaf CP (2014) NR2F1 mutations cause optic atrophy with intellectual disability. *Am J Hum Genet* **94:** 303-309

Bovolenta P, Liem RK, Mason CA (1987) Glial filament protein expression in astroglia in the mouse visual pathway. *Brain Res* **430:** 113-126

Carelli V, La Morgia C, Ross-Cisneros FN, Sadun AA (2017) Optic neuropathies: the tip of the neurodegeneration iceberg. *Hum Mol Genet* **26:** R139-R150

Chen CA, Bosch DG, Cho MT, Rosenfeld JA, Shinawi M, Lewis RA, Mann J, Jayakar P, Payne K, Walsh L, Moss T, Schreiber A, Schoonveld C, Monaghan KG, Elmslie F, Douglas G, Boonstra FN, Millan F, Cremers FP, McKnight D, Richard G, Juusola J, Kendall F, Ramsey K, Anyane-Yeboa K, Malkin E, Chung WK, Niyazov D, Pascual JM, Walkiewicz M, Veluchamy V, Li C, Hisama FM, de Vries BB, Schaaf C (2016) The expanding clinical phenotype of Bosch-Boonstra-Schaaf optic atrophy syndrome: 20 new cases and possible genotype-phenotype correlations. *Genetics in medicine : official journal of the American College of Medical Genetics*

Chou SJ, Babot Z, Leingartner A, Studer M, Nakagawa Y, O'Leary DD (2013) Geniculocortical input drives genetic distinctions between primary and higher-order visual areas. *Science* **340:** 1239-1242

Chu Y, Hughes S, Chan-Ling T (2001) Differentiation and migration of astrocyte precursor cells and astrocytes in human fetal retina: relevance to optic nerve coloboma. *FASEB journal : official publication of the Federation of American Societies for Experimental Biology* **15:** 2013-2015

Chun BY, Rizzo JF, 3rd (2017) Dominant Optic Atrophy and Leber's Hereditary Optic Neuropathy: Update on Clinical Features and Current Therapeutic Approaches. *Semin Pediatr Neurol* **24:** 129-134

Conforti L, Gilley J, Coleman MP (2014) Wallerian degeneration: an emerging axon death pathway linking injury and disease. *Nat Rev Neurosci* **15:** 394-409

Deiner MS, Kennedy TE, Fazeli A, Serafini T, Tessier-Lavigne M, Sretavan DW (1997) Netrin-1 and DCC mediate axon guidance locally at the optic disc: loss of function leads to optic nerve hypoplasia. *Neuron* **19:** 575-589

Faedo A, Tomassy GS, Ruan Y, Teichmann H, Krauss S, Pleasure SJ, Tsai SY, Tsai MJ, Studer M, Rubenstein JL (2008) COUP-TFI coordinates cortical patterning, neurogenesis, and laminar fate and modulates MAPK/ERK, AKT, and beta-catenin signaling. *Cereb Cortex* **18:** 2117-2131

Flore G, Di Ruberto G, Parisot J, Sannino S, Russo F, Illingworth EA, Studer M, De Leonibus E (2017) Gradient COUP-TFI Expression Is Required for Functional Organization of the Hippocampal Septo-Temporal Longitudinal Axis. *Cereb Cortex* **27:** 1629-1643

Glasgow SM, Zhu W, Stolt CC, Huang TW, Chen F, LoTurco JJ, Neul JL, Wegner M, Mohila C, Deneen B (2014) Mutual antagonism between Sox10 and NFIA regulates diversification of glial lineages and glioma subtypes. *Nat Neurosci* **17:** 1322-1329

Heavner W, Pevny L (2012) Eye development and retinogenesis. *Cold Spring Harb Perspect Biol* **4**

Hernandez MR, Miao H, Lukas T (2008) Astrocytes in glaucomatous optic neuropathy. *Prog Brain Res* **173:** 353-373

Jurado-Parras MT, Gruart A, Delgado-Garcia JM (2012) Observational learning in mice can be prevented by medial prefrontal cortex stimulation and enhanced by nucleus accumbens stimulation. *Learning & memory* **19:** 99-106

Jurkute N, Yu-Wai-Man P (2017) Leber hereditary optic neuropathy: bridging the translational gap. *Current opinion in ophthalmology* **28:** 403-409

Kaiwar C, Zimmermann MT, Ferber MJ, Niu Z, Urrutia RA, Klee EW, Babovic-Vuksanovic D (2017) Novel NR2F1 variants likely disrupt DNA binding: molecular modeling in two cases, review of published cases, genotype-phenotype correlation, and phenotypic expansion of the Bosch-Boonstra-Schaaf optic atrophy syndrome. *Cold Spring Harbor molecular case studies* **3**

Lenaers G, Hamel C, Delettre C, Amati-Bonneau P, Procaccio V, Bonneau D, Reynier P, Milea D (2012) Dominant optic atrophy. *Orphanet journal of rare diseases* **7:** 46

Lintas A, Schwaller B, Villa AE (2013) Visual thalamocortical circuits in parvalbumin-deficient mice. *Brain Res* **1536:** 107-118

Lodato S, Rouaux C, Quast KB, Jantrachotechatchawan C, Studer M, Hensch TK, Arlotta P (2011a) Excitatory projection neuron subtypes control the distribution of local inhibitory interneurons in the cerebral cortex. *Neuron* **69:** 763-779

Lodato S, Tomassy GS, De Leonibus E, Uzcategui YG, Andolfi G, Armentano M, Touzot A, Gaztelu JM, Arlotta P, Menendez de la Prida L, Studer M (2011b) Loss of COUP-TFI alters the balance between caudal ganglionic eminence- and medial ganglionic eminence-derived cortical interneurons and results in resistance to epilepsy. *J Neurosci* **31:** 4650-4662

Madronal N, Lopez-Aracil C, Rangel A, del Rio JA, Delgado-Garcia JM, Gruart A (2010) Effects of enriched physical and social environments on motor performance, associative learning, and hippocampal neurogenesis in mice. *PLoS One* **5:** e11130

Martin-Hernandez E, Rodriguez-Garcia ME, Chen CA, Cotrina-Vinagre FJ, Carnicero-Rodriguez P, Bellusci M, Schaaf CP, Martinez-Azorin F (2018) Mitochondrial involvement in a Bosch-Boonstra-Schaaf optic atrophy syndrome patient with a novel de novo NR2F1 gene mutation. *Journal of human genetics*

Meeren HK, Van Luijtelaar EL, Coenen AM (1998) Cortical and thalamic visual evoked potentials during sleep-wake states and spike-wave discharges in the rat. *Electroencephalography and clinical neurophysiology* **108:** 306-319

Najm FJ, Madhavan M, Zaremba A, Shick E, Karl RT, Factor DC, Miller TE, Nevin ZS, Kantor C, Sargent A, Quick KL, Schlatzer DM, Tang H, Papoian R, Brimacombe KR, Shen M, Boxer MB, Jadhav A, Robinson AP, Podojil JR, Miller SD, Miller RH, Tesar PJ (2015) Drug-based modulation of endogenous stem cells promotes functional remyelination in vivo. *Nature* **522:** 216-220

Ono K, Yoshii K, Tominaga H, Gotoh H, Nomura T, Takebayashi H, Ikenaka K (2017) Oligodendrocyte precursor cells in the mouse optic nerve originate in the preoptic area. *Brain Struct Funct* **222:** 2441-2448

Parisot J, Flore G, Bertacchi M, Studer M (2017) COUP-TFI mitotically regulates production and migration of dentate granule cells and modulates hippocampal Cxcr4 expression. *Development* **144:** 2045-2058

Patel A, Sowden JC (2017) Genes and pathways in optic fissure closure. *Semin Cell Dev Biol*

Pekny M, Wilhelmsson U, Pekna M (2014) The dual role of astrocyte activation and reactive gliosis. *Neurosci Lett* **565:** 30-38

Qiu Y, Krishnan V, Zeng Z, Gilbert DJ, Copeland NG, Gibson L, Yang-Feng T, Jenkins NA, Tsai MJ, Tsai SY (1995) Isolation, characterization, and chromosomal localization of mouse and human COUP-TF I and II genes. *Genomics* **29:** 240-246

Ridder WH, 3rd, Nusinowitz S (2006) The visual evoked potential in the mouse--origins and response characteristics. *Vision research* **46:** 902-913

Ritchie HH, Wang LH, Tsai S, O'Malley BW, Tsai MJ (1990) COUP-TF gene: a structure unique for the steroid/thyroid receptor superfamily. *Nucleic Acids Res* **18:** 6857-6862

Sanz-Rodriguez M, Gruart A, Escudero-Ramirez J, de Castro F, Delgado-Garcia JM, Wandosell F, Cubelos B (2018) R-Ras1 and R-Ras2 Are Essential for Oligodendrocyte Differentiation and Survival for Correct Myelination in the Central Nervous System. *J Neurosci* **38:** 5096-5110

Schwarz M, Cecconi F, Bernier G, Andrejewski N, Kammandel B, Wagner M, Gruss P (2000) Spatial specification of mammalian eye territories by reciprocal transcriptional repression of Pax2 and Pax6. *Development* **127:** 4325-4334

Sofroniew MV (2009) Molecular dissection of reactive astrogliosis and glial scar formation. *Trends Neurosci* **32:** 638-647

Stolt CC, Lommes P, Friedrich RP, Wegner M (2004) Transcription factors Sox8 and Sox10 perform non-equivalent roles during oligodendrocyte development despite functional redundancy. *Development* **131:** 2349-2358

Stolt CC, Rehberg S, Ader M, Lommes P, Riethmacher D, Schachner M, Bartsch U, Wegner M (2002) Terminal differentiation of myelin-forming oligodendrocytes depends on the transcription factor Sox10. *Genes Dev* **16:** 165-170

Su X, Tang W, Luan Z, Yang Y, Wang Z, Zhang Y, Wang Q, Suo L, Huang Z, Wang X, Yuan H (2018) Protective effect of miconazole on rat myelin sheaths following premature infant cerebral white matter injury. *Experimental and therapeutic medicine* **15:** 2443-2449

Sun D, Moore S, Jakobs TC (2017) Optic nerve astrocyte reactivity protects function in experimental glaucoma and other nerve injuries. *The Journal of experimental medicine* **214:** 1411-1430

Swindell EC, Bailey TJ, Loosli F, Liu C, Amaya-Manzanares F, Mahon KA, Wittbrodt J, Jamrich M (2006) Rx-Cre, a tool for inactivation of gene expression in the developing retina. *Genesis* **44:** 361-363

Tang K, Rubenstein JL, Tsai SY, Tsai MJ (2012) COUP-TFII controls amygdala patterning by regulating neuropilin expression. *Development* **139:** 1630-1639

Tang K, Tsai SY, Tsai MJ (2015) COUP-TFs and eye development. *Biochim Biophys Acta* **1849:** 201-209

Tang K, Xie X, Park JI, Jamrich M, Tsai S, Tsai MJ (2010) COUP-TFs regulate eye development by controlling factors essential for optic vesicle morphogenesis. *Development* **137:** 725-734

Tripodi M, Filosa A, Armentano M, Studer M (2004) The COUP-TF nuclear receptors regulate cell migration in the mammalian basal forebrain. *Development* **131:** 6119-6129

Tsai HH, Miller RH (2002) Glial cell migration directed by axon guidance cues. *Trends Neurosci* **25:** 173-175; discussion 175-176

Wang LH, Ing NH, Tsai SY, O'Malley BW, Tsai MJ (1991) The COUP-TFs compose a family of functionally related transcription factors. *Gene expression* **1:** 207-216

Wiggins RC, Fuller GN, Dafny N (1982) Propagation of photic evoked responses recorded from the retina, optic chiasm, lateral geniculate body, and visual cortex of the nutritionally rehabilitated rat visual system. *Exp Neurol* **77:** 644-653

Zhou C, Tsai SY, Tsai MJ (2001) COUP-TFI: an intrinsic factor for early regionalization of the neocortex. *Genes Dev* **15:** 2054-2059

CHAPTER 5
SUMMARY

The transcription factor Sox2 is expressed in the nervous system from the beginning of its development where it is required for stem cells maintenance. In humans, *SOX2* heterozygous mutations are linked to various central nervous system defects, including visual defects. The visual system is composed of the eye, the dorsolateral geniculate thalamic nucleus (dLGN) and the visual cortex, which are highly interconnected. The eye, in fact, sends retinal afferent to a specific dorsal thalamic nucleus, the dLGN, whose neurons in turn project to the visual cortical area. The visual cortex elaborates visual inputs and projects back to the dLGN in a complex circuit. Several genes are important for the correct development of the visual system and Sox2 is one of them. Sox2 is expressed in all the three components of the visual system in mice; while its role in the development of the retina is well characterized little is known about its role in the thalamus. To investigate Sox2 requirement in the thalamus for the correct establishment of the visual axis, we generated a thalamic *Sox2* conditional knock-out in post-mitotic neurons. We observed that Sox2 loss in the dLGN leads to a strong reduction in size of the dLGN, aberrant retino-geniculate, thalamo-cortical and cortico-thalamic neural projections and, consequently, to a defective patterning of the cortical visual area. We found that in *Sox2* thalamic mutants the *Efna5* gene, important in guiding retinal axons towards the dLGN, and the serotonin transporters encoding genes *SERT* and *vMAT2*, involved in the establishment of thalamo-cortical projections, are strongly

downregulated in the mutant dLGN. To identify all the potential genes that could mediate Sox2 function in the thalamus, we performed RNA sequencing (RNA-seq) on control and *Sox2* mutant dLGNs. We noticed that misregulated genes are enriched in genes encoding axon guidance molecules and molecules involved in neurotransmission and synapses. Interestingly, thalamic ablation of another transcription factor, COUP-TF1, leads to defects of the visual system similar to the ones described for Sox2. In addition, heterozygous mutations in the *COUP-TF1* gene in human lead to optic atrophy and intellectual disabilities. Interestingly, we found that Sox2 and COUP-TF1 are co-expressed in the same post-mitotic neurons of the DLG. Surprisingly, *COUP-TF1* expression does not vary in *Sox2* thalamic mutants, arising the possibility that Sox2 and COUP-TF1 have common target in the thalamus. Therefore, we looked at the expression, in *COUP-TF1* mutants, of genes downregulated in *Sox2* thalamic mutants and we found that they appear upregulated, suggesting that the two transcription factors could act on the same genes but in an opposite way. To further understand whether the two transcription factors regulate common genes, we are performing gene expression analyses by RNA-seq also on *COUP-TF1* thalamic mutants, with the aim to identify an overlap with Sox2 regulated genes. Moreover, we are generating *Sox2* and *COUP-TF1* double mutant mice to unveil how these genes regulate gene expression; it is plausible that they regulate common genes to balance their expression in thalamic neurons.

CONCLUSIONS AND FUTURE PERSPECTIVES

1. Sox2 is required not only in neural stem cells but also in differentiated neurons of the thalamus

The transcription factor Sox2 is widely known as a stem cell gene (Avilion et al., 2003, Pevny and Nicolis 2010, Mercurio et al., 2019), and it is able to reprogram terminally differentiated cells into induced pluripotent stem cells (Takahashi and Yamanaka 2016). Recently, the Nicolis laboratory revealed Sox2 relevance in shaping chromatin connectivity by mediating distal enhancer-promoter interactions in mouse-derived neural stem cells; *Sox2* deletion reduces long-range interactions and gene expression, highlighting Sox2 requirement in neural stem cells maintenance (Bertolini et al., 2019). However, Sox2 exerts important functions also in differentiated cells, such as neurons and glia (reviewed in Mercurio et al., 2019. You can find the review in Chapter 6).

Sox2 expression in all the three components of the visual system, highly interconnected, is consistent with the idea that Sox2 acts by orchestrating the development of the visual system.

We demonstrated that Sox2 is highly expressed in post-mitotic neurons of the dLGN, and that its deletion strongly affects the development of the thalamus with its connections to the eyes as well as the visual cortex. However, we still do not know the causes of the dLGN reduction in size when Sox2 is missing. In other brain regions, *Sox2* conditional ablation is associated to an increased cellular death. For example, *Sox2* deletion in the mouse embryonic brain leads to loss of neurogenesis and neural stem cells in the dentate gyrus of the hippocampus, due to apoptotic cell

death, demonstrating Sox2 requirement in hippocampal neural stem cells maintenance (Favaro et al., 2009). In another mutant, where *Sox2* is deleted in the developing telencephalon, *Sox2* ablation causes ventral telencephalon tissue loss (Ferri et al., 2013) and affects the developing olfactory epithelium (Panaliappan et al., 2018) by increased apoptotic events. Therefore, Sox2 is important for cellular survival and so when it is ablated cells die. However, from preliminary analyses on *Sox2* thalamic mutants we don't see signs of cellular death in the thalamus.

It could be that dLGN size reduction in *Sox2* thalamic mutants is due to reduced innervation from the retina to the dLGN. In fact, retinal innervation is required for dLGN development, particularly in the early postnatal phase, when indeed the increase in size of the dLGN is not due to an increase in the number of relay neurons. During the first postnatal week, dendritic branches of relay neurons undergo an expansion in terms of length and complexity, and during the second and third postnatal weeks the dendritic field of dLGN relay neurons appears increased, leading to the expansion of the dLGN area (Guido 2018). In mice lacking retinal afferents, the dLGN is smaller and the dendritic growth pattern of relay neurons in disrupted, suggesting that retinofugal projections give trophic support for relay neurons of the dLGN (El Danaf et al., 2015; Guido 2018).

The retina is not affected in our *Sox2* thalamic mutant, infact the number and distribution of RGCs in adults is comparable beween control and mutant mice, as shown in Chapter 2 (Figure S2), indicating that *Sox2* thalamic deletion does not affect the viability of these cells. The analyses of retino-geniculate projections at postnatal stages, shown in Chapter 2, reveals that the total innervation of retinal fibers that reach

the LGN appears unchanged between control and mutant mice; however, in thalamic mutants the fraction of retinal afferents that reach the dLGN is reduced, while the fraction of afferents that reach the vLGN is increased, suggesting misrouting of retinal fibers.

Interestingly, at postnatal day 1, when the dLGN size is still comparable in control and mutant mice, the contralateral projections reaching the dLGN are already reduced. Thus, the defects in *Sox2* thalamic mutants could be likely due to dLGN inability to correctly attract retinal axons. In support of a role of Sox2 in axon guidance we found, by RNA sequencing performed on dLGN neurons at postnatal day 0, that many axon guidance molecules are downregulated in the mutant dLGN compared to controls. Therefore, we aim to study potential axon guidance defects in a simplified system, using explants *in vitro.* Retinae and thalami explant systems represent a good strategy to study retino-geniculate axis, as shown by Guido et al., 1997. In fact, the use of co-cultures of dissected retinas and thalami would allow us to observe how retinal projections grow towards a control or a Sox2-mutant thalamus. If the axon growth pattern is affected by *Sox2* loss in the thalamus, we could try to rescue these defects by adding back to the mutant thalamus some of the deregulated axon guidance molecules.

To re-introduce some specific deregulated genes into the *Sox2* mutant dLGN we could use viral stereotaxic injections or we could add, in explant systems, secreted molecules by beads realizing them before the defective phenotype occurs. We would then analyse dLGN morphology and retina-thalamo and thalamo-cortical connections to see if the growth defects of the dLGN and the defective connections between the

eye and the visual cortex could be rescued after the reintroduction of the deregulated genes.

Interestingly, RNA sequencing revealed that among the most downregulated genes there are also genes involved in glutamatergic synapse. It could be that *Sox2* deletion in thalamic neurons leads to the production of fewer and less efficient excitatory synapses. Therefore, the combination of axon guidance and synaptic defects could overall lead to the developmental defects observed after Sox2 loss in the thalamus.

2. S*OX2* defective function in the thalamus could be linked in humans to cerebral visual impairment

Sox2 is considered the major causative gene of eye disorders. *SOX2* mutations in human patients result in different degrees of ocular phenotype severity, with some common extraocular defects. (Ragge et al., 2005; Kelberman et al., 2006; Sisodya et al., 2006; Schneider et al., 2009; Williamson and FitzPatrick, 2014). The mouse represents a good model to study Sox2 function also in a pathological context. Indeed, *Sox2* deficiency in different mouse models leads to defective neurogenesis (Ferri et al., 2004), ataxia (Cerrato et al., 2018) and to many ocular defects depending on the Sox2 gene dosage (Taranova et al., 2006). *Sox2* conditional knock-outs in retinal progenitors in mice suggest that the disruption of Sox2 function in the neural retina could contribute to the eye-defects observed in human patients (Taranova et al., 2006).

However, Sox2 expression and crucial function in post-mitotic neurons of the visual thalamus in mouse arises the possibility that, in humans, *SOX2* mutations could also lead to cerebral visual impairment (CVI).

CVI results from a malfunctioning of parts of the brains involved in the visual system, such as the optic tracts and the cortex and it is usually diagnosed when no ocular defects can explain the vision defects. CVI patients show reduced visual acuity, visual field defects, abnormal visual behaviour, and often intellectual disability and epilepsy (Bosch et al., 2016). Interestingly, among the downregulated genes in the *Sox2* mutant dLGN we found also other SOX family members, such as Sox5 that has been reported as a candidate gene for cerebral visual impairment (Bosch et al., 2016).

Recently, *de novo* heterozygous mutations in the human *COUP-TF1* gene have been linked to CVI, causing the autosomal dominant optic atrophy syndrome (Bosch et al., 2014).

Interestingly, the haploinsufficiency of *COUP-TF1* in the mouse recapitulates the human visual pathological defects (see Chapter 4) and thus gives an important contribution for our understanding of the human disease. In addition to optic nerve abnormalities, these mice show a defective dLGN development suggesting that also thalamic defects could be responsible for the vision abnormalities in patients.

The evidence that Sox2 and COUP-TF1 are expressed in the same neurons of the dLGN in mice and that, in humans, *COUP-TF1* is linked to CVI, makes us think that also *SOX2* could be related to the cerebral vision disease.

We have already identified several deregulated genes in the *Sox2* mutant dLGN, and I plan to characterize some of them by means of *in*

vitro assays, such as retina-thalamus explants, and *in vivo* assays, such as the injection of deregulated genes in the thalamus of mutant mice. Moreover, I am going to identify also deregulated genes, by RNA sequencing, in *COUP-TF1* mutant thalamic dLGN. I will compare these data to *Sox2* mutant transcriptome, in order to identify any potential common target gene.

In human patients, SOX2 and COUP-TF1 could have a role in the development of the dLGN that could lead to CVI. It could be that the same genes that are deregulated in the visual thalamus in mutant mice are also deregulated in the visual thalamus of human patients.

Overall, the identification of genes that mediate Sox2 and COUP-TF1 functions in the visual system, and in particular in the thalamus, will allow to better understand the human vision disease and the development of potential therapeutic approaches.

3. Sox2 and COUP-TF1: why are they co-expressed in thalamic neurons?

Sox2 and *COUP-TF1* thalamic mutants show some important similarities; infact, in both mutants the size of the dLGN is highly reduced, as well as the thalamo-cortical projections, and the visual cortical patterning is similarly and strongly compromised.

Interestingly, we found that SOX2 and COUP-TF1 are largely co-localized in the same cells in the mouse dLGN, raising the hypothesis that they could interact in the development of the visual system. As shown in Chapter 3, we observed that the two transcription factors do not regulate each other, and thus our hypothesis is that they could regulate common target genes in the visual thalamus.

To our knowledge, there is no evidence of the interaction between SOXs and COUP-TFs in the brain. Srinivasan et al., in 2010 showed that Sox18 and COUP-TFII, important for the development of mammalian vascular and lymphatic systems, cooperate in lymphatic endothelial cell (LEC) progenitors to initiate the specification of these cells and to maintain their identity.

However, it is possible that in the brain Sox2 and COUP-TF1 could need to interact to modulate correct gene expression levels in distinct thalamic neurons. For example, as reported in Chapter 2 and 3, Sox2 activates the expression of *EphrinA5* in the dLGN and when *Sox2* is deleted *EphrinA5* is downregulated. We were expecting *EphrinA5* expression to be reduced also in *COUP-TF1* thalamic mutants, but we surprisingly found that its expression appears upregulated in the dLGN when *COUP-TF1* is ablated. Therefore, COUP-TF1 seems to repress *EphrinA5* expression. Interestingly, ChIP sequencing experiments performed by Nicolis and Studer laboratories revealed that there are both Sox2 and COUP-TF1 binding sites on the *Efna5* gene. It could be possible that they both bind the *EphrinA5* gene and finely modulate the precise expression level of the protein. Therefore, when one of the two genes is ablated this fine balance is lost.

To explore this possibility, I plan to analyse *Sox2* and *COUP-TF1* double mutant mice, that we have generated, to see what happens to dLGN size and morphology, connectivity with the eye and the cortex and to the corex itself. It will be interesting to see whether the simultaneous deletion of the two transcription factors could balance gene expression levels into thalamic neurons and, potentially, partially rescue the defects observed in the development of the visual axis.

However, the identification by RNA sequencing of deregulated genes in the thalamic projective neurons of *COUP-TF1* mutant mice and, subsequently, the comparison with the genes deregulated in the *Sox2* thalamic mutant, will allow us to dissect the gene regulatory network downstream of these transcription factors and common or distinct pathways.

References

Avilion, A.A., Nicolis, S.K., Pevny, L.H., Perez, L., Vivian, N., Lovell-Badge, R., 2003. Multipotent cell lineages in early mouse development depend on SOX2 function. Genes Dev 17(1), 126-140.

Bertolini, J. A., Favaro, R., Zhu, Y., Pagin, M., Ngan, C. Y., Wong, C. H., Tjong, H., Vermunt, M. W., Martynoga, B., Barone, C., Mariani, J., Cardozo, M. J., Tabanera, N., Zambelli, F., Mercurio, S., Ottolenghi, S., Robson, P., Creyghton, M. P., Bovolenta, P., Pavesi, G., Guillemot, F., Nicolis, S. K. & Wei, C. L. 2019. Mapping The Global Chromatin Connectivity Network For Sox2 Function In Neural Stem Cell Maintenance. Cell Stem Cell, 24, 462-476 E6.

Bosch DG, Boonstra FN, de Leeuw N, Pfundt R, Nillesen WM, de Ligt J, Gilissen C, Jhangiani S, Lupski JR, Cremers FP, de Vries BB, 2016. Novel genetic causes for cerebral visual impairment. European journal of human genetics: EJHG 24: 660-665.

Bosch DG, Boonstra FN, Gonzaga-Jauregui C, Xu M, de Ligt J, Jhangiani S, Wiszniewski W, Muzny DM, Yntema HG, Pfundt R, Vissers LE, Spruijt L, Blokland EA, Chen CA, Baylor-Hopkins Center for Mendelian G, Lewis RA, Tsai SY, Gibbs RA, Tsai MJ, Lupski JR, Zoghbi HY, Cremers FP, de Vries BB, Schaaf CP, 2014. NR2F1 mutations cause optic atrophy with intellectual disability. Am J Hum Genet 94: 303-309

Cerrato, V., Mercurio, S., Leto, K., Fuca, E., Hoxha, E., Bottes, S., Pagin, M., Milanese, M., Ngan, C. Y., Concina, G., Ottolenghi, S., Wei, C. L., Bonanno, G., Pavesi, G., Tempia, F., Buffo, A. & Nicolis, S. K. 2018. Sox2 conditional mutation in mouse causes ataxic symptoms, cerebellar vermis hypoplasia, and postnatal defects of Bergmann glia. Glia.

El-Danaf, R. N., Krahe, T. E., Dilger, E. K., Bickford, M. E., Fox, M. A. & Guido, W. 2015. Developmental Remodeling Of Relay Cells In The Dorsal Lateral Geniculate Nucleus In The Absence Of Retinal Input. Neural Dev, 10, 19.

Favaro, R., Valotta, M., Ferri, A. L., Latorre, E., Mariani, J., Giachino, C., Lancini, C., Tosetti, V., Ottolenghi, S., Taylor, V. & Nicolis, S. K. 2009. Hippocampal development and neural stem cell maintenance require Sox2-dependent regulation of Shh. Nature neuroscience, 12, 1248-56.

Ferri, A., Favaro, R., Beccari, L., Bertolini, J., Mercurio, S., Nieto-Lopez, F., Verzeroli, C., La Regina, F., De Pietri Tonelli, D., Ottolenghi, S., Bovolenta, P. & Nicolis, S. K. 2013. Sox2 is required for embryonic development of the ventral telencephalon through the activation of the ventral determinants Nkx2.1 and Shh. Development, 140, 1250-61.

Guido, W., Lo, FS., Erzurumlu, RS., 1997. An in vitro model of the kitten retinogeniculate pathway. J Neurophysiol. 1997 77(1):511-6.
Guido W., 2018. Development, form, and function of the mouse visual thalamus. J Neurophysiol. 120(1): 211-25.

Kelberman, D., Rizzoti, K., Avilion, A., Bitner-Glindzicz, M., Cianfarani, S., Collins, J., Chong, W.K., Kirk, J.M., Achermann, J.C., Ross, R., Carmignac, D., Lovell-Badge, R., Robinson, I.C., Dattani, M.T., 2006. Mutations within Sox2/SOX2 are associated with abnormalities in the hypothalamo-pituitary-gonadal axis in mice and humans. J Clin Invest 116(9), 2442-2455.

Matsushima, D., Heavner, W., Pevny, L.H., 2011. Combinatorial regulation of optic cup progenitor cell fate by SOX2 and PAX6. Development 138(3), 443-454.

Mercurio, S., Serra, L., Nicolis, SK., 2019. More than just Stem Cells: Functional Roles of the Transcription Factor Sox2 in Differentiated Glia and Neurons. Int J Mol Sci. 20(18). pii: E4540. doi: 10.3390/ijms20184540.

Panaliappan, T. K., Wittmann, W., Jidigam, V. K., Mercurio, S., Bertolini, J. A., Sghari, S., Bose, R., Patthey, C., Nicolis, S. K. & Gunhaga, L. 2018. Sox2 is required for olfactory pit formation and olfactory neurogenesis through BMP restriction and Hes5 upregulation. Development, 145.

Pevny, L. H. & Nicolis, S. K. 2010. Sox2 Roles In Neural Stem Cells. Int J Biochem Cell Biol, 42, 421-4.

Pfeiffenberger, C., Cutforth, T., Woods, G., Yamada, J., Rentería, R.C., Copenhagen, D.R., Flanagan, J.G., Feldheim, D.A., 2005. Ephrin-As and

neural activity are required for eye-specific patterning during retinogeniculate mapping. Nature Neuroscience 8(8), 1022-27.

Sisodiya, S.M., Ragge, N.K., Cavalleri, G.L., Hever, A., Lorenz, B., Schneider, A., Williamson, K.A., Stevens, J.M., Free, S.L., Thompson, P.J., van Heyningen, V., Fitzpatrick, D.R., 2006. Role of SOX2 mutations in human hippocampal malformations and epilepsy. Epilepsia 47(3), 534-542.

Srinivasan, RS., Geng, X., Yang, Y., Wang, Y., Mukatira, S., Studer, M., Porto, MP., Lagutin, O., Oliver, G., 2010. The nuclear hormone receptor Coup-TFII is required for the initiation and early maintenance of Prox1 expression in lymphatic endothelial cells. Genes Dev. 24(7):696-707.

Takahashi, K. & Yamanaka, S. 2016. A Decade Of Transcription Factor-Mediated Reprogramming To Pluripotency. Nat Rev Mol Cell Biol, 17, 183-93.

Taranova, O.V., Magness, S.T., Fagan, B.M., Wu, Y., Surzenko, N., Hutton, S.R., Pevny, L.H., 2006. SOX2 is a dose-dependent regulator of retinal neural progenitor competence. Genes Dev 20(9), 1187-1202.

Williamson, KA., FitzPatrick, DR., 2014. The genetic architecture of microphthalmia, anophthalmia and coloboma. Eur J Med Genet. 57(8):369-80.

The following review, that I wrote with Dr. Sara Mercurio and Prof. Silvia K. Nicolis, represents an additional discussion about the importance and requirement of Sox2 non only in stem cells, but also in differentiated cells, such as neurons and glia.

CHAPTER 6

Review

More than just Stem Cells: Functional Roles of the Transcription Factor Sox2 in Differentiated Glia and Neurons

Sara Mercurio [1], [*], Linda Serra [1, 2] and Silvia K. Nicolis [1],[*]

[1]Department of Biotechnology and Biosciences, University Milano-Bicocca, 20126 Milano, Italy

[2]CNRS, Inserm, iBV, Université Côte d'Azur, 06108 Nice, France

*Correspondence: sara.mercurio@unimib.it (S.M.); silvia.nicolis@unimib.it

Published: 13 September 2019 in *International Journal of Molecular Sciences*

Abstract: The Sox2 transcription factor, encoded by a gene conserved in animal evolution, has become widely known because of its functional relevance for stem cells. In the developing nervous system, Sox2 is active in neural stem cells, and important for their self-renewal; differentiation to neurons and glia normally involves Sox2 downregulation. Recent evidence, however, identified specific types of

fully differentiated neurons and glia that retain high Sox2 expression, and critically require Sox2 function, as revealed by functional studies in mice and in other animals. Sox2 was found to control fundamental aspects of the biology of these cells, such as the development of correct neuronal connectivity. Sox2 downstream target genes identified within these cell types provide molecular mechanisms for cell-type-specific Sox2 neuronal and glial functions. SOX2 mutations in humans lead to a spectrum of nervous system defects, involving vision, movement control, and cognition; the identification of neurons and glia requiring Sox2 function, and the investigation of Sox2 roles and molecular targets within them, represents a novel perspective for the understanding of the pathogenesis of these defects.

Keywords: sox2; neurons; glia; transcription factors; neural stem cells; cerebellum; thalamus; dorsolateral geniculate nucleus; visual cortex; Bergmann glia; Müller glia

1. Introduction

1.1. Sox2 as a "Stem Cell Gene"

The transcription factor Sox2 has become widely known because of its functional connection to the stem cell state (reviewed in references [1–4]). In mammals, Sox2 is expressed, and required, from the earliest stages of embryonic development in the pluripotent stem cells of the blastocyst inner cell mass; its knock-out in mice causes early embryonic lethality [5]. Conversely, Sox2 can reprogram differentiated cells to induced pluripotent stem cells (iPSCs), acting with a small number of other factors [6]. At later developmental stages, Sox2 is maintained (at

least preferentially) in stem cells of different tissues [1], among which, prominently, the developing (and postnatal) nervous system [2,7]. Here, Sox2 is highly expressed in neural stem/precursor cells, constituting the ventricular zone of the developing neural tube and, in general, it is downregulated in differentiating cells as they progressively move out of the ventricular zone into the outer layers of the neural tube. Sox2 conditional deletion in the developing neural tube impacts neural stem cell (NSC) function, both in vitro and in vivo [2,8,9]. Recently, Sox2 was also found to be absolutely required for the development of the mouse olfactory neuroepithelium [9,10], a neurogenic epithelium containing Sox2-positive, long-term self-renewing stem-like cells [11].

1.2. SOX2 and Neurodevelopmental Genetic Disease

SOX2 heterozygous mutations in humans lead to a characteristic spectrum of nervous system abnormalities that includes eye defects and hippocampal defects, together with intellectual disability, seizures, and motor control defects [12–14]. In mouse models, severe eye defects are reproduced following Sox2 conditional deletion in the neural stem/progenitor cells of the developing retina [4,15]. Hippocampal defects are reproduced in mouse models of conditional Sox2 deletion in the neural tube at mid-embryogenesis (embryonic day 11.5, E11.5), and are explained by a loss of stem cells of the hippocampus dentate gyrus [8]. Administration of a drug, mimicking the effect of a cytokine (SHH) lost from the mutant hippocampus, encoded by a Sox2 target gene, rescues hippocampal NSC, and hippocampal growth [8]. Sox2 hippocampal function is likely to contribute to the seizures, as well as the cognitive defects, observed in patients.

Earlier deletion of Sox2 (E10.5) also compromises the development of the primordia of the basal ganglia in the ventral forebrain (medial ganglionic eminence, MGE), pointing to stage-specific functions of Sox2; in the context of the early MGE, an important downstream target of Sox2 is the gene encoding transcription factor Nkx2.1, a master regulator of ventral forebrain development [9].

Sox2 is very conserved in evolution, with homologs in Drosophila, C. elegans, chick, and zebrafish, in addition to mouse and human [3]. It is noteworthy that some Sox2 homologs in invertebrates can replace mouse Sox2 function in preserving embryonic stem cell fate [16].

1.3. Recent Perspectives on SOX2 Molecular Mechanisms of Action

SOX2 targets, and molecular modes of action, in NSC, are the object of strong interest (reviewed in references [2,3,17]). These issues have been recently investigated from a genomic perspective, using NSC cultured in vitro from the normal, or Sox2-deleted, mouse brain as a model system [18]. In brain-derived NSC, ChIPseq shows that SOX2 binds predominantly to distal enhancers, connected to promoters via RNApolII-mediated long-range interactions, identified by ChIA-PET analyses [18]. Distal SOX2-bound enhancers are active in vivo, in the developing forebrain of transgenic zebrafish and mouse embryos. Sox2-deleted cells show downregulation of some 700 genes by RNAseq; these genes are highly enriched in connections with SOX2-bound enhancers, and SOX2 loss from these interactions is the single most important factor underlying differences in gene expression in Sox2-mutant cells (more than SOX2 loss at promoters) [18]. Sox2 loss leads to the loss, or decrease, of a high number of long-range

interactions, pointing to Sox2 as an “architectural” factor in 3D functional chromatin organization [18]. Of note, genes bound by SOX2 and involved in long-range interactions include many genes involved in neurodevelopmental diseases, showing phenotypic overlap with the abnormalities detected in Sox2-deficient patients, or Sox2-mutant mice. In addition, the functional study of genes regulated by Sox2 through long-range interactions identified Socs3, encoding a signaling molecule, as an important mediator of Sox2 function in maintaining NSC self-renewal [18]. Intriguingly, SOX2-bound genes also include genes that are still transcriptionally silent in NSC but will be activated following neuronal or glial differentiation (some of which will be discussed later in this Review). This suggests the possibility that SOX2-bound chromatin loops constitute a form of “priming” of neural genes for later activity in differentiation. SOX2 was also found to bind to genes carrying “bivalent” epigenetic histone modifications characteristic of “poised” genes, meaning genes that will become fully active only following differentiation. Conditional ablation [8] of SOX2 in adult hippocampal NSC, impaired the activation of pro-neural and neurogenic genes, during differentiation, supporting a functional role for SOX2 binding in NSC in establishing a permissive epigenetic state of neuronal/glial genes [19]. Recently, an additional architectural role of Sox2 in NSC chromatin was suggested by the finding of its interaction with the nucleoporin Nup153, a protein that is part of the nuclear pores [20]; SOX2 and Nup153 share a high fraction of binding sites on DNA, and their binding is enriched on genes deregulated following downregulation of Nup153. It is possible that Sox2 acts on chromatin architecture at the level of long-range interactions

maintenance, as well as by possibly tethering genes to the nuclear pore. It will be interesting to ask if the SOX2-bound regions involved show any overlap.

The evidence summarized above demonstrates critical roles for Sox2 in NSC (recently reviewed more in detail in references [2,17]) and begins to unravel molecular mechanisms and targets mediating Sox2 function. However, is Sox2 function in neural development limited to its roles in NSC?

Recent evidence shows that this is not the case. In this Review, we will present and discuss the unexpected critical functions played by Sox2 within specific classes of differentiated glial and neuronal cells.

2. Sox2 Functions in Differentiated Glia and Neurons

NSC produce, by controlled proliferation and differentiation, the various types of neuronal and glial cells that constitute the mature nervous system. Typically, NSC differentiation involves the downregulation of Sox2 expression. However, expression studies (e.g., by immunofluorescence with anti-SOX2 antibodies) revealed a high level of SOX2 within specific types of differentiated glial and neuronal cells; these studies, in turn, prompted functional investigations of Sox2 roles within these cells (Table 1).

2.1. Sox2 in Glial Cells

2.1.1. Bergmann Glia and Müller Glia

Bergmann Glia in the cerebellum

During development, Sox2 is expressed in the primordium of the cerebellum, and, postnatally, it is maintained in the Bergmann glia (BG), a unipolar cell type (that originates from radial glia) with the soma in the Purkinje cell (PC) layer and their radial processes going through the molecular layer and reaching the pia [40] (Figure 1A). BG are essential for granule cell migration during development and in postnatal life, and they are important for Purkinje cells function by regulating ion homeostasis and synapse stability (reviewed in references [41,42]). Conditional knock-out of Sox2 in the developing cerebellum (mediated by Wnt1-Cre recombinase) results, postnatally, in hypoplasia of the central portion of the cerebellum, the vermis, and ataxia. In addition, a cell type that appears particularly affected by Sox2 loss is the Bergmann glia. BG cell bodies are found outside of the Purkinje cell layer, where they are usually localized, and their radial morphology is lost in Sox2 mutants (Figure 1A). Other glial cells that express Sox2, like parenchymal and prospective white matter astrocytes, appear unaffected by Sox2 loss, indicating a specific requirement for Sox2 in BG, but not in other glial cell types [29]. Since Wnt1-Cre-mediated Sox2 deletion occurs during early phases of embryogenesis, the observed phenotype could have been due to a problem occurring in the first phases of Bergmann glia differentiation from radial glia [40]. However, even postnatal conditional ablation of Sox2 in Bergmann glia—with a tamoxifen-inducible-Cre recombinase knocked-in the GLAST locus—showed that Sox2 is required to maintain BG radial morphology and their correct position in the PC-layer, in agreement with Sox2 maintaining an important role in postnatal, fully differentiated BG (Figure 1A). Interestingly, this later

Sox2 ablation was accompanied by mild ataxia, while the vermis appeared normal, suggesting a likely direct role of Sox2-expressing BG in regulating neuronal activity [29]. One important role of BG that influences neuronal function, is the removal of glutamate from the synaptic cleft via the glutamate transporter GLAST. Defects in glutamate uptake in humans lead to ataxia [43]. This function of BG seems to be influenced by Sox2 loss since Sox2 mutant BG were found defective in glutamate uptake [29].

What genes does Sox2 regulate that mediate its function in determining the position, the morphology, and the activity of BG?

To date, no direct Sox2 targets in BG have been identified, but many Sox2 targets in NSC and glial cells in culture [18,29,44] are also expressed in BG and could mediate Sox2 function. In addition, mutations in some of these potential targets lead to ataxia and BG defects reminiscent of the ones due to Sox2 loss, for example mutations in the tumor suppressor adenomatous polyposis coli (APC) [45] and in the transcription factor Sox4 [46].

Finally, it has been reported that BG translocation is a marker for vanishing white matter disease, a severe leukoencephalopathy due to mutations in the eukaryotic translation initiation factor 2B (eI2B) and that glial abnormality may be important in the pathogenesis of the disease [47].

Müller Glia in the Retina

Another macroglia type that expresses Sox2 is the Müller glia in the retina [4,27,28]. Müller glia (MG) develop from retinal progenitor cells

(RPC) after they have given rise to all the different retinal neurons [48]. MG have a radial morphology that spans across the whole retina; MG cells have their cell bodies in the inner nuclear layer (INL) (Figure 1B). MG are essential for the establishment and maintenance of the laminar organization of the postnatal retina, and for providing trophic support to neurons [49,50]. Ablation of Sox2 at the height of MG genesis in mice (P5) using a tamoxifen inducible Cre recombinase line (GLAST-Cre-ER) led to the disruption of MG processes, that worsened with time and led to a thinner retina. In the Sox2 mutants, adherens junctions were shorter and not oriented correctly. The lack of Sox2 not only affected MG, but also the development of neuronal processes that probably required a functional MG to correctly differentiate [27].

In addition, MG cell bodies, usually localized in the INL, were located ectopically in the outer plexiform layer (OPL) and outer nuclear layer (ONL) in Sox2 mutants [27](Figure 1B). This same phenotype was also obtained by ablating Sox2 postnatally in differentiated MG with a tamoxifen inducible Cre recombinase (CAGG-Cre-ER); in this mouse model, retinas were treated with Tamoxifen in vitro, cultured for a few days and imaged with time-lapse videos. The time-lapse videos showed that the mis-localization of MG was an indication that they had re-entered the cell cycle and, therefore, interkinetic nuclear migration had occurred. MG display a similar nuclear movement when they re-enter the cell cycle following retinal damage [28]. In conclusion, Sox2 has a key role in maintaining MG shape and quiescence state, in order to prevent their premature re-entering of the cell cycle and subsequent depletion through cell divisions.

What genes does Sox2 regulate that mediate its function in determining the morphology, the position, and the quiescence of MG?

The Notch signaling pathway has been shown to be important, not only to regulate NPC fate decisions but also to maintain MG identity [51,52]. In addition, Notch1, a downstream target of Sox2 in RPC [15,53], is downregulated in Sox2 mutant MG, and ectopic activation of the Notch pathway in Sox2 mutant MG can rescue the radial morphology. However, Notch signaling does not seem to be involved in the maintenance of the MG quiescence state [28].

Can Sox2 Expressing BG and MG Include Cells with Stem Cell Features?

Both BG and MG express markers of stem cells, including Sox2, suggesting that they might have the capacity to re-enter the cell cycle and produce new neurons and glia upon damage. In the adult cerebellum, cells with properties of NSC-like cells were found to be localized in the Purkinje cell layer, intermingled with BG, and to express Sox2 [54]. MG maintains neurogenic capacity in the adult retina, and it has been shown to be able to re-enter the cell cycle in response to retinal injury [55,56]. These findings indicate that Sox2 may retain some of its stem cell-related functions, acting within subpopulations of differentiated glia, as they occasionally resume stem cell character.

2.1.2. Myelinating Glial Cells: Oligodendrocytes and Schwann Cells

In vertebrates, axons are wrapped by myelin sheaths that allow rapid information transmission. Myelination is essential for the proper

function of axons, and defects in its development or myelin damage can lead to serious diseases in humans like leukodystrophies and multiple sclerosis.

Oligodendrocytes

Oligodendrocytes are the myelinating glia of the central nervous system, and they originate from neural stem cells after neurons have been generated. Sox2 is expressed in oligodendrocyte progenitor cells (OPCs) during development and in early differentiating oligodendrocytes, while Sox2 expression in OPCs in the adult brain is still controversial [22–25]. Overexpression of Sox2 and Sox3 in oligodendrocytes precursors cells (OPC) converts them to neural stem cells [57], however, the role of Sox2 in differentiating oligodendrocytes was not clear until recently.

Conditional ablation in the oligodendrocyte lineage of Sox2 was generated in mice (by Sox10-Cre recombinase that leads to complete ablation by E15.5), and while no effect on proliferation, migration, and survival were observed at embryonic stages, at early postnatal stages terminal differentiation was impaired [22] (Figure 1C). When OPC proliferation was analyzed at postnatal stages, a strong reduction of OPCs was instead observed [24,25]. Since Sox2 expression peaks in the early stages of oligodendrocyte differentiation, its deletion, specifically at this stage of the oligodendrocyte lineage, was obtained (by CNP-Cre recombinase), and a diminished rate of oligodendrocyte generation was observed, accompanied, in the forebrain, by hypomyelination [23,24] (Figure 1C).

One way in which Sox2 is thought to influence myelination is by inhibiting the expression of miR145, a negative regulator of genes important for oligodendrocyte differentiation like Sox9, Med12, and Myrf [22] (Figure 1C). In addition, Sox2 binds the myelin basic protein promoter, but it is a much weaker activator than Sox10 (a marker of the whole oligodendrocyte lineage); this observation led to the idea that Sox2 could be important to poise the chromatin for Sox10, since SoxB1 factors have been shown to do this in neural stem cells [58,59].

Schwann Cells

Schwann cells (SC) originate from the neural crest and are the myelinating glia of the peripheral nervous system, involved in myelinating axons during normal development and in their remyelination following injury. While many positive regulators of myelination in the PNS have been identified, including Krox20 and Sox10, just a few negative regulators have been characterized, and Sox2 is one of them.

Overexpression of Sox2 in vitro using SC/dorsal root ganglion co-cultures had been shown to inhibit the induction of Krox-20 by cAMP and, therefore, myelination [30]. Recently, a role for Sox2 in inhibiting myelination has been shown also in vivo in mice. Sox2 was conditionally overexpressed in Schwann cells (by means of a conditionally overexpressing Sox2 allele [60], that gets activated by Cre recombination, in this case, P0-Cre [61]) and this resulted in animals smaller than their littermates, with clasping behavior (sign of abnormal motor function) and hypomyelination [31] (Figure 1D). In addition, SC overexpressing Sox2 did not associate correctly with axons and

produced many processes, but little myelin compared to controls. Sox2-overexpressing SCs proliferated more, and presented features of immature non-myelinating Schwann cells, like an increase of N-cadherin (usually expressed in developing nerves and downregulated during myelination), and of Jun (a marker of promyelinating SCs) [31]. In conclusion, Sox2 appears to have a role in regulating the onset of myelination during development in the PNS.

Could Sox2 Have a Role in Remyelination?

Remyelination is the process by which myelinating glia of the nervous system get activated by a demyelinating lesion and stimulated to proliferate, migrate to the demyelinated area, and differentiate into new myelin-producing glia. Understanding how remyelination occurs is essential to be able to design cures for demyelinating diseases like multiple sclerosis.

Sox2 expression in OPCs and early differentiating oligodendrocytes make it a good candidate regulator of remyelination in the CNS. Indeed, in vivo studies of remyelination in mice, after induced demyelination in the CNS, have shown that Sox2 is important for OPC recruitment to the lesion site, OPC proliferation, and differentiation [24,25]. Interestingly, Sox2 is expressed in OPCs in the human brain and these OPCs can be differentiated into mature OL in vitro [62], suggesting that even in humans it could be an important regulator of remyelination.

Sox2 might also have a role in remyelination in the PNS; indeed, Sox2 overexpression in SC, following crush nerve injury, results in impairment of remyelination and of functional recovery [31].

Therefore, even in the PNS, Sox2 seems to have a role in remyelination and it appears to be required to regulate the onset of myelination [31].

2.2. Sox2 in Neurons

Sox2 is usually considered a marker of neural stem cells in different embryonic and adult brain regions; however, its expression has also been described in differentiated neurons in various regions of the nervous system, but until recently little was known about Sox2 function in these post mitotic neurons. Sox2 expression in pyramidal and GABAergic interneurons in the cerebral cortex and in different thalamic neurons in mice had been described [26]. In addition, a potential role of Sox2 in differentiated neurons was suggested by the identification of neurons with inclusions typical of neurodegenerative disorders and by GABAergic interneurons with aberrant morphology in the cortex of hypomorph Sox2 mutants [26,39]. Defects in post-mitotic neurons could be due to the lack of Sox2 in neural progenitors that might influence their correct differentiation, but Sox2 could also have a role after neuronal differentiation has occurred, and recently Sox2 ablation in post-mitotic neurons has been performed and this question can start to be addressed.

Three examples of the role of Sox2 in differentiated neurons will be described.

Thalamic Projection Neurons

Sox2 is expressed in post-mitotic neurons of thalamic sensory nuclei from late gestation to adulthood, these nuclei are the medial geniculate nucleus (MGN, that receives auditory information), the dorsolateral

geniculate nucleus (dLGN, that receives visual information), and the ventro-posterior nucleus (VPN, that receives somato-sensory information from the periphery) and they project to the auditory cortex, the primary visual cortex, and the somatosensory cortex, respectively. Recently, the role of Sox2 in the neuronal development of these sensory thalamic nuclei has been investigated by means of conditional thalamic ablation within post-mitotic neurons. Particular attention has been given to the role of Sox2 in the dLGN and on how its thalamic ablation influences the development of the visual system [35].

Neurons in the dLGN receive input from the retina and project to the visual cortex. Projections from the dLGN to the visual cortex are required for the correct patterning of the visual cortex, if projections from dLGN neurons to the cortex are reduced/absent, the primary visual cortex and the adjacent higher order visual cortical areas are not correctly defined [35,63]. Sox2 deletion in these dLGN neurons, when they are already post-mitotic (by means of a thalamus specific Cre recombinase (Rorα-Cre expressed from E14.5)), results in a reduction of the size of the dLGN postnatally (Figure 2A). Interestingly, even before the reduction of the dLGN is observed, the arrival of retinal fibers to the dLGN is compromised. In addition, dLGN neuronal projections to the primary visual cortex are reduced concomitantly with the projections from the cortex to the thalamus. Even though Sox2 is not deleted in the primary visual cortex (V1), the development of V1 is strongly compromised in the Sox2 thalamic mutants, this is likely due to reduced projections from the dLGN to V1 known to be required for proper patterning of V1 [63] (Figure 2A).

Neurons in the VP also appear to require Sox2 for their correct development since their projections to the somatosensory cortex are reduced in Sox2 thalamic mutants and not correctly organized. On the other hand, projections from the MG to the auditory cortex appear less affected by Sox2 loss in the same thalamic mutants described above, but their development should be studied in more detail to properly address Sox2 requirement [35].

Retinal axons reaching the Sox2 mutant dLGN not only are reduced in number, compared to their control littermates, but they also do not segregate in the correct manner within the dLGN. In addition, a portion of axons are misrouted to the adjacent ventrolateral geniculate nucleus (vLGN). A misrouting phenotype suggests that deregulation of an axon guidance molecule could be involved. In fact, ephrin-A5 (efna5) was found to be downregulated in the Sox2 mutant dLGN, even at stages preceding the misrouting phenotype. It is thought that Efna5 could be a direct Sox2 target since Sox2 binding sites were identified in an intron, that behaves as an enhancer activated by Sox2 in in vitro co-transfection assays [18,35].

Another signaling pathway affected by thalamic Sox2 loss is the serotonin pathway. Serotonin uptake by thalamo-cortical axons in the first two postnatal weeks has been shown to be important in patterning cortical areas, in particular, the somatosensory cortex. Alterations of the serotonin pathway in mouse brains have been shown to affect the organization of barrel fields in the somatosensory cortex [64–66]. Serotonin uptake by dLGN neurons is affected in the thalamic Sox2 cKO, since expression of the serotonin transporters, SERT and vMAT, is strongly downregulated in the mutant dLGN. As a consequence (at

least in part) of this, the amount of serotonin-positive fibers reaching the visual cortex is greatly reduced [35].

In conclusion, Sox2 expression is required in post-mitotic thalamic sensory neurons, and in particular in the visual thalamus, to properly receive and process visual information [35].

Clock Neurons in the Suprachiasmatic Thalamic Nucleus

Other thalamic nuclei where Sox2 expression has been described in differentiated neurons are the Suprachiasmatic nuclei (SCN)—small paired structures in the anterior hypothalamus just above the optic chiasm [67] (Figure 2B). They receive visual stimuli for light or dark through indirect or direct retina-SCN pathways. The SCN is considered the central circadian pacemaker in mammals since it is the site of a master circadian clock in the mammalian brain that generates circadian rhythms. Each neuron in the SCN is capable of independent cellular oscillations. Different clock genes have been identified that are involved in a series of transcription–translation feedback loops (TTFL) that make up the molecular clock (reviewed in reference [68]). Among the key genes involved in the molecular clock are period1 and period2. To synchronize oscillations within the SCN, different SCN populations synthetize neuropeptides including vasoactive intestinal peptide (VIP), arginine vasopressin (AVP), and gastrin-releasing peptide (GRP). On the other hand, the production of neuropeptides such as prokineticin 2 (PK2 and Prok2) can function as outputs of the SCN to other brain regions [34,69].

Cheng et al. 2019 found that almost all PER2+ cells in the adult SCN express SOX2. To understand how Sox2 loss could affect the activity

of SCN neurons, a conditional knock-out was generated in which Sox2 was deleted in all GABA-ergic interneurons (using a vescicular GABA transporter Cre recombinase). While the structural organization of the SCN was not affected by Sox2 conditional ablation, the expression of PER2 and of neuropeptide genes was greatly reduced. These mice have a deficit in light induced entrainment and display widespread changes in behavioral rhythms [34] (Figure 2B).

Sox2 was found to regulate the clock activity of SCN neurons by directly activating, in vitro and in vivo, the period2 gene. In addition, RNAseq experiments identified a reduction of transcription of other clock genes and also of neuropeptides. Therefore, Sox2 is thought to regulate signaling within the SCN nucleus and between the SCN nucleus and other parts of the brain [34].

In conclusion, Sox2 is required in clock neurons of the SCN for their proper regulation of circadian rhythms.

Neurons in C.elegans

The genome of the nematode C. elegans contains two *SoxB* genes: *sox2* (SoxB1) and *sox3* (SoxB2). On the other hand, there are 5 SoxB genes in mammals: *Sox1*, *Sox2*, *Sox3* (SoxB1) and *Sox14*, *Sox21* (SoxB2). *C. elegans sox2* has functional conservation with vertebrate Sox2 [36].

It has been recently shown that *C. elegans* SoxB genes are not required for neurogenesis in the developing nervous system, but for the differentiation of specific cell types. In particular, *sox2*, the SoxB1 gene, has been shown to be expressed throughout the life of several glutamatergic and cholinergic neurons and is required for their terminal differentiation. These neurons are born in sox2-null worms, but their

differentiation in a specific neuron-type is compromised [37] (Figure 2C).

A role for *C. elegans sox2* in regulating the final differentiation of a specific neuronal class has also been shown for olfactory neurons. Three pairs of olfactory neurons are dedicated to sensing volatile odorants, AWA, AWB, and AWC, and their identity is regulated by regulatory programs involving neuron-type specific transcription factors. Distinct homeodomain proteins compete for cooperation with Sox2 to drive neuron specific gene expression. The Sox2/Lim4 pair drives the differentiation of the AWC neurons while the Sox2/Ceh-36 (Otx-type) pair drives the AWB differentiation program [36].

3. Conclusions and Perspectives

The identification of functional roles for Sox2 in specific types of differentiated neurons and glia opens a new perspective in the understanding of the function of this transcription factor in neural development and disease, enlarging Sox2 functional roles beyond those it plays within stem cells. Sox2 function in thalamic neurons is an example of an important role for Sox2 in aspects of neural cell biology central to their "differentiated" characteristics: the development of neuron-to-neuron connectivity, involving the correct establishment of the retina–thalamus–brain connections. These new roles provide an unexpected potential new explanation for the visual defects observed in Sox2 patients, acting together with Sox2 functions in the eye. The identification of the Sox2 target genes within these differentiated neural cells, and a more in-depth understanding of the gene regulatory networks mediating Sox2 function in them will provide a better

understanding of Sox2 function in neural development and its pathology, with potential implications for new therapy approaches.

Author Contributions: S.M. and S.K.N. wrote the review; L.S. discussed the review and prepared the Figures and Table 1.

Funding: The Nicolis laboratory is supported by ERANET NEURON funding (ImprovVision grant, NEURON8-Full-815-091). L.S. is the recipient of a Vinci PhD fellowship from the Università Italo-Francese. S.M. is the recipient of a research fellowship (Assegno di Ricerca) from the Department of Biotechnology and Biosciences, University of Milano-Bicocca.

Conflicts of Interest: The authors declare no conflict of interest.

Figures

Table1. SOX2 expression and function in glia and neurons.

Glia	Sox2 expression	Sox2 function	References
Macroglia in the Central nervous system			
Astrocytes	Yes	Cellular maturation and morphology (retina)	[21]
OPC and Oligodendrocytes	Yes	Proliferation, differentiation, myelination	[22–25]
Ependymal cells	Yes	Cellular structure (cilia reduction in Sox2 mutants)	[26]
Müller glia (retina)	Yes	Cellular structure and positioning	[27,28]
Bergmann glia (cerebellum)	Yes	Cellular morphology and positioning (in Sox2 mutants, defective motor control)	[29]
Macroglia in the Peripheral nervous system			
Schwann cells	Yes	Myelination	[30,31]
Satellite cells	Yes	Survival	[32,33]
Neurons	**Sox2 expression**	**Sox2 function**	**References**
Clock neurons in Suprachiasmatic nucleus	Yes	Regulation of circadian rhythms	[34]
Sensory thalamic nuclei (including DLG)	Yes	Signalling to incoming retinal axons; DLG growth; development of thalamic neurons projections to the visual and somatosensory cortex	[35]
Specific glutamatergic and cholinergic neurons in C.elegans	Yes	Differentiation of specific neuron-types	[36,37]
Cholinergic amacrine neurons	Yes	Cell positioning and dendritic stratification	[38]
GABA-ergic interneurons, rare pyramidal cells in the cortex	Yes	Morphology and maturation (impaired GABAergic neuroblast migration and differentiation; intraneuronal aggregates)	[26,39]
Some striatal cells	Yes	N.A.	[26]
Thalamic cells	Yes	N.A.	[26]

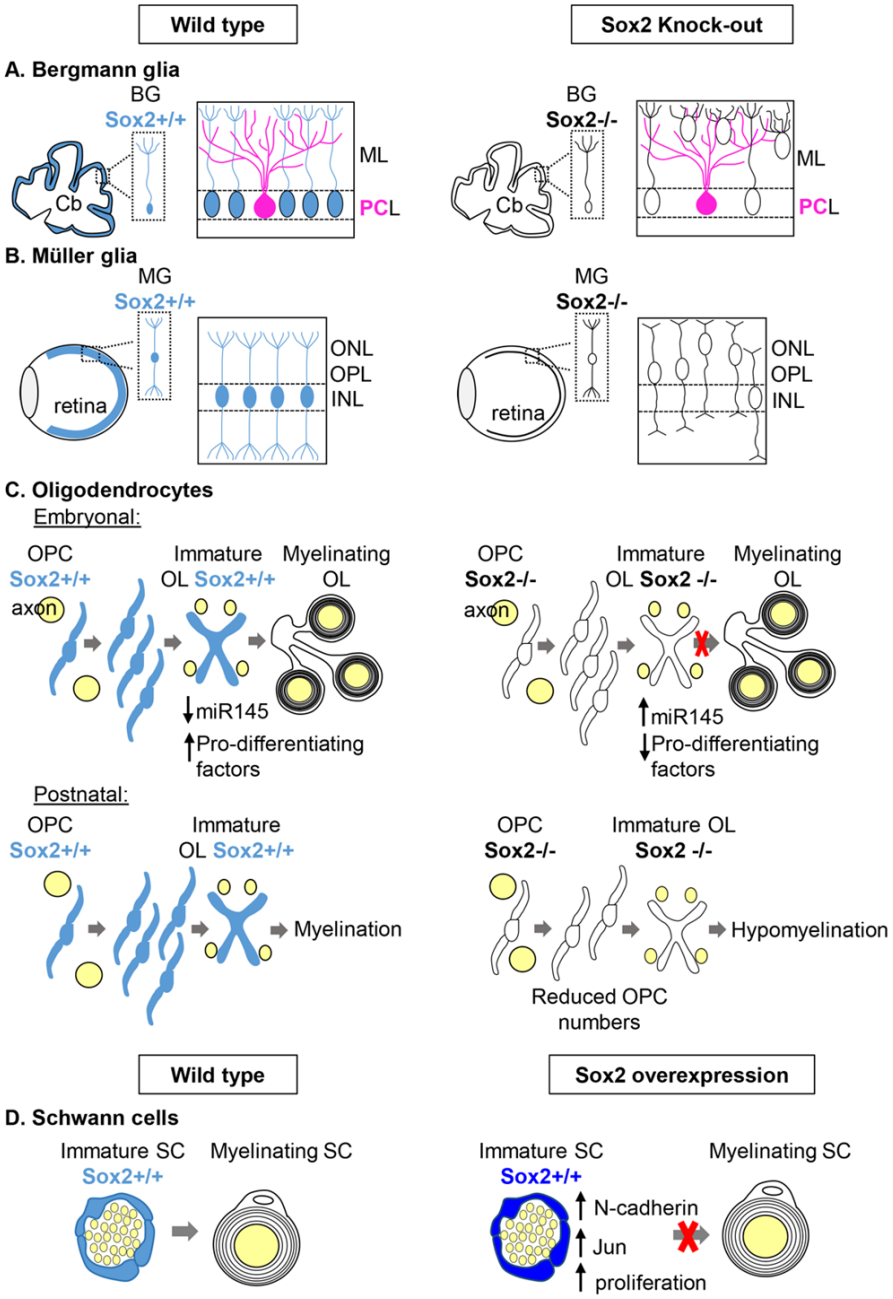

Figure 1. Differentiated glial cells requiring Sox2 function. Glial cells expressing Sox2 in wild type (left) are colored in blue. The corresponding cell types in Sox2 knock-out mice (right) are uncolored. (A) Bergmann glia in the cerebellum. Sox2-positive Bergmann glia cells (blue), forming an ordered

array in wild type, that also includes Purkinje neurons (pink), are displaced and abnormal in Sox2 mutants (see text). Abbreviations: Cb, cerebellum; BG, Bergmann glia; ML: molecular layer; PCL, Purkinje cells layer. (B) Müller glia in the retina. Sox2-positive Müller glia cells (blue), forming an ordered array in wild type, are displaced and abnormal in Sox2 mutants, in the context of a thinner retina (see text). Abbreviations: MG, Müller glia; INL, inner nuclear layer; OPL, outer plexiform layer; ONL, outer nuclear layer. (C) Oligodendrocytes. In wild type embryonic oligodendrogenesis (top), Sox2-positive oligodendrocyte precursor cells and immature oligodendrocytes differentiate into oligodendrocytes, thereby, decreasing the expression of miR145, and increasing the expression of myelinating factors; in Sox2 mutants, differentiation of oligodendrocytes is abnormal, as cells retain immature features, and show higher expression of miR145 and lower expression of myelinating factors relative to the controls (see text). In postnatal oligodendrogenesis (bottom), Sox2 loss leads to reduced numbers of oligodendrocyte precursors, and to hypomyelination (see text). Abbreviations: OPC, oligodendrocyte precursor cells; OL, oligodendrocytes. (D) Schwann cells. Wild type immature, Sox2-positive Schwann cells produce correctly differentiated Schwann cells (left); Sox2 overexpression (right, dark blue cells) leads to cells retaining immature features, with upregulation of N-cadherin, Jun, an increase of proliferation, and failing to properly differentiate (see text). Abbreviations: SC, Schwann cells.

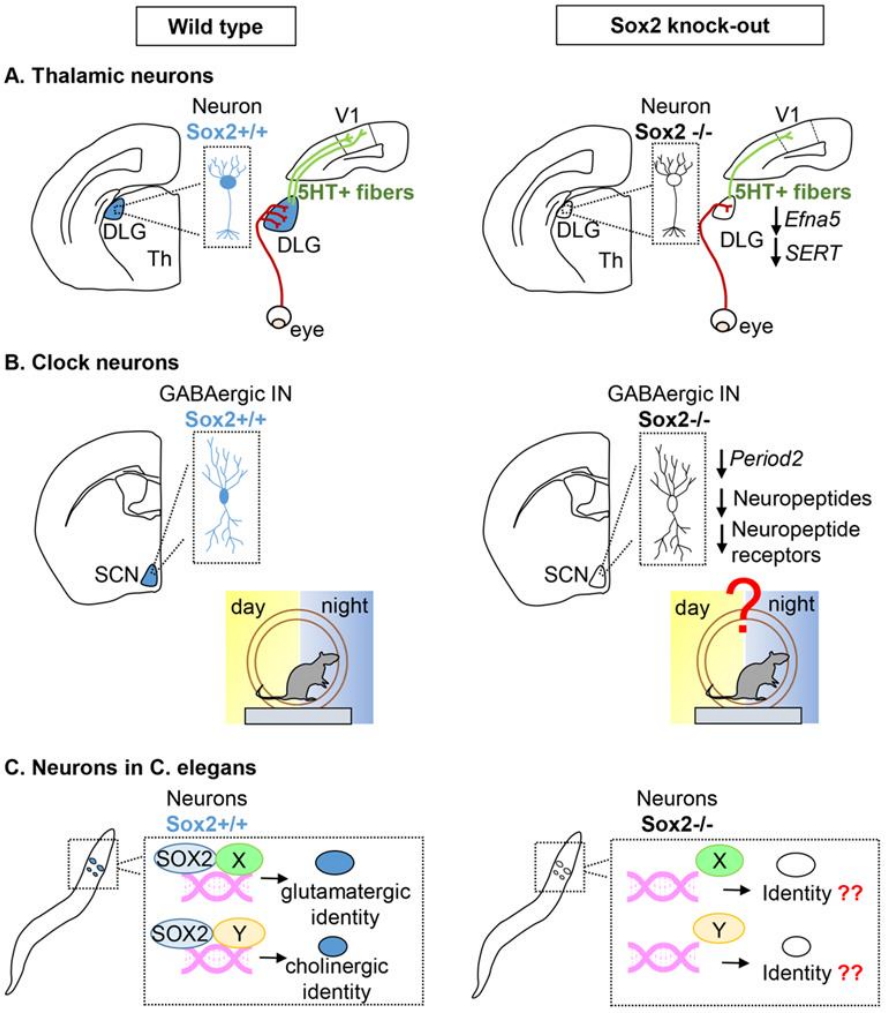

Figure 2. Differentiated neuronal cells requiring Sox2 function. Neuronal cells expressing Sox2 in wild type (left) are colored in blue. The corresponding cell types in Sox2 knock-out mice (right) are uncolored. (A) Thalamic neurons within the mouse sensory thalamic nuclei. In wild type animals, axons outgrowing from the retina reach the DLG in a spatially ordered pattern; DLG neurons develop 5HT-positive projections to the primary visual cortical area (V1). In mutant animals, the DLG is reduced, and the eye-DLG projections are reduced and disorganized; the DLG-V1

projections are also defective. A reduction of the expression of Efna5 and SERT in the mutant contributes to the defects. Abbreviations: DLG, dorsolateral geniculate nucleus; Th, thalamus; V1, primary visual area of the cerebral cortex; 5HT, 5-hydroxytryptamine, i.e., serotonin. (B) Clock neurons within the mouse suprachiasmatic nucleus. In wild types, Sox2-expressing GABAergic interneurons in the SCN are essential for establishing circadian rhythms. In mutants, circadian rhythms are perturbed; a decrease in the expression of Period2, and of neuropeptides and their receptors contribute to the defect. Abbreviations: SCN, suprachiasmatic nucleus; IN, interneurons. (C) Neurons of C. elegans. In wild types, Sox2 is expressed in specific neuronal cell types, both glutamatergic and cholinergic, and binds to DNA with different partners (X, Y). In mutants, the terminal differentiation of these neuron types is defective.

References

1. Arnold, K.; Sarkar, A.; Yram, M.A.; Polo, J.M.; Bronson, R.; Sengupta, S.; Seandel, M.; Geijsen, N.; Hochedlinger, K. Sox2(+) adult stem and progenitor cells are important for tissue regeneration and survival of mice. Cell Stem Cell 2011, 9, 317–329, doi:10.1016/j.stem.2011.09.001.
2. Bertolini, J.; Mercurio, S.; Favaro, R.; Mariani, J.; Ottolenghi, S.; Nicolis, S.K. Sox2-dependent regulation of neural stem cells and CNS development. In Sox2, Biology and Role in Development and Disease; Kondoh, H., Lovell-Badge, R., Eds.; Elsevier: Amsterdam, The Netherlands, 2016.
3. Kondoh, H.; Lovell-Badge, R. Sox2, Biology and Role in Development and Disease; Elsevier: Amsterdam, The Netherlands; Associated Press: New York, NY, USA, 2016; ISBN: 978-0-12-800352-7.

4. Pevny, L.H.; Nicolis, S.K. Sox2 roles in neural stem cells. Int. J. Biochem. Cell Biol. 2010, 42, 421–424, doi:10.1016/j.biocel.2009.08.018.

5. Avilion, A.A.; Nicolis, S.K.; Pevny, L.H.; Perez, L.; Vivian, N.; Lovell-Badge, R. Multipotent cell lineages in early mouse development depend on SOX2 function. Genes Dev. 2003, 17, 126–140, doi:10.1101/gad.224503.

6. Takahashi, K.; Yamanaka, S. A decade of transcription factor-mediated reprogramming to pluripotency. Nat. Rev. Mol. Cell Biol. 2016, 17, 183–193, doi:10.1038/nrm.2016.8.

7. Zappone, M.V.; Galli, R.; Catena, R.; Meani, N.; De Biasi, S.; Mattei, E.; Tiveron, C.; Vescovi, A.L.; Lovell-Badge, R.; Ottolenghi, S.; et al. Sox2 regulatory sequences direct expression of a (beta)-geo transgene to telencephalic neural stem cells and precursors of the mouse embryo, revealing regionalization of gene expression in CNS stem cells. Development 2000, 127, 2367–2382.

8. Favaro, R.; Valotta, M.; Ferri, A.L.; Latorre, E.; Mariani, J.; Giachino, C.; Lancini, C.; Tosetti, V.; Ottolenghi, S.; Taylor, V.; et al. Hippocampal development and neural stem cell maintenance require Sox2-dependent regulation of Shh. Nat. Neurosci. 2009, 12, 1248–1256, doi:10.1038/nn.2397.

9. Ferri, A.; Favaro, R.; Beccari, L.; Bertolini, J.; Mercurio, S.; Nieto-Lopez, F.; Verzeroli, C.; La Regina, F.; De Pietri Tonelli, D.; Ottolenghi, S.; et al. Sox2 is required for embryonic development of the ventral telencephalon through the activation of the ventral determinants Nkx2.1 and Shh. Development 2013, 140, 1250–1261, doi:10.1242/dev.073411.

10. Panaliappan, T.K.; Wittmann, W.; Jidigam, V.K.; Mercurio, S.; Bertolini, J.A.; Sghari, S.; Bose, R.; Patthey, C.; Nicolis, S.K.; Gunhaga, L. Sox2 is required for olfactory pit formation and olfactory neurogenesis through BMP restriction and Hes5 upregulation. Development 2018, 145, doi:10.1242/dev.153791.

11. Schwob, J.E.; Jang, W.; Holbrook, E.H.; Lin, B.; Herrick, D.B.; Peterson, J.N.; Hewitt Coleman, J. Stem and progenitor cells of the mammalian olfactory epithelium: Taking poietic license. J. Comp. Neurol. 2017, 525, 1034–1054, doi:10.1002/cne.24105.

12. Fantes, J.; Ragge, N.K.; Lynch, S.A.; McGill, N.I.; Collin, J.R.; Howard-Peebles, P.N.; Hayward, C.; Vivian, A.J.; Williamson, K.; van Heyningen, V.; et al. Mutations in SOX2 cause anophthalmia. Nat. Genet. 2003, 33, 461–463, doi:10.1038/ng1120.

13. Ragge, N.K.; Lorenz, B.; Schneider, A.; Bushby, K.; de Sanctis, L.; de Sanctis, U.; Salt, A.; Collin, J.R.; Vivian, A.J.; Free, S.L.; et al. SOX2 anophthalmia syndrome. Am. J. Med. Genet. A 2005, 135, 1–7, discussion 8, doi:10.1002/ajmg.a.30642.

14. Sisodiya, S.M.; Ragge, N.K.; Cavalleri, G.L.; Hever, A.; Lorenz, B.; Schneider, A.; Williamson, K.A.; Stevens, J.M.; Free, S.L.; Thompson, P.J.; et al. Role of SOX2 mutations in human hippocampal malformations and epilepsy. Epilepsia 2006, 47, 534–542, doi:10.1111/j.1528-1167.2006.00464.x.

15. Taranova, O.V.; Magness, S.T.; Fagan, B.M.; Wu, Y.; Surzenko, N.; Hutton, S.R.; Pevny, L.H. SOX2 is a dose-dependent regulator of retinal neural progenitor competence. Genes Dev. 2006, 20, 1187–1202, doi:10.1101/gad.1407906.

16. Niwa, H.; Nakamura, A.; Urata, M.; Shirae-Kurabayashi, M.; Kuraku, S.; Russell, S.; Ohtsuka, S. The evolutionally-conserved function of group B1 Sox family members confers the unique role of Sox2 in mouse ES cells. BMC Evol. Biol. 2016, 16, 173, doi:10.1186/s12862-016-0755-4.

17. Feng, R.; Wen, J. Overview of the roles of Sox2 in stem cell and development. Biol. Chem. 2015, 396, 883–891, doi:10.1515/hsz-2014-0317.

18. Bertolini, J.A.; Favaro, R.; Zhu, Y.; Pagin, M.; Ngan, C.Y.; Wong, C.H.; Tjong, H.; Vermunt, M.W.; Martynoga, B.; Barone, C.; et al. Mapping the Global Chromatin Connectivity Network for Sox2 Function in Neural

Stem Cell Maintenance. Cell Stem Cell 2019, 24, 462–476, doi:10.1016/j.stem.2019.02.004.

19. Amador-Arjona, A.; Cimadamore, F.; Huang, C.T.; Wright, R.; Lewis, S.; Gage, F.H.; Terskikh, A.V. SOX2 primes the epigenetic landscape in neural precursors enabling proper gene activation during hippocampal neurogenesis. Proc. Natl. Acad. Sci. USA 2015, 112, E1936–E1945, doi:10.1073/pnas.1421480112.

20. Toda, T.; Hsu, J.Y.; Linker, S.B.; Hu, L.; Schafer, S.T.; Mertens, J.; Jacinto, F.V.; Hetzer, M.W.; Gage, F.H. Nup153 Interacts with Sox2 to Enable Bimodal Gene Regulation and Maintenance of Neural Progenitor Cells. Cell Stem Cell 2017, 21, 618–634, doi:10.1016/j.stem.2017.08.012.

21. Kautzman, A.G.; Keeley, P.W.; Nahmou, M.M.; Luna, G.; Fisher, S.K.; Reese, B.E. Sox2 regulates astrocytic and vascular development in the retina. Glia 2018, 66, 623–636, doi:10.1002/glia.23269.

22. Hoffmann, S.A.; Hos, D.; Kuspert, M.; Lang, R.A.; Lovell-Badge, R.; Wegner, M.; Reiprich, S. Stem cell factor Sox2 and its close relative Sox3 have differentiation functions in oligodendrocytes. Development 2014, 141, 39–50, doi:10.1242/dev.098418.

23. Zhang, S.; Rasai, A.; Wang, Y.; Xu, J.; Bannerman, P.; Erol, D.; Tsegaye, D.; Wang, A.; Soulika, A.; Zhan, X.; et al. The Stem Cell Factor Sox2 Is a Positive Timer of Oligodendrocyte Development in the Postnatal Murine Spinal Cord. Mol. Neurobiol. 2018, 55, 9001–9015, doi:10.1007/s12035-018-1035-7.

24. Zhang, S.; Zhu, X.; Gui, X.; Croteau, C.; Song, L.; Xu, J.; Wang, A.; Bannerman, P.; Guo, F. Sox2 Is Essential for Oligodendroglial Proliferation and Differentiation during Postnatal Brain Myelination and CNS Remyelination. J. Neurosci. 2018, 38, 1802–1820, doi:10.1523/JNEUROSCI.1291-17.2018.

25. Zhao, C.; Ma, D.; Zawadzka, M.; Fancy, S.P.; Elis-Williams, L.; Bouvier, G.; Stockley, J.H.; de Castro, G.M.; Wang, B.; Jacobs, S.; et al. Sox2

Sustains Recruitment of Oligodendrocyte Progenitor Cells following CNS Demyelination and Primes Them for Differentiation during Remyelination. J. Neurosci. 2015, 35, 11482–11499, doi:10.1523/JNEUROSCI.3655-14.2015.

26. Ferri, A.L.; Cavallaro, M.; Braida, D.; Di Cristofano, A.; Canta, A.; Vezzani, A.; Ottolenghi, S.; Pandolfi, P.P.; Sala, M.; DeBiasi, S.; et al. Sox2 deficiency causes neurodegeneration and impaired neurogenesis in the adult mouse brain. Development 2004, 131, 3805–3819, doi:10.1242/dev.01204.

27. Bachleda, A.R.; Pevny, L.H.; Weiss, E.R. Sox2-Deficient Muller Glia Disrupt the Structural and Functional Maturation of the Mammalian Retina. Investig. Ophthalmol. Vis. Sci. 2016, 57, 1488–1499, doi:10.1167/iovs.15-17994.

28. Surzenko, N.; Crowl, T.; Bachleda, A.; Langer, L.; Pevny, L. SOX2 maintains the quiescent progenitor cell state of postnatal retinal Muller glia. Development 2013, 140, 1445–1456, doi:10.1242/dev.071878.

29. Cerrato, V.; Mercurio, S.; Leto, K.; Fuca, E.; Hoxha, E.; Bottes, S.; Pagin, M.; Milanese, M.; Ngan, C.Y.; Concina, G.; et al. Sox2 conditional mutation in mouse causes ataxic symptoms, cerebellar vermis hypoplasia, and postnatal defects of Bergmann glia. Glia 2018, 66, 1929–1946, doi:10.1002/glia.23448.

30. Le, N.; Nagarajan, R.; Wang, J.Y.; Araki, T.; Schmidt, R.E.; Milbrandt, J. Analysis of congenital hypomyelinating Egr2Lo/Lo nerves identifies Sox2 as an inhibitor of Schwann cell differentiation and myelination. Proc. Natl. Acad. Sci. USA 2005, 102, 2596–2601, doi:10.1073/pnas.0407836102.

31. Roberts, S.L.; Dun, X.P.; Doddrell, R.D.S.; Mindos, T.; Drake, L.K.; Onaitis, M.W.; Florio, F.; Quattrini, A.; Lloyd, A.C.; D'Antonio, M.; et al. Sox2 expression in Schwann cells inhibits myelination in vivo and induces influx of macrophages to the nerve. Development 2017, 144, 3114–3125, doi:10.1242/dev.150656.

32. Koike, T.; Wakabayashi, T.; Mori, T.; Hirahara, Y.; Yamada, H. Sox2 promotes survival of satellite glial cells in vitro. Biochem. Biophys. Res. Commun. 2015, 464, 269–274, doi:10.1016/j.bbrc.2015.06.141.

33. Koike, T.; Wakabayashi, T.; Mori, T.; Takamori, Y.; Hirahara, Y.; Yamada, H. Sox2 in the adult rat sensory nervous system. Histochem. Cell Biol. 2014, 141, 301–309, doi:10.1007/s00418-013-1158-x.

34. Cheng, A.H.; Bouchard-Cannon, P.; Hegazi, S.; Lowden, C.; Fung, S.W.; Chiang, C.K.; Ness, R.W.; Cheng, H.M. SOX2-Dependent Transcription in Clock Neurons Promotes the Robustness of the Central Circadian Pacemaker. Cell Rep. 2019, 26, 3191–3202, doi:10.1016/j.celrep.2019.02.068.

35. Mercurio, S.; Serra, L.; Motta, A.; Gesuita, L.; Sanchez-Arrones, L.; Inverardi, F.; Foglio, B.; Barone, C.; Kaimakis, P.; Martynoga, B.; et al. Sox2 Acts in Thalamic Neurons to Control the Development of Retina-Thalamus-Cortex Connectivity. iScience 2019, 15, 257–273, doi:10.1016/j.isci.2019.04.030.

36. Alqadah, A.; Hsieh, Y.W.; Vidal, B.; Chang, C.; Hobert, O.; Chuang, C.F. Post-mitotic diversification of olfactory neuron types is mediated by differential activities of the HMG-box transcription factor SOX-2. EMBO J. 2015, 34, 2574–2589, doi:10.15252/embj.201592188.

37. Vidal, B.; Santella, A.; Serrano-Saiz, E.; Bao, Z.; Chuang, C.F.; Hobert, O.C. elegans SoxB genes are dispensable for embryonic neurogenesis but required for terminal differentiation of specific neuron types. Development 2015, 142, 2464–2477, doi:10.1242/dev.125740.

38. Whitney, I.E.; Keeley, P.W.; St John, A.J.; Kautzman, A.G.; Kay, J.N.; Reese, B.E. Sox2 regulates cholinergic amacrine cell positioning and dendritic stratification in the retina. J. Neurosci. 2014, 34, 10109–10121, doi:10.1523/JNEUROSCI.0415-14.2014.

39. Cavallaro, M.; Mariani, J.; Lancini, C.; Latorre, E.; Caccia, R.; Gullo, F.; Valotta, M.; DeBiasi, S.; Spinardi, L.; Ronchi, A.; et al. Impaired

generation of mature neurons by neural stem cells from hypomorphic Sox2 mutants. Development 2008, 135, 541–557, doi:10.1242/dev.010801.

40. Yamada, K.; Watanabe, M. Cytodifferentiation of Bergmann glia and its relationship with Purkinje cells. Anat. Sci. Int. 2002, 77, 94–108, doi:10.1046/j.0022-7722.2002.00021.x.

41. Buffo, A.; Rossi, F. Origin, lineage and function of cerebellar glia. Prog. Neurobiol. 2013, 109, 42–63, doi:10.1016/j.pneurobio.2013.08.001.

42. De Zeeuw, C.I.; Hoogland, T.M. Reappraisal of Bergmann glial cells as modulators of cerebellar circuit function. Front. Cell. Neurosci. 2015, 9, 246, doi:10.3389/fncel.2015.00246.

43. Jayadev, S.; Bird, T.D. Hereditary ataxias: Overview. Genet. Med. 2013, 15, 673–683, doi:10.1038/gim.2013.28.

44. Lodato, M.A.; Ng, C.W.; Wamstad, J.A.; Cheng, A.W.; Thai, K.K.; Fraenkel, E.; Jaenisch, R.; Boyer, L.A. SOX2 co-occupies distal enhancer elements with distinct POU factors in ESCs and NPCs to specify cell state. PLoS Genet. 2013, 9, e1003288, doi:10.1371/journal.pgen.1003288.

45. Wang, X.; Imura, T.; Sofroniew, M.V.; Fushiki, S. Loss of adenomatous polyposis coli in Bergmann glia disrupts their unique architecture and leads to cell nonautonomous neurodegeneration of cerebellar Purkinje neurons. Glia 2011, 59, 857–868, doi:10.1002/glia.21154.

46. Hoser, M.; Baader, S.L.; Bosl, M.R.; Ihmer, A.; Wegner, M.; Sock, E. Prolonged glial expression of Sox4 in the CNS leads to architectural cerebellar defects and ataxia. J. Neurosci. 2007, 27, 5495–5505, doi:10.1523/JNEUROSCI.1384-07.2007.

47. Dooves, S.; Bugiani, M.; Wisse, L.E.; Abbink, T.E.M.; van der Knaap, M.S.; Heine, V.M. Bergmann glia translocation: A new disease marker for vanishing white matter identifies therapeutic effects of Guanabenz treatment. Neuropathol. Appl. Neurobiol. 2018, 44, 391–403, doi:10.1111/nan.12411.

48. Livesey, F.J.; Cepko, C.L. Vertebrate neural cell-fate determination: Lessons from the retina. Nat. Rev. Neurosci. 2001, 2, 109–118, doi:10.1038/35053522.

49. Bringmann, A.; Pannicke, T.; Grosche, J.; Francke, M.; Wiedemann, P.; Skatchkov, S.N.; Osborne, N.N.; Reichenbach, A. Muller cells in the healthy and diseased retina. Prog. Retin. Eye Res. 2006, 25, 397–424, doi:10.1016/j.preteyeres.2006.05.003.

50. Willbold, E.; Berger, J.; Reinicke, M.; Wolburg, H. On the role of Muller glia cells in histogenesis: Only retinal spheroids, but not tectal, telencephalic and cerebellar spheroids develop histotypical patterns. J. Hirnforsch. 1997, 38, 383–396.

51. Furukawa, T.; Mukherjee, S.; Bao, Z.Z.; Morrow, E.M.; Cepko, C.L. rax, Hes1, and notch1 promote the formation of Muller glia by postnatal retinal progenitor cells. Neuron 2000, 26, 383-394, doi:10.1016/s0896-6273(00)81171-x.

52. Jadhav, A.P.; Roesch, K.; Cepko, C.L. Development and neurogenic potential of Muller glial cells in the vertebrate retina. Prog Retin Eye Res 2009, 28, 249-262, doi:10.1016/j.preteyeres.2009.05.002.

53. Matsushima, D.; Heavner, W.; Pevny, L.H. Combinatorial regulation of optic cup progenitor cell fate by SOX2 and PAX6. Development 2011, 138, 443-454, doi:10.1242/dev.055178.

54. Ahlfeld, J.; Filser, S.; Schmidt, F.; Wefers, A.K.; Merk, D.J.; Glass, R.; Herms, J.; Schuller, U. Neurogenesis from Sox2 expressing cells in the adult cerebellar cortex. Sci. Rep. 2017, 7, 6137, doi:10.1038/s41598-017-06150-x.

55. Dyer, M.A.; Cepko, C.L. Control of Muller glial cell proliferation and activation following retinal injury. Nat. Neurosci. 2000, 3, 873–880, doi:10.1038/78774.

56. Gorsuch, R.A.; Lahne, M.; Yarka, C.E.; Petravick, M.E.; Li, J.; Hyde, D.R. Sox2 regulates Muller glia reprogramming and proliferation in the

regenerating zebrafish retina via Lin28 and Ascl1a. Exp. Eye Res. 2017, 161, 174–192, doi:10.1016/j.exer.2017.05.012.

57. Kondo, T.; Raff, M. Chromatin remodeling and histone modification in the conversion of oligodendrocyte precursors to neural stem cells. Genes Dev. 2004, 18, 2963–2972, doi:10.1101/gad.309404.

58. Bergsland, M.; Ramsköld, D.; Zaouter, C.; Klum, S.; Sandberg, R.; Muhr, J. Sequentially acting Sox transcription factors in neural lineage development. Genes Dev. 2011, 25, 2453–2464, doi:10.1101/gad.176008.111.

59. Wegner, M. SOX after SOX: SOXession regulates neurogenesis. Genes Dev. 2011, 25, 2423–2428, doi:10.1101/gad.181487.111.

60. Lu, Y.; Futtner, C.; Rock, J.R.; Xu, X.; Whitworth, W.; Hogan, B.L.; Onaitis, M.W. Evidence that SOX2 overexpression is oncogenic in the lung. PLoS ONE 2010, 5, e11022, doi:10.1371/journal.pone.0011022.

61. Feltri, M.L.; D'Antonio, M.; Previtali, S.; Fasolini, M.; Messing, A.; Wrabetz, L. P0-Cre transgenic mice for inactivation of adhesion molecules in Schwann cells. Ann. N. Y. Acad. Sci. 1999, 883, 116–123.

62. Oliver-De La Cruz, J.; Carrion-Navarro, J.; Garcia-Romero, N.; Gutierrez-Martin, A.; Lazaro-Ibanez, E.; Escobedo-Lucea, C.; Perona, R.; Belda-Iniesta, C.; Ayuso-Sacido, A. SOX2+ cell population from normal human brain white matter is able to generate mature oligodendrocytes. PLoS ONE 2014, 9, e99253, doi:10.1371/journal.pone.0099253.

63. Chou, S.J.; Babot, Z.; Leingartner, A.; Studer, M.; Nakagawa, Y.; O'Leary, D.D. Geniculocortical input drives genetic distinctions between primary and higher-order visual areas. Science 2013, 340, 1239–1242, doi:10.1126/science.1232806.

64. Chen, X.; Ye, R.; Gargus, J.J.; Blakely, R.D.; Dobrenis, K.; Sze, J.Y. Disruption of Transient Serotonin Accumulation by Non-Serotonin-Producing Neurons Impairs Cortical Map Development. Cell Rep. 2015, 10, 346–358, doi:10.1016/j.celrep.2014.12.033.

65. Gaspar, P.; Cases, O.; Maroteaux, L. The developmental role of serotonin: News from mouse molecular genetics. Nat. Rev. Neurosci. 2003, 4, 1002–1012, doi:10.1038/nrn1256.

66. Persico, A.M.; Mengual, E.; Moessner, R.; Hall, F.S.; Revay, R.S.; Sora, I.; Arellano, J.; DeFelipe, J.; Gimenez-Amaya, J.M.; Conciatori, M.; et al. Barrel pattern formation requires serotonin uptake by thalamocortical afferents, and not vesicular monoamine release. J. Neurosci. 2001, 21, 6862–6873.

67. Hoefflin, S.; Carter, D.A. Neuronal expression of SOX2 is enriched in specific hypothalamic cell groups. J. Chem. Neuroanat. 2014, 61–62, 153–160, doi:10.1016/j.jchemneu.2014.09.003.

68. Reppert, S.M.; Weaver, D.R. Molecular analysis of mammalian circadian rhythms. Annu. Rev. Phys. 2001, 63, 647–676, doi:10.1146/annurev.physiol.63.1.647.

69. Cheng, M.Y.; Bullock, C.M.; Li, C.; Lee, A.G.; Bermak, J.C.; Belluzzi, J.; Weaver, D.R.; Leslie, F.M.; Zhou, Q.Y. Prokineticin 2 transmits the behavioural circadian rhythm of the suprachiasmatic nucleus. Nature 2002, 417, 405–410, doi:10.1038/417405a.